Int. J. Adv. Eng. Pure Sci. 2019, 4: 267-272
DOI: 10.7240/jeps.453159

RESEARCH ARTICLE / ARAŞTIRMA MAKALESİ

A Vehicle Routing Model for Postal Service Operations and an Application

Posta Hizmeti Operasyonları İçin Bir Araç Rotalama Modeli ve Uygulama

Şeymanur Ebru ŞENSU[1], Zeynep ARSLAN[1], Rabia Döndü EKİNCİ[1], Gülfem TUZKAYA[1]

[1] *Marmara University, Faculty of Engineering, Department of Industrial Engineering, 34722, Istanbul, Turkey*

Öz

Günümüzde firmalar arası rekabetin kilit taşını müşteri memnuniyeti oluşturmaktadır. Daha az maliyet, daha çok üretim gibi hedefler müşteri memnuniyetini sağlanmadıkça firmalar için yeterli olmaz. Bu nedenle küçükten büyüğe bütün firmaların amacı müşteriye en iyi, en hızlı şekilde hizmet sunmak ve müşteri memnuniyeti sağlamaktır. Bir ürün veya hizmetin başlangıç noktasından varış noktasına kadar olan süreçte lojistik ağının çok iyi kurulması ve sürecin işlemesi bir firma için önemlidir. Özellikle temel görevi taşımacılık olan kargo firmalarının araç, ürün ve çalışan sayısı gibi kısıtlar ve zaman açısından çok iyi bir sürece sahip olması gerekmektedir. Bu amaçla, bu çalışmada posta hizmetleri için Araç Rotalama Problemi (ARP) üzerine çalışılmıştır. Araçlarını rotalarken önce dağıtım merkezlerine sonrasında kabul merkezlerine gönderen posta hizmetlerinin çok fazla şubesi bulunabilmektedir. Merkez sayısı çoğaldıkça en iyi çözümü veren algoritmalar bu problemi çözemeyeceği için merkezlerin birbirine olan uzaklıkları temel alınarak kümeleme metodu kullanılmıştır. Böylece birbirine yakın olan merkezler kendi içlerinde planlanarak toplam kat edilen uzaklık azaltılmaya çalışılmıştır.

Anahtar Kelimeler: Geri Toplamalı Araç Rotalama Problemi, Kümeleme, Karma Tamsayılı Programlama

Abstract

Customer satisfaction is an important factor for the success of the companies. Efforts for cost reduction and production productivity are not enough for companies unless customer satisfaction is provided. For this reason, the aim of companies from all sizes is to provide the best and fastest service to customers. Therefore, the establishment and operation of a logistics network is important for a company from the original point to the point of arrival of a product or service. In cargo companies, transportation is the main procedure in terms of time and capacity constraints such as the number of vehicles, products and employees. With this aim, Vehicle Routing Problem with Backauls (VRPB) is investigated to reduce the total distance travelled by vehicles for a hypothetical postal service firm. It is assumed that there are more than a hundred centers of the firm that send their vehicles to the reception centers after the distribution centers are visited. The P-Median clustering model is used based on the distances of the centers to each other, since the exact algorithms cannot solve this problem due to a great number of centers. Then, vehicles in each cluster routed by using a modified mathematical model.

Keywords: Vehicle Routing Problem with Backhauls, Clustering, Logistics

I. INTRODUCTION

VRP generally deals with the management of distribution and/or pick-up activities. It is related to decision of how to use the available vehicle fleet and resources. It is expected to meet the requirements by using the resources effectively. Hence, routes for existing vehicles are tried to be defined **[1]**.

In the classic VRP, the route starts and ends at the storage point and that is the main constraint. Other common constraints may be capacity, demand, duration, time-window and priority **[2].** Some of the application areas of VRP are:

Sorumlu yazar/Corresponding Author: Gulfem TUZKAYA, **Tel:** +90 216 348 0292-1228, **e-posta:** gulfem.tuzkaya@marmara.edu.tr
Gönderilme/Submitted: 13.08.2018, **Düzenleme/Revised:** 26.09.2019, **Kabul/Accepted:** 10.10.2019

- Transportation and logistics sectors
- Waste collection
- Flight charts
- Delivery of online shopping
- Distribution of goods (such as newspaper, mail, bread and drinks)
- Routing of service vehicles

In transportation and logistics applications, the routes of vehicles from factories to warehouses, from warehouses to customers are ensured. In the transportation sector, especially public transportation vehicles are routed **[3].**

Solution techniques of the Vehicle Routing Problem (VRP) can be grouped into three main categories as exact, heuristics and meta-heuristics solution techniques in general. With exact solution methods it is possible to find the optimal solution to a problem; whereas with heuristic and meta-heuristic approaches optimality is not guaranteed, however, solutions can be found in close-range to optimal solution **[4].**

In this study, one of the types of VRP, Vehicle Routing Problem with Bachauls (VRPB) is applied to the postal service operations. In literature review part, VRP studies are investigated based on two main topics which are postal service operations and types of VRP. After that, the purpose of the study is explained in Applied Mathematical Models section. Moreover in this part, the models that are used in this paper have shown in a detailed way. In the Application and Results part, a vehicle routing problem for a hypothetical firm is investigated. In order to solve this problem, clusters that contain distribution and reception centers are generated by using p-median model. In the results part of this section, Goetschalckx and Jacobs-Blecha's vehicle routing model **[5]** modified and applied. Finally, concluding remarks are given.

II. LITERATURE REVIEW

Related literature is reviewed in terms of two main topics which are VRP in postal service operations and types of VRP. VRP types that investigated are VRPB, capacitated VRP, VRP with time windows, and VRP with delivery and pick-up.

Ji and Chen studied on the vehicle routing problem in postal service operations in Hong Kong in 2007. At that time, scheduling of postal vehicles carried out manually. In the problem, there are a General Post Office and a set of District Post Offices. The study aimed to minimize costs and to maximize resource utilization. To find an optimal solution, an integer linear programming model was built **[6].**

For Vehicle Routing Problem with Backhauls (VRPB), as Jacobs-Blecha and Goetschalckx mentioned, pick-up is not allowed until distribution is finished. Jacobs-Blecha and Goetschalckx **[7]** introduced a linehaul-backhaul (LHBH) heuristics for VRPB in 1992. For routing, TSP, 2-opt and 3-opt heuristics are used. LHBH produces routes which are adaptable and flexible. This allows the user to interactively make modifications to the solutions needed in real time applications **[7]**. Another type of VRP is capacitated VRP and as an example, the study prepared by Nazif and Lee is investigated. They solved capacitated vehicle routing problem by using genetic algorithm. The aim of the study is to find the optimal set of delivery routes by minimizing total cost. A comparison with some other heuristic approaches is also presented in that study **[8]**. VRP with time windows is another type of VRP and Yassen et al. **[9]** studied on this type and used Solomon's data to test their algorithms. They developed an adaptive hybrid algorithm and carried out some experiments to examine impact of using local search algorithms, effect of performed mechanisms on the search ability and validate efficiency of the adaptive hybrid algorithm. The outputs showed that adaptive hybrid algorithm achieved better results in comparison to the other methods **[9]**. The paper presented by Righini et al. **[10]** can be given as an example of VRP with delivery and pick-up. They applied branch-and-price technique for this problem. Two different solution methods compared to solve the pricing subproblem: state space relaxation and exact dynamic programming **[10]**.

In literature survey, firstly the studies applied for postal service operations are investigated. Only one study was found about vehicle routing problem applied in postal service. This study was prepared for Hong Kong Postal Service **[6]**. However, there are many practices about VRP in cargo firms. Then, a brief literature survey is realized for different types of VRP. Due to the NP-hard nature of the VRP problems, meta-heuristics and heuristics are the mostly used solution algorithms. As exact solution methods, Branch and Bound Algorithm and Branch and Cut Algorithms are the mostly used ones.

III. MATHEMATICAL MODELS

The aim of this study is minimizing the total distance for postal service operations of a hypothetical firm. This firm's post route can be seen in Figure 1.

A vehicle delivers the posts from Processing Center to the Distribution Centers after that same vehicle collects the new posts from Reception Centers for the aim of returning them to the Processing Center. Vehicles departed and arrived to a single depot. If the distribution is not finished, vehicles can

Figure 1. Route of a post in the firm

not visit the Reception Centers. Therefore, this is a type of Vehicle Routing Problem with Backhauls. In this study, to solve the vehicle routing problem with backhauls for postal service operations, a modified model is used. Before solving the model, to decrease the number of centers, p-median model is used and clusters are generated. In the following, brief literature and the applied mathematical model are given.

The first study in this area was conducted by Dantzig and Ramser in 1959 **[11]** and the fundamental of this problem is based on Travelling Salesman Problems (TSP). Then, Jacobs-Blecha and Goetschalckx in 1989 **[5]** studied on Vehicle Routing Problem with Backhauls.

Since the VRPB problems are NP-hard type, an optimization software may not be sufficient to find optimal solutions for large problem instances. Therefore, it is determined to use a clustering method. As the first step of the solution, it is decided to cluster the distribution and reception centers by using P-Median model given in **[12].**

Parameters

P: Number of clusters

D: Number of distribution centers, *d=1, 2, .., D*

R: Number of reception centers, *d=D+1, D+2, ..., D+R*

d_{ij}: Distance of direct travel from center i to center *j* (*i, j =1, ..., D, D+1, ..., D+R*)

Variables

$$x_{ij} = \begin{cases} 1, \text{ if the vehicle directly travels from center } i \text{ to } j, \\ \qquad\qquad i,j = 1,..,D,...,D+R \\ 0, \text{ otherwise} \end{cases}$$

Minimize

$$\sum_{i=1}^{D+R} \sum_{j=1}^{D+R} d_{ij} x_{ij} \quad (1)$$

Subject to

$$\sum_{j=1}^{D+R} x_{ij} = 1 \qquad i = 1,2,\dots,D+R \quad (2)$$

$$\sum_{j=1}^{D+R} x_{jj} = P \qquad j = 1,2,\dots,D+R \quad (3)$$

$$x_{ij} \leq x_{jj} \qquad i,j = 1,2, \dots, D+R \quad (4)$$

$$x_{ij} = 0 \text{ or } 1 \qquad i,j = 1,2, \dots, D+R \quad (5)$$

By applying P-Median Model, 11 clusters are found.

Jacobs-Blecha and Goetschalckx's vehicle routing model **[5]** modified and applied for this study after clustering the centers. There are distribution and reception centers, and the objective function is minimization of the total distance travelled. It is assumed that the firm has heterogeneous fleet, therefore vehicle index is used. To eliminate subtours and loops, a subtour elimination constraint is added. In addition, it is considered in the tenth constraint that each vehicle must service to centers in total working hours everyday.

Afterwards, a mathematical model is built for the problem as follows:

Parameters

K: Number of vehicles

D: Number of distribution centers, *d= 1, 2,..., D* (index *0* indicates the depot)

R: Number of reception centers, *d= D+1, D+2,..., D+R*

T: Total service time in a day

C_k: Capacity of the vehicles (*k =1,2,..,K*)

a_i: Demand of distribution center *i* (*i =1, 2,..., D*)

b_i: Supply of reception center *i* (*i = D+1, D+2,..., D+R*)

d_{ij}: Distance of direct travel from center i to center *j* (*i, j = 0,1,..., D, D+1,..., D+R*)

t_{ij}: Travel time between center i and center *j* (*i, j = 0,1,..., D, D+1, ..., D+R*)

y_j: Service time in each center (*j =1,...,D+R*)

Variables

$u_{ik=}$ { 1, if distribution center i is serviced by vehicle k, $i = 0,1,..,D$; 0, otherwise

$v_{jk=}$ { 1, if reception center j is serviced by vehicle k, j = D+1,..,D+R and j=0 ; 0, otherwise

$x_{ijk=}$ { 1, if vehicle k travels directly from center i to j, $i, j = 0,1,..,D,...,D+R$; 0, otherwise

s_j= Subtour elimination variable $j=1,....,D+R$

s_i= Subtour elimination variable $i=1,....,D+R$

Objective function

$$Min \sum_{k=1}^{K} \sum_{i=0}^{D+R} \sum_{j=0}^{D+R} d_{ij}\, x_{ijk} \quad (6)$$

Subject to

$$\sum_{i=1}^{D} a_i\, u_{ik} \le C_K \qquad k = 1,2,\dots,K \quad (7)$$

$$\sum_{i=D+1}^{D+R} b_i\, v_{ik} \le C_K \qquad k = 1,2,\dots,K \quad (8)$$

$$\sum_{k=1}^{K} u_{ik} = 1 \qquad i = 1,2,\dots,D \quad (9)$$

$$\sum_{k=1}^{K} v_{ik} = 1 \qquad i = D+1, D+2,\dots,D+R \quad (10)$$

$$u_{0k} = 1 \qquad k = 1,2,\dots,K \quad (11)$$

$$v_{0k} = 1 \qquad k = 1,2,\dots,K \quad (12)$$

$$\sum_{i=0}^{D} \sum_{\substack{j=D+1 \\ and \\ j=0}}^{D+R} x_{ijk} = 1 \qquad k = 1,2,\dots,K \quad (13)$$

$$\sum_{j=0}^{D+R} x_{ijk} = \begin{cases} u_{ik,} \text{ if } i = 0,1,...,D \\ v_{ik,,} \text{ if } i = D+1, D+2,..., D+R \; k = 1,2,..., K \end{cases} \quad (14)$$

$$\sum_{i=0}^{D+R} x_{ijk} = \begin{cases} u_{jk,} \text{ if } j = 1,...,D \\ v_{jk,} \text{ if } j = D+1, D+2,..., D+R \text{ and } j=0 \; k = 1,2,...,K \end{cases} \quad (15)$$

$$\sum_{i} \sum_{j} x_{ijk} t_{ij} + \sum_{i} \sum_{j} x_{ijk} y_j \le T \qquad k=1,2,...,K \quad (16)$$

$$s_i - s_j + (D+R+1) * \sum_{k=1}^{K} x_{ijk} - (D+R) \le 0 \qquad i \ne j,\ i,j=1,...,D+R \quad (17)$$

$$u_{ik} = 0 \text{ or } 1 \qquad i = 1,2,\dots,D \quad k = 1,2,\dots,K \quad (18)$$

$$v_{ik} = 0 \text{ or } 1 \qquad i = D+1, D+2,\dots,D+R \quad k = 1,2,\dots,K \quad (19)$$

$$x_{ijk} = 0 \text{ or } 1 \qquad i,j = 0,...., D+R \; k = 1,2, ..., K \quad (20)$$

$$s_i \ge 0 \; s_j \ge 0 \qquad i,j = 1,...., D+R \quad (21)$$

Constraints (7) and (8) ensure that the trucks cannot be loaded more than their capacities for distribution and reception centers, respectively.

Constraint (9) ensures that only one vehicle can be assigned to the distribution center's route.

Constraint (10) ensures that only one vehicle can be assigned to the reception center's route and only K, number of vehicles, can leave or turn back to the depot.

Constraints (11) and (12) ensure that each vehicle must start from and turn back to depot.

Constraint (13) ensures that there is only one link traveled by each vehicle from last distribution center to first reception center in one route.

Constraints (14) and (15) ensure that exactly one vehicle leaves from each center and exactly one vehicle enters each center and depot.

Constraint (16) ensures that total service time of each vehicle and process times at the centers can not be more than total working time in a day.

Constraint (17) is the subtour elimination constraint. $D+R+1$ represents total number of centers including depot.

Constraints (18), (19) and (20) ensure that the decision variables must have binary solution values.

Constraint (21) is the nonnegativity constraint for subtour elimination variables.

IV. APPLICATION AND RESULTS

Vehicles that can carry cargo and posts are considered and 4 types of vehicles are decided to be used in the study. Their capacities are assumed as 14 m^3, 17 m^3, 22 m^3 and 40 m^3. By assuming 1 m^3 carries 26 kg. load, capacities of vehicles

are calculated in terms of grams. Table 1 demonstrates capacities of vehicles.

Table 1. Capacities of the vehicles

14 m^3	364,000 gr
17 m^3	442,000 gr
22 m^3	572,000 gr
40 m^3	1,040,000 gr

To determine the routes of vehicles, a distance matrix is needed. Then a matrix that includes one hundred and sixteen centers is created. Total demand is 8,093,680 gr. in distribution centers while total supply amount is 8,598,620 gr. in reception centers.

In this paper, 11 clusters are created according to relative distances of the centers by using p-median model. Then, each cluster is solved in LINGO 17.0 and the routes of the vehicles are determined. The results obtained are given in Table 2.

Table 2. Total travelled distances of Clusters

Clusters	Total Travelled Distances (m)
Cluster 1	168,544
Cluster 2	133,775
Cluster 3	179,731
Cluster 4	487,822
Cluster 5	354,368
Cluster 6	164,492
Cluster 7	54,110
Cluster 8	122,953
Cluster 9	116,936
Cluster 10	97,337
Cluster 11	114,015
Total	1,994,083

Total travelled distance and route for cluster 1 is shown in figure 2.

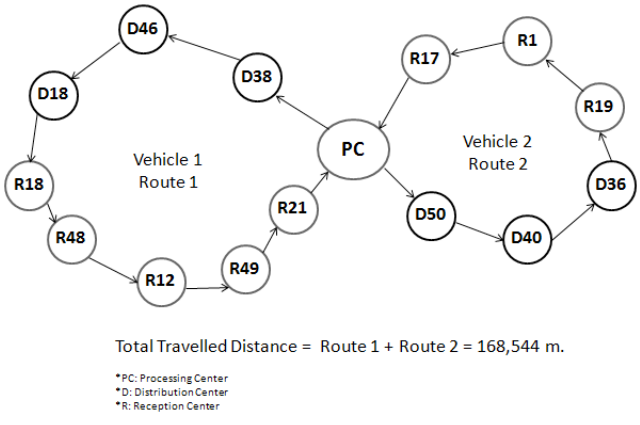

Figure 2. Route for cluster 1

Optimal routes for cluster 7, 8 and 9 are given below. For these routes only one vehicle in each cluster is required in the optimal solution.The optimal route of cluster 7 for its vehicle is PC, D7, D8, R56 and PC. The route for cluster 8 is PC, D16, D41, D14, D58, D57, D27, R51, R53, R14, R41 and PC. Lastly, the route is PC, D59, D30, D44, R28, R35, R 55 and PC for cluster 9.

Results are anaylsed based on changes of vehicle speed, process times at each center and demand, supply amounts made a huge difference in the clusters. To observe the variations, cluster 1 is analysed. Initially, it was assumed that vehicle speed is 60 km/h for each vehicle. To analyse the results, it is increased to 90 km/h. For this increase in the speed, optimal route for the cluster did not change.Then, the vehicle speed is decreased to 40 km/h due to traffic congestion at the main roads. As in 90 km/h, the optimal route for the cluster did not change. It was assumed in the paper that unloading the vehicles takes 25 minutes at each center. For analysis this time it is altered to 15 minutes. The optimal route for the cluster remained the same as the previous case. Also, assuming that a vehicle broke down at the first reception center and it took 125 minutes to get repaired. Again, it doesn't effect the optimal route. Finally, supply amount changes are analysed.Supply amounts of the distribution centers were 117020, 27380, 53720, 81260, 149480, 58520, 17180, 19974 gr. and demanded amounts in the reception centers were 14320, 39440, 4260, 251900, 2808400, 29700 gr. To observe the difference amounts at the distribtution centers changed into 100000, 150000, 50000, 40000, 20000, 90000, 20000 and 50000 gr. The amounts in the reception centers became 100000, 140000, 250000, 50000, 30000 and 50000 gr. With this experiment, objective value calculated as 166648 meters and as expected, the optimal routes have changed in the cluster for two vehicles.

V. CONCLUSION

Vehicle routing is one of the important problem areas for logistics management literature. Vehicles routes may have a direct effect on cost effectiveness, on time delivery ratios and as a result, on custumer satisfaction levels. Especially for postal services, this problem becomes the main problem for the companies. Considering this importance level, in this study, vehicle routing problem with backhauls (VRPB) is examined for postal service operations. Considering the possibility of having large number of points for such networks, initially, a clusturing model, p-median model, from literature is applied. Following clustering phase, a modified VRPB model is applied to find proper routes for the vehicles. Finally, results are analysed for some variations

in the data. For the future researches, instead of decreasing the size of the problem by using a clustering approach, a real size problem can be solved by applying a proper heuristic or meta-heuristic algorithm.

REFERENCES

[1] Atasagun, G., (2015). Zaman bağımlı eş zamanlı topla dağıt araç rotalama problem. *Selçuk Üniversitesi Fen Bilimleri Enstitüsü Endüstri Mühendisliği Anabilim Dalı Yüksek Lisans Tezi*, pp.15-16.

[2] Laporte, G., (1992). The Vehicle-Routing Problem – an Overview of Exact and Approximate Algorithms. *European Journal of Operational Research*, 59(3), 345-358.

[3] Keskintürk, T., Topuk, N. & Özyeşil, O., (2015). Araç Rotalama Problemleri ile Çözüm Yöntemlerinin Sınıflandırılması ve Bir Uygulama. *İşletme Bilimi Dergisi*, 3(2), 80.

[4] El-Sherbeny, N.A., (2010). Vehicle routing with time windows: An overview of exact, heuristic and metaheuristic methods. *Journal of King Saud University – Science*, 22(3), 123-131.

[5] Jacobs-Blecha C. & Goetschalckx M., (1989). The vehicle routing problem with backhauls. *European Journal of Operational Research*, 42, 39-51.

[6] Ji, P. & Chen, K., (2007). The Vehicle Routing Problem: The Case of the Hong Kong Postal Service. *Transportation Planning and Technology*, 30(2-3), 167-182.

[7] Jacobs-Blecha C. & Goetschalckx M., (1992). A Vehicle Routing Problem Backhauls: Properties and Solution Algorithms. *Computer Science and Information Technology Laboratory*, Georgia Tech Research Institute.

[8] Nazif, H. & Lee, L.S. (2012). Optimised crossover genetic algorithm for capacitated vehicle routing problem. *Applied Mathematical Modeling*, 36, 2110-2117.

[9] Yassen, E.A., Ayob, M., Nazri, M.Z.A. & Sabar, N.R., (2017). An Adaptive Hybrid Algorithm for Vehicle Routing Problems with Time Windows. *Computers & Industrial Engineering*, 113, 382-391.

[10] Righini, G., Salani, M. & Dell'Amico M., (2006). A branch-and-price approach to the vehicle routing problem with simultaneous distribution and collection. *Transportation Science*, 40 (2), 235-247.

[11] Dantzig, G.B. & Ramser, J.H., (1959). The truck dispatching problem. *Management Science*, pp. 6-80.

[12] Heragu S.S., (2006). *Facilities Design,* CRC Press, Taylor&Francis Group.

Int. J. Adv. Eng. Pure Sci. 2019, 4: 273-279
DOI: 10.7240/jeps.468836

RESEARCH ARTICLE / ARAŞTIRMA MAKALESİ

Bakım Planlamalı Uçuş Atama Modeli ve Bir Uygulama

Flight Planning with Maintenance Consideration and an Application

Mehmet Anıl ŞAHİN[1], **Gülfem TUZKAYA**[1]

[1]*Marmara Üniversitesi, Mühendislik Fakültesi, Endüstri Mühendisliği Bölümü, 34722, İstanbul/Türkiye*

Öz

Bu çalışmanın amacı, hava yolları endüstrisinin karmaşık problemlerinden biri olan bakım rotalama problemine yeni bir çözüm önerisi getirmektir. Çalışma kapsamında öncelikle, hava yolları endüstrisi operasyonlarının temel uygulama ve problemleri, bu uygulamaların literatürdeki yeri temel düzeyde ele alınmıştır. Hava yolları endüstrisi literatürü "Filo Atama, Uçak Rotalama, Bakım Rotalama ve Mürettabat Çizelgeleme" başlıkları altında incelenmiştir. Önerilen, bakım planlamalı uçuş atama modeli, gerçek uçuş verileri ve tasarlanan uçuş filosu için uygulanmış ve bir uçuş programı oluşturulmuştur. Model iki amaç fonksiyonuna sahiptir. Birinci amaç fonksiyonu, kullanılmayan kalan yasal zamanı minimize etmeye çalışırken, ikinci amaç fonksiyonu kullanılmamış uçak kapasitesini minimize etmeye çalışır. İki amaçlı model öncelikli hedef programlama ile çözülmüştür.

Anahtar Kelimeler: Bakım planlama, Uçuş atama

Abstract

As the main concentration of this study, maintenance routing is one of the most complicated problems of airline industry. In this study, airline industry operations' main applications and subjects are basically summarized and a literature review is briefly presented. Study is conducted under headings of; "Fleet Assignment, Aircraft Routing, Maintenance Routing and Crew Scheduling". A problem consist of real time flight data and a small size fleet is generated and the proposed model is solved to create a route with maintenance consideration. Model which solves the problem has two objective functions. While first objective function tries to minimize remaining legal flight hours of the aircrafts second objective function tries to maximize the capacity utilization of an aircraft according to the demand for the covered flight. The model is solved by using preemptive goal programming.

Keywords: Maintenance Planning, Flight Planning

1. GİRİŞ

Ticari havacılık endüstrisi, en güvenli ve en hızlı seyahat yollarından birini sunmaktadır. Çok önemli bir iş alanı olan bu endüstride, yöneylem araştırması tekniklerinden sıklıkla faydalanılmaktadır. Havacılık endüstrisinde rotalama ve çizelgeleme problemlerini dört ana başlık altında inceleyebiliriz: Filo atama, uçak rotalama, bakım rotalama ve mürettebat çizelgeleme. ***Filo atama*** probleminde rotaların tamamlanacağı uçaklar belirlenmeye çalışılır. Bu filolar bazen yalnızca bir uçak tipinden, bazen birkaç farklı modelden oluşurlar. Karışık filolarda, tüm ihtiyaçları karşılamak için çeşitli kapasite ve menzile sahip uçaklar bulunmaktadır. ***Uçak rotalama*** esas olarak uçuş programındaki belirli sayıda uçuşun her birinin filodaki hangi uçakla yapılacağına karar veren çalışmadır. ***Bakım rotalama***, belirli bir periyot için gerçekleşecek uçuşlara uçak ataması yapılırken, uçakların Avrupa Havacılık Güvenliği Ajansı (EASA–European Aviation Safety Agency) yönergelerine göre bakım ihtiyaçlarının da değerlendirilmesini içerir. Bu bakım ihtiyaçları uçaktan uçağa farklılık gösterebilir. Dolayısıyla uçuş programında uçakların her biri için kalan uçuş süresi hesaplanır ve düzenli bakımlar için uçaklara boşluklar yaratılır. ***Mürettebat çizelgeleme***, uçuşlara pilot ve kabin ekibi atanması ile ilgilenir ve gerekli planları yapar **[1-2].**

Bir uçuş programını planlarken, en önemli noktalardan biri, uçuş saatlerine uygun olarak uçağın bakımının da planlanmasıdır. Her markanın farklı tipte uçakları farklı zaman ve mesafeler sonrasında planlı bakım gerektirir. Bakım süreleri EASA

Sorumlu yazar/Corresponding Author: Gulfem TUZKAYA, **Tel:** +90216 3480292-1228, **e-posta:** gulfem.tuzkaya@marmara.edu.tr,
Gönderilme/Submitted: 09.10.2018, **Düzenleme/Revised:** 26.09.2019, **Kabul/Accepted:** 14.10.2019

tarafından düzenlenmektedir. Bu bakımlar, orta, uzun vadeli bakımlar ve uçuş öncesi kontrolleri başlıklarında üç bölüme ayrılır. Uzun süreli bakımlar ve uçuş öncesi kontrolleri haftalık uçuş planında listelenmemektedir. Çünkü uzun vade bakımları için uçağın filodan alınması ve hangara çekilmesi gerekecektir. Uçuş kontrolleri ise her uçuştan önce yapılır ve çok az zaman alır. EASA yönetmelikleri ile düzenlenen orta vadeli bakımlar, parça değişiklikleri için uçağın hangara alınmasını gerektirir. Firmalar genellikle, uçuş saatleri ile çakışmaması için, bakımlarını uçuş yapılmayacak gece saatlerinde yapmayı planlar. Yukarıda belirtilen nedenlerden dolayı, uçuş planlarını hazırlarken kalan uçuş sürelerinin dikkate alınması, uçakları aktif tutmak için bir avantaj sağlar **[3].**

Bakım kısıtlı uçuş planlama probleminde temel amaç, bakım gereksinimlerine uygun olarak her uçak için uçuş rotaları oluşturmaktır. Geleneksel bakım kısıtlı uçuş planlama problemleri modelleri yüksek sayıda uçak ve rota seçeneği için çalışır. Plandaki uçuşların sayısı arttıkça, çözüm ve çözüm zamanı için alternatifler katlanarak artmaktadır. Sorunu hafifletmek için bu tür modeller, sütun oluşturma veya satır oluşturma yaklaşımlarıyla adım adım çözülür. Diğer taraftan, Liang ve Chaovalitwongse **[3]** günlük bakım kısıtlı uçuş rotası problemi için haftalık rotasyon-tur ağı modeli geliştirmişlerdir. Bu çalışmada, uçuş sayısındaki artış çözümün aralığını doğrusal olarak etkilemektedir **[3].**

Bakım kısıtlı uçuş planlama, havayolu endüstrisinin planlama ihtiyaçlarından sadece biridir. Bu problem hem yolcu uçuşları hem de kargo uçuşları için çözülmelidir, ancak iki problem çeşitli farklılıklar içerir. Yolcu uçuşlarında gecikmelerde sorunlar oluşabilir ve iptal durumları söz konusu olabilir. Kargo uçuşları için ağırlık ve kütle problem oluşturabilir **[1].**

Bakım kısıtlı uçuş planlama probleminde iki husus önemlidir. Bunlardan biri, uçuş bağlantılarının ihtiyaç duyulandan daha kısa sürede kurulduğu durumları cezalandırmak, diğeri ise bağlı uçuşların değerini arttırmaktır. "Dönüş süresi", uçağın "minimum bekleme süresinden" kısaysa, gerekli işlemler için yeterli zaman olmayacaktır ve kısa bağlantı süresi cezası uygulanacaktır. Dönüş süresi, bir uçağın inmesi ile bir sonraki kalkışı arasındaki süreyi açıklayan bir terimdir. Uçağın minimum bekleme süresi, kabin görevlilerinin uçuşlar arasındaki uçakları değiştirmesi için gereken minimum süreyi açıklayan bir terimdir. Kısa bağlantı, 'Takım kurma problemi' için pratik olmayan veya yüksek maliyetli sonuçlara neden olabileceğinden istenmeyen bir olaydır. Bağlı uçuşların değerini arttıran faktör, iki bağlı uçuş arasında uçakta kalan yolcu miktarıdır.

Uçuş dizilerinin bağlanması ve rotaların belirlenmesi konunun literatürdeki en yaygın rastlanan iki problemidir. Kararlar, istasyonlar arasında bakım hizmetini verebilecek, bakım istasyonlarından birinde sona eren uygulanabilir uçuş sıralarını bulmakla ilgilidir **[3].**

Havayolu sektöründe en büyük maliyetlerden birini bakım giderleri oluşturur. Bu nedenle, bir uçağın yasal uçuş süresini azami ölçüde kullanarak, planlanan bakım süresini limitler dahilinde geciktirerek maliyetleri düşürmek önemlidir. Ekipmanların en son kullanma sürelerine kadar kullanılmaması ekstra maliyet getirecektir **[4].** Daha önce de belirtildiği gibi, bakım için zaman limitleri Avrupa Havacılık Güvenliği Ajansı tarafından belirlenir. Bakımlar dört kategori altında, kendi aralarında frekans, içerik ve zaman ile bölünmektedir **[5].** A kategori bakımı yaklaşık 65 saatlik uçuş ya da bir haftalık süre ardından yapılsa da, birçok şirket bu bakımları 45 saatlik uçuş sonrasında bir önlem olarak yapmaktadır. Bu bakım içeriği motorlar ve iniş takımları gibi temel parçaların kontrolünü içerir ve genelde bir gecede yapılır. B kategori bakımları 300-600 saatlik uçuşları takiben yapılır ve uçağın genel görsel kontrolü ile hareketli tüm parçaların yağlanmasını içerir. C ve D tipi bakımlar ise 1-4 yılda bir yapılır. Uçağın yapısal bütünlüğünün kontrolü de dahil olmak üzere uçağın tamamen sökülüp tekrardan birleştirilmesini içerir. Bu işlem uçağın yaklaşık bir ay filodan alınması anlamına gelmektedir **[1].**

Bu alandaki çalışmalarda, maliyetlerin en aza indirilmesi ve kar maksimizasyonu gibi yaygın amaç fonksiyonlarından kalan uçuş süresinin en aza indirilmesi gibi spesifik örneklere kadar farklı amaç fonksiyonları görülmektedir. Yapılan araştırmalar, erken yapılmış bakımların maliyetleri yıllık bazda önemli bir ölçüde artırdığını göstermiştir **[3-6-7-8].** Bu nedenle, bir uçuş planı belirlenirken, filodaki uçakların kalan uçuş süreleri, bir bakım ihtiyacı için durmadan önce mümkün olan en fazla miktarda kullanılmalıdır. Literatürde bu yaklaşıma göre modelleme yapan ve amaç fonksiyonu oluşturan iki çalışma olduğu görülmüştür. Amaç fonksiyonu, bakımdan önce uçakların kullanılmayan yasal uçuş süresini en aza indirmektir. Bu çalışmalardan ilki, modelde tanımlanan kritik statüyle bir uçağın gelecek uçuş döneminde bakım ihtiyacı olup olmadığına karar vermektedir. Uçağın kalan uçuş süresi, planlanacak periyodun en uzun uçuş ağından daha kısa ise uçak, modele kritik bir uçak olarak katılacaktır. Kritik durumda olmayan uçaklar seti, bakım kısıtlamalarını dikkate almadan haftalık uçuş programını tamamlayacaktır. Öte yandan kritik set, bakım ihtiyaçlarını karşılayabileceği havalimanlarının bulunduğu ağlarda uçurulacaktır **[6].** İkinci çalışmada, uçaklar kalan uçuş sürelerine bağlı olmayan bir kuralla düzenlemekte ve bakım verebilecek rotalarda daha az zamanı kalan uçaklara atama

önceliği tanınmaktadır **[8].** Tablo 1'de ilgili çalışmaların sınıflandırılması görülebilmektedir.

Tablo 1. Bakım kısıtlı uçak rotalama çalışmaları

Yazar	Yıl	Veri	Amaç Fonksiyonu	Notlar	Programlama
Liang vd. **[7]**	2015	Gerçek	Gecikme min.	Bakım	IP
Basdere ve Bilge **[6]**	2013	Gerçek	Kalan uçuş süresi min.	Bakım	IP
Diaz-Ramirez vd. **[9]**	2013	Gerçek	Kar maks.	Bakım	IP
Liang ve Chaovalitwongse **[3]**	2013	Gerçek	Toplam ceza puanı min.	Bakım, Filo Atama	Karma IP
Orhan vd. **[8]**	2011	Gerçek	Kalan uçuş süresi min.	Bakım	IP
Lapp ve Cohn **[10]**	2011	Gerçek	Bakım uyuşmazlığı min.	Bakım	LP
Afsar vd. **[11]**	2009	Gerçek değil	Fayda maks.	Bakım	LP
El Moudani ve Mora-Camino **[12]**	2000	Gerçek	Maliyet min.	Bakım	DP

IP: Tamsayılı Programlama (Integer Programming), LP: Doğrusal Programlama (Linear Programming), DP: Dinamik Programlama (Dynamic Programming)

önceki bölümde özetlenen literatür incelenmiş ve konunun uygulaması araştırılmıştır. Bu aşamada, uçakların bakım süresinden önce yasal uçuş saatlerini kullanmalarına ve böylece kullanım verimliliğini artırmalarına ve dolayısıyla bakım maliyetlerini düşürmelerine imkân tanıyan bir yaklaşım geliştirilmiştir. Aynı zamanda, uçuşlar atanırken uygun kapasiteli uçuşlara atanması hedeflenmiştir. Bu hedefler doğrultusunda model iki amaç fonksiyonuna sahip olacak şekilde geliştirilmiştir. Birinci amaç fonksiyonu, kullanılmayan kalan yasal zamanı minimize etmeye çalışırken, ikinci amaç fonksiyonu kullanılmamış uçak kapasitesini minimize etmeye çalışır. Kapasite kullanımını artırmak ve ihtiyacı karşılamak için iki yöntem takip edilmiştir. İlk olarak, uçuş taleplerini dikkate alarak, filoda en çok talep gören uçuşu karşılayabilecek kapasiteye sahip bir uçak seçilmiştir. Bu atama esnasında uçağın, talebi düşük olan herhangi bir uçuşta boş kalmaması için makul koltuk sayısında olması dikkate alınmıştır. İkincisi, uçuş talebi ile kapasitenin daha etkin kullanılması için, atanacak uçakların kapasitesi ile uçuşa olan talep arasında minimum fark olmasını sağlayacak bir amaç fonksiyonu oluşturulmuştur.

Bu bilgilerin ışığında, bir havayolu şirketinin örnek bir uçuş programı oluşturulmuş ve bu haftalık uçuş programını kapsayan bir filo tespit edilmiştir. Problem, bu veri ve matematiksel modeli kullanarak LINGO programında çözülmüştür. Programlama esnasında kullanılan indisler, parametreler, setler ve karar değişkenleri Tablo 2'de özetlenmiştir.

II. MATERYAL VE YÖNTEM

Bakım planlamalı uçuş atama modeli geliştirilirken, bir

Tablo 2. İndisler, parametreler, setler ve karar değişkenleri

i	Gerçekleştirilen uçuş indisi
j	*(i)* uçuşunu takip edecek uçuş indisi
k	Uçak indisi
t_i	Uçuş (i) süresi
r_k	Uçak (k) kalan uçuş süresi
c_k	Uçak (k) yolcu kapasitesi
d_i	Uçuş (i) yolcu talebi
I	Uçuş seti
S(i)	Uçuş (i)'yi takip edebilecek uçuşlar seti
P(i)	Uçuş (i)'ye öncül olabilecek uçuşlar seti
M(i)	Uçuş (i)'yi takip eden bakımlar seti
$\{0,T\}$	Yapay başlangıç ve bitiş noktaları
Xijk	Belirlenen haftada bakım görmeden (k) uçağının sırasıyla (i) ve (j) uçuşlarını tamamlaması durumunda 1 değerini alır, diğer durumlarda 0 değerini alır.
Yijk	Belirlenen haftada bakım gördükten sonra (k) uçağının sırasıyla (i) ve (j) uçuşlarını tamamlaması durumunda 1 değerini alır, diğer durumlarda 0 değerini alır.

Amaç fonksiyonu 1:

$$\min \quad \sum_{k\in K}\left(1-\sum_i^I\sum_j^I \frac{t_i x_{ijk}}{r_k}\right) \qquad \text{(Denk. 1)}$$

Amaç fonksiyonu 2:

$$\min \quad \sum_{i\in I}\sum_{j\in S(i)}\sum_{k\in K}\left(\frac{(x_{ijk}+y_{ijk})(c_k-d_i)}{I}\right) \qquad \text{(Denk. 2)}$$

Kısıt 1:

$$\sum_{j\in P(i)U\{0\}} x_{jik} = \sum_{j\in S(i)U\{T\}} x_{ijk} + \sum_{j\in M(i)} y_{ijk} \qquad \forall_i, \forall_k \quad \text{(Denk. 3)}$$

Kısıt 2:

$$\sum_k (x_{ijk} + y_{ijk}) c_k \geq d_i \quad \forall_i, \forall_j \qquad \text{(Denk. 4)}$$

Kısıt 3:

$$\sum_i \sum_{j \in S(i)} t_i x_{ijk} \leq r_k \quad \forall_k \qquad \text{(Denk. 5)}$$

Kısıt 4:

$$\sum_{j \in P(i) U \{0\}} y_{jik} = \sum_{j \in S(i) U \{T\}} y_{ijk} \qquad \forall_i, \forall_k \qquad \text{(Denk. 6)}$$

Kısıt 5:

$$\sum_{j \in P(i) U \{0\}} (x_{jik} + y_{jik}) = 1 \qquad \forall_i \qquad \text{(Denk. 7)}$$

Kısıt 6:

$$\sum_{j \in M(i)} y_{ijk} + \sum_{j \in S(i) U \{T\}} (x_{ijk} + y_{ijk}) = 1 \qquad \forall_i, \forall_k \qquad \text{(Denk. 8)}$$

Kısıt 7:

$$x_{ijk}, y_{ijk} \in \{0,1\} \quad \forall_i, \forall_j, \forall_k \qquad \text{(Denk. 9)}$$

Amaç fonksiyonları ve kısıtların açıklamaları aşağıdaki gibidir:

İlk amaç fonksiyonu (Denk. 1), uçakların planlanan bakımdan önce mümkün olduğunca kullanılmasını amaçlamaktadır. EASA yönetmeliklerine göre uçaklar belirli bir uçuş saatinden sonra bakıma alınmalıdır. Bu amaç fonksiyonu, uçakların uçuş saat limitlerini aşmadan olabildiğince fazla uçuş saatini tamamlamasını sağlamaya çalışmaktadır. Örneğin, bir uçağın 5 saat daha uçuş saati varsa ve hemen bir bakım almasına veya 4 saatlik başka bir rotaya uçmasına olanak sağlayan bir ikilemdeyse, uçakları rotayı uçurmaya zorlar.

İkinci amaç fonksiyonu (Denk. 2), uçakların kapasitelerinin en iyi şekilde kullanılmasını sağlamaya çalışmaktadır. Uçağın kapasitesi gerçekleştirilecek uçuşa olan talebi karşılamalıdır, bu kısıtlarda sağlanmaktadır. Bu amaç fonksiyonu, uçağın verimini en üst düzeye çıkarmak için uçağın, talep düzeyine en yakın kapasitede seçilmesini sağlamaktadır.

Modelde sekiz kısıt vardır. İlk kısıt (Denk. 3), uçuş planını içeren hafta boyunca bakıma girmeyen uçaklar için uçuşları, takip eden uçuşlara ve bakımı dahil eden X_{ijk}-Y_{ijk} dönüşümü uçuşlarına bağlar. Bir uçuş bir uçak tarafından gerçekleştirildiğinde, uçak gerçekleştirdiği uçuşu takip edebilecek uçuşların biriyle yoluna devam edebilmektedir. Öncül ve takip eden uçuşlar, kalkış ve iniş havaalanlarından yararlanılarak tasarlanmıştır. Uçağın son iniş yaptığı havalimanından kalkış yapması zorunludur. Uçuş takibi için başka bir kriter de iniş ve kalkış saatleridir. Takip eden uçuşun iniş saatinden 30 dakika sonra kalkması gerekir. Buna ek olarak ilk kısıt bahsedildiği gibi planlanan uçuş programı döneminde bakım alacak uçaklarla ilgili dönüşümleri sağlar. Kısıt, hem tüm uçuşlar hem de uçaklar için oluşturulmuştur. Bir uçak bakıma girdiğinde, uçağın kalan uçuş saatlerini hesaplamamak için model bu uçağın dahil olduğu uçuşların karar değişkenini değiştirmektedir. Ayrıntılı olarak: eğer bir uçağın uçuşu bakım olarak tanımlanan uçuşlardan biri ise, bu uçak bakım sonrasında bakım uçuşunu takip edebilecek uçuşlarından biri ile uçuş programına devam eder.

İkinci kısıt (Denk. 4), seçilen uçağın ilgili uçuşa olan talepten fazla bir kapasiteye sahip olmasını garantilemektedir. Burada 120 ve 150 kapasiteli 2 uçak bulunmaktadır. Uçuş talepleri her uçuş için 100 ila 150 arasında rassal olarak tanımlanmıştır. İkinci amaç fonksiyonu (Denk. 2) uçağın kapasitesi ile uçuşa olan talep arasındaki farkı en aza indirmeye çalışırken, bu kısıt talebin uçağın kapasitesini aşmasını önler. Bu kısıt sayesinde uçuş talebi göz önünde bulundurularak yolcu kapasitesi yetersiz bir uçak atanamamaktadır. Bu kısıt X_{ijk} ve Y_{ijk} karar değişkenleri yardımıyla hem bakıma girmiş hem de girmemiş uçakları kapsamaktadır.

İlk amaç fonksiyonu (Denk. 1), uçakların bakımdan önce kullanılmayan izin verilmiş uçuş saatlerini en aza indirmeye çalışmaktadır. Başka bir deyişle, ilk amaç fonksiyonu uçakları mümkün olduğunca kullanmaya çalışır. Bu nedenle model, uçakların kalan uçuş saatlerini aşmamak için bir sınırlamaya ihtiyaç duyar. Burada üçüncü kısıt (Denk. 5) bir sınırlayıcı olarak işlev görür. Uçuşun uçuş süresini (t_i) karar değişkeniyle ($Xijk$) çarpar ve uçuş programında bu uçak tarafından gerçekleştirilen her uçuşun süresini toplayarak toplam uçuş süresini hesaplar. Burada toplam uçuş saati, uçağın kalan uçuş saatlerini (r_k) aşmamalıdır. Sınırı aşmadan önce, uçak bakım altına alınmalı ve ilk kısıt içerisinde önerilen dönüşüm yapılmalıdır. Bu dönüşüm uçakların, bahse konu uçuş programı sırasında başka bir bakıma ihtiyaç duymayacağı anlamına gelmektedir. Dolayısıyla, üçüncü kısıt Y_{ijk} değişkenini içermez, çünkü model bakımdan sonra uçağın başka bir bakıma daha ihtiyaç duymayacağı bilgisi doğrultusunda bu uçakların uçuş saatlerini hesaplamayı bırakır.

Filodaki uçaklar modele göre bir kere bakım gördükten sonra, tekrar bakıma ihtiyaç duymadan haftalık uçuş programını tamamlayabilmektedir. Herhangi bir uçak bakım gördükten sonra, birinci kısıtın (Denk. 3) yardımıyla karar değişkenini Y_{ijk}'ye çevirir. Bu dönüşüm modelde uçağın haftalık uçuş programının sonuna kadar tekrar bakım gerektirmeyeceğini garanti altına alır. Karar değişkeni Y_{ijk}'ye dönüştükten sonra, önceki ve sonraki uçuşlar dördüncü kısıt (Denk. 6) yardımıyla birbirine bağlanır.

Uçuş programı belirlendiğinde, uçuşların birbirini izlediği bir sıra organize edilir. Burada, uçağın kalkış ve iniş havalimanlarının takibi yapılmamaktadır. Bunun yerine, uçuşların kalkış ve iniş saatleri, kalkış ve iniş şehirleri bilgileri kullanılarak alt setlerle tanımlanan uçuş bağlantıları kullanılır. Beşinci kısıt (Denk. 7), öncül uçuşların bağlantılarını sağlamaktadır. Bu kısıtla bir uçuşa öncül uçuş olabilecek seçenekler belirlenmekte ve bu seçeneklerden sadece bir tanesinin seçilmesi sağlanmaktadır. Kısıtın ilk bölümünde *Xijk* karar değişkeni, bakım uçuşlarının öncül uçuşlarını takip etmektedir. Bu bölüm, bakım olarak tanımlanan uçuşlardan önce hangi uçuşların yapılabileceğini belirtir. İkinci bölüm ise normal uçuşlar için aynı şekilde çalışır ve normal uçuşlar öncesinde hangi uçuşların yapılabileceğini belirler. Dolayısıyla, bir uçak, yalnızca önceden tanımlanan uçuşlardan birini yapabilir.

Altıncı kısıt (Denk. 8) ise her hangi bir uçuştan sonra yapılabilecek uçuşları tanımlar. Denklemin ilk kısmı, bakımları takip eden muhtemel uçuşları tanımlarken, ikinci kısmı ise, bakım dışındaki uçuşlarla ilgilidir.

Son kısıt (Denk. 9) ise karar değişkenlerinin 0-1 değerlerini alabileceği ile ilgilidir.

Modelin çözümünde çok amaçlı modellerin çözümü için yaygın olarak kullanılan Öncelikli Hedef Programlama yöntemi kullanılmıştır. Bu metot n adet amaç fonksiyonu olan bir modelin, amaç fonksiyonlarının önem sırasına göre sıralanması ile başlar. En yüksek öneme sahip amaç fonksiyonu dikkate alınarak, diğer amaç fonksiyonları devre dışı bırakılarak model çözülür. Bulunan amaç fonksiyonu değeri kısıt olarak eklenerek, model ikinci derecede öneme sahip amaç fonksiyonu için çözülür. Bu sayede daha yüksek önem sırasına sahip olan amaç fonksiyonunun aldığı en iyi değerin korunmasını garanti altına alınır. Süreç bu şekilde tüm amaç fonksiyonları için tekrarlanır **[13].** Bu modelde Öncelikli Hedef Programlama metodun kullanılmasının en önemli sebebi de bu temele dayanır. Uçakların bakıma kadar yasal sınırlar dahilinde uçabilecekleri en fazla saati uçmaları ve uçağın bakımlar arası uçuş süresi veriminin artırılması en önemli amaçtır. Kapasitenin verimli kullanılması ise ikinci öncelikli amaçtır.

III. BULGULAR VE TARTIŞMA

Modelin çözümü için gerekli veriler, küçük bir hava yolu şirketinin çevrimiçi yayımlanan uçuş programından alınmıştır. Bu uçuş programı 4 şehirden ve 38 uçuştan oluşan bir ağdır. Uçuş programı yeni şehir ve uçuşlar eklenerek büyütülebilir. Tablo 3 detaylı olarak uçuş programını göstermektedir. Tablo 4 ise filodaki uçakların detaylarını göstermektedir.

Tablo 3. Uçuş programı

Uçuş No	Uçuş	Muhtemel takip eden uçuşlar			Muhtemel Bakımlar
		1	2	3	
1	İS-İZ 10.20-11.20	2	8	14	
2	İZ-İS 12.00-13.00	4	7	9	
3	İS-T 12.50-14.10	5	10		
4	İS-A 14.00-15.20	6	13		
5	T-İS 14.50-16.10	7	9	11	
6	A-İS 16.00-17.20	7	9	11	
7	İS-İZ 10.20-11.20	8	14	20	
8	İZ-İS 12.00-13.00	11	12	15	
9	İS-T 12.50-14.10	10	17		
10	T-İS 14.50-16.10	11	12	15	
11	İS-A 17.30-18.50	13	18		
12	İS-İZ 19.00-20.00	14	20	24	
13	A-İS 19.20-20.40	15	16	19	
14	İZ-İS 20.40-21.40	15	16	19	*M1
15	İS-T 12.50-14.10	17	28		
16	İS-A 14.00-15.20	18	22		
17	T-İS 14.50-16.10	19	21	23	
18	A-İS 16.00-17.20	19	21	23	
19	İS-İZ 19.00-20.00	20	24	26	
20	İZ-İS 20.40-21.40	21	23	25	*M2
21	İS-A 17.10-18.30	22	34		
22	A-İS 19.10-20.30	25	27	29	
23	İS-İZ 20.10-21.10	24	26	30	
24	İZ-İS 21.50-22.50	25	27	29	*M3
25	İS-İZ 10.40-11.40	26	30	36	
26	İZ-İS 12.10-13.10	29	31	32	
27	İS-T 12.50-14.10	28	33		
28	T-İS 14.50-16.10	29	31	32	*M4
29	İS-İZ 10.20-11.20	30	36		
30	İZ-İS 12.00-13.00	32	35	37	
31	İS-T 12.50-14.10	33			
32	İS-A 14.00-15.20	34	38		
33	T-İS 16.00-17.20	35	37		*M5
34	A-İS 16.00-17.20	35	37		*M6
35	İS-İZ 9.10-10.10	36	T		
36	İZ-İS 10.40-11.40	37	T		
37	İS-A 13.00-14.20	38	T		
38	A-İS 16.00-17.20	T			

Tablo 4. Filo uçakları

Uçaklar	Kalkış Havalimanı	Kalan uçuş süresi	Uçak kapasitesi
1	İstanbul	360 saat	150
2	İstanbul	1900 saat	120

Bu bölümde model Lingo programı ile çözdürüldüğünde yapılan gözlemler özetlenmiştir. 1. amaç fonksiyonu uçakların kalan sürelerini oranlar yardımıyla tespit ederek olabildiğince fazla *Xijk* değişkenli uçuş yaptırmaya çalışmıştır. Böylece

uçakların kalan uçuş saatleri mümkün olduğunca kullanılmıştır. 3. kısıt yardımıyla uçakların bu sınırları aşmamaları ve yasal engellere takılmamaları sağlanmıştır. Uçağın bakım görmeden önce uçabileceği uçuş saatleri uçağın kalan uçuş süresini aşamayacağı için 1. uçak 14. uçuşu tamamladıktan sonra bakıma yönlendirilmiştir. İkinci uçak ise kalan uçuş saatleri yapabileceği uçuşların toplam saatinden daha fazla olduğu için bakım ihtiyacı olmadan uçuş programını tamamlamıştır. Uçuş programı Tablo 5 içerisinde gösterilmiştir.

Tablo 5. Tamamlanmış uçuş programı

	Uçuklar	
Uçuşlar	**1**	**2**
1		X 1.2.2
2		X 2.4.2
3	X 3.5.1	
4		X 4.6.2
5	X 5.7.1	
6		
7	X 7.8.1	
8	X 8.12.1	
9		X 9.10.2
10		X 10.11.2
11		X 11.13.2
12	X 12.14.1	
13		X 13.15.2
14	Y 14.16.1	
15		X 15.17.2
16	Y 16.18.1	
17		X 17.19.2
18	Y 18.23.1	
19		X 19.20.2
20		X 20.21.2
21		X 21.22.2
22		X 22.25.2
23	Y 23.24.1	
24	Y 24.27.1	
25		X 25.26.2
26		X 26.31.2
27	Y 27.28.1	
28	Y 28.29.1	
29	Y 29.30.1	
30	Y 30.32.1	
31		X 31.33.2
32	Y 2.34.1	
33		X 33.35.2
34	Y 34.T.1	
35		X 35.36.2
36		X 36.37.2
37		X 37.38.2
38		X 38.T.2

Veri setinde uçuşların büyük çoğunluğu iki uçağın da karşılayabileceği gibi 120 talepli seçilmiştir. Bu durumda düşük kapasiteli uçağın daha fazla kullanılması beklenmiştir. Burada belirli aralıklarla 150 talepli uçuşlar belirlenerek modelin 2. kısıt desteği ile bu ihtiyacı karşıladığı tespit edilmiştir. Yaklaşık yüzde 60 uçuş kapasitesi daha düşük olan ikinci uçak tarafından gerçekleştirilmiştir. Uçuş talepleri genel olarak 120 seviyesinde seyreden uçuşlarda ikinci amaç fonksiyonu sayesinde mümkün olan tüm seçeneklerde kapasite ile talep arasındaki farkı minimumda tutmak adına beklenildiği gibi düşük kapasiteli ikinci uçak atanmıştır.

Çalışma uçuşların bağlanma şekli olarak literatürdeki çalışmaların neredeyse tümünden ayrılmaktadır. Bu anlamda sadece bir çalışma ile aynı metodu kullanmıştır. Bu çalışmada da, Başdere ve Bilge **[6]** tarafından hazırlanan çalışmada olduğu gibi uçuşlar, zaman ve havalimanı kısıtlarına dahil edilmeyerek, direkt olarak alt setlerle bağlamıştır. Setler de yine zaman ve havalimanı kısıtları göz önüne alınarak belirlenmiştir. Yine literatürde birçok çalışmada maliyetin azaltılması ya da kazancın artırılması sağlanmaya çalışılarak rota belirlenmeye çalışılırken, bu çalışmada uçakların kalan sürelerinin en üst düzeyde kullanılması amaç fonksiyonu olarak ele alınmıştır. Buna ek olarak literatürde tek olacak şekilde bu amaçla birlikte ikinci amaç olarak uçak kapasiteleri ile atandıkları uçuşun talebi arasındaki farkın minimize edilmesi hedeflenmiştir.

Dinamik fiyatlandırma çalışmalarında uçuşlar için gelişen anlık talep değişimleri sonuçları etkilemektedir. Büyük hacimli olmayan filo-uçuş programı ikilileri için anlık talep değişikliklerinde maksimum kar elde etmek adına atanan uçuşların kapasitelerinin uygun olması sağlanabilir. Tam tersi şekilde, büyük bir uçağın atandığı uçuştaki anlık talep düşüşünün programın tekrar çalıştırılması sayesinde daha küçük bir uçakla karşılanması ve zararın azaltılması adına ikinci amaç fonksiyonu faydalı olacaktır. Şekil.1'de de görüleceği üzere daha az kapasiteye sahip ikinci uçak daha sık kullanılmıştır. Yüksek talep barındıran daha az uçuş olması dolayısıyla, küçük uçağın daha sık kullanılması ikinci amaç fonksiyonunun varlığı sonucunda beklenen bir durumdur.

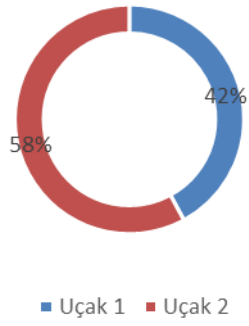

Şekil 1. Uçakların uçuş tamamlama yüzdeleri

IV. SONUÇ

Bu çalışmada, uçuş setinin atama kararlarının çözümüne ulaşmak adına öncelikle veri setleri gerçek zamanlı uçuşlardan alınarak oluşturulmuş, filo büyüklüğüne karar verilmiştir. Uçakların kapasitesi, kalkış havalimanları ve bakım şehirleri şekillendirilmiştir. Takip eden ve öncül uçuşlar belirlenerek uçuş programının nasıl ilerleyebileceğine, hangi seçeneklerle sonucun farklılaşabileceğine karar verilmiştir. Daha sonra uçuşların nasıl bağlanacağı incelenmiştir. Genel olarak ilgili literatürde şehirlerin ve zamanların bağlanması yolunun izlendiği görülmüştür. Şehir ve zaman kısıtları, kalkışlar, varışlar bu setlerin içerisinde tanımlanarak bağlantı sorunu giderilmiştir. Uçuşlar ilk amaç fonksiyonu sayesinde uçakların kullanılan yasal uçuş saati limitlerinin en yüksek düzeyde kullanılarak bakım almaları için en doğru şekilde sıralanmıştır.

Model göreceli olarak küçük bir veri seti ile çalıştırılmıştır. Uçuş sayısı 38 olan set için 2 uçakla yapılan çalışmada Lingo 9.0 programının 2.8 GHz işlemci hızına sahip bilgisayar ile çözümü bulması 0.8 saniye sürmüştür. Ancak çözümün bulunma hızı gerçek yaşamda, daha büyük boyutlu problemlerde yeterli olmayacaktır. Gelecek çalışmalarda, problemin sezgisel ya da meta-sezgisel metotlarla çözülmesi düşünülebilir.

KAYNAKLAR

[1] Barnhart, C., Bolant, N., Clarke, L.W., Johnson, E., Nemhauser G., & Shenoi R.G., (1998). Flight String Models for Aircraft Fleeting and Routing. *Transportation Science*, 32 (3), 208-220.

[2] Clausen, J., Larsen, A., Larsen, J., & Rezanova, N.J., (2010). Disruption Management in the Airline Industry–Concepts, models and methods. *Computers and Operations Research*, 37(5), 809-821.

[3] Liang, Z. & Chaovalitwongse, W.A., (2013). A Network Based Model for the Integrated Weekly Aircraft Maintenance Routing and Fleet Assignment Problem. *Transportation Science,* 47(4), 493-507.

[4] Teodorovic, D. & Stojkovic, G., (1995). Model to Reduce Airline Schedule Disturbances. *Journal of Transportation Engineering*, July/August, 324-342.

[5] Clarke, L., Johnson, E., Nemhauser, G., & Zhu, Z., (1997). The Aircraft Rotation Problem. *Annals of Operations Research*, 69(0), 33-46.

[6] Başdere, M. & Bilge, Ü., (2013). Operational Aircraft Maintenance Routing Problem with Remaining Time Consideration. *European Journal of Operational Research*, 235, 315-328.

[7] Liang, Z., Feng, Y., Zhang, X., Wu, T., & Chaovalitwongse, A., (2015). Robust Weekly Aircraft Maintenance Routing Problem and the Extension to the Tail Assignment Problem. *Transportation Research Part B*, 78, 238–259.

[8] Orhan, I., Kapanoğlu, M., & Karakoç, T.H., (2011). Concurrent Aircratf Routing and Maintenance Scheduling. *Journal of Aeronautics and Space Technologies*, 5(1), 73-79.

[9] Diaz-Ramirez, J., Huertas, J.I., & Trigos, F., (2013). Simultaneous Schedule Design and Routing with Maintenance Constraints for Single Fleet Airlines. *International Journal of Engineering and Applied Sciences*, 2(2), 23-35.

[10] Lapp, M. & Cohn, A., (2011). Modifying Lines-of-Flight in the Planning Process for Improved Maintenance Robustness. *Computers and Operations Research*, 37, 2051-2062.

[11] Afsar, H.M., Espinouse, M.-L., & Penz, Z., (2009). Building Flight Planning for an Airline Company Under Maintenance Consideration. *Journal of Quality in Maintenance Engineering*, 15(4), 430-443.

[12] El Moudani, W. & Mora-Camino, F., (2000). A Dynamic Approach for Aircraft Assignment and Maintenance Scheduling by Airlines. *Journal of Air Transport Management*, 6, 233-237.

[13] Taha, H.A., (2002). Operations Research: An Introduction, 7st Edition. Macmillan Publishing Company, US.

Int. J. Adv. Eng. Pure Sci. 2019, 4: 280-285
DOI: 10.7240/jeps.470175

RESEARCH ARTICLE / ARAŞTIRMA MAKALESİ

PV Panelinin Altına Serbest Olarak Yerleştirilen Siyah Emici Plakanın Termal Kapasitesinin Belirlenmesi

Determination of Thermal Capacity of Black Absorber Plate that Freely Placed to Beneath of the PV Panel

Mustafa ATMACA[1], İmdat Zafer PEKTEMİR[2]

[1]Marmara Üniversitesi, Teknoloji Fakültesi, Makine Mühendisliği Bölümü, 34722, İstanbul, Türkiye

[2]Marmara Üniversitesi, Fen Bilimleri Enstitüsü, 34722, İstanbul, Türkiye

Öz

Fotovoltaik termal sistemler, aynı yüzeyden hem termal hem elektrik enerjisi kazanmak için oldukça popülerdir. Bu çalışmada, PV panelin altına yerleştirilmiş siyah boyalı absorber plakanın ısı kazancı deneysel olarak araştırılmıştır. Bu amaçla bakır borulu bir ısı değiştirici dizayn edilmiştir. Ayrıca siyah boyalı bir alüminyum emici plaka dizayn edilerek absorber ve ısı değiştirici ısıl iletken bir yapıştırıcı sayesinde birleştirilmiştir. En sonunda absorber, PV panelin arkasına yerleştirilmiş ve ısı yalıtım malzemesi ile yalıtılmıştır. Ayrıca sistem, bir su ısıtma sistemi ile birleştirilmiş olup absorber plakanın ısı kazancı farklı iklim koşulları için araştırılmıştır. Araştırma, farklı güneş ışınımı, çevre sıcaklığı ve rüzgar hızları için yürütülmüştür.Sonuçlar, soğutmadan önce, absorber plaka sıcaklığının 70-80 °C seviyelerine ulaştığını göstermiştir. Ayrıca absorberin iyi oranda termal güneş enerjisi kazandığı görülmüştür. Bu enerji kolaylıkla su ısıtma sistemlerinde kullanılabilir. Ayrıca, su ısıtma sistemi sayesinde absorber sıcaklığının optimum değerlere düşürülebileceği görülmüştür.

Anahtar Kelimeler: Fotovoltaik, Emici levha, Termal sistemler, Güneş ışınımı

Abstract

Photovoltaic – thermal systems are very popular for gaining both thermal and electrical energy from same surface. In this study, thermal gain of black colored absorber plate that placed at beneath of PV panel was investigated experimentally. For this purpose, it was designed that copper tubes heat exchanger. Also it was designed that a black painted aluminum absorber plate. Absorber and heat exchanger were joined by means of thermally conductive adhesive. Finally, absorber was placed to beneath of the PV panel and it was insulated using heat insulation material. Also absorber system was integrated with a water heating system. Thermal gain of absorber plate was investigated for different climatic conditions. Research was conducted for different solar irradiance, ambient temperature, wind speed, relative humidity values.Results show that absorber temperature reaches up to 70 – 80 °C before the cooling. Also it has been seen that absorber, gained well amount solar thermal energy. This energy can be used for water heating systems easily. Also it has been seen that absorber temperature can be decrease to optimum value by means of water heating system.

Keywords: Photovoltaic, Absorber plate, Thermal systems, Solar irradiance

I. GİRİŞ

Enerji, hayatımızın önemli parçalarından biri fakat enerji kaynakları sınırlıdır. Yenilenebilir enerji kaynaklarının daha fazla kullanımı bu sorun için bir çözüm olabilir. Başlıca yenilenebilir enerji kaynağı olan güneş enerjisinin uygulamaları iki ana bölümden oluşmaktadır. Birincisi PV paneller sayesinde elektrik üretimidir. Diğer türü ise, termal kolektörler sayesinde termal enerji üretimidir. Ayrıca bu alanda, fotovoltaik-termal (PV/ T) sistemler vardır. Bu sistemler, fotovoltaik panel ve ona entegre edilmiş ısı değiştirici ünitelerden oluşur.

Sorumlu yazar/Corresponding Author: Mustafa ATMACA, **Tel:** +902163365770/1315, **e-posta:** matmaca@marmara.edu.tr,
Gönderilme/Submitted: 13.10.2018, **Düzenleme/Revised:** 26.09.2019, **Kabul/Accepted:** 16.10.2019

Güneş pilleri yüksek güneş radyasyonuna maruz kaldığında daha fazla elektrik üretir, sıcaklığı arttığında verimi düşer. Sonuçlar, bir hibrit PV/T modülün elektrik üretiminin, artan panel sıcaklığı ile azaldığını göstermektedir [1].

İşletme sıcaklığı, fotovoltaik süreçlerde önemli bir yere sahiptir [2]. PV panellerin elektriksel verimi çalışma sıcaklığına bağlıdır, performansın iyileştirilebilmesi için efektif soğutma gerekir [3]. Rawat ve arkadaşları [4] bakır absorber plaka kullanılansu bazlı bir PV/T sistem üzerinde çalışmışlar ve PV/T sistemin elektriksel ve termal performansının PV modül performansına göre daha fazla olduğunu tespit etmişlerdir.İşte fotovoltaik-termal (PV/T) sistemler, artan PV panel sıcaklığını düşürmesinin yanısıra, farklı şekillerde enerji dönüşümlerine olanak sağlarlar. Bu sistemlerin başlıcaları, hava esaslı ve su esaslı sistemlerdir.

Soni ve arkadaşları [5] su bazlı bir PV/T sistem üzerinde çalışmışlar ve soğutma yapılmadığında maksimum PV panel sıcaklığını 79.31 °C bulmuşlar, optimum debi değeriyle soğutma yapıldığında ise, PV panel sıcaklığının 47.13 °C değerine düştüğünü tespit etmişlerdir.

Bu çalışmada, bir su esaslı PV/ T sisteme entegre edilen siyah emici yüzeyin ısıl kapasitesi belirlenmeye çalışılmıştır. Bu ısıl kapasite, güneş radyasyonu ile birlikte diğer meteorolojik değişkenlere doğrudan bağlıdır. Meteorolojik değişkenlere bağlı olarak, PV panellerin sıcaklığını belirlemek için çeşitli çalışmalar yapılmıştır. Örneğin, Muzathik [6], rüzgar hızının da hesaba katıldığı aşağıdaki formülasyonu ortaya koymuştur.

$$T_{modul}\ (^{o}C)=0,943xT_{amb.}+0,0195xIrridance-1,528xWindspeed+0,3529 \quad (1)$$

Bu formülasyonda, üç önemli meteorolojik parametre olan, hava sıcaklığı, güneş radyasyonu ve rüzgar hızına bağlı olarak modül sıcaklığının değişimi incelenmiştir.

Meteorolojik parametrelere bağlı olarak, artan panel sıcaklığının azaltılması ve kazanılan enerjinin su ısıtma sistemlerinde kullanımı ile ilgili çeşitli çalışmalar yapılmıştır.

Kalogirou ve Tripanagustopoulos [7] yaptıkları çalışmada, tipik bir termal güneş kolektörüne entegre ettikleri amorf silikon ve polikristal güneş pilleri ile, doğal dolaşımlı ve cebri dolaşımlı su ısıtma üniteleri kullanarak, sistemlerin elektriksel ve termal enerji kazançlarının belirlenmesi üzerine çalışmışlardır. Çalışma sonuçlarına göre; cebri dolaşımlı aktif sistem performansının doğal dolaşımlı sisteme göre oldukça yüksek olduğu görülmüştür. Güneş enerjisi kazancı, konuma bağlı olarak %60 ve %87 arasında değişmektedir. Hibrid olmayan PV sistem %38 civarında fazla elektrik üretmesine rağmen bu sistem, binaların sıcak su ihtiyacını yüksek oranda karşılayabilme özelliğine sahiptir.

Rekha ve arkadaşları [8] yaptıkları, çalışmada, düzlemsel güneş kolektörü ile iyileştirilmiş bir PV/T sistemin, ısıl, elektriksel ve ekserji performansını sayısal olarak araştırmışlardır. Çalışma sonucunda, ortalama toplam elektriksel, enerji ve ekserji verimleri sırasıyla; 11%, 63% ve 15% olarak belirlenmiştir. Bir başka çalışmada Hossain ve arkadaşları [9] paralel serpantin borulu bir su bazlı PV/T sistem üzerinde çalışmışlar ve sistemin maksimum termal verimini 76.58% bulmuşlardır.

Bu çalışmada, PV panelin arkasına yerleştirilen siyah boyalı absorber plakanın termal kazanımı belirlenmeye çalışılmıştır. Deneylerin yürütüldüğü atmosferik koşulların değişimi de şekillere aktarılarak, bu konuda yapılacak çalışmalara ışık tutulmaya çalışılmıştır.

II. MATERYAL VE METOT

Bu çalışmada, siyah boyalı alüminyum plaka ile bakır ısı değiştirici, 0.88 W/ mK ısıl iletkenlik değerine sahip ısıl iletken bir yapıştırıcı ile birleştirilerek bir absorber ünite oluşturulmuştur. Siyah boyalı alüminyum plaka, yapıştırıcının daha düzgün yayılabilmesi için, şekil 1' de görüldüğü gibi üç parça halinde su serpantini ile birleştirilmiştir. Absorber ünite, bir monokristal PV panelin altına serbest olarak yerleştirilmiştir (Şekil 2). Sistem, 33˚ eğimli bir platform üzerine sabitlenmiş ve 50 mm kalınlığında ve 0.035 W/mK ısı iletkenlik değerine sahip, taş yünü esaslı yalıtım malzemesi ile yalıtılmıştır. Tablo 1'de kullanılan malzemeler ve özellikleri görülmektedir.

Tablo 1. Deney seti temel parça özellikleri

No	Adı	Özellikler
1	PV panel	TPSM6U Monocristalline 200W, V_{oc}: 45.4 V,I_{sc}: 5.77, 808x1580mm
2	Absorber plaka	Alüminyum, 0.4 mm, siyah boyalı, 808x1580mm
3	Su serpantini	Bakır (λ: 394 W/ mK) kolektör çapı: 32mm, boru çapı: 10mm
4	Boyler	Isı değiştirici serpantinli, 100 lt
5	Pompa	Frekans konvertörlü

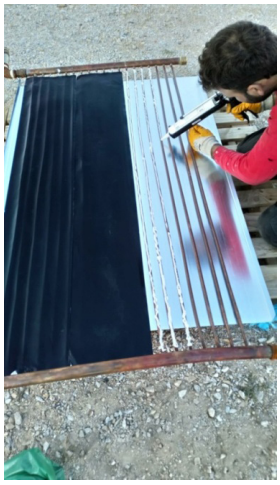

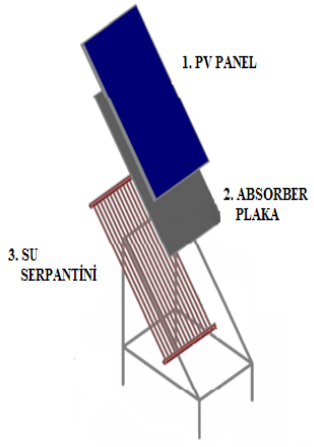

Şekil 1. Absorber montajı **Şekil 2.** Deney seti montaj şeması

Absorber ünite, şekil 3'de görüldüğü gibi su ısıtma devresi ile irtibatlandırılmıştır. Su ısıtma devresi, boyler, pompa, vanalar ve boru hattından oluşmaktadır. Ayrıca bir genleşme deposu, boyler serpantin seviyesini aşacak şekilde yerleştirilmiştir (Şekil 3).Tablo 1'de de belirtildiği gibi serpantin malzemesi olarak ısıl iletkenliği 394 W/mK olan bakır borular kullanılmıştır. Dağıtıcı borular 10 mm , alt ve üst kolektörler ise 32 mm çapında seçilmiştir. Absorber plaka ise; siyah boyalı alüminyumdan imal edilmiştir.

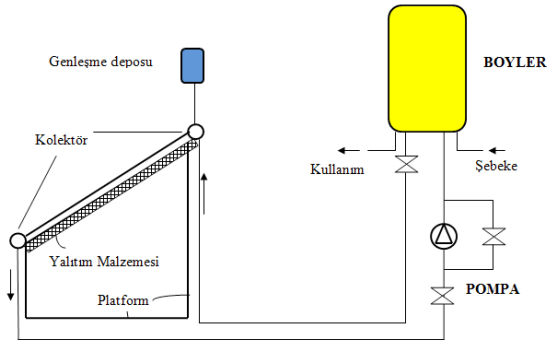

Şekil 3. Su ısıtma devresi şeması

Isı değiştirici akışkan olarak, donma riskine karşı, 1/3 oranında etilen glikol (antifiriz) içeren su – antifiriz karışımı kullanılmıştır. Bu orandaki karışımın özgül ısısı ve yoğunluğu, Duffie ve Beckman [10] tarafından yapılan çalışma baz alınarak, 20 – 40 ˚C için yaklaşık; C_p = 3700 j/ kg˚C= 0.885 kcal/ kg˚C, ρ= 1050 kg/m³ olarak alınmıştır.

Tablo 2'de veri alma cihazlarının özellikleri ve Şekil 4'de bilgi algılama sistemi ve sensör yerleşimi görülmektedir. Veri alma sisteminde; veri alma cihazlarından alınan veriler, analog 4-20 mA, Pt 100, mV okuma kabiliyetine sahip endüstriyel modüllere aktarılmaktadır. Modüller bu verileri, okunarak bilgisayar diline çevrilmesi için, RS-485 Modbus RTU protokolüne çevirmektedir. Bilgisayara aktarılan veriler ise bir program vasıtasıyla raporlanıp değerlendirilmektedir.

Tablo 2. Veri alma cihaz özellikleri

No	Adı	Yerleştirilme şekli	Özellikler
1	Sıcaklık sensörü	Su serpantini giriş, çıkışına ve absorber plakanın merkez noktasına yerleştirildi.	Pt 100
3	Piranometre	PV açısıyla aynı olacak şekilde 33˚ eğimli olarak yerleştirildi.	EKO MS – 410 Hassasiyet 11.78 µV/Wm^{-2},0-2000 W/m²
4	Dış hava nem ve sıcaklık sensörü	Güneş ışınlarına doğrudan maruz kalmayacak şekilde, yerden 1 m yukarıya yerleştirildi.	Sıcaklık ve nem için iki farklı analog çıkışa sahip.
5	Rüzgar hız sensörü	PV panelin üst kenarı seviyesine yerleştirildi.	Encoder pulse' leri 4-20 mA akıma çevrilmektedir.

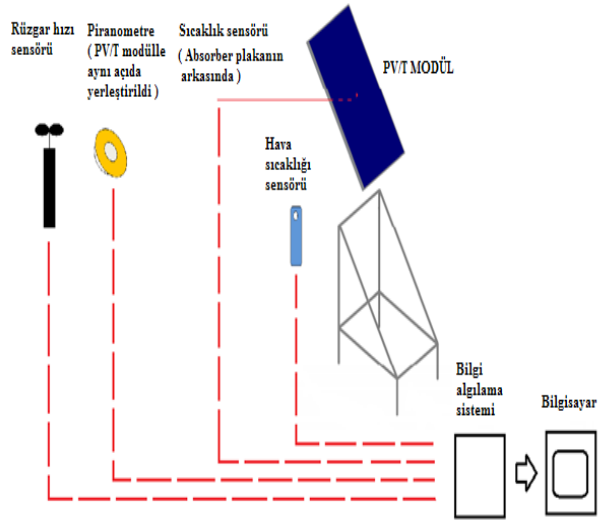

Şekil 4. Bilgi algılama sistemi ve sensör yerleşimi [11,12]

III. BULGULAR

Çalışmalar, 37˚N enlemi ile 32˚E meridyenindeki Konya İli'nde, Şubat ve Mart ayları içerisinde farklı meteorolojik parametrelere sahip günlerde yürütülmüştür. Ölçümler, soğutmadan önce absorber sıcaklığının oldukça yüksek olduğunu ve soğutma işlemiyle sıcaklığının optimum değerlere

düşürülebildiğini göstermektedir (Şekil 5). Tablo 3'den anlaşılacağı üzere, ele alınan her üç günün, termal dönüşüm oranı ortalaması yaklaşık % 50 seviyesinde olmuştur. İletim boruları yalıtımsız olduğu için iletim hattından havaya ısı transferi oldukça yüksek seviyededir. Bu boruların yalıtılması ile birlikte boyler toplam ısı kazancı artacak, iletim hattından havaya olan ısı transferi azalacaktır.

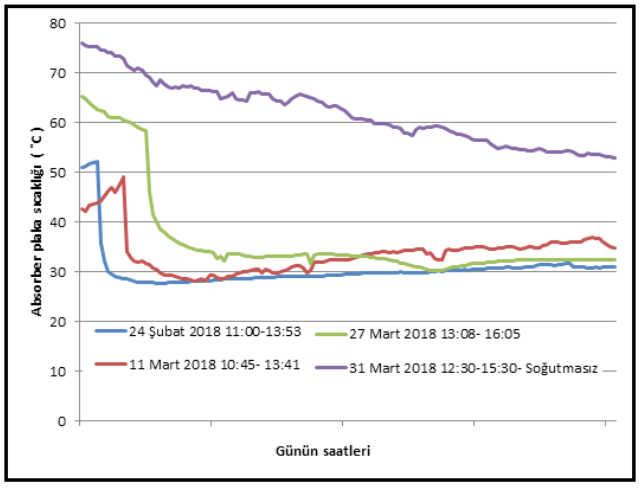

Şekil 5. Soğutmasız gün ve soğutma yapılan günlerdeki absorber plaka sıcaklıklarının karşılaştırılması.

Boyler toplam ısı kazancı: $Q_{boy} = m\ C_p\ (T_s - T_i)$ (2)

Boyler ısı kazancı $q_{boy} = ((Q_{boy}/\text{toplam saat})/860)1000$ (3)

Ortalama boru hattı sıcaklığı: $T_{ort} = (T_g + T_ç) / 2$ (4)

Boru hattından havaya ısı kaybı $q_{b-h} = 2\pi L\ \lambda\ (T_{ort} - T_h) / \ln(r_2/r_1)$ (5)

(Boru hattı özellikleri: L= 20m, Ø32x5,4 mm PP-R 80 PP3 boru λ= 0.24 W/mK , boru hattı yalıtılmamıştır.)

Absorberden çekilen ısı: $q_t = q_{boy} + q_{b-h}$ (6)

Termal dönüşüm oranı: $\eta_{th} = q/ (I x A_p)$ (7)

Tablo 3. Farklı günlere ait termal değerlerin karşılaştırılması

Parametre	**24 Şubat 2018 11:30 – 14:30**	**11 Mart 2018 11:00-14:00**	**27 Mart 2018 13:40-18:40**
Ortalama absorber plaka Sıcaklığı (ºC)	29.97	33.03	31.19
Ortalama soğutma suyu giriş Sıcaklığı (ºC)	22.60	22.58	24.79
Ortalama soğutma suyu çıkış sıcaklığı (ºC)	23.51	24.33	28.98
Ortalama hava sıcaklığı (˚C)	16.03	17.13	23.73
Ortalama ışınım değeri (W/m²)	1142.03	1152.09	581.93
Ortalama rüzgar hızı (m/s)	2.66	1.41	3.21
Boyler ilk sıcaklığı (˚C)	11.80	18.80	17.60
Boyler son sıcaklığı (˚C)	19.80	24.10	23.90
Boyler toplam ısı kazancı (kcal)	708	530	630
Boyler ısı kazancı (W)	274.42	205.43	146.51
Boru hattından havaya ısı kaybı (W)	514.32	463.43	230.98
Absorberden çekilen ısı (W)	788.74	668.86	377.49
Termal dönüşüm oranı (%)	54.38	45.71	51.07

Şekil 6 da; 24 Şubat 2018 , Şekil 7 de; 11 Mart 2018 ve Şekil 8 de; 27 Mart 2018 gününe ait absorber plaka termal kazancını etkileyen, termal ve meteorolojik parametrelerin değişimleri görülmektedir. Bu şekillerde sağda yer alan birincil düşey eksende W/m^2cinsinden güneş ışınımı, solda yer alan ikincil düşey eksende ise, °C cinsinden sıcaklık skalası yer almaktadır. Yatay eksen ise, gün içinde deneysel verilerin alındığı saatleri göstermektedir. 24 Şubat ve 11 Mart günleri ele alınan saatler, güneş ışınımının en yüksek olduğu öğlen saatleri iken, 27 Mart günü öğleden sonrayı da tam kapsayacak şekilde seçilmiştir. 27 Mart günü, ortalama rüzgar hızı ve ortalama hava sıcaklığı diğer günlerden fazladır. Her üç durumda da, absorber plakanın ısı kazanımının ortalama ışınım değerine oranı, 50 % seviyelerine yakın olarak gerçekleşmiştir. 11 Mart ve 27 Mart günleri gün boyunca, bulutluluk nedeniyle güneş ışınımında dalgalanmalar oluşmuştur(Şekil 7 ve 8). 24 Şubat günü ise 13:30 dan sonra kısmen ışınım dalgalanmaları oluşmuştur (Şekil 6). Her üç durumda da meteorolojik parametreler değişkenlikler göstermekle birlikte, absorber plaka sıcaklıklarının 30-35˚C civarında olduğu görülmektedir (Şekil 6-8). 50 mm yalıtım uygulanmış olması, absorber sıcaklığını daha kararlı hale getirmiştir. Kesin sayısal sonuç elde etmekten ziyade, montaj ve uygulama tekniği açısından, bu alanda yapılacak çalışmalara ışık tutmak amaçlandığından, belirsizlik analizi yapılmasına gerek duyulmamıştır.

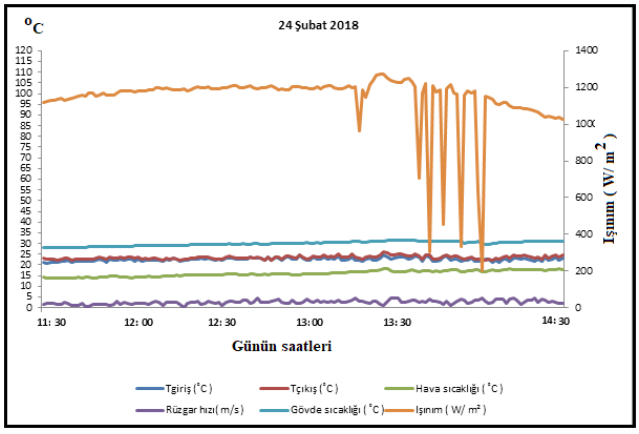

Şekil 6. 24 Şubat 2018 11:30 – 14:30 arasında elde edilen değerler.

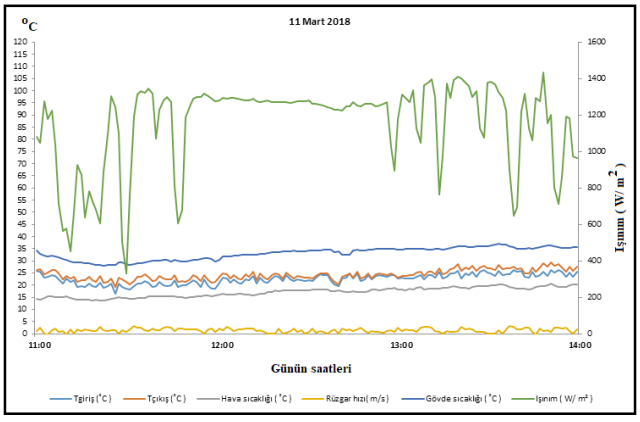

Şekil 7. 11 Mart 2018 11:00 – 14:00 arasında elde edilen değerler.

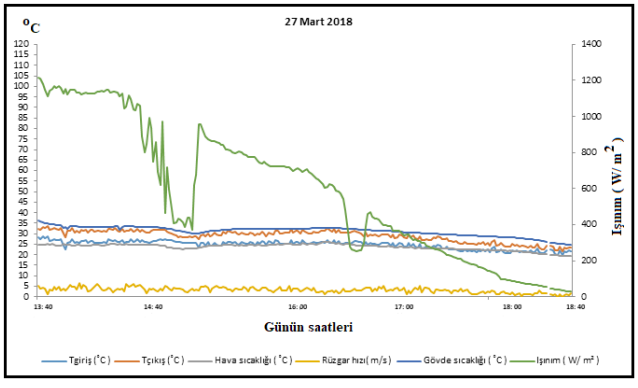

Şekil 8. 27 Mart 2018 13:40 – 18:40 arasında elde edilen değerler.

IV. SONUÇLAR

Yapılan çalışma, PV panelin arkasına serbest olarak yerleştirilen siyah boyalı plakanın oldukça yüksek sıcaklıklara ulaştığını ve PV/T sistemlerde kolaylıkla kullanılabileceğini göstermektedir. Uygulanan hesap metoduna göre, absorber plaka ısı kazanımı, incelenen her üç günün ortalaması alınırsa 50% olarak gerçekleşmiştir. Soğutma işlemi ile, sıcaklık optimum PV çalışma sıcaklığı seviyelerine düşürülebilir ve kazanılan termal enerji su ısıtma sistemlerinde kullanılabilir. Bu çalışmada, sadece termal kazanım incelenmekle birlikte, bu şekilde yapılacak bir uygulama ile, aynı alandan hem elektriksel hem de termal enerji kazanılacağından, toplam verim oldukça yüksek olacaktır. Sıcak su iletim hatlarına, boyler ısı transfer oranının yetersiz kalabileceği düşünülerek ilk etapta yalıtım yapılmamıştır. Yalıtım yapılmış olsaydı, boylerden kullanım suyuna ısı transferi artacağından boyler suyu, kullanım için optimum değerlere çıkarılabilecekti. Sonuçlar, bu şekilde bir uygulama ile oldukça iyi termal kazanım elde edilebileceğini göstermektedir.

TERMİNOLOJİ

T_m Ortalama absorber plaka sıcaklığı (˚C)

T_g Ortalama soğutma suyu giriş sıcaklığı (˚C)

$T_ç$ Ortalama soğutma suyu çıkış sıcaklığı (˚C)

T_{ort}: Ortalama boru hattı sıcaklığı (˚C)

T_h Ortalama hava sıcaklığı (˚C)

I Ortalama ışınım değeri (W/m²)

V_r Ortalama rüzgar hızı (m/s)

T_i Boyler ilk sıcaklığı (˚C)

T_s Boyler son sıcaklığı (˚C)

Q_{boy} Boyler toplam ısı kazancı (kcal)

q_{boy} Boyler ısı kazancı (W)

q_{b-h} Boru hattından havaya ısı kaybı (W)

q_t Absorberden çekilen ısı (W)

A_p Absorber alanı (PV panel alanı) (m²)

η_{th} Termal dönüşüm oranı (%)

C_p Sabit basınçta özgül ısı (kcal/ kg ˚C)

ρ Yoğunluk (kg/m³)

m Boyler kütlesi (kg)

λ Isı iletkenlik katsayısı (W/mK)

r_2 Boru dış yarıçapı (m)

r_1 Boru iç yarıçapı (m)

TEŞEKKÜR

Bu çalışmayı, 2017 FEN-C-DRP-070.317.0111 nolu proje ile destekleyen, Marmara Üniversitesi Bilimsel Araştırma Projeleri Birimi' ne ve proje tesisatı için yer sağlayan, Konya İnnopark yönetimine teşekkür ederiz.

KAYNAKLAR

[1] Sirinivas, M., Jayaraj, S., (2013). Investigation on the performans of double pass hybrid – type (PV/T) solar air heater. *International Journal of Energy and Environment*, 4, 687-698.

[2] Dubey S, Sarvaiya J.N, Seshadri B., (2013). Temperature dependent photovoltaic (PV) efficiency and its effect on PV production in The World – a review, *Energy Procedia*, 33:311-321

[3] Alizadeh H, Ghasempour R, Shafii M.B, Ahmadi M.H, Yan W.M, Nazari M.A., (2018). Numerical simulation of PV cooling by using single turn pulsating heat pipe, *International Journal of Heat and Mass Transfer*, 127: 203-208.

[4] Rawat P, Debbarma M, Mehrotra S, Sudhakar K., (2014). Design, Development and Experimental Investigation of Solar Photovoltaic/ Thermal (PV/T) Water Collector System, *International Journal of Science, Environment and Technology*, 3,3, 1173-1183.

[5] Sanjeev J, Soni M.S, Gakkhar N., (2016). Parametric modeling and simulation of photovoltaic panels with earth water heat exchanger cooling, *Geothermal Energy*, 4:10

[6] Muzathik, A.M. (2014). Photovoltaic modules operating temperature estimation using a simple correlation. *International Journal of Energy Engineering*, 4,151-158.

[7] Kalogirou, S.A. and Tripanagnostopoulos, Y. (2006). Hybrid PV/T solar systems for domestic hot water and electricity production. *Energy Conversion &Management* 47, 3368-3382.

[8] Rekha, L. Vijayalakshmi, M.M. and Natarajan, E. (2013). Photovoltaic thermal hybrid solar system for residental applications. *International Journal of Research in Engineering and Technology*, 2,10,277-283.

[9] Hossain M.S, Pandey A.K, Selvaraj J, Rahim N.A, Rivai A, Tyagi V.V., (2019). Thermal performance analysis of parallel serpentine flow based photovoltaic/thermal (PV/T) system under composite climate of Malaysia, *Applied Thermal Engineering*, 153, 861-871.

[10] Duffie, J.A. and Beckman, W.A. (1980). *Solar engineering of thermal processes*. J. Wiley&Sons,

[11] Atmaca M, Pektemir I.Z and Yılmaz E., (2018).Investigation of possibilities obtain heating, hot water and electricity from same solar panel by means of a new design called "Solenam" (Solar Energy Absorber Machine) 432 *3.International Multidisciplinary Studies Congress Kiev*, Ukrain,, pp 156-166.

[12] Atmaca M and Pektemir I.Z., (2019). An Investigation on the Effect of the Total Efficiency of Water and Air Used Together as aWorking Fluid in the Photovoltaic Thermal Systems, *Processes*,7,516, pp 1-19

Int. J. Adv. Eng. Pure Sci. 2019, 4: 286-294
DOI: 10.7240/jeps.492429

RESEARCH ARTICLE / ARAŞTIRMA MAKALESİ

Thermoeconomic Performance Analysis of Steam Boilers of a Power Plant Operating with Various Fuels

Çeşitli Yakıtlarla Çalışan Bir Santralin Buhar Kazanlarının Termoekonomik Performans Analizi

Mehmet Selçuk MERT[1]

[1] *Yalova University, Energy Systems Engineering Department, 77200, Yalova, Turkey*

Abstract

Energy consumption is one of the most concerned topics of the industry, and the cost of energy represents a large proportion of operating expenditure for energy-intensive sectors. In the analysis and design of industrial processes, mainly thermodynamics is often used with economic principles to obtain the optimum design for energy-efficient systems. The performance of the system can be analyzed via applying the conservation principles of energy that is defined by the first law of thermodynamics. However, only regarding the conservation of energy is not sufficient to determine the real performance of the system. At this point, an exergy analysis is done to predict the useful part of the energy, also to provide the magnitudes and places of the irreversibilities and losses within the system. Moreover, the thermoeconomic analysis is done for providing useful information to design and operate a cost-effective system. In this study, thermoeconomic analysis of the steam boilers in a power plant was performed. The simulations of the steam boilers were done by using the Aspen HYSYS simulation software. The mass, energy and cost balance equations were obtained for the boilers to determine the effect of various fuels on the process economics.

Keywords: Energy, Exergy, Thermoeconomic Analysis, Steam Boiler, Simulation.

Öz

Enerji tüketimi, endüstrinin en önemli konularından biridir ve enerji maliyeti, enerji yoğun sektörler için işletme giderlerinin büyük bir bölümünü oluşturur. Endüstriyel proseslerin analizinde ve tasarımında, enerji verimli bir sistem için en uygun tasarımı elde etmek üzere temel olarak termodinamik ve ekonomik prensipler birlikte kullanılır. Sistemin performansı, termodinamiğin birinci yasası tarafından tanımlanan enerji korunumu prensipleri uygulanarak analiz edilebilir. Ancak, sadece enerji korunumu prensibi sistemin gerçek performansını belirlemek için yeterli değildir. Bu noktada, enerjinin yararlı kısmının belirlenmesi için ekserji analizi yapılır, ayrıca sistem içindeki tersinmezliklerin ve kayıpların büyüklüklerini ve yerleri de belirlenir. Buna ilaveten, maliyet-etkin bir sistem tasarlamak ve işletmek üzere faydalı bilgi sağlamak için termoekonomik analiz yapılır. Bu çalışmada, bir santralin buhar kazanlarının termoekonomik analizi gerçekleştirilmiştir. Buhar kazanlarının simülasyonları Aspen HYSYS simülasyon yazılımı kullanılarak yapılmıştır. Kazanlar için kütle, enerji ve maliyet dengesi denklemleri çeşitli yakıtların proses ekonomisi üzerindeki etkisini belirlemek üzere elde edilmiştir.

Anahtar Kelimeler: Enerji, Ekserji, Termoekonomik Analiz, Buhar Kazanı, Simülasyon.

1. INTRODUCTION

The basis of conservation of energy called as the first law of thermodynamics, defines that energy cannot be created or eliminated in a system; it can only transform its form [1]. Moreover, the second law of thermodynamics introduces the difference in quality between various forms of energy, and also states that all irreversible processes progress to maximize entropy; that is, to become more randomized and to transform energy into a less useful form [2].

Sorumlu yazar/Corresponding Author: Mehmet Selçuk MERT, **Tel:** +902268155371, **e-posta:** msmert@yalova.edu.tr,
Gönderilme/Submitted: 11.12.2018, **Düzenleme/Revised:** 26.09.2019, **Kabul/Accepted:** 16.10.2019

Unlike energy, exergy or the available part of energy is not conserved in actual processes. Exergy is explained as the maximum amount of work that can be obtained by a system or a flow of matter or energy as it approaches into balance with a reference environment, and it is always expended or eliminated throughout a real process in proportion to the entropy generation because of the irreversibilities related with that process [3]. Exergy analysis is a practical method for system performance assessment and improvement since it enables accurate magnitudes of the losses to be identified.

In literature, many studies related to energy conversion and storage systems were reported by researchers for various applications. Sari and Kaygusuz [4] studied energy and exergy evaluations of energy storage systems. Ozturk performed an exergy analysis of biological energy conversion [5]. Mert et al. investigated a chemical heat pump system to progress the low level thermal energy to upper levels [6]. Tsatsaronis and Cziesla summarized the definitions and fundamentals of thermoeconomics [7]. A brief summary of exergy based economic-analysis approaches for analyzing thermal processes were done by Dincer and Rosen [8]. A systematic methodology for describing and calculating exergetic efficiencies and exergy related costs in thermal processes is offered by Lazzaretto and Tsatsaronis [9]. Atmaca carried out exergy analysis of a cogeneration system including steam and gas turbines [10]. Gümüş and Atmaca investigated the exergy analyses of a compression ignition engine using diesel and compressed natural gas as fuels [11]. Thermoeconomic evaluation of a geothermal power plant was studied by Yildirim and Ozgener [12]. Kwak et al. have done the exergoeconomic analysis for a 500 MW combined cycle plant [13]. Sahoo performed the exergoeconomic analysis and optimization of a cogeneration system using evolutionary programming [14]. El-Emam and Dincer performed the thermodynamic and economic analyses of a geothermal regenerative organic Rankine cycle based energy and exergy concepts [15]. Pellegrini et al. have done a comparative thermoeconomic study of supercritical steam cycles and biomass integrated gasification combined cycles for sugarcane mills [16]. The exergetic and economic evaluations of an iron and steel factory were done by Mert et al. [17]. A detailed thermoeconomic cost analyzes of a 600 MW oxy-combustion coal-fired power plant were studied by Xiong et al [18]. Exergoeconomic comparison of absorption refrigeration systems have done by Farshi et al. [19]. Gungor et al. performed exergoeconomic analysis of a gas engine driven heat pump drier and food drying process [20]. Ozgeners presented exergy efficiencies and exergoeconomic parameters of geothermal district heating systems [21]. The optimization of integrated heat, mass and pressure exchange network using exergoeconomic method was studied by Dong et al. [22].

In this work, thermoeconomic analysis of steam boilers with steam production capacities of 80 ton/h and 100 ton/h in a power plant in Turkey was studied. The mass, energy, exergy and cost balance equations were obtained for steam boilers, and their simulation was done by using the Aspen HYSYS Simulation Software to investigate the effect of fuel types on the process economics. Thus, the examinations of the steam boilers, which have relatively large capacity, were carried out by using exergy and thermoeconomics methods in order to determine the place of thermodynamic irreversibilities and the feasible improvements.

II. EXERGY ANALYSIS

Exergy analysis is a functional tool for constructing, assessing and improving energy conversion systems. Exergy of a system in a given state can be described as the maximum work that can be obtained through interaction of the system with the reference environment as it reaches chemical, mechanical and thermal equilibrium [23]. Here, the reference environment is considered to be so large, that its parameters are not influenced by interaction with the system under consideration [24].

The total exergy of a system has been composed of four components when the other energy effects were neglected [7,8]:

$$\dot{\Xi} = \dot{\Xi}^{ph} + \dot{\Xi}^{ch} + \dot{\Xi}^{pt} + \dot{\Xi}^{kn} \tag{1}$$

$\dot{\Xi}^{ph}$, $\dot{\Xi}^{ch}$, $\dot{\Xi}^{pt}$ and $\dot{\Xi}^{kn}$ denotes the physical, chemical, potential and kinetic exergy components, respectively. Kinetic and potential exergies are neglected in the exergy analysis of this study. The reason for this is the variations of velocity and elevations are insignificant and do not result in a substantial change in exergy [25].

Physical exergy of a system or a stream is the available part of the energy of that system when the system delivered to initial to environmental states via taking only a physical process.

$$\dot{\Xi}^{ph} = \dot{m}\left[(h - h_0) - T_0(s - s_0)\right] \tag{2}$$

The chemical exergy of a stream can be explained as the maximum work that can be achieved by taking the stream to compositional equilibrium with the environment:

$$\dot{\Xi}^{ch} = \dot{m}\left(\sum y_i \bar{e}^{ch} + RT_0 \sum y_i \ln y_i\right) \tag{3}$$

The place, amount and cause of the thermodynamic inefficiencies in a thermal system could be determined by an exergy analysis [7]. The general exergy balance equation can be written for the k^{th} component of a system, as follows:

$$\dot{\Xi}_{F,k} = \dot{\Xi}_{P,k} + \dot{\Xi}_{L,k} + \dot{\Xi}_{D,k} \tag{4}$$

Here the F, P, L, and D denote the fuel, product, loss and destruction, respectively. The exergy of fuel is the exergy entering the system, and the exergy of product is the exergy of exiting

stream or work. Exergy loss is the thermodynamic loss due to the exergy transfer to the surroundings. Exergy destruction is the loss caused by the irreversibilities within the system limits, and when the limits are assumed as the reference temperature T_0, the exergy loss is zero, and the thermodynamic inefficiencies composed of solely of exergy destruction.

Exergy loss and exergy destruction can be written as follows, respectively:

$$X_{L,k} = Q_k \cdot (1 - T_o / T) \quad (5)$$

$$X_{D,k} = T_0 S_{gen,k} \quad (6)$$

The exergetic efficiency (ε) of a system can be formulated as:

$$e_k = X_{P,k} / X_{F,k} = 1 - (X_{D,k} / X_{F,k}) \quad (7)$$

III. THERMOECONOMIC ANALYSIS

Thermoeconomic analysis relates thermodynamic assessments relies on an exergy analysis with economic principles, in order to allow the designer or operator of a system that is beneficial to the design and operate of a cost-effective system, but not acquirable by classical economic and exergy analysis. Thermoeconomics stands to the concept that exergy is the exclusively acceptable base for determining pecuniary costs to the interactions that a system experiences with its surroundings and to the causes of thermodynamic inefficiencies within it [7, 26, 27].

The cost balance for a system operating at the steady state can be written as;

$$C_{P,tot} = Z_k + C_{F,tot} \quad (8)$$

Here, $C_{P,tot}$ signifies the total cost rate of the products, $C_{F,tot}$ is the total cost rate of the fuels and Z_k is the sum of the cost rates related with the capital investment ($\dot{Z}_{tot}^{CI}$) and operating & maintenance costs ($\dot{Z}_{tot}^{OM}$) | [7, 26]:

$$\dot{Z}_k = \dot{Z}_{tot}^{CI} + \dot{Z}_{tot}^{OM} \quad (9)$$

In exergy costing, a cost is correlated with each exergy stream. So, Equations (10-11) are written for the entering (i) and exiting (o) streams of matter with corresponding exergy transfer rates. Equations (12-13) are written for the exergy transfer rate associated with heat and power [7, 26]:

$$C_i = c_i X_i = c_i (m_i . e_i) \quad (10)$$

$$C_o = c_o X_o = c_o (m_o . e_o) \quad (11)$$

$$C_q = c_q X_q = c_q Q_q (1 - T_o / T) \quad (12)$$

$$C_w = c_w X_w = c_w W \quad (13)$$

Here, c_i, c_o, c_w and c_q indicates the average costs per unit of exergy transfer rate ($/GJ) so the units of C_i, C_o, C_w and C_q are dollars per hour ($/h).

Exergy costing includes cost balances commonly defined for each component individually. The cost equation for a component that gets heat and generates power is [7, 26];

$$\sum_o C_{o\,k} + C_{w\,k} = \sum_i C_{i\,k} + C_{q\,k} + Z_k \quad (14)$$

Equation (14) defines that the total cost of exiting exergy streams equals the total outgoings to achieve them. By applying above cost equations (Equations (10-14)), the Equation (15) can be written [7, 26];

$$\sum_o (c_o X_o)_k + (c_w X_w)_k = \sum_i (c_i X_i)_k + (c_q X_q)_k + Z_k \quad (15)$$

IV. STEAM BOILERS

In this work, the energy, exergy and thermoeconomic analyses of two individual steam boilers (SB-1 and SB-2), with steam production capacities of 80 ton/h and 100 ton/h were done. The simulation screen view of the steam boiler-1 is presented in Figure 1 while steam boiler-2 has identical view with its own stream numbers.

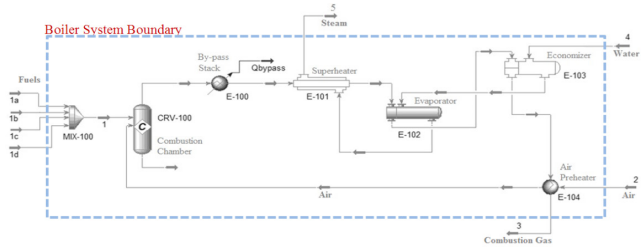

Figure 1. Steam boiler SB-1 and SB-2

The considered steam boilers were individually composed of an air preheater, an economizer, an evaporator, a superheater and a combustion chamber, and have the ability of combusting different types of liquid and gaseous fuels. Here, SB-1 was firing blast furnace gas (BFG), coke gas (CG), steelworks off-gas (SOG) and coal tar (CT) while SB-2 was firing blast furnace gas (BFG), coke gas (CG), steelworks off-gas (SOG) and natural gas (NG). The stream properties of steam boilers were given in Table 1 and the compositions of air and fuels were given in Figure 2.

Table 1. Flow stream properties of the boilers

Steam Boiler-1 (SB-1)				Steam Boiler-2 (SB-2)			
Stream	$\dot{m}$ (kg/s)	P (bar)	T (K)	Stream	$\dot{m}$ (kg/s)	P (bar)	T (K)
1a (BFG)	0.3	1	298	6a (BFG)	11.5	1	298
1b (CG)	0.1	1	298	6b (CG)	0.5	1	298
1c (SOG)	8.4	1	298	6c (SOG)	8.0	1	298
1d (CT)	0.8	8	353	6d (NG)	0.1	16	353
2 (Air)	28.1	1	298	7 (Air)	43.1	1	298
3 (CMB)	37.8	1	419	8 (CMB)	62.4	1	424
4 (WT)	16.1	55	383	9 (WT)	23.6	55	383
5 (ST)	16.1	45	716.2	10 (ST)	23.6	45	716.2

V. RESULTS AND DISCUSSION

The thermoeconomic analysis of the steam boilers has been carried out with the following assumptions:

- The boilers were operated at the steady-state during the analysis.
- Kinetic and potential energy effects were insignificant.
- Combustion reaction was occurred completely.
- Fuel/air ratio was kept constant.
- The reference state that used in calculations was 298.15 K and 1.013 bar.

The equations required for thermoeconomic analysis of steam boilers were given in Table 2.

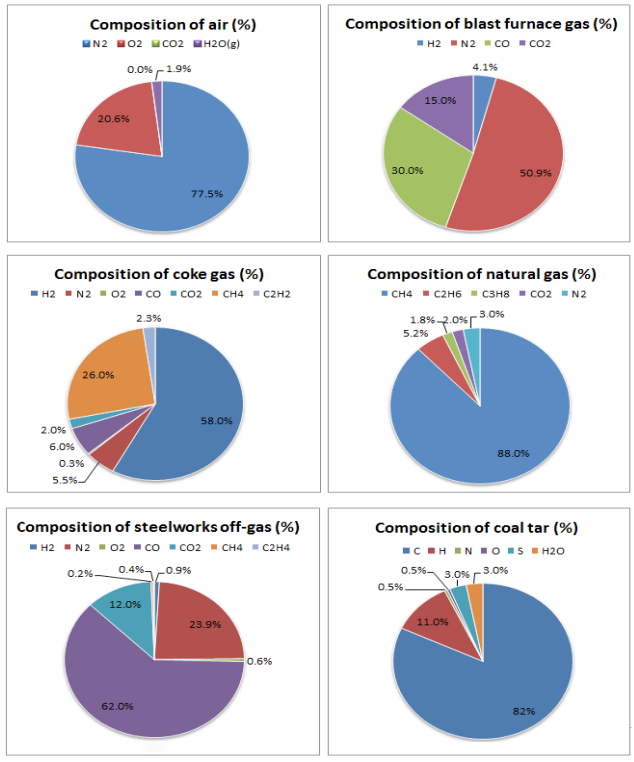

Figure 2. The compositions of air and fuels

Table 2. The mass, energy and exergy balances, exergy destruction, exergy efficiency, energy efficiency, improvement potential and cost equations for the boilers

Steam Boiler-1	Steam Boiler-2
$\dot{m}_{1a} + \dot{m}_{1b} + \dot{m}_{1c} + \dot{m}_{1d} + \dot{m}_2 = \dot{m}_3$, $\dot{m}_4 = \dot{m}_5$	$\dot{m}_{6a} + \dot{m}_{6b} + \dot{m}_{6c} + \dot{m}_{6d} + \dot{m}_7 = \dot{m}_8$, $\dot{m}_9 = \dot{m}_{10}$
$\dot{E}_{1a} + \dot{E}_{1b} + \dot{E}_{1c} + \dot{E}_{1d} + \dot{E}_2 + \dot{E}_4 = \dot{E}_3 + \dot{E}_5$	$\dot{E}_{6a} + \dot{E}_{6b} + \dot{E}_{6c} + \dot{E}_{6d} + \dot{E}_7 + \dot{E}_9 = \dot{E}_8 + \dot{E}_{10}$
$\dot{\Xi}_{1a} + \dot{\Xi}_{1b} + \dot{\Xi}_{1c} + \dot{\Xi}_{1d} + \dot{\Xi}_2 + \dot{\Xi}_4 = \dot{\Xi}_3 + \dot{\Xi}_5 + \dot{\Xi}_L + \dot{\Xi}_D$	$\dot{\Xi}_{6a} + \dot{\Xi}_{6b} + \dot{\Xi}_{6c} + \dot{\Xi}_{6d} + \dot{\Xi}_7 + \dot{\Xi}_9 = \dot{\Xi}_8 + \dot{\Xi}_{10} + \dot{\Xi}_L + \dot{\Xi}_D$
$\dot{\Xi}_D = \dot{\Xi}_{1a} + \dot{\Xi}_{1b} + \dot{\Xi}_{1c} + \dot{\Xi}_{1d} + \dot{\Xi}_2 + \dot{\Xi}_4 - \dot{\Xi}_3 - \dot{\Xi}_5$	$\dot{\Xi}_D = \dot{\Xi}_{6a} + \dot{\Xi}_{6b} + \dot{\Xi}_{6c} + \dot{\Xi}_{6d} + \dot{\Xi}_7 + \dot{\Xi}_9 - \dot{\Xi}_8 - \dot{\Xi}_{10}$
$\varepsilon = (\dot{\Xi}_5 - \dot{\Xi}_4)/(\dot{\Xi}_{1a} + \dot{\Xi}_{1b} + \dot{\Xi}_{1c} + \dot{\Xi}_{1d} + \dot{\Xi}_2)$	$\varepsilon = (\dot{\Xi}_{10} - \dot{\Xi}_9)/(\dot{\Xi}_{6a} + \dot{\Xi}_{6b} + \dot{\Xi}_{6c} + \dot{\Xi}_{6d} + \dot{\Xi}_7)$
$\eta = \dot{E}_5/(\dot{E}_{1a} + \dot{E}_{1b} + \dot{E}_{1c} + \dot{E}_{1d} + \dot{E}_2 + \dot{E}_4)$	$\eta = \dot{E}_{10}/(\dot{E}_{6a} + \dot{E}_{6b} + \dot{E}_{6c} + \dot{E}_{6d} + \dot{E}_7 + \dot{E}_9)$
$\dot{I}_{pot} = \dot{\Xi}_D(1-\varepsilon) + \dot{\Xi}_3$	$\dot{I}_{pot} = \dot{\Xi}_D(1-\varepsilon) + \dot{\Xi}_8$
Cost balance	Cost balance
$\dot{C}_{1a} + \dot{C}_{1b} + \dot{C}_{1c} + \dot{C}_{1d} + \dot{C}_2 + \dot{C}_4 + \dot{Z}_{SB-1} = \dot{C}_3 + \dot{C}_5$	$\dot{C}_{6a} + \dot{C}_{6b} + \dot{C}_{6c} + \dot{C}_{6d} + \dot{C}_7 + \dot{C}_9 + \dot{Z}_{SB-2} = \dot{C}_8 + \dot{C}_{10}$
$c_{1a}.\dot{\Xi}_{1a} + c_{1b}.\dot{\Xi}_{1b} + c_{1c}.\dot{\Xi}_{1c} + c_{1d}.\dot{\Xi}_{1d} + c_2.\dot{\Xi}_2 + c_4.\dot{\Xi}_4 + \dot{Z}_{SB-1} = c_3.\dot{\Xi}_3 + c_5.\dot{\Xi}_5$	$c_{6a}.\dot{\Xi}_{6a} + c_{6b}.\dot{\Xi}_{6b} + c_{6c}.\dot{\Xi}_{6c} + c_{6d}.\dot{\Xi}_{6d} + c_7.\dot{\Xi}_7 + c_9 \cdot \dot{\Xi}_9 + \dot{Z}_{SB-2} = c_8.\dot{\Xi}_8 + c_{10}.\dot{\Xi}_{10}$
Variable calculated from cost balance	Variable calculated from cost balance
$c_5 = \left[c_{1a}.\dot{\Xi}_{1a} + c_{1b}.\dot{\Xi}_{1b} + c_{1c}.\dot{\Xi}_{1c} + c_{1d}.\dot{\Xi}_{1d} + c_4 \cdot \dot{\Xi}_4 + \dot{Z}_{SB-1} \right] / (\dot{\Xi}_5)$	$c_{10} = \left[c_{6a}.\dot{\Xi}_{6a} + c_{6b}.\dot{\Xi}_{6b} + c_{6c}.\dot{\Xi}_{6c} + c_{6d}.\dot{\Xi}_{6d} + c_9 \cdot \dot{\Xi}_9 + \dot{Z}_{SB-2} \right] / (\dot{\Xi}_{10})$

According to the data obtained from the power plant, the unit exergetic cost of BFG, CG, SOG, CT and NG were taken as 4.05 $/GJ, 3.08 $/GJ, 4.42 $/GJ, 4.25 $/GJ, 8.49 $/GJ, respectively. On the other hand, the sum of the cost rates related with equipment were taken as 222.08 $/h and 256 $/h for SB-1 and SB-2. Furthermore, since there is no additional cost to intake the air required for combustion in steam boilers, the costs of air sucked from the environment were taken as zero. Likewise, there is no additional cost to exhaust the formed combustion gases.

The calculated values for the exergy of fuels (MW), exergy of products (MW), exergy destruction (MW), energy and exergy efficiencies (%) and improvement potential (MW) of the steam boilers were given in Figure 3. The results of thermoeconomic analysis were presented in Figure 4 for SB-1 and SB-2.

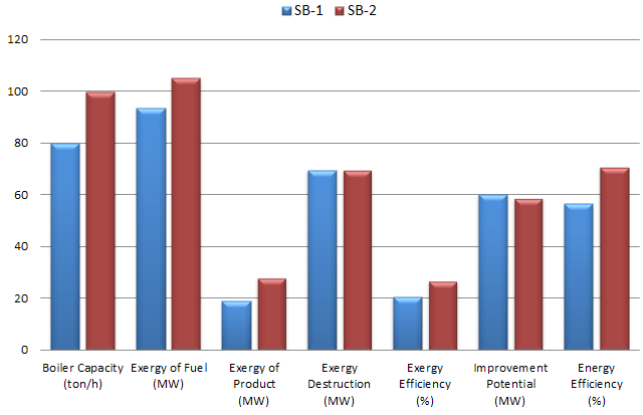

Figure 3. Results of the exergy analysis

According to the Figure 3, the exergy destruction rates were almost the same for the boilers. While the improvement potential of SB-1 was slightly higher than the improvement potential of SB-2 based on the losses and the exergetic efficiencies of the boilers. It was obvious from the Figure 3 that steam boiler-2 operates more efficiently based on its higher steam generation capacity. Figure 4 shows the cost distribution of generated steam from the boilers. It was understood from the figure that the exergetic cost of steam produced from SB-2 was higher than that of SB-1 based on the different feed compositions of the fuels. Since the analyzed boilers were a part of power cycle, which was operating in a closed cycle, the addition or consumption of water in the boilers and their costs were negligible as mentioned in the assumptions.

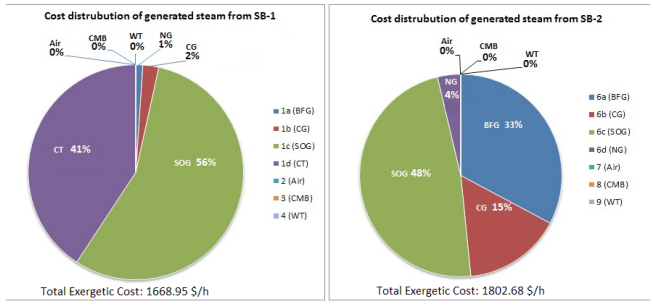

Figure 4. Results obtained from the thermoeconomic analysis

In the second part of this work, determination of the impact of fuel types on the process economics were carried out by using software called Aspen HYSYS [28]. The steam boiler-2 (SB-2) was chosen to investigate the effect of various fuels. Once the real operating condition of SB-2 was simulated as Base Case, which was firing mixture of BFG, CG, SOG and NG, then the effect of individual types of fuel namely, BFG, CG, SOG and NG were simulated respectively among Case1 to Case 4. Assumptions were made as steady-state operation, the constant fuel/air ratio, the constant O_2 moles % at flue gas, and complete combustion.

According to the simulation results, comparison of the percentages of fuel composition of the cases, comparison of fuel / CO_2 mass flow rate and comparison of the unit exergetic cost / CO_2 mass flow rates of the cases were obtained as in Figure 5, Figure 6 and Figure 7, respectively. The simulations demonstrated that the lowest fuel flows observed in case 2 and case 4 due the fuels higher energy content. As a result, CO_2 flow rates in these case considerably low

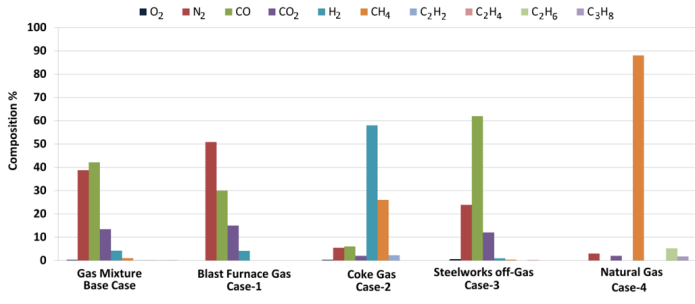

Figure 5. Comparison of the percentages of fuel composition of the cases

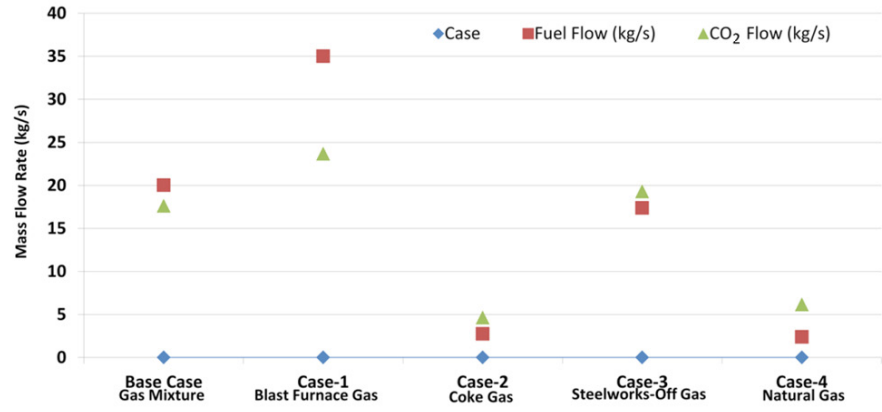

Figure 6. Comparison of fuel and CO_2 mass flow rate of the cases

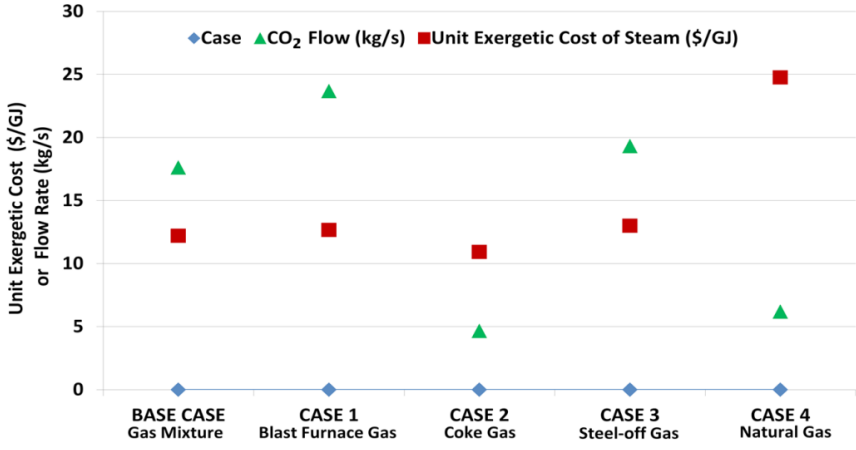

Figure 7. Comparison of the unit exergetic cost and CO_2 mass flow rate

compared to the other cases. While the unit exergetic cost of natural gas was the highest (Figure 7).

The mole compositions of combustion gases (%), depending on the fixed oxygen content (%) in the flue gas during boiler operation were given in Table 4. Accordingly, CO_2 mass flow rate in the combustions gas was highest in Case 3 based on the higher CO and CO_2 content of SOG. The mass flow rates of the fuels and the amount of CO_2, which were obtained by using Aspen HYSYS simulation, were compared in Table 5. Based on the simulations and calculations, the results of exergy and exergoeconomic analyses were shown in Table 6 and Table 7, respectively.

Table 6 illustrates the results obtained from the boiler exergy analysis based on the constant amount of steam production scenarios during operation. It was understood from the table that the highest exergy destruction was occurred in Case 2 while the lowest energy and exergy efficiencies realized in this case. Conversely, the most efficient scenario was Case 3 while it has the lowest exergy destruction rates. Moreover, the exergetic costs of the generated steam in Case 2 was the lowest (1613.70 $/h) and Case 4 was the highest (3662.45 $/h) due to the unit exergetic costs of the fuels. The mass flow rates, the exergy amounts and the cost of each stream in the cases were summarized in Table 7. The results were demonstrated that the cost of generated steam which were higher than the Base Case (1802.68 $/h) except the Case 2, were following the order of Case 4 > Case 3 > Case 1 > Case 2.

Table 4. Mole compositions of combustion gases (%), depending on the fixed oxygen content (%) in the flue gas during boiler operation

Composition (%)	O_2	N_2	CO_2	H_2O
Base Case	5.000	69.965	19.590	5.445
Case 1 (BFG)	5.000	71.560	20.400	3.041
Case 2 (CG)	5.000	70.694	5.796	18.510

Case 3 (SOG)	5.000	68.694	24.960	2.146
Case 4 (NG)	5.000	72.285	7.305	15.410

Table 5. Simulation results: Fuel type, fuel and CO_2 mass flow rate

SB-2	Base Case	Case1	Case2	Case3	Case4
Fuel Type	Gas Mix.	BFG	CG	SOG	NG
Fuel Flow (kg/s)	20.0	35.0	2.8	17.4	2.4
CO_2 Flow (kg/s)	17.6	23.7	4.6	19.3	6.2

Table 6. The results obtained from the boiler exergy analysis based on the constant amount of steam production scenarios during operation

SB-2	$\dot{E}_F$ (MW)	$\dot{E}_P$ (MW)	$\dot{E}_D$ (MW)	ε (%)	I_{pot} (MW)	η (%)
BASE CASE	105.16	28.00	69.56	26.62	58.57	70.76
CASE 1	111.05	28.00	71.75	25.21	64.88	65.47
CASE 2	122.61	28.00	89.44	22.84	74.11	63.70
CASE 3	104.90	28.00	68.71	26.69	58.48	70.78
CASE 4	111.56	28.04	78.33	25.10	63.83	64.61

Table 7. Results obtained from exergoeconomic analysis

Stream	$\dot{m}$ **(kg/s)**	$\dot{E}$ **(MW)**	c **($/GJ)**	$\dot{C}$ **($/h)**
		CASE 1		
$6a^{CS-1}$ (BFG)	35.0	110.93	4.045	1615.36
7^{CS-1} (Air)	47.3	0.12	0.000	0.00
8^{CS-1} (CMB)	82.3	11.25	0.000	0.00
9^{CS-1} (WT)	23.6	13.04	0.000	0.00
10^{CS-1} (ST)	23.6	41.09	12.650	1871.24
		CASE 2		
$6b^{CS-2}$ (CG)	2.8	122.49	3.079	1357.73
7^{CS-2} (Air)	47.1	0.12	0.000	0.00
8^{CS-2} (CMB)	49.9	5.13	0.000	0.00
9^{CS-2} (WT)	23.6	13.04	0.000	0.00
10^{CS-2} (ST)	23.6	41.09	10.909	1613.70
		CASE 3		
$6c^{CS-3}$(SOG)	17.4	104.80	4.419	1667.20
7^{CS-3} (Air)	38.9	0.10	0.000	0.00
8^{CS-3} (CMB)	56.3	8.15	0.000	0.00
9^{CS-3} (WT)	23.6	13.04	0.000	0.00
10^{CS-3} (ST)	23.6	41.09	13.001	1923.16
		CASE 4		
$6d^{CS-4}$ NG)	2.4	111.44	8.491	3406.45
7^{CS-4} (Air)	51.2	0.13	0.000	0.00
8^{CS-4} (CMB)	53.6	5.19	0.000	0.00
9^{CS-4} (WT)	23.6	13.04	0.000	0.00
10^{CS-4} (ST)	23.6	41.09	24.759	3662.45

Exergy flows and improvement potential of the cases were demonstrated in Figure 8. Thus, the magnitudes of exergy flows of the cases were compared. Based on the constant amount of steam production scenarios, it can be said that the highest amount of exergy was supplied in Case 2 and this resulted a highest exergetic destruction rate. Furthermore, the performance analyses of the cases were shown in Figure 9. It was found that the exergetic efficiencies slightly differ in the cases however, these differences are greater in energy efficiencies.

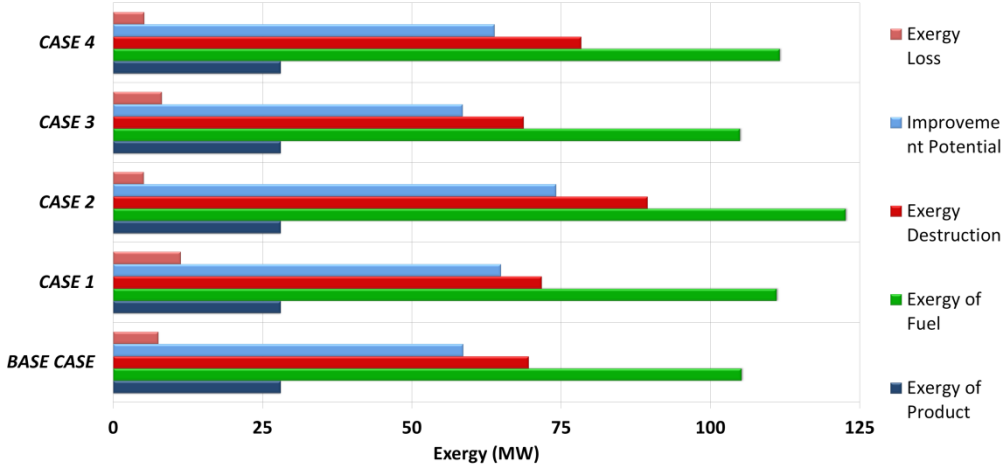

Figure 8. Exergy flows and improvement potential of the cases

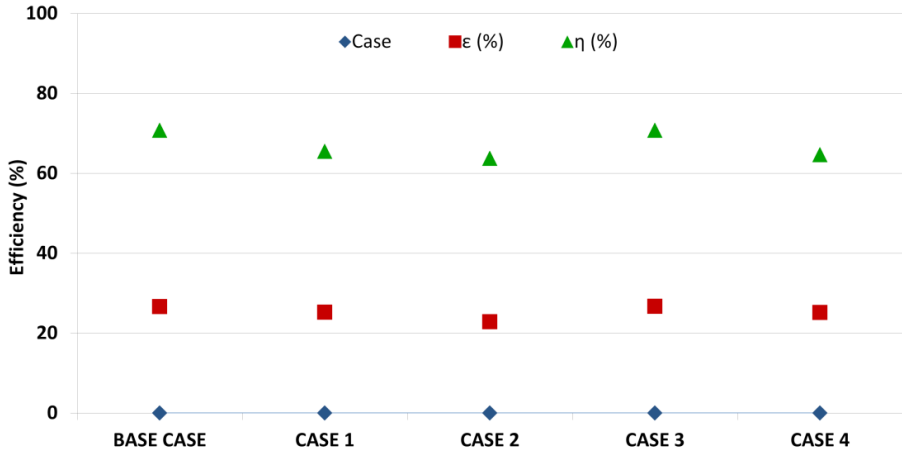

Figure 9. The demonstration of energy and exergy efficiencies

VI. CONCLUSIONS

The steam boilers of a power plant were analyzed, and the following results were achieved. Due to the exergy analysis, the energy efficiencies were found to be 56.79% and 70.76%, and exergetic efficiencies were found to be 20.47% and 26.62% for SB-1 and SB-2, respectively. Furthermore, the amounts of exergy destructions were 69.40 MW and 69.56 MW; the improvement potentials were 60.16 MW and 58.57 MW, and the exergy destruction rates were 74.22% and 66.15% for SB-1 and SB-2 respectively. Due to the thermoeconomic evaluation, it was found that the costs of fuel of SB-1 and SB-2 were 1446.90 $/h and 1546.62 $/h. The costs of steam generated by SB-1 and SB-2 were 1668.95 $/h and 1802.68 $/h or as 28.76 $/ton and 21.21 $/ton, respectively.

On the other hand, in order to investigate the effect of the type of fuel further simulations were done for SB-2 by using Aspen HYSYS simulation software. According to the simulation case studies, the following results were obtained. The energy efficiencies were found to be 65.47%, 63.70%, 70.78% and 64.61%, and exergetic efficiencies were found to be 25.25%, 22.87%, 26.73% and 25.14%, for the fuel BFG, CG, SOG and NG, respectively. Based on the thermoeconomic assessment, the costs of fuels were calculated (Table 7). It was found that CG has the lowest and NG has the highest exergetic costs as 1357.73 $/h and 3406.45 $/h, respectively. In general, the results indicate that the cost of fuels were following the order of CG < BFG < SOG < NG. In other words, the costs of steam were 18.98 $/ton and 43.09 $/h while the CO_2 mass flow rate was 4.6 kg/s and 6.2 kg/s for CG and NG, respectively.

Consequently, thermoeconomic analysis that identifies place amount and causes of thermodynamic inefficiencies in a system with an economic viewpoint is a very helpful tool to reduce environmental impacts, improve the energy conversion systems and increase benefits. This study illustrates the picture of system's exergetic costs and can be used as guiding study for the resembling systems.

NOMENCLATURE

BFG	Blast Furnace Gas
c	Cost per Exergy Unit, $/GJ
C	Cost Rate, $/h
CI	Capital Investment
CG	Coke Gas
COMB	Combustion Gas
CT	Coal Tar
e	Specific Exergy, kJ/kg
h	Specific Enthalpy, kJ/kg
m	Mass Flow, kg/s
NG	Natural Gas
OM	Operating And Maintenance Cost
SB	Steam Boiler
SOG	Steelworks Off-Gas
P	Pressure, Bar
s	Specific Entropy, kJ/kgK
ST	Steam
T	Temperature, K
WT	Water
X	Mole Composition, %
Z	Capital Investment and Operating & Maintenance Cost
Greek Letters	
X	Exergy Flow Rate, MW
e	Exergy Efficiency
I_{pot}	Improvement Potential, MW

h	Energy Efficiency
Subscripts	
ch	chemical
CS	case
i	in
kn	kinetic
o	out
ph	physical
pt	potential

REFERENCES

[1] Cengel, Y.A. and Boles, M.A. (2006). Thermodynamics: An Engineering Approach, 5th ed, McGraw-Hill.

[2] Dincer, I. and Cengel, Y.A. (2001). Energy, Entropy and Exergy Concepts and Their Roles in *Thermal Engineering. Entropy* 3: 116-149.

[3] Cengel, Y.A., Wood, B. and Dincer, I. (2002). Is bigger thermodynamically better? *Exergy, an International Journal* 2: 62–68.

[4] Sari, A. and Kaygusuz K. (2000). Energy and Exergy Calculations of Latent Heat Energy Storage Systems. *Energy Sources*, 22:2, 117-126.

[5] Ozturk, M. (2012). An Exergy Analysis of Biological Energy Conversion. *Energy Sources, Part A: Recovery, Utilization, and Environmental Effects*, 34:21, 1974-1983.

[6] Mert, M.S., Salt, I., Karaca, F., Mert, H.H. and Bolat, E. (2015). Multiple Regression Analysis of Catalytic Dehydrogenation of Isopropanol in a Chemical Heat Pump System. *Chemical Engineering & Technology* 38:3, 399–408.

[7] Tsatsaronis, G. and Cziesla, F. (2002). Thermoeconomics, In: Meyers Robert A. (Ed.) Encyclopedia of Physical Science and Technology, 3rd ed. Academic Press.

[8] Dincer, I. and Rosen, M.A. (2013). Exergoeconomic Analysis of Thermal Systems, In: Dincer, I., Rosen, M.A. (Eds.) *Exergy* 2nd ed. Elsevier Science p. 393-423.

[9] Lazzaretto, A. and Tsatsaronis, G. (2006). SPECO: A systematic and general methodology for calculating efficiencies and costs in thermal systems. *Energy*, 31: 1257–1289.

[10] Atmaca M. (2010). Efficiency Analysis of Combined Cogeneration Systems with Steam and Gas Turbines. *Energy Sources, Part A: Recovery, Utilization, and Environmental Effects*, 33:4, 360-369.

[11] Gümüş M. and Atmaca M. (2013).Energy and Exergy Analyses Applied to a CI Engine Fueled with Diesel and Natural Gas. *Energy Sources, Part A: Recovery, Utilization, and Environmental Effects*, 35:11, 1017-1027.

[12] Yildirim, D. and Ozgener, L. (2012). Thermodynamics and exergoeconomic analysis of geothermal power plants. *Renewable and Sustainable Energy Reviews,* 16: 6438–6454.

[13] Kwak, H.Y., Kim, D.J. and Jeon, J.S. (2003). Exergetic and thermoeconomic analyses of power plants. *Energy*, 28: 343–360.

[14] Sahoo, P.K. (2008). Exergoeconomic analysis and optimization of a cogeneration system using evolutionary programming. *Applied Thermal Engineering*, 28 (13):1580–1588.

[15] El-Emam, R.S. and Dincer, I. (2013). Exergy and exergoeconomic analyses and optimization of geothermal organic Rankine cycle. *Applied Thermal Engineering,* 59: 435 – 444.

[16] Pellegrini, L.F., Junior, O.S. and Burbano, J.C. (2010). Supercritical steam cycles and biomass integrated gasification combined cycles for sugarcane mills. *Energy,* 35: 1172–1180.

[17] Mert, M.S., Dilmaç, Ö.F., Özkan, S., Karaca, F. and Bolat, E. (2012). Exergoeconomic analysis of a cogeneration plant in an iron and steel factory. *Energy,* 46: 78-84.

[18] Xiong, J., Zhao, H. and Zheng, C. (2012). Thermoeconomic cost analysis of a 600 MWe oxy-combustion pulverized-coal-fired power plant. *International Journal of Greenhouse Gas Control* 9: 469–48.

[19] Farshi, L.G., Mahmoudi, S.M.S. and Rosen, M.A. (2013). Exergoeconomic comparison of double effect and combined ejector-double effect absorption refrigeration systems. *Applied Energy*, 103: 700-711.

[20] Gungor, A., Erbay, Z. and Hepbasli, A. (2011). Exergoeconomic analyses of a gas engine driven heat pump drier and food drying process. *Applied Energy*, 88(8): 2677-2684.

[21] Ozgener, L. and Ozgener, O. (2009). Monitoring of energy exergy efficiencies and exergoeconomic parameters of geothermal district heating systems (GDHSs). *Applied Energy*, 86(9): 1704-1711.

[22] Dong, R., Yu, Y. and Zhang, Z. (2014). Simultaneous optimization of integrated heat, mass and pressure exchange network using exergoeconomic method. *Applied Energy*, 136: 1098–1109.

[23] Rakopoulos, C.D. and Giakoumis, E.G. (2006). Second-law analyses applied to internal combustion engines operation. *Progress in Energy and Combustion Science,* 32: 2-47.

[24] Cornelissen, R.L. and Hirs, G.G. (2002). The value of the exergetic life cycle assessment besides the LCA. *Energy Conversion and Management*, 43: 1417–1424.

[25] Meratizaman, M., Amidpour, M., Jazayeri, S.A. and Naghizadeh, K. (2010). Energy and exergy analyses of urban waste incineration cycle coupled with a cycle of changing LNG to pipeline gas. *Journal of Natural Gas Science and Engineering,* 2: 217-221.

[26] Bejan, A., Tsatsaronis, G. and Moran, M. (1996). Thermal Design and Optimization, John Wiley and Sons, USA

[27] Tsatsaronis, G. (2007). Definitions and nomenclature in exergy analysis and exergoeconomics. *Energy,* 32: 249–253.

[28] Aspen HYSYS V.10, Aspen Technology, Inc. aspenONE, Massachusetts, USA.

Int. J. Adv. Eng. Pure Sci. 2019, 4: 295-304
DOI: 10.7240/jeps.512240

RESEARCH ARTICLE / ARAŞTIRMA MAKALESİ

Hydroxyapatite/Cerium Oxide Composites: Sintering, Microstructural, Mechanical and In-vitro Bioactivity Properties

Hidroksiapatit/Seryum Oksit Kompozitleri: Sinterlenebilme, Mikroyapısal, Mekanik ve İn-vitro Biyoaktivite Özellikleri

Serdar PAZARLIOĞLU[1]

[1]*Marmara University, Technology Faculty, The Department of Metallurgy and Material Science Engineering, Goztepe Campus, Istanbul/Turkey*

Abstract

In the present study, the effects of cerium oxide (CeO_2) additive on the sinterability, microstructural, mechanical and in-vitro bioactivity properties of a commercially synthetic hydroxyapatite (HA) was investigated. HA without CeO_2 additive started to decompose at 1100 ^oC, but the decomposition temperature of the CeO_2 added samples decreased up to 900 ^oC. Decomposition rate of the sintered samples increased by increasing sintering temperature. It was about 5.8% for pure HA, and increased to 11.4% when the CeO_2 additive to HA reached to 2.5 wt%. SEM images showed that an excessive grain growth as well as microcracks occured on the surface of pure HA when it was sintered at the temperatures than that of 1100 ^oC. The microcracks were also observed on the surface of HA-CeO_2 composites, when they were sintered at 1300 ^oC. The composite of HA-0.5CeO_2 sintered at 1100 ^oC possess the higher fracture toughness (Kıc) (2.510 ± 0.225 $MPam^{-1/2}$) and the higher compressive strength (152.73 ± 6.31 MPa) compared to other HA-CeO_2 composites, and its mechanical properties are higher than that of pure HA at about 2-3 times. In-vitro bioactivity test results showed that apatite layers on the surface of the samples were in the different morphologies.

Keywords: Hydroxyapatite, Cerium Oxide, Sintering

Öz

Bu çalışmada, seryum oksit (CeO_2) ilavesinin ticari saflıktaki bir sentetik hidroksiapatitin (HA) sinterlenebilme, mikroyapısal, mekanik ve in-vitro biyoaktivite özelliklerine etkileri incelenmiştir. CeO_2 ilavesiz HA 1100 ^oC sıcaklıkta dekompoze olmaya başlamış, CeO_2 ilave edilmiş numunelerde dekompoze olma sıcaklığı ise 900 ^oC' ye kadar düşmüştür. Sinterlenmiş numunelerin dekompoze olma oranı sinterleme sıcaklığının artmasıyla artmıştır. Saf HA' nın dekompoze olma oranı yaklaşık % 5.8 iken, HA' ya yapılan CeO_2 katkı maddesi ağırlıkça% 2.5' e ulaştığında %11.4' e yükselmiştir. SEM görüntüleri 1100 ^oC' nin üstündeki sıcaklıklarda sinterlenen saf HA' nın yüzeyinde aşırı tane büyümelerinin yanı sıra mikroçatlakların meydana geldiğini göstermiştir. Mikroçatlaklar ayrıca HA-CeO_2 kompozitlerinin yüzeyinde, 1300 ^oC sıcaklıkta sinterlendiklerinde gözlemlenmiştir. 1100 ^oC' de sinterlenmiş HA-0.5CeO_2 kompoziti, diğer HA-CeO_2 kompozitlerine kıyasla daha yüksek kırılma tokluğu (Kıc) (2.510 ± 0.225 $MPam^{-1/2}$) ve daha yüksek basma dayanımına (152.73 ± 6.31 MPa) sahiptir ve mekanik özellikleri saf HA' dan yaklaşık 2-3 kat daha yüksektir. İn-vitro biyoaktivite testi sonuçları, numunelerin yüzeyindeki apatit katmanlarının farklı morfolojilerde olduğunu göstermiştir.

Anahtar Kelimeler: Hidroksiapatit, Seryum oksit, Sinterleme

I. INTRODUCTION

Owing to the ageing populations worldwide, there is a strong need for developing biomaterials for tissue engineering applications. Accordingly, hydroxyapatite (HA) is considered as the most common bioceramic which can be used extensively

Sorumlu yazar/Corresponding Author: Serdar PAZARLIOĞLU, **Tel:** +902163365770/1364, **e-posta:** spazarlioglu@marmara.edu.tr,
Gönderilme/Submitted: 13.01.2019, **Düzenleme/Revised:** 31.08.2019, **Kabul/Accepted:** 16.10.2019

for repairing as well as reconstructing diseased or damaged hard tissues as a result of its excellent chemical similarity with the mineral phase of bone over other biomaterials [1]. However, the advantage of the HA chemical similarity with the mineral phase of bone is outweighed by its poor mechanical properties that prevent its bulk use in orthopedic implants. It has been investigated that load resistant HA bioceramics reinforced with other second-phase ceramic materials with moderate tolerable compressive strengths powders (for instance, zirconia, titania, magnesia or alumina) [2].

As an oxide ceramic, cerium oxide (CeO_2), is a promising material that has potential use in a number of applications such as high-temperature ceramics, catalysts, capacitor devices, UV blocking materials, oxygen sensor, fuel cells, and biodiesel production [3-6]. Apart from these applications, because of it's excellent biological properties such as protection of primary cells from the detrimental effects of radiation therapy, prevention of retinal degeneration induced by intracellular peroxides and neuroprotection to spinal cord neurons, anti-inflammatory, it can be also used as a coating material and also an additive material to hydroxyapatite, which has derived from bovine femur bone [7-12]. The study about the bovine derived hdroxyapatite-cerium oxide composites has the experimental datas on the density, hardness, and compressive strength of that bioceramics, depending on the sintering temperatures as well as cerium oxide ratio. However, the effect of cerium oxide additives were not investigated on the phase stability, fracture toughness, grain growth, porosity, and in-vitro bioactivity properties of commercially available hydroxyapatite in Ref [12].

The aim of the present study was to investigate the effect of cerium oxide on a commercially available hydroxyapatite. A series of test were applied to physical and mechanical properties of sintered HA with and without cerium oxide additive. The type and amount of phases and grain size measurements were carried out using X-ray diffraction patterns and scanning electron microscope. In-vitro test were also performed to the samples having best mechanical properties.

II. EXPERIMENTAL PROCEDURE

II.1 Sample Preparation

The raw materials used in the present study were HA (Across Organics, Belgium) and CeO_2 (Sigma Aldrich, Germany) powders, and CeO_2 powder were added to HA to obtain the composites as shown in **Table 1**. The composite powders were mixed by a ball milling device at 180 rpm for 2 h. The mixed powders were uniaxially pressed to prepare the pellets according to our previous study [13]. Sintering process was performed at 900 ºC, 1000 ºC, 1100 ºC, 1200 ºC, and 1300 ºC for 4h.

Table 1. Abbreviation and composition of the samples.

Name	Abbreviation	Composition (wt/wt %)
Hydroxyapatite and cerium oxide composites	HA	HA (100)
	HA-0.5C	HA (99.5) + CeO_2 (0.5)
	HA-1.5C	HA (98.5) + CeO_2 (1.5)
	HA-2.5C	HA (97.5) + CeO_2 (2.5)

II.2 Microstructural Characterization

Microstructural characterization of the samples were analyzed by a Philips X'Pert XRD machine using Cu-Kα as the radiation source in the range of 2θ values between 25° and 50°. The percentage of the phases detected by XRD analysis was determined by Rietveld analysis. The changes in the surface morphology of the sintered samples were determined by FEI Sirion XL30 SEM machine. The changes in the average grain size of the sintered samples were determined by the linear intercept method.

II.3 The Determination of Physical and Mechanical Properties

While the green and sintered densities of the samples were calculated according to **Equation 1**, the porosity ratios were calculated using **Equation 2**.

$$d = \frac{m}{v} \quad (1)$$

$$p = 100 - dr \quad (2)$$

Where; d is the green and/or sintered density (g/cm^3), m is the weight (g), v is the volume (cm^3), p is the porosity (%), dr is the relative density of the sintered sample.

The theoretical densities of the pelletized and sintered samples were calculated according to **Equation 3**, and the relative density values of the samples were calculated according to **Equation 4**.

$$d_t = \frac{m_t}{(\frac{m_1}{d_1} + \frac{m_2}{d_2})} \quad (3)$$

$$d_r = \frac{d}{dt} x100 \quad (4)$$

Where; d_t is the theoretical density (g/cm^3), m_t is the total weight (g), m_1 is the weight of HA in mixture (g), d_1 is the theoretical density of HA (3.156 g/cm^3 [14]), m_2 is the weight of CeO_2 in mixture (g), d_2 is the theoretical density of CeO_2 (7.220 g/cm^3 [15]).

The shrinkage rate of the sintered samples were calculated using **Equation 5**.

$$\text{Shrinkage} = \left(\frac{L1 - L2}{L1}\right) \text{x } 100 \quad (5)$$

Where; L1 and L2 are the lengths of green bodies and sintered bodies, respectively.

The micro (μ) – hardness of the samples was calculated using **Equation 6** by Shimadzu HMV2 microindentor at load of 200 g for 20 s. The fracture toughness (K_{ic}) of the samples were calculated by **Equation 7** according to Ref [16] using load of 300 g for 10 s.

$$HV = 0{,}0018544*(P/d^2) \quad (6)$$

Where; HV is the vickers hardness (GPa), P is the applied load (g), and d is the diagonal indent length (mm)

$$Kıc = 0.203(c/a)^{-1.5}(HV)(a)^{0.5} \quad (7)$$

Where; a is the half diagonal of the indentation (m), c is the radial crack dimension (m) measured from the center of the indent impression, and L is the crack length (m). Compression tests were done using an universal testing machine (Devotrans FU 50kN, Turkey) under a loading rate of 2 $mm.min^{-1}$. The in-vitro bioactivity properties of the samples, which had the higher compressive strength of HA with and without CeO_2, were determined by simulated body fluid (SBF) prepared according to Ref [17]. The apatite layers on the surface of samples immersed in SBF solutions were investigated by SEM.

III. RESULTS & DISCUSSION

Figure 1 shows the XRD patterns of pure HA. The extra peak observed at 2θ angle of 31.03 was attributed to the β-TCP, when pure HA sintered at 1100 ºC, and 1200 ºC. At 1300 ºC, α-TCP and CaO peaks were detected in addition to HA and β-TCP phases. The XRD patterns revealed that HA powder used in the present study started to decompose at 1100 ºC. **Table 2** summarizes the decomposition rates of HA to secondary phases. While pure HA started to decomposition at 1100 ºC, the decomposition of CeO_2 started at dissimilar temperatures depending on additive ratios. The increase in sintering temperatures led to an increase in decomposition rates of HA-CeO_2 composites, as in pure HA. The decomposition in HA ceramics can be explained as following reactions [18]. ($Ca_3(PO4)_2$ is β-TCP, and $Ca_3P_2O_8$ is α-TCP)

$$Ca_{10}(PO_4)_6(OH)_2 \Longrightarrow Ca_{10}(PO_4)_6(OH)_{2(1-x)} + xH_2O_{gaz} \quad (R.\ 1)$$

$$Ca_{10}(PO_4)_6(OH)_{2(1-x)} \Longrightarrow 3Ca_3(PO_4)_2 + CaO + (1-x)H_2O \quad (R.\ 2)$$

$$Ca_{10}(PO_4)_6(OH)_2 \Longrightarrow 2Ca_3(PO4)_2 + Ca_3P_2O_8 + CaO + H_2O \quad (R.\ 3)$$

Previous studies have reported that the decomposition temperatures of HA begin at different sintering temperatures between 700 ºC and 1400 ºC [19-24], depending on the production process and the water vapor in the furnace atmosphere. The pure HA used in the present study started to decompose at 1100 ºC. The decomposition rate of pure HA also agreed with previous reports [25-27].

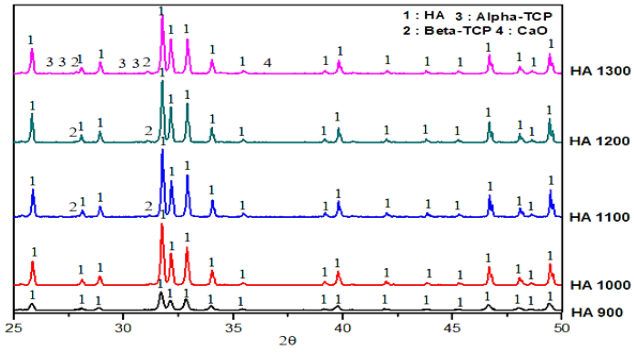

Figure 1 XRD analyzes of pure HA depending on the sintering temperatures

Table 2. The amount of HA and its decomposition rates in the sintered samples

Sample	Phase	Sintering temperature (ºC)				
		900	1000	1100	1200	1300
HA	HA	100	100	97.8	96.2	94.2
	β-TCP	-	-	2.2	3.8	4.1
	α-TCP	-	-	-	-	1.6
	CaO	-	-	-	-	0.1
HA-0.5C	HA	99.2	92.5	90.5	90.6	90.2
	β-TCP	-	7.0	8.8	8.9	8.8
	α-TCP	-	-	-	-	-
	CaO	-	-	-	-	0.4
HA-1.5C	HA	98.3	92.1	90.2	89.7	87.9
	β-TCP	-	7.6	8.9	9.1	9.6
	α-TCP	-	-	-	-	1.1
	CaO	-	-	-	-	0.3
HA-2.5C	HA	96.8	91.1	89.1	88.7	86.9
	β-TCP	1.0	8.2	9.2	8.3	9.5
	α-TCP	-	-	-	0.9	1.3
	CaO	-	-	-	0.1	0.6

HA-CeO_2 composites consisted of CeO_2, Ce_7O_{12}, $Ce_{11}O_{20}$, $Ca_{0.167}Ce_{0.7}PO_4$ and $Ca_{19}Ce(PO_4)_{14}$ in addition to HA, β-TCP, α-TCP and CaO, as shown **Figure 2 (a)-(c)**. The CeO_2 phase detected at all sintering temperatures in the composites, regardless CeO_2 ratio, and its peak intensities at 2θ of 28.544º, and 47.479º increased as CeO_2 ratio. The Ce_7O_{12}, and $Ce_{11}O_{20}$ phases were only detected up to 1100 ºC, which had due to the formation of oxygen vacancies in CeO_2, as stated in previous reports [28-30]. The $Ca_{0.167}Ce_{0.7}PO_4$ and $Ca_{19}Ce(PO_4)_{14}$ phases detected at dissimilar temperatures depending on the additive ratios. The $Ca_{0.167}Ce_{0.7}PO_4$ and $Ca_{19}Ce(PO_4)_{14}$ phases are formed due to the ion radii of the elements are close to each other. The ionic radii are 0.97 Å for Ce^{4+}, 0.99 Å

for Ca^{2+}, 1.07 Å for P^{5+}, and 0.66 Å for O^{2+}, respectively [31,32]. In the CeO_2 added samples, the decomposition rates increased with increase in the sintering temperatures as well as CeO_2 ratios. The decomposition of HA composited with CeO_2 at amount of 1.5 and 2.5wt % sintered at 1300 ºC can be explained by Reaction 4.

$$\mathbf{3}Ca_{10}(PO_4)_6(OH)_2 + CeO_2 \Longrightarrow Ca_{19}Ce(PO_4)_{14} + Ca_3(PO_4)_2 + Ca_3P_2O_8 + \mathbf{5}CaO + \mathbf{3}H_2O \quad \text{(R. 4)}$$

The amount of HA% phase in HA-CeO_2 composites decreased to the minimum value of 86.9% at 1300 ºC, as shown in **Table 2**. Although the addition of CeO_2 led to an increase in the decomposition rates of HA, it was found to be lower than that of previous studies. For example the amount of HA phase in a commercially available HA-SiO_2 composites decreased to the minimum value of 18.2% at 1200 ºC [33], whereas it decreased to the minimum value of 57.0% for HA composited with ZrO_2 [34]. The low decomposition rate of HA-CeO_2 composites than that of the other HA based composites are due to the following reasons. 1 – The difference in sintering regime and methods. 2 – The difference in the average grain size of the raw materials. 3 – The difference in the ionic radii of the additives. The ionic radii of the Si is 0.40 Å [35], Zr^{4+} is 0.84 Å [36].

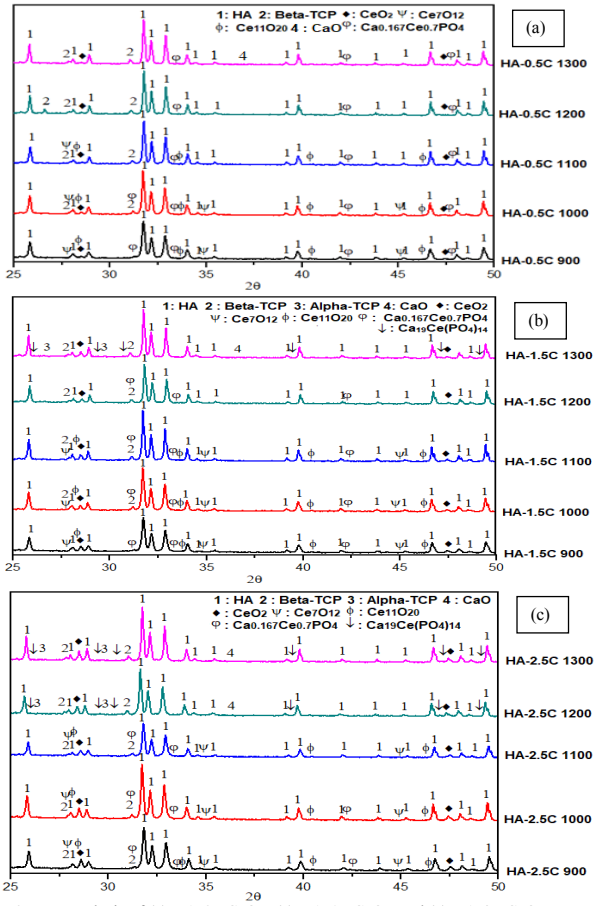

Figure 2. XRD analysis of (a) HA-0.5CeO2, (a) HA-1.5CeO2, and (a) HA-2.5CeO2 composites

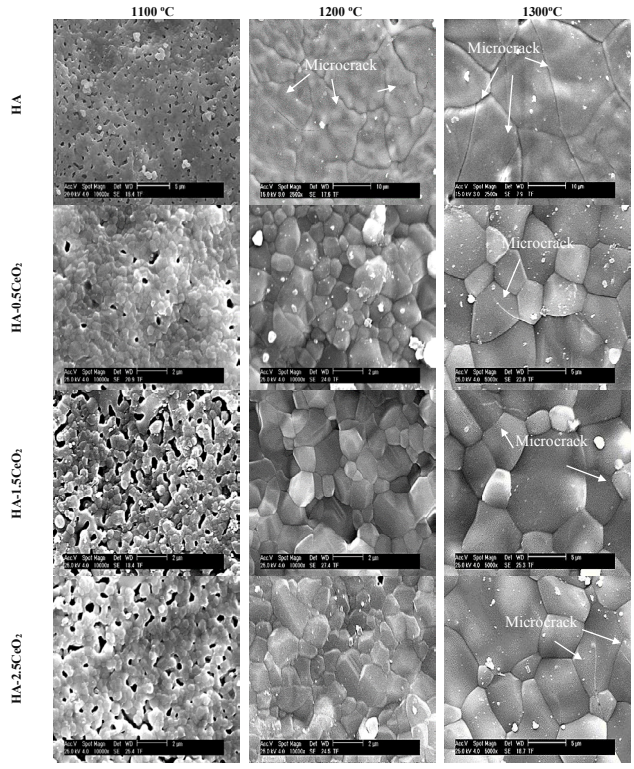

Figure 3 SEM microstructure images of samples sintered between 1100 ºC and 1300 ºC

Figure 3 shows the SEM images of samples sintered between 1100ºC and 1300ºC. As shown in **Figure 3** the samples sintered at 1100 ºC showed a high amount of pores that remained between the grains. These observations corresponded to the low shrinkage and the low density of sintered samples. The SEM micrographs of pure HA sintered above 1100 ºC evidence a significant grain growth. For these temperatures, the average grain sizes of pure HA were measured as 7.955±1.616 µm and 17.167±2.156 µm, respectively. The microcracks on the surface of pure HA was in transgranular form. Furthermore, microcracking was also observed on the surface of pure HA. This is related to the thermal expansion anisotropy (TEA) of the HA, which leads to the generation of thermal and residual stress fields as well as it results in contraction of individual grains from neighboring grains at different rates when the pure HA ceramics sintered using conventional sintering process. If the differences in thermal contraction rates are large enough, the induced stresses can cause microcracks [37], when the grain size, G, of the HA exceeds, Gcr, the critical grain size [38].As reported by Ref [39], the critical grain size is about 0.4 µm to the formation of microcracking in HA ceramics. In the present study, no microcracking observed for the pure HA at about the average grain size of 0.473 ± 0.035 µm, which is good agreement with that paper. The microcracks were also

observed to the CeO_2 added samples sintered at 1300 °C, when the grain sizes reached to 3.565 ± 0.411 μm in HA-0.5CeO_2, 4.114 ± 0.456 μm in HA-1.5CeO_2 and 4.283 ± 0.541 μm in HA-2.5CeO_2, respectively. As can be seen in the results for grain size, the presence of CeO_2 inhibited the grain growth of HA particles. However, microcracks in CeO_2 added samples were found to in a shorter form than that of pure HA, and they were trapped in the grains. The microcracks on the surface of CeO_2 added samples mainly are caused by the difference in thermal expansion coefficient (TEC) of the HA, CeO_2, β-TCP, α-TCP, CaO, $Ca_{0.167}Ce_{0.7}PO_4$ and $Ca_{19}Ce(PO_4)_{14}$ phases (HA ≈ 16.9 x 10^{-6} °C^{-1} [40], CeO_2 ≈ 14 x 10^{-6} °C^{-1} [41], β-TCP ≈ 14.2 x 10^{-6} °C^{-1} [42], CaO ≈ 13.8 × 10^{-6} ∘C^{-1} [43]). **Table 3** summarizes the green and relative density values of pelleted samples. It is obviously seen that the green and relative density values of the pelleted samples decreased, as the CeO_2 ratio increase. This may be related to the harder structure of CeO_2 than that of HA.

Table 3. The green and relative density values of pelleted samples

Sample ID	Theoretical density (g/cm^3)	Green density (g/cm^3)	Relative density of green bodies (%)
HA	3.156	1.651±0.016	52.316±0.529
HA-0.5CeO_2	3.165	1.606±0.054	50.755±1.723
HA-1.5CeO_2	3.184	1.596±0.071	50.133±2.257
HA-2.5CeO_2	3.203	1.577±0.064	49.258±2.006

Table 4. The physical properties of HA with and without CeO_2 additive, depending on the sintering temperatures

Property	T(°C)	HA	HA-0.5CeO_2	HA-1.5CeO_2	HA-2.5CeO_2
Shrinkage (%)	900	5.333±0.571	4.817±0.315	4.703±0.310	4.438±0.179
	1000	8.940±0.383	7.240±0.180	7.230±0.163	6.797±0.315
	1100	13.534±0.505	12.074±0.317	11.739±0.906	11.202±0.435
	1200	17.734±0.704	18.444±0.619	17.891±1.537	17.873±1.083
	1300	18.209±0.622	18.826±0.869	18.742±1.413	18.459±0.541
Porosity (%)	900	39.868±0.406	42.658±1.329	43.701±1.041	45.054±1.552
	1000	34.978±1.722	39.585±1.516	40.642±2.128	40.940±0.642
	1100	21.910±1.541	30.496±3.172	31.617±4.520	32.2.951±
	1200	6.832±0.224	6.797±1.690	7.930±1.477	9.903±3.361
	1300	6.304±0.469	3.793±0.370	7.157±1.786	8.661±1.366
Density (g/cm^3)	900	1.897±0.012	1.825±0.042	1.822±0.051	1.803±0.033
	1000	2.052±0.054	1.958±0.021	1.923±0.048	1.901±0.068
	1100	2.464±0.048	2.305±0.105	2.177±0.143	2.163±0.094
	1200	2.940±0.070	2.988±0.11	2.973±0.057	2.948±0.053
	1300	2.957±0.077	3.063±0.045	3.029±0.043	2.967±0.047
Relative density (%)	900	58.061±0.570	57.575±1.627	57.341±1.329	56.298±1.041
	1000	65.557±0.848	59.059±0.642	60.414±1.516	59.357±2.128
	1100	73.410±0.895	69.503±3.172	68.382±4.520	67.543±2.951
	1200	95.981±0.595	93.202±1.690	92.069±1.786	90.096±3.361
	1300	97.087±0.769	96.206±1.370	92.842±1.477	91.338±1.366

Table 4 shows the physical properties of the sintered samples. **Table 4** showed that little improvements in the physical properties were achieved up to 1100 °C. For the pure HA, the final shrinkage was 18.209 ± 0.622%, whereas the final shrinkage was about 18.459-18.826% for CeO_2 added samples. The densities after sintering at or above 1200 °C reached to 2.940 ± 0.071 g/cm^3 and 2.957 ± 0.077 g/cm^3 for pure HA. However, although the grain sizes were lower, the HA-CeO_2 composites had higher densities than pure HA at these temperatures. This can be related to the higher theoretical densities of CeO_2 (7.220 g/cm^3), CaO (3.37 g/cm^3), $Ca_{0.167}Ce_{0.7}PO_4$ (4.40 g/cm^3), and $Ca_{19}Ce(PO_4)_{14}$ (3.23 g/cm^3) phases than that of HA (3.156 g/cm^3). The relative density of pure HA was higher than the CeO_2-HA composites regardless of the sintering temperature used, which is due to the low theoretical density of HA than that of CeO_2. Taking theoretical density of HA as 3.156 g/cm^3, the relative density of its attained to 97.087 ± 0.769% after sintering at 1300 °C, which is higher than that of the data in literature. For

example in Ref. [44] the authors claimed that relative density after sintering at 1300 ºC was about 87%; contrary to authors of [45] who reported a relative density of ≈ 62-76% for samples sintered at 1300 ºC. The higher relative density of pure HA used in the present study could be attributed to the various reasons: First is the utilization of higher pelletizing pressure in the present study. Second is the HA used in this study decomposed to secondary phases at a lower rate than that of others. Third is the lower starting particulate size of HA powder. Fourth is the difference in the sintering regime and sintering time. As reported by Ref [46], the sintered density of the compacts increased with applied pelletizing pressure because a comparatively rapid grain growth occured. It is well-known that increase in the decomposition rates of HA leads to the decreasing in the final density because of the lower density values of the β-TCP (3.07 g/cm3 [47]), and α-TCP (2.86 g/cm3 [48]) phases. As reported Ref [49] that the difference in the particle sizes of the HA powders leads to the difference in the degree of packing during compaction. Even if the same pelletizing pressure applied to the HA powders derived from meleagris gallopova in our previous study [50], the difference in the degree of packing during compaction are reflected in the relative density values of the final products.

Table 5. The mechanical properties of HA with and without CeO_2 additive, depending on the sintering temperatures

Property	T (ºC)	HA	HA-0.5CeO_2	HA-1.5CeO_2	HA-2.5CeO_2
μ-hardness (GPa)	900	0.76±0.06	0.78±0.01	0.76±0.03	0.73±0.02
	1000	1.11±0.03	0.83±0.03	0.82±0.02	0.79±0.02
	1100	1.51±0.08	1.79±0.09	1.43±0.09	1.12±0.06
	1200	4.76±0.22	4.89±0.22	4.83±0.15	4.78±0.16
	1300	4.87±0.09	4.99±0.44	4.89±0.25	4.74±0.19
$\sigma_{compressive}$ (MPa)	900	91.00±6.80	84.41±5.34	77.58±16.50	60.54±6.61
	1000	102.00±10.20	91.99±11.89	99.10±6.47	86.92±21.18
	1100	130.00±6.22	152.73±15.58	123.06±23.76	115.86±18.21
	1200	101.00±5.01	139.08±6.31	116.32±11.62	112.36±8.28
	1300	65.00±5.59	107.04±5.98	69.71±3.43	58.76±10.14
Kıc (MPa $m^{1/2}$)	900	0.68±0.05	0.69±0.03	0.68±0.09	0.67±0.08
	1000	0.88±0.09	0.70±0.13	0.70±0.10	0.69±0.09
	1100	0.96±0.05	2.51±0.22	2.32±0.15	2.02±0.14
	1200	0.92±0.06	1.86±0.23	1.65±0.29	1.45±0.26
	1300	0.71±0.13	1.45±0.28	1.22±0.09	0.8±

Table 5 shows the mechanical properties of the sintered samples. Although the $\sigma_{compressive}$ of pure HA reached the maximum value of 130 ± 6.22 MPa at sintering temperature of 1100 °C, it decreased to 101.8 ± 5.01 and 65.6 ± 5.59 MPa, when it was sintered at 1200 ºC and 1300 ºC. Given the significant improvement in densification achieved at 1300 ºC, the reduction in $\sigma_{compressive}$ can be attributed to the presence of microcracks, and increasing in the average grain sizes. Microcracks reduce the mechanical strength of HA ceramics, so HA ceramics containing TCP is not the proper material for surgical implants that require high mechanical strength [51]. It has been well established that a decrease in grain size increased the mechanical properties according to the Hall-Petch equation ($\sigma = \sigma_o + kd^{-1/2}$) [52]. The maximum $\sigma_{compressive}$ value of pure HA obtained at sintering temperature of 1100 ºC increased to 152.73 ± 15.58 MPa with 0.5 CeO_2 additive. However, the $\sigma_{compressive}$ of HA-0.5CeO_2 composites decreased to 115.86 ± 18.21 MPa with increase in the amount of CeO_2 ratio at the same temperature. The $\sigma_{compressive}$ of HA-CeO_2 composites decreased with increasing temperature even if the relative densities of their reached to above 90%.

Hovewer; the maximum $\sigma_{compressive}$ value of 152.73 ± 15.58 MPa for HA-0.5CeO_2 composites obtained in the present study is higher than that of a previous study (107 MPa), at about 42% [12]. Increasing the sintering temperature from 900 ºC to 1100 ºC significantly improved the Kıc values of samples, but the more temperature caused to reduction the Kıc values. The peak Kıc value of pure HA of 0.967±0.056

$MPam^{1/2}$ is inside the range of 0.6-1.5 $MPam^{1/2}$, as stated Ref [18]. The maximum Kıc value of pure HA significantly improved to 2.510 ± 0.225 $MPam^{1/2}$ by the CeO_2 additive at amount of 0.5 wt%. The higher Kıc values of HA-0.5CeO_2 composite compared to pure HA can be attributed to two major factors: (i) grain size refinement and (ii) crack bridging by CeO_2. The addition of CeO_2 to HA more than 0.5 wt% led to reduction the Kıc values of the composites at all temperatures. It can be explained by decreasing the decomposition ratio of the samples depending on the decreasing CeO_2 content as shown in **Table 2**. The peak value of 2.510±0.225 $MPam^{1/2}$ measured to HA-0.5CeO_2 is also compatible with the Kıc value of human cortical bone (2-6 $MPam^{1/2}$). The samples sintered at below 1100 ºC had the low µ-hardness values than 2 GPa. Increasing in the sintering temperature from 1100 ºC to 1200 ºC contributed to the sharply improvement in µ-hardness values and reached to at above 4.7 GPa. The lower hardness observed for the composites is associated with the lower density of the sintered bodies as depicted in **Table 4**. The hardness of ceramics is typically a function of porosity, density, relative density and average grain size [53]. The hardness increase with decreasing grain size is typically attributed to the reduced free path for dislocations in both metals and ceramics [54]. **Figure 4** shows the relationship between hardness and the porosity, density, relative density and average grain size of sintered samples. The figure showed that hardness of the sintered samples increased with increasing density and relative density. Moreover, the decrease in porosity and average grain size of the sintered samples led to increasing the hardness.

Figure 5 shows the SEM images of pure HA and HA-0.5CeO_2 samples after SBF test. The surface morphology of the samples changed with the soaking time, and for 7 day of SBF immersion a layer consisted of dendritic apatitic structures on the materials could be observed. The dendritic apatite structures on the surface of pure HA were found to the more thickness after 15 days of waiting time. Hovewer, the dendritic apatite layer on the surface of HA-0.5CeO_2 composite changed to flake like layers at same waiting time. When the immersing time reached to 30 days, all of the surfaces of pure HA and HA-0.5CeO_2 composite were covered by apatite layers. The micrographs clearly exhibited that the apatite crystals has dissimilar morphologies on the surface samples. It is obviously seen that the apatite crystals on the surface CeO_2 added sample has a thicker and smooth without drying cracks. The same structures were also imaged in a previous study [55]. The positive effect of CeO_2 on the in-vitro bioactivity of hydroxyapatite may also related to the $Ca_{0.167}Ce_{0.7}PO_4$ phase, which accelerate the increasing intracellular calcium ions (ubiquitous intracellular messenger) by

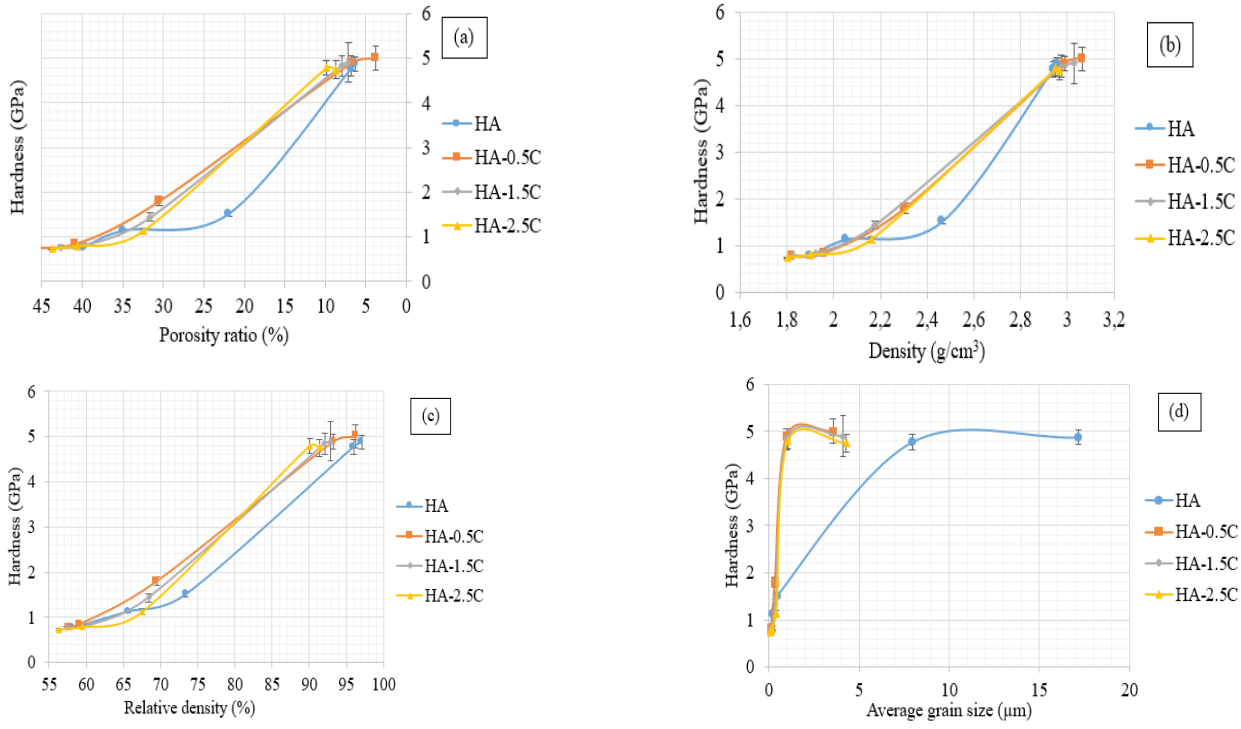

Figure 4. The relationship between microhardness and (a) the porosity, (b) the density, (c) the relative density, and (d) the average grain size of sintered samples

activation of Ca^{2+} receptor found in the membranes up-regulating signaling pathways speeding up the adhesion and proliferation of osteoblasts, as reported Ref [36]. As stated in **Table 2** that HA-0.5CeO_2 composites include β-TCP phase at amount of 8.0% in addition to HA peaks. That type combination known as biphasic calcium phosphate, which has the more bioactivity property compared to pure hydroxyapatite

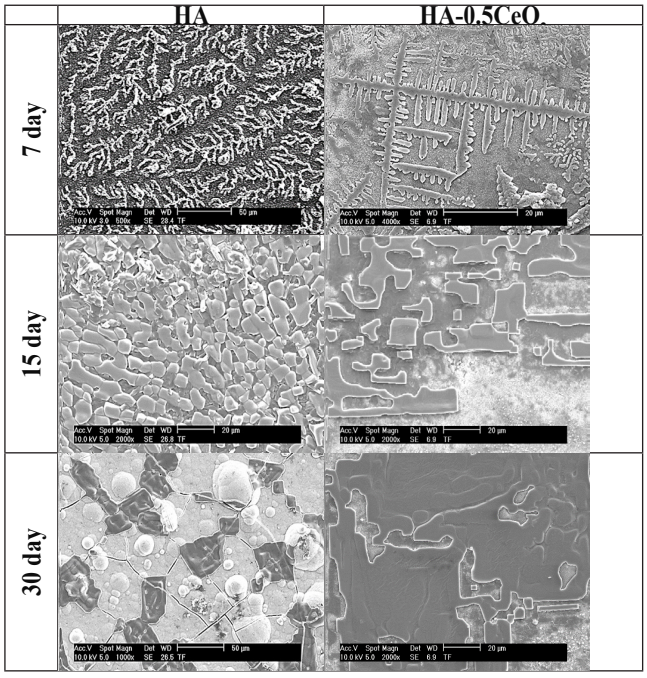

Figure 5 SEM images of pure HA and HA-0.5CeO_2 samples after SBF test

IV. CONCLUSION

In this research hydroxyapatite/CeO_2 composites were sintered at various temperature by pressureless sintering. X-ray diffraction and scanning electron microscopy results clearly revealed that the pure decomposed at 1100 ºC, and when sintering temperatures at elevated temperatures an excessive grain growth with microcracks observed. By adding CeO_2 the grain growth was inhibited, but the decomposition temperature decreased to 900 ºC depending on the increasing CeO_2 ratio. The mechanical properties of hydroxyapatite could be improved when it was doped with CeO_2 at amount of 0.5 wt%. The composite of HA/0.5CeO_2 can be used in human body, because it has enough fracture toughness, compressive strength and in-vitro bioactivity properties.

REFERENCES

[1] Youness, R.A., Taha, M.A., & Ibrahim, M.A., (2017). Effect of sintering temperatures on the in vitro bioactivity, molecular structure and mechanical properties of titanium/carbonated hydroxyapatite nanobiocomposites. *J. Mol. Struct.*, 1150, 188-195.

[2] Yetmez, M., Erkmen, Z.E., Kalkandelen, C., Ficai, A., & Oktar, F.N., (2017). Sintering effects of mullite-doping on mechanical properties of bovine hydroxyapatite. *Mater. Sci. Eng.*, C 77 , 470-475.

[3] Zhou, Y., & Rahaman, M.N., (1997). Effect of redox reaction on the sintering behavior of cerium oxide. *Acta Mater.*, 45(9), 3635-3639.

[4] Wang, X., Deng, L.L., Wang, L.Y., Dai, S.M., Xing, Z., Zhan, X.X., Lu, X.Z., Xie, S.Y., Huang, R.B., & Zheng, L.S., (2017). Cerium oxide standing out as an electron transport layer for efficient and stable perovskite solar cells processed at low temperature. *J. Mater. Chem. A*, 5, 1706-1712.

[5] Nakane, S., Tachi, T., Yoshinaka, M., Hirota, K., & Yamaguchi, O., (1997). Characterization and sintering of reactive cerium(IV) oxide powders prepared by the hydrazine method. *J. Am. Ceram. Soc.*, 80(12), 3221-3224.

[6] Yan, B., Zhang, Y., Chen, G., Shan, R., Ma, W., & Liu, C., (2016). The utilization of hydroxyapatite-supported CaO-CeO_2 catalyst for biodiesel production. *Energ. Conver. Manage.*, 130, 156-164.

[7] Patil, S., Sandberg, A., Heckert, E., Self, W., & Seal, S., (2007). Protein adsorption and cellular uptake of cerium oxide nanoparticles as a function of zeta potential. *Biomater.*, 28, 4600-4607.

[8] Hirst, S.M., Karakoti, A.S., Tyler, R.D., Sriranganathan, N., Seal, S., & Reilly, C.M., (2009). Anti-inflammatory properties of cerium oxide nanoparticles. *Small*, 5(24), 2848-2856.

[9] Gopi, D., Murugan, N., Ramya, S., Shinyjoy, E., & Kavitha, L., (2015). Ball flower like manganese, strontium substituted hydroxyapatite/cerium oxide dual coatings on the AZ91 Mg alloy with improved bioactive and corrosion resistance properties for implant applications. *RSC Adv.*, 5, 27402-27411.

[10] Li, K., Yu, J., Xie, Y., You, M., Huang, L., & Zheng, X., (2017). The effects of cerium oxide incorporation in calcium silicate coating on bone mesenchymal stem cell and macrophage responses. *Biol. Trace Elem. Res.*, 177, 148-158.

[11] Ivanchenko, L.A., Pinchuk, N.D., Parkhomei, A.R., Golovkova, M.E., Molchanovskaya, M.I., & Syabro, A.N., (2009). Effect of cerium dioxide on the properties of biogenic hydroxyapatite sintered with borosilicate glass. *Powder Metall. Met. Ceram.*, 48 (5-6), 305-310.

[12] Gunduz, O., Gode, C., Ahmad, Z., Gökçe, H., Yetmez, M., Kalkandelen, C., Sahin, Y.M., & Oktar, F.N., (2014). Preparation and evaluation of cerium oxide-bovine hydroxyapatite composites for biomedical engineering applications. *J. Mech. Behav. Biomed. Mater.*, 35, 70-76.

[13] Pazarlioglu, S., & Salman, S., (2017). Sintering effect on the microstructural, mechanical, and in vitro bioactivity properties of a commercially synthetic hydroxyapatite. *J. Aust. Ceram. Soc.*, 53, 391-401.

[14] Majling, J., Znáik, A., Palová, S., Stevīk, S., Kovalīk, D.K., & Roy, A.R., (1997). Sintering of the ultrahigh pressure densified hydroxyapatite pure xerogels. *J. Mater. Res.*, 12(1), 198-202.

[15] Ozawa, M. (2004). Effect of oxygen release on the sintering of fine CeO_2 powder at low temperature. *Scripta Mater.*, 50, 61-64.

[16] Pazarlioglu, S., & Salman, S., (2019). Effect of yttria on thermal stability, mechanical and in vitro bioactivity properties of hydroxyapatite/alumina composite. *J. Ceram. Process Res.*, 20(1), 99-112.

[17] Kokubo, T., Yamamuro T., Hench L.L., & Wilson J., (1990). Handbook on Bioactive Ceramics: Bioactive Glasses and Glass-Ceramics. Vol. 1., CRC Press, Boca Raton, U.S.A. s. 1-5.

[18] Ruys, A.J., Wei, M., Sorrell, C.C., Dickson, M.R., Brandwood, A., & Milthorpe, B.K., (1995). Sintering effects on the strength of hydroxyapatite. *Biomater.*,16, 409-415.

[19] Fathi, M.H., Hanifi, A., & Mortazavi, V., (2008). Preparation and bioactivity evaluation of bone-like hydroxyapatite nanopowder. *J. Mater. Process. Technol.*, 202, 536-542.

[20] Wang, A.J., Lu, Y.P., Zhu, R.F., Li, S.T., Xiao, G.Y., Zhao, G.F., & Xu, W.H., (2008). Effect of sintering on porosity, phase, and surface morphology of spray dried hydroxyapatite microspheres. *J. Biomed. Mater. Res. A*, 87(2), 557-562.

[21] Dorozhkin, S.V., (2008). Green chemical synthesis of calcium phosphate bioceramics. *J. Appl. Biomater. Biomech.*, 6(2), 104-109.

[22] Mateus, A.Y.P., Barrias, C.C., Ribeiro, C., Ferraz, M.P., & Monteiro, F.J., (2008). Comparative study of nanohydroxyapatite microspheres for medical applications. *J. Biomed. Mater. Res. A*, 86(2), 483-493.

[23] Locardi, B., Pazzaglia, V.E., Gabbi, C., & Profilo, B., (1993). Thermal behaviour of hydroxyapatite intended for medical applications. *Biomater.*, 44, 437-441.

[24] Muralithran, G., & Ramesh, S., (2000). The effects of sintering temperature on the properties of hydroxyapatite. *Ceram. Inter.*, 26, 221-230.

[25] Frayssinet, P., Rouquet, N., Fages, J., Durand, M., Vidalain, P.O., & Bonell, G., (1997). The influence of sintering temperature on the proliferation of fibroblastic cells in contact with HA-bioceramics. *J. Biomed. Mater. Res.*, 35, 337-347.

[26] Fanovich, M.A., Castro, M.S., & Lòpez, J.M.P., (1998). Improvement of the microstructure and microhardness of hydroxyapatite ceramics by addition of lithium. *Mater. Lett.*, 33, 269-272.

[27] Habibovic, P., Yuan, H., van der Valk, C.M., Meijer, G., van Blitterswijka, C.A., & de Groot, K., (2005). 3D micro environment as essential element for osteoinduction by biomaterials. *Biomater.*, 26, 3565-3575.

[28] Hull, S., Norberg, S.T., Ahmed, I., Eriksson, S.G., Marrocchelli, D., & Madden, P.A., (2009). Oxygen vacancy ordering within anion-deficient ceria. *J. Solid State Chem.*, 182, 2815-2821.

[29] Zinkevich, M., Djurovic, D., & Aldinger, F., (2006). Thermodynamic modelling of the cerium-oxygen system. *Solid State Ionics*, 177, 989-1001.

[30] Kümmerle, E.A., & Heger G., (1999). The Structures of C-$Ce_2O_{3+\delta}$, Ce_7O_{12}, and $Ce_{11}O_{20}$. *J. Solid State Chem.*, 147, 485-500.

[31] Morais, D.S., Fernandes, S., Gomes, P.S., Fernandes, M.H., Sampaio, P., Ferraz, M.P., Santos, J.D., Lopes, M.A., & Hussain, N.S., (2015). Novel cerium doped glass-reinforced hydroxyapatite with antibacterial and osteoconductive properties for bone tissue regeneration. *Biomed. Mater.*, 10(5), 055008.

[32] Gamoke, B., Neff, D., & Simons, J., (2009). Nature of PO bonds in phosphates. *J. Phys. Chem. A*, 113, 5677-5684.

[33] Li, X.W., Yasuda, H.Y., & Umakoshi, Y., (2006). Bioactive ceramic composites sintered from hydroxyapatite and silica at 1200ºC: preparation, microstructures and in vitro bone-like layer growth. *J. Mater. Sci. Mater. Med.*, 17, 573-581.

[34] Evis, Z. (2007). Reactions in hydroxylapatite-zirconia composites, *Ceram. Inter.*, 33, 987-991.

[35] Upasani, M. (2017). Synthesis of $Y_3Al_5O_{12}$:Tb & $Y_3Al_5O_{12}$:Tb,Si phosphor by combustion synthesis: Comparative investigations on the structural and spectral properties. *Opt. Mater.*, 64, 70-74

[36] Mikhailov, M.M., Vlasov, V.A., Yuryev, S.A., Neshchimenko, V.V., & Shcherbina, V.V., (2015). Optical properties and radiation stability of TiO_2 powders modified by Al_2O_3, ZrO_2, SiO_2, TiO_2, ZnO, and MgO nanoparticles. *Dyes and Pigments*, 123, 72-77.

[37] Tan, C.Y., Yaghoubi, A., Ramesh, S., Adzila, S., Purbolaksono, J., Hassan, M.A., & Kutty, M.G., (2013). Sintering and mechanical properties of MgO-doped nanocrystalline hydroxyapatite. *Ceram. Inter.*, 39, 8979-8983.

[38] Hoepfner, T.P., & Case, E.D., (2004). An estimate of the critical grain size for microcracks induced in hydroxyapatite by thermal expansion anisotropy. *Mater. Lett.*, 58, 489 – 492.

[39] Case, E.D., Smith, I.O., & Baumann, M.J., (2005). Microcracking and porosity in calcium phosphates and the implications for bone tissue engineering. *Mater. Sci. Eng. A*, 390, 246-254.

[40] Miao, X., Chen, Y., Guo, H., & Khor, K.A., (2004). Spark plasma sintered hydroxyapatite-yttria stabilized zirconia composites. *Ceram. Inter.*, 30, 1793-1796.

[41] Sameshima, S., Kawaminami, M., & Hirata, Y., (2002). Thermal expansion of rare-earth-doped ceria ceramics, *J. Ceram. Soc. Jpn.*, 110(7), 597-600.

[42] Ruseska, G., Fidancevska, E., & Bosser, J., (2006). Mechanical and thermal-expansion characteristics of $Ca_{10}(PO_4)_6(OH)_2$-$Ca_3(PO_4)_2$ composites. *Science of Sintering*, 38, 245-253.

[43] Chen, M., Lu, C., & Yu, J., (2007). Improvement in performance of MgO-CaO refractories by addition of nano-sized ZrO_2. *J. Eur. Ceram. Soc.*, 27, 4633-4638.

[44] Herliansyah, M.K., Hamdi, M., Ide-Ektessabi, A., Wildan, M.W., & Toque, J.A., (2009). The influence of sintering temperature on the properties of compacted bovine hydroxyapatite. *Mater. Sci. Eng. C*, 29, 1674-1680.

[45] Wang, P.E., & Chaki, T.K., (1993). Sintering behaviour and mechanical properties of hydroxyapatite and dicalcium phosphate. *J. Mater. Sci. Mat. Med.*, 4, 150-158.

[46] Rootare, H.M., & Craig, R.G., (1974). Characterization of the compaction and sintering of hydroxyapatite powders by mercury porosimetry, *Powder Technol.*, 9, 199-211.

[47] Miao, X., Chen, Y., Guo, H., & Khor, K.A., (2004). Spark plasma sintered hydroxyapatite-yttria stabilized zirconia composites. *Ceram. Inter.*, 30, 1793-1796.

[48] Wang, X., Fan, H., Xiao, Y., & Zhang, X., (2006) . Fabrication and characterization of porous hydroxyapatite/β-tricalcium phosphate ceramics by microwave sintering. *Mater. Lett.*, 60, 455-458.

[49] Alymov, M.I., Bakunova, N.V., Barinov, S.M., Belunik, I.A., Fomin, A.S., Ievlev, V.M., & Soldatenko, S.A., (2011). Specific features of the densification of hydroxyapatite nanopowders upon pressing. *Nanotechnologies in Russia*, 6(5-6), 353-356.

[50] Pazarlioglu, S.S., Gokce, H., Ozyegin, L.S., & Salman, S., (2014). Effect of sintering on the microstructural and mechanical properties of meleagris gallopova hydroxyapatite. *Bio-Med. Mater. Eng.*, 24, 1751-1769.

[51] Ryu, H.S., Youn, H.J., Hong, K.S., Chang, B.S., Lee, C.K., & Chung, S.S., (2002). An improvement in sintering property of β-tricalcium phosphate by addition of calcium pyrophosphate. *Biomater.*, 23, 909-914.

[52] Mansour, S.F., El-dek, S.I., & Ahmed, M.K., (2017). Physico-mechanical and morphological features of zirconia substituted hydroxyapatite nano crystals. *Sci. Rep.*, 7, 43202.

[53] Hoepfner, T.P., & Case, E.D., (2003). The influence of the microstructure on the hardness of sintered hydroxyapatite. *Ceram. Inter.*, 29, 699-706.

[54] Wang, J., & Shaw, L.L., (2009). Nanocrystalline hydroxyapatite with simultaneous enhancements in hardness and toughness. *Biomater.*, 30, 6565-6572.

[55] Zhu, Q., Ablikim, Z., Chen, T., Cai, Q., Xia, J., Jiang, D., & Wang, S., (2017). The preparation and characterization of HA/β-TCP biphasic ceramics from fish bones. *Ceram. Inter.*, 43, 12213-12220.

Int. J. Adv. Eng. Pure Sci. 2019, 4: 305-315
DOI: 10.7240/jeps.554409

RESEARCH ARTICLE / ARAŞTIRMA MAKALESİ

Evaluation of Performance by Operating Process Improvement Modeling on a Company with Pump Manufacturing

Pompa İmalatı Yapan Bir Firmada Süreç İyileştirme Modellemesiyle İşletmenin Performansının Değerlendirilmesi

Ahmet Talat İNAN [1], Mehmet Akif KARTAL [2]

[1] Marmara University, Faculty of Technology, Department of Mechanical Engineering, 34722, Göztepe – İstanbul / Turkey

[2] Bandırma Onyedi Eylül University, Central Campus, 10200, Bandırma – Balıkesir / Turkey

Abstract

There may be more than one element affecting quality and efficiency in the manufacturing organizations. As a result of multiple elements occurring at the same time, permanent losses occur in final production and quality. Both the customer sense of trust and their satisfaction are negatively affected because of those problems.

Failure to achieve targeted levels of quality and productivity in the organization reduces customer satisfaction. Quality and productivity in the organization are affected by inefficiency in resource utilization, bottlenecks in the production and inefficient workflow design within the organization.

This study aims to improve production process in a manufacturer of air operated diaphragm pumps by simulation analysis. Most efficient way of utilizing raw materials, manpower, vehicles and equipment is sought by simulation based process improvement. Discrete-event simulation software (Arena) is used to detect problems in the production process such as: transportation, blockage and/or layout. Simulation is used to experiment with process improvement approaches without making changes in the real-world production system.

Simulation models of the current state and the proposed future state with improvements to the layout of the production system are created. The results from the models were compared with each other and evaluations were made. The future state simulation model utilizes existing resources for process improvement, without the requirement for additional resource acquisition. Comparison of current state model and future state model simulation output data, suggests a 67% increase in the number of products produced per month. It is foreseen that this increase can greatly affect the operational efficiency and future managerial decisions, and suggestions are made for future works.

Keywords: Assembly Line, Process Improvement Simulation, Pump, Pump Process Improvement.

Öz

İmalat organizasyonlarında kaliteyi ve verimliliği etkileyen birden fazla unsur olabilir. Aynı anda meydana gelen çoklu elemanların bir sonucu olarak, nihai üretim ve kalitede kalıcı kayıplar meydana gelir. Bu sorunlar nedeniyle hem müşteri güven duygusu hem de memnuniyeti olumsuz yönde etkilenmektedir.

Kuruluşta hedeflenen kalite ve verimlilik seviyelerinin sağlanamaması müşteri memnuniyetini azaltır. Kurumdaki kalite ve verimlilik, kaynak kullanımındaki yetersizlik, üretimdeki darboğazlar ve organizasyon içindeki yetersiz iş akışı tasarımından etkilenir.

Bu çalışma, simülasyonlu analizle hava ile çalışan bir diyafram pompa üreticisindeki üretim sürecini iyileştirmeyi amaçlamaktadır. Simülasyona dayalı süreç iyileştirme ile hammadde, insan gücü, araç ve gereç kullanmanın en etkili yolu aranmaktadır. Kesikli olay simülasyon yazılımı (Arena), üretim sürecindeki sorunları tespit etmek için kullanılır: ulaşım, tıkanma ve / veya düzen. Simülasyon, gerçek dünya üretim sisteminde değişiklik yapmadan süreç iyileştirme yaklaşımlarını denemek için kullanılır.

Sorumlu yazar/Corresponding Author: Ahmet Talat İNAN, **Tel:** +905326549884, **e-posta:** inantalat@gmail.com,
Gönderilme/Submitted: 16.04.2019, **Düzenleme/Revised:** 31.08.2019, **Kabul/Accepted:** 15.10.2019

Üretim sisteminin düzeninde iyileştirmelerle mevcut durumun ve önerilen gelecek durumun simülasyon modelleri oluşturulmuştur. Modellerin sonuçları birbirleriyle karşılaştırıldı ve değerlendirmeler yapıldı. Gelecekteki durum simülasyon modeli, ek kaynak edinme şartı olmadan, süreç iyileştirme için mevcut kaynakları kullanır. Mevcut durum modeli ve gelecekteki durum modeli simülasyonu çıktı verilerinin karşılaştırılması, ayda üretilen ürün sayısında % 67 artış olduğunu göstermektedir. Bu artışın operasyonel verimliliği ve gelecekteki yönetim kararlarını büyük ölçüde etkileyebileceği ve gelecekteki çalışmalar için önerilerde bulunacağı öngörülmektedir.

Anahtar Kelimeler: Montaj Hattı, Süreç İyileştirme Simülasyonu, Pompa, Pompa Süreç İyileştirme.

1. INTRODUCTION

Production planning and control is a predetermined process, which includes the use of human resource, raw materials, machines etc. PPC is the technique to plan every step in a long series of separate operation. Therefore, it is the other name of the function that determines the levels or limits of the future activities and which takes precautions at the required times. Production planning and control functions and objectives are to organize the production facilities like machines, men, etc., to achieve stated production objectives with respect to quantity and quality time and cost. In addition, it is to conform to delivery commitments. Also, coordinate with other departments relating to production to achieve regular balanced and uninterrupted production flow.

Companies strive for continuous improvement of their business processes and production systems in order to main their competitiveness and/or status quo under fierce global competition. Therefore, it can be said that the importance of process management and process improvement is of great importance.

In recent year's textile and apparel companies in Turkey are threatened by increased competition especially from their Asian rivals that have the advantage of low labor costs. Therefore, companies should prioritize rational use of their resources and place emphasis on efficiency and efficacy of their business operations.

In most of the enterprises operating in the sector, there are basic problems such as inability to use resources effectively, bottlenecks in production lines or unbalanced workflows. These problems reduce efficiency / productivity; which adversely affects product quality, customer satisfaction and service levels.

In this study a simulation analysis based process improvement methodology is proposed to improve layout in a discrete parts manufacturer of diaphragm pumps which in turn positively affects productivity and quality levels. Simulation analysis point to problems in the current layout of the enterprise which hinder effective usage of resources. Current production process also includes bottlenecks and capacity utilization is lower than expected. The main purpose of this study is to propose a simulation analysis based methodology for layout improvement. Manufacturing system layout of a discrete parts manufacturer of diaphragm parts is analyzed to propose an improved future state with gains in productivity and quality levels.

In the second part of the study, information was given about the studies carried out on process improvement. In the third chapter, the application related to the process improvement in a pump manufacturer is explained. As a result, a general performance evaluation was made and recommendations were made for future studies.

2. LITERATURE REVIEW ON PROCESS MODELING AND IMPROVEMENT

This section includes a review of existing literature on process improvement in manufacturing sector.In the production management process, it is simply a series of operations where inputs are transformed into output through a production process. Process planning is the design and implementation of a production system that will enable the production of the desired product or service in the desired amount, at the most appropriate time and with acceptable cost [1]. Process management aims to ensure continuous monitoring and improvement of processes. Within this scope, continuous evaluation, analysis and improvements are carried out in order to design and maintain the processes and to better meet customer expectations and needs [2].

In a study carried out in the textile sector, bottlenecks in the production line of a manufacturer of jeans were identified and a process improvement was proposed to eliminate bottlenecks. A simulation based assembly line balancing approach was proposed and resulting improvements were analyzed. Comparison of future and current state simulation models indicate 47% improvement in productivity [3].

In the study carried out in an automotive supplier industry, physical resources such as labor, materials, machinery and equipment have been re-designed in a way to minimize the total material and transportation cost and process development has been studied. Effects machine-equipment layout changes on the manufacturing system performance were examined. In the study, LayOPT package program was used for the placement of the physical resources, and the new settlement plan and the improvements made by the ARENA simulation program were used to measure the performance

of the new placement method and it was observed that the improvements have a positive affection the performance [4].

In a study carried out in an aviation company that collaborates with global partners such as Airbus and Boeing on research and development (RD) and manufacturing projects, a new manufacturing model was proposed that enhances quality control and improvement in the manufacturing process. The firm's current quality control approach is to avoid errors with close to 100% inspection. The proposed system has mechanisms that take into account changes in the variety and quantity of products, improvements in the system and capacity constraints. According to the results obtained from carrying out statistical process control, failure modes and effects analysis (FMEA) and measurement system analysis, quality levels were improved not just in the final product but also on other areas such as workforce training, lean production system and product design. [5].

Another study was conducted on Total Productive Maintenance (TPM); a general approach to maintenance that aims to improve production and quality levels. TPM is a guideline that aims to achieve zero percent failure and error goal with active participation from all level of employees. Results of the analysis indicate significant improvements in production levels as a result of changes in traditional maintenance approaches, continuous training, inter-departmental coordination, sharing of responsibility and usage of computer software [6].

Referring to the importance of methodical approach in machining optimization, Six Sigma study was conducted in the sector to reduce the breakage rate of cutting tools. Accordingly, cutting tool breaks have been reduced by 85%, it earned a profit of over €1000000 [7].

The program of TRIZ, which has been used in design and manufacturing processes, has been carried out by using this technique which helps to develop creative solutions to problems in "Theory of Inventive Problem Solving". The implementation of TRIZ in the manufacturing process was discussed and the effects on the process were evaluated with the results of the sample application. The results show that TRIZ may contribute to the optimization of the manufacturing process [8].

In order to measure the effectiveness of business assets, a study was performed by using Overall Equipment Effectiveness (OEE) analysis. In this context, OEE analysis was carried out by expressing the equations related to machine and equipment conformity, performance efficiency, quality product ratio calculations in a firm that produces aspirators. A method for improvement such as single minute exchange of dies (SMED) and process planning was proposed. Results indicate improvement in process performance [9].

A process improvement study was carried out at the factory that manufactures hydraulic gear pumps. Engineering system analysis was made to improve material handling and man-machine utilization time. Man-machine utilization charts and Group Technology (GT) techniques were proposed to improve man-machine utilization and material handling [10].

Process development work was carried out in a company producing pump impellers. Since the propeller shape has a direct effect on the efficiency and performance of the pump, 3D designs have been made. According to propeller shape, performance and yield values were compared. According to the findings, the results of the propellers designed with the 3D designs made in place have been added to the yield and performance values [11].

A process improvement study was carried out for the transition to a lean manufacturing system in a company that uses batch production. Batch production; a production system in which similar or same-type products are produced in batches to meet a certain order or continuous demand. Lean manufacturing is a concept aimed at reducing waste, increasing quality and adding value to the company. Toyota Manufacturing System (TMS) is the precursor to lean manufacturing (LM) system with the latter born out of efforts of Western practitioners to adopt TMS to Western companies. The study synchronizes and increases adaptability of the manufacturing system using process improvement methods during transition to improve efficiency and performance. Transition from batch production system to lean manufacturing system resulted in improvements in levels of productivity, efficiency and performance rates [12].

Chan and Spedding examined quality and cost assessment with total Quality Management for business process restructuring and process improvement [13]. Schiefer emphasized the importance of case studies on the application of environmental management concepts in industry by attracting attention to environmental issues for process improvement and process efficiency in supply chain management [14].

Freire and Alarcon proposed an improvement methodology for the design processes of construction projects. In this study, it is aimed to ensure efficiency with improvements related to cycle times and waiting times [15]. Rohleder and Silver conducted a literature review on process improvement, emphasizing the strategic importance of business process improvement and, based on personal experience [16].

Kayışkan carried out process management practices and process improvement studies in a food business. The aim

of this study is to determine the processes, measure the data related to the process, implement the process management, monitor the applications and improve the processes in the process through process improvement techniques [17].

The details of the process development project at BSH were studied [18]. Karaman has implemented corporate process improvement in a finance company [19]. Etleç (2017), by the application of the process improvements in lean manufacturing techniques have been applied in a cosmetics company [20].

A company that performs ice cream production was carried out. The current situation analysis was conducted by examining all stages of business processes. After the analysis, the problems were determined and the studies were carried out to solve the problems by selecting the appropriate methods. As a result of the application, the main problems were identified and workmanship errors, cleaning and hygiene, and factory layout solutions were produced. Some of the solutions produced have been implemented and provided significant improvements in a short time, while some of the proposals were evaluated by taking into consideration the medium-term targets of the organization [21].

The study focuses on Jishuken technique. In order to better understand the technique, the Japanese business management style, the logic of lean manufacturing and the philosophy of continuous improvement are explained. Then, the concepts and features of the Jishuken technique, training and implementation steps of the process, as well as the application of the method to show the selected examples were emphasized. The result of this study is that it is a recommended way of working to reduce unwanted costs in enterprises, to train qualified managers, to strengthen internal communication, to adopt the principle of continuous improvement of the managers, to adopt the process, to reduce the resistance to lean transformation in enterprises and to establish a working philosophy in the enterprise [22].

Şenol (2017), the energy saving potential of the pumps and pumping systems used in the water plant unit of an enterprise operating in the iron and steel sector was investigated. As a result, the energy consumption has been reduced from 240 kWh to 109 kWh in winter, and from 347 kWh to 125 kWh in summer, bringing the total value from approximately 2.241.000 kWh / year to 920.000 kWh / year [23].

Alpaslan (2018), conducted a process improvement study focused on customer satisfaction at an automotive service department [24].

3. MATERIAL AND METHODS

Computer simulation models are created to mimic the behavior of the real-world system. Simulation modeling provides us with the flexibility to work on the model of the engineering system considered, avoiding the difficulties associated with making changes in the real-world environment. Simulation modeling allows us to anticipate the effects of changes made to the engineering system before changes are made. In this study, Arena 13.0 discrete-event simulation software was used.

When developing a simulation model, a number of steps must be followed. These are; analysis of the system, formulation of the model, verification and validation of the model logic, planning of experiments, analysis and interpretation of results [25].

Simulation method has advantages and disadvantages as other methods. The advantages of the simulation method can be listed as follows:

- Most complex systems cannot be analytically evaluated and accurately defined by mathematical models. In such cases, simulation is the only research method.
- Simulation makes it easy to estimate an existing system according to changing conditions.
- It is possible to find out which of the proposed different system designs will best meet the desired target by simulation method.
- Once the model of the system is created, it can be used as many times as needed in the analysis of different situations.
- It is inexpensive to obtain data for the system.
- Simulation is the most appropriate method when system data is not very detailed.
- Simulation enables the examination of dynamic structures by emphasizing the universality of the systems.

The disadvantages of the simulation method can be listed as follows:

- Hide critical assumptions that invalidate the model,
- Not applicable to deterministic problems,
- May not propose a solution methodology,
- May not provide optimal solution,
- Requires expertise to build complex and comprehensive models,
- Data collection, modeling and analysis can be costly.

There are different package programs developed for simulation. In this study, ARENA 13.9 package program was used.

Arena is a popular simulation program with a Windows interface developed by Systems Modeling Corporation, which also introduced Siman. Arena program includes detailed and comprehensive functions such as animation, analysis of input and output data required for successful simulation.

When creating a program model, Arena uses Siman commands to run the created model. But the feature of this program is that almost no command information is needed. In Arena, you can create your model program by adding the modules that are given shortcuts in the templates to your program page and by entering the desired information (arrival time, stack size, next station name, etc.) in the window that opens when you double-click these modules.

Since the Arena runs under Windows, it provides great convenience for working with toolbars, menus, and windows. The strength of the Arena model system is that it allows special applications in environments such as production, health sector, flow lines, computer networks. Therefore, it was deemed appropriate to use Arena simulation program.

Simulation was used as a method in the study. Simulation is the imitation of the behavior of the real system in a computer environment. Simulation provides important insights into what kind of changes we can make to a system without changing or stopping it. It also allows us to anticipate the impact of future changes to the system on the system.

The flowchart showing the steps of the simulation process can be expressed as follows:

- Problem identification,
- Setting up the computer model,
- Ensuring the validity of the model,
- Designing experiments
- Collecting necessary data,
- Performing the simulation,
- Evaluate statistical outputs,
- Review the simulation,
- Further data collection and analysis,
- Reporting

3.1. Current Situation Simulation Model

The following pictures are taken from the Arena program we used.

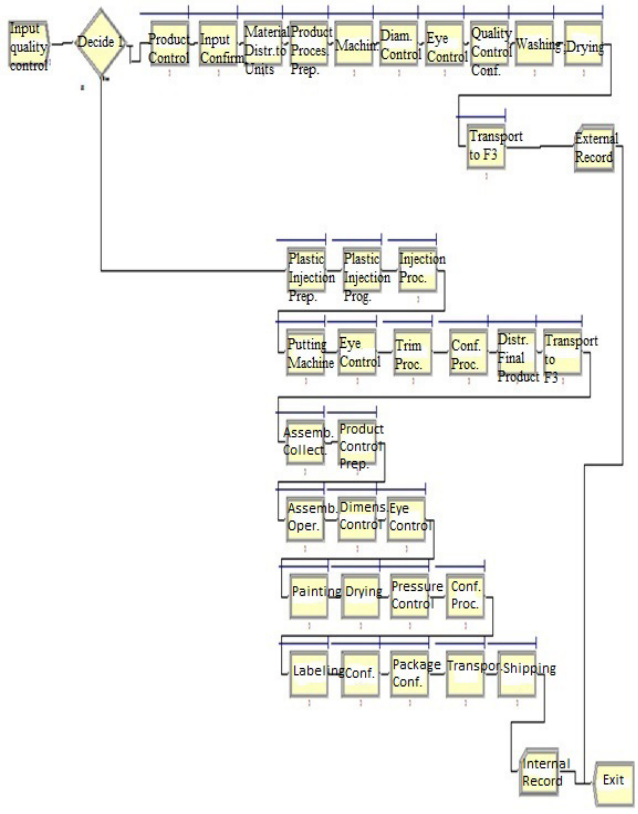

Figure 1. Current Situation Simulation Model

3.2. Future Situation Simulation Model

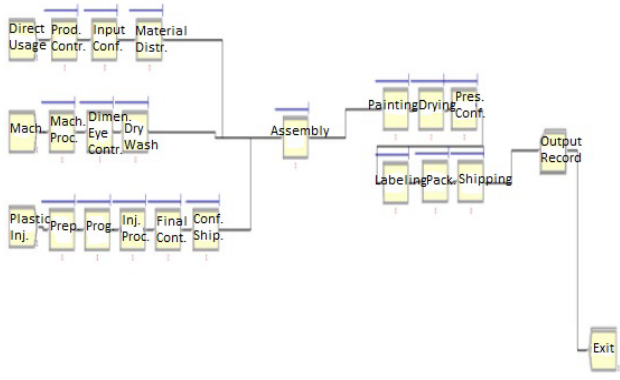

Figure 2. Future Situation Simulation Model

Verification: It is performed to verify that the simulation model reflects the real system in the same way. All the flows from the first entry to the system with the create module with the dispose module from the system are followed step by step and the inputs are passed through all the necessary steps in the system respectively. From this it was concluded

that the system was verified. So the model represents the actual system adequately.

Validation: It is a stage in which the outputs obtained from the simulation model are compared with the outputs of the real system. At this stage, the outputs from the simulation and the outputs of the actual system are compared. If there is no statistically significant difference between the two main findings, it is concluded that the model is valid.

Finally, In the validity test phase of the model "Final Number of Products" is taken as performance measure. When the historical data of the real system for the 12-month period between January and December 2017 were obtained, it was seen that the number of final products was 4391. On the other hand, the number of final products obtained from the simulation model was found to be 4396. The results were found to be very close to each other. It is concluded that the model has been verified.

Herein, future situation simulation model and current situation simulation model were created. In these models, each square box shows a process in production. The operation times of these processes is entered into the program according to the information received from the company. The compiled version of these data are given in Table 1. When this information is entered into the related operations and the model is executed, the result gives us the number of final products. In the same way, the future situation simulation model is developed and improvements are made and the final product number is obtained. The yield ratio is obtained by comparing these two final product numbers.

4. APPLICATION

4.1 Firm's Basics

Since 2001, the company has been producing diaphragm pumps, it is a medium-sized firm and has about 70 employees. It is a firm that manufactures both air and electric diaphragm pumps and has a wide place in domestic market and exports to many countries.

Pump manufacturing process involves sand casting of a component that is done at a subcontractor which is then shipped to the company. Sand-casted pump part is then machined, machining process is followed by production of the pump's diaphragm component using plastic injection. Pump assembly and quality control of the finished product takes place next. After quality inspection the pump is transferred to paint shop. The painted pump is then stored in the finished goods area.

4.2 Product Flow in Firm

The production flow diagram of the diaphragm pump is as follows [26]:

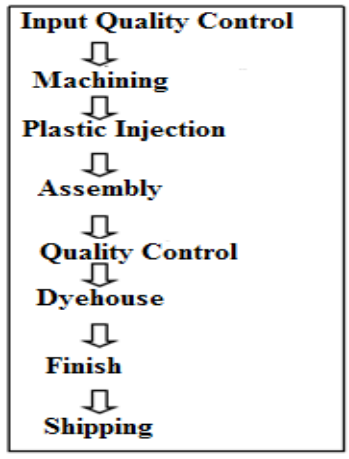

Figure 3. Production Flow Chart

In the ground floor of the manufacturing facility there is a quality control section for raw materials and semi-finished goods. The machining department is also located on the ground floor with multiple vertical milling machines and lathes with a storage area for machined components. Quality control section in the ground floor inspects incoming materials and if the procured material passes inspection approval is granted to use the material in downstream production processes. On the 2nd floor, a plastic injection machine produces several pump components in batches. A single batch of injection moulded parts are produced in a single production run followed by visual inspection and splitting of individual parts that are interconnected [27].

Painting shop and assembly area are located on the third floor where components are painted and assembled to create the finished product. Assembly area is separated from other areas by glass walls requiring movement of components to be assembled into this area manually. There is a final quality inspection of finished goods before shipping. If finished-product passes quality inspection, it is transported to the packaging area.

4.3 Problems in Production Flow and the Proposed Future-State for Solving Those Issues

The situation in which the process has been improved after the changes that are planned to be made in the current situation is shown by the future-state model. A number of improvements have been obtained with the future-state model. A

number of problems have been observed in the current production flow. The main problems identified are [28]:

- It was determined that human resources and equipment was not utilized effectively in the shop-floor.
- Inefficient usage of workforce leads to lack of efficiency in production and decreases productivity.
- Line balancing becomes an issue since bottlenecks in the production process cannot be detected and remedied. For instance, insufficient number of personals was identified as a bottleneck in the production and the problem was solved by transferring personal from other departments to the assembly department.
- Even though the ground floor has adequate space, it is not used effectively since only the machining department is located at this floor. There are also problems with workflow since assembly, painting and quality control departments are located at the third floor. At the same time, the installation, paint shop and quality control departments on the third floor cause confusion in the workflow.
- Work flow and inter-departmental disturbances cause loss of time, which prevents timely delivery of products and therefore delivery times are usually not met [29].
- Overtime work is done to meet delivery times which leads to additional production costs and negatively affects employee performance. The rapid work done to meet the delivery times cause quality problems in the line and this prevents the coordination between the employees. Delays and quality problems arising from rapid work also negatively affect customer satisfaction and lead to loss of confidence [30].
- In the present case, a future simulation model is proposed to solve the above problems. To solve the space and workflow issues on the ground floor, it was suggested to carry the finishing and packaging section to the ground floor and to the assembly and paint shop area. Quality Control area on the third floor was moved to the second floor. Thus, it is estimated that lead-time and disturbances in production flow will be alleviated with new layout.

A number of arrangements have been made for the simulation model of the future and current state. These regulations are as follows:

- Several personnel were relocated to detected bottleneck operations in the assembly area from the quality control area since they were not used effectively in their current area.
- The quality control section was moved to the second floor. Thus, the time of transport of the materials is reduced.
- The joker milling machine in the machining section with low efficiency is placed as main band. Thus, performance and efficiency of the machining area was improved.
- The processed products section on the ground floor was removed from there and moved to an upper floor.
- Assembly and painting areas were relocated to the ground floor.
- Two personnel are relocated to the assembly section which is determined as a bottleneck and product collection and control operations have been made faster.
- The drying process of the parts from the machining process is taken from the ground floor
- In order to ensure interdepartmental coordination, the division of labor has been increased and the division of work that is done on the same workstation among workers has been eliminated. For instance, removal of part from the plastic injection machine and checking for defects was aggregated into a single operation to be completed using a single operator.

4.4 Utilizing the Simulation Method to See the Impact of the Proposed Flow in the Future

The proposed improved process for the future situation has been utilized as a result of the simulation method to see what will change in the current system and how the existing system will be affected. In this context, firstly, the current state simulation model was established and it was confirmed that this model represents the current system in full. Later on, a current state simulation model has been created by making some changes on the existing simulation model. It is seen that the proposed process for the future situation is effective by comparing the future situation simulation model with the outputs of the current situation simulation model.

4.4.1 Current state simulation model for product flow in firm

The scope of application is modeled by simulating the existing production flow simulation in the machining, plastic injection process, assembly, quality control, painting and finish sections. The ARENA 13.9 package program was used to create simulation models. Table 1 is shown that statistical distributions for operation times.

Table 1. Statistical Distributions of Operation Times

DEPARTMENT	OPERATION	DISTRIBUTION	TIME (MINUTE)
Input Quality Control	Product Inspection	Expression	75
	Input Confirmation	Expression	30
	Distribution of Materials to Units	Expression	23
	Product Process Preparation	Expression	5
Machining	Machining	Expression	7
	Measure Control	Expression	8
	Eye control	Expression	2
	Quality Control Approval	Expression	10
	Washing	Expression	12
	Drying	Expression	45
	Moving to 3rd Ground	Expression	35
Plastic Injection Department	Plastic Injection Preparation	Expression	12
	Plastic Injection Programming	Expression	8
	Injection Process	Expression	6
	Taking of the product from the machine	Expression	2
	Eye Control Process	Expression	2
	Trimming Process	Expression	2
	Approval Process	Expression	3
	Separation to the finished product section	Expression	3
	Dispatch Process to 3rd Ground	Expression	35
Assembly	Collecting Parts	Expression	45
	Product Preparation	Expression	12
	Mounting Operation	Expression	32
	Dimension Control	Expression	5
	Eye Control Operation	Expression	2
Dyehouse	Dyeing Process	Expression	10
	Drying Process	Expression	120
	Pressure Control Operation	Expression	20
	Approval Operation	Expression	5
Finish	Labeling Operation	Expression	2
	Approval Products	Expression	15
	Packaging Operation	Expression	10
	Trucking	Expression	75
	Shipment Operation	Expression	55

4.4.2 Verification of the current state of the simulation model and validity testing

Verification: It is performed to verify that the simulation model reflects the real system in the same way. All the flows from the first entry to the system with the create module with the dispose module from the system are followed step by step and the inputs are passed through all the necessary steps in the system respectively. From this it was concluded that the system was verified. So the model represents the actual system adequately.

Validation: It is a stage in which the outputs obtained from the simulation model are compared with the outputs of the real system. At this stage, the outputs from the simulation and the outputs of the actual system are compared. If there is no statistically significant difference between the two main findings, it is concluded that the model is valid.

In the validity test phase of the model ”Final Number of Products” is taken as performance measure. When the historical data of the real system for the 12-month period between January and December 2017 were obtained, it was seen that the number of final products was 4391. On the other hand, the number of final products obtained from the simulation model was found to be 4396. The results were found to be very close to each other. It is concluded that the model has been verified.

4.5 Analysis of Simulation Results and General Evaluation of Simulation Results

In the future status simulation model, more resources of the same quality are provided by working with the same resources without adding extra resources with the existing resources. The final product number, which is taken as the performance criterion, is compared according to the current situation simulation model and the data obtained from the future situation simulation model. According to the current situation simulation model data, the one-year number of Final Products was 4396 and the number of Final Products was 366 per month.

On the other hand, according to the data of the future case simulation model, the one-year number of Final Products was 7352 and the number of Final Products was 613 per month. It is determined that there are 2956 differences between the current situation simulation model and the final product number of the future situation simulation model and 246 items per month. Based on these findings, it is seen that there is a 67% increase in the number of the final case simulation model compared to the current situation simulation model data.

Table 2. Comparisons of Data Obtained from Present Status Simulation Model and Data Obtained from Future Status Simulation Model

Period	Data from the Current Situation Simulation Model (Final Number of Products)	Data from the Future Situation Simulation Model (Final Number of Products)
12 Months	4396	7352
Average	366	613
Increase		**% 67**

Table 3. Comparisons of Time Data Obtained from Present Status Simulation Model and Data Obtained from Future Status Simulation Model

VA Time (Minute)	Average	Minimum Value	Maximum Value
Time Data from the Current Situation Simulation Model	**7.0980**	**6.1667**	**8.0167**
Time Data from the Future Situation Simulation Model	**3.5568**	**3.1500**	**4.3333**
Difference	**3.5412**	**3.0167**	**3,6834**

With VA Time, Current Situation Simulation Model Average process time which is 7.0980 minutes is shortened to 3.5568 minutes. That is why the difference between current status and future status is 3.5412 minutes. On the other hand, Current Situation Simulation Model Minimum process time which is 6.1667 minutes is shortened to 3.1500 minutes. That is why the difference between current status and future status is 3.0167 minutes. For the last value, Current Situation Simulation Model Maximum process time which is 8.0167 minutes is shortened to 4.3333 minutes. That is why the difference between current status and future status is 3.6834 minutes.

5. CONCLUSIONS

The purpose of this work is to improve process in a manufacturing enterprise. In this context, an enterprise operating in the manufacturing sector was dealt with and the flow of one of the products produced by this enterprise was examined and the problems in the production of the said enterprise were determined and they were tried to be eliminated.

The current situation is compared with the future situation and the performance evaluation of the company has been done. According to this study, the results and evaluations are as follows;

- A future situation model for eliminating the problems encountered in the current situation is proposed. At this stage, the simulation model of the current situation was developed. Once this model has been verified and tested for validity, the proposed future situation simulation model has been developed.
- Future situation simulation model and the sources which are not used effectively in the installation section are evaluated at the determined bottleneck points. In addition, two personnel were given to the assembly section which was seen as the bottleneck point and the human resource was reinforced. The product collection and control operations there were made faster.
- At the same time, it has been suggested that the processed products section on the ground floor is removed and moved to an upper floor. Mounting and paint sections on the third floor was moved to the ground floor to the vacated place. Thus, the work flow problems and loss times between the sections were eliminated.
- When the current situation is compared with the future situation, it is determined that there are 2956 differences between the current situation simulation model and the final product number of the future simulation model and it corresponds to 246 units as the average of the month. Based on these findings, it is seen that there is a 67% increase in the number of the final case simulation model in the final case compared to the current situation simulation model data.

The application of this study has been carried out with a focus on one of the products (models) produced by the pump manufacturer. Therefore, it is possible to realize the implementation of the applications in the different sectors that are concerned with the process improvement as well as the contribution of the results obtained from the study to the sector.

It is believed that study for the future studies would be contributed to the sector and the companies manufacturing pump in terms of total cost reduction, improving quality, increasing competitiveness, customer satisfaction, annual production capacity, number of final products, reduction of scrap rate and efficiency improvement works.

Acknowledgment

This study was conducted by Lecturer Mehmet Akif KARTAL under the supervision of Assistant Professor AHMET TALAT İNAN, was completed in Marmara University, Institute of Science and Technology, Department of Mechanical Engineering Department and it is derived from the master thesis titled of " Evaluation of Performance by Operating Process Improvement Modeling On a Company with Pump Manufacturing".

REFERENCES

[1] Monks, J., G. (1996) "İşlemler Yönetimi" S. Üreten (2. Bas. Çev.), İstanbul, Nobel Yayıncılık.

[2] Bozkurt, R. (2003) "Süreç İyileştirme" 3. Basım, Ankara, MPM.

[3] Takcı, E.: 'Bir İmalat İşletmesinde Simülasyon Yardımıyla Süreç İyileştirme Uygulaması Kayseri Gürkar Tekstil Örneği', Yüksek Lisans Tezi, Nevşehir Hacı Bektaş Veli Üniversitesi Sosyal Bilimler Enstitüsü, Nevşehir, Türkiye, (2013).

[4] Yurdakul, M.; Eşkin, S.; İç, Yusuf T.İ.:'Bir İmalat Sisteminin Yerleşim Düzeninin İyileştirilmesi', Gazi Üniversitesi Mühendislik Fakültesi, Başkent Üniversitesi Mühendislik Fakültesi, Ankara, Türkiye, (2009).

[5] Özateş, M.; Şahin, M.; Şenol, S.; Terzi, F.; Yörükoğlu, S.; Köksal, G.; Serin, Y.:'Düşük Hacimli Üretim İçin Kalite Kontrol Sistemi Tasarımı', Orta Doğu Teknik Üniversitesi Mühendislik Fakültesi, Ankara, Türkiye, (2012).

[6] Yurdakul, M.; Türkbaş, S.; Altınova, S.:'Bir İmalat Tesisinde Toplam Verimli Bakım (TVB) Uygulaması', Gazi Üniversitesi Mühendislik-Mimarlık Fakültesi, Ankara, Mercedes-Benz Türk A.Ş. Aksaray Fabrikası, Aksaray, (2008).

[7] Oran, A.:'Talaşlı İmalat Optimizasyonunda Metodik Yaklaşım ve Sektörel Bir Altı Sigma Proje Uygulaması', BOSCH San. ve Tic. A.Ş. Teknik Fonksiyonlar 1 Departmanı, Bursa, Türkiye, (2012).

[8] Şahin, Ş.; Öztürk, F.:'İmalat Süreçlerindeki Problemlere Optimum Çözüm Arama ve Bir Uygulama', Uludağ Üniversitesi Mühendislik-Mimarlık Fakültesi, Bursa, (2009).

[9] Görener, A.:'Toplam Verimli Bakım ve Ekipman Etkinliği: Bir İmalat İşletmesinde Uygulama', Electronic Journal of Vocational Colleges, İstanbul, (2012).

[10] Kathiriya$_1$, J. J.; Amareliya$_2$, V.D.; Kapadiya$_3$, S. H.:'Production Process Analysis On Manufacturing of Hydraulic Gear Pump', [1]Department of Mechanical, Shantilal Shah Engineering College, Bhavnagar, Gujarat, INDIA$_2$ Department of Mechanical, Mahatma Gandhi Institute of Technical Education and Research Centre, Navsari, Gujarat, INDIA$_3$ Department of Mechanical, Mahatma Gandhi Institute of Technical Education and Research Centre, Navsari, Gujarat, INDIA, (2014).

[11] Kaljahi, B. Z.:'Reverse Engineering of Pump Impeller Utilizing Rapid Prototyping Technology', Eastern Mediterranean University the Institute of Graduate Studies and Research, Gazimağusa, North Cyprus, (2015).

[12] Tamlander, J.:'Defining a Manufacturing Planning and Control Model for a Lean Manufacturing Company', Bachelor's Thesis, JAMK University of Applied Sciences, Technology Degree Programme in Logistics Engineering, Jyväskylä, Finland, (2016).

[13] Chan, K., K. ve Spedding T., A. (2003). An Integrated Multidimensional Process Improvement Methodology for Manufacturing Systems. Computers & Industrial Engineering, 44(4): 673-693.

[14] Schiefer, G. (2002). Environmental Control for Process Improvement and Process Efficiency in Supply Chain Management – the Case of the Meat Chain. International Journal of Production Economics, 78(2): 197-206.

[15] Freire, J. ve Alarcon, L. (2002). Achieving Lean Design Process: Improvement Methodology. Journal of Construction Engineering and Management, 128(3): 248-256.

[16] Rohleder, T., R. ve Silver, E., A. (1997). A Tutorial on Business Process Improvement. Journal of Operations Management, 15(2): 139-154.

[17] Özveri, O. ve Kayışkan, D. (2016). Bir Gıda İşletmesinde Süreç Yönetimi ve Süreç İyileştirme Uygulaması, s. 12-25.

[18] Er, Ö. (2016). Process Improvement and an Industrıal Example Over Company BSH, Bahçeşehir University, Master Thesis, İstanbul.

[19] Karaman U. (2017). Bir Finans Şirketinde Kurumsal Süreç İyileştirme ve Uygulaması, Maltepe Üniversitesi, Yüksek Lisans Tezi, İstanbul.

[20] Etleç, B. (2017). Yalın Üretim Tekniklerine Bağlı Süreç İyileştirmelerinin Bir Kozmetik Firmasında Uygulanması, Arel Üniversitesi, Sosyal Bilimler Üniversitesi, Yüksek Lisans Tezi, İstanbul.

[21] Berber, G. (2017). Bir Gıda İşletmesinde Süreç İyileştirme Uygulaması: Dondurma Fabrikası Örneği, İnönü Üniversitesi, Sosyal Bilimler Enstitüsü, Yüksek Lisans Tezi, Malatya.

[22] Sönmez, Y. (2017). Otomotiv Sektörü Süreç İyileştirmede Jishuken Uygulamaları, Sakarya Üniversitesi, Fen Bilimleri Enstitüsü, Yüksek lisans Tezi, Sakarya.

[23] Şenol, G. K. (2017). Pompa Sistemlerinde Enerji Tasarrufu ve Demir Çelik Sektöründe Örnek Bir Uygulama, İskenderun Teknik Üniversitesi, Mühendislik ve Fen Bilimleri Enstitüsü, Yüksek Lisans Tezi, Hatay.

[24] Alpaslan, İ. (2018). Otomotiv Yetkili Servisinde Müşteri Memnuniyeti Odaklı Süreç İyileştirme Çalışması: Bir Uygulama Örneği, İstanbul Medeniyet Üniversitesi / Sosyal Bilimler Enstitüsü, Yüksek Lisans Tezi, İstanbul.

[25] Sarıaslan, H. (1986) "Sıra Bekleme Sistemlerinde Simülasyon Tekniği" 1. Basım, Ankara, Ankara Üniversitesi Siyasal Bilgiler Fakültesi Yayınları.

[26] Prasad M. M., Aravindh A., Baskar R. and Kannan S. D.:'Implementation of Lean Manufacturing in Centrifugal Pump Assembly', Sri Krishna College of Engineering & Technology, Kuniamuthur, Coimbatore-641008, Tamilnadu, India, (2017) 134-140. http://www.ijirset.com/upload/2017/tapsa/17_mech_017.PDF.

[27] Aravinth K. A., Dr. Rajenthirakumar D.:'Lean Implementation through Enhancing Productivity in a Pump Industry', Department of Mechanical Engineering, United Institute of Technology, Coimbatore, TN India, (2016) 430-433. http://ijer.in/publication/v5/097.pdf.

[28] Kumar D.K.R., Shivashankar G.S. and Rajeshwar S. K.:'Application of Value Stream Mapping in Pump Assembly Process: A Case Study', Industrial Engineering & Management, Barcelona, Spain (2015) 1-11. DOI: 10.4172/2169-0316.100.0162.

[29] Parthiban M., Perumalsamy M. and Aravinddinesh G.:'Manufacturing Lead Time Reduction in Monoblock (SWJ) Pump Industry', International Research Journal of Engineering and Technology (IRJET), Tamilnadu, India, (2017) 1801-1807. https://www.irjet.net/archives/V4/i12/IRJET-V4I12331.pdf

[30] Prabhu C. and Aravindha B. S.:'Product and Process Improvement Using Simulation Based Value Stream Mapping: An Case Study', International Journal of Innovative Research in Science, Engineering and Technology, Tamilnadu, India, (2014) 1186-1190. http://www.rroij.com/open-access/product-and-process-improvement-usingsimulation-based-value-stream-mapping-ancase-study.pdf.

Int. J. Adv. Eng. Pure Sci. 2019, 4: 316-327
DOI: 10.7240/jeps.578024

REVIEW / DERLEME

A Review of Biomedical Engineering Research in Turkey During the Period 2008-2018

Türkiye'de 2008-2018 Döneminde Yapılan Biyomedikal Mühendisliğindeki Araştırmaların Derlemesi

Mehlika KARAMANLIOGLU [1]

[1] *Istanbul Gelisim University, Faculty of Engineering and Architecture, Biomedical Engineering, 34310, Istanbul, Turkey*

Abstract

Biomedical engineering is one of the fastest developing research disciplines in the past 60 years with the aid of rapid advances in technology. Biomedical engineering has emerged in Turkey in late 1970s but the research conducted in this area has been developing only in the past 15 years. The aim of this review is to summarize the problems regarding biomedical engineering in Turkey; to present the main subjects that are conducted in biomedical field in Turkey; and to summarize the prominent research papers conducted by Turkish Institutes published during the period 2008-2018 that contribute and/or have a potential to contribute to research and development (R&D) in biomedical engineering field in Turkey. These studies were divided into categories of tissue engineering, biosensors and biomedical devices; and summarized in this review.

Keywords: Biomedical engineering, tissue engineering, biosensors, biomedical devices, research and development, Turkey

Öz

Biyomedikal mühendisliği, teknolojideki hızlı gelişmelerin yardımıyla son 60 yılda en hızlı gelişen araştırma disiplinlerinden biri olmuştur. Biyomedikal mühendisliği Türkiye'de 1970'lerin sonunda ortaya çıkmış, ancak bu alanda yapılan araştırmalar sadece son 15 yılda gelişmeye başlamıştır. Bu derlemenin amacı, Türkiye'de biyomedikal mühendisliği ile ilgili sorunları özetlemek; Türkiye'de biyomedikal alanında yürütülen ana konuları sunmak; ve 2008-2018 yılları arasında yayınlanan ve Türkiye'de biyomedikal mühendisliği alanında araştırma ve geliştirmeye (AR-GE) katkıda bulunan/bulunma potansiyeline sahip olan ve Türk Enstitüleri tarafından yürütülen önde gelen araştırma makalelerini özetlemektir. Bu araştırmalar doku mühendisliği, biyosensörler ve biyomedikal cihazlar konularına ayrılarak incelenmiştir.

Anahtar Kelimeler: Biyomedikal mühendisliği, doku mühendisliği, biyosensörler, biyomedikal cihazlar, araştırma ve geliştirme, Türkiye

I. INTRODUCTION

Biomedical engineering is the application of engineering principles to biology and medicine for mainly diagnosis and treatment of patients [1, 2]. Therefore, biomedical engineering aims to use technologies to design and develop instruments to improve human life and to be used for research purposes.

1.1. A Brief History of Biomedical Engineering in the World

The field of biomedical engineering emerged in the 1950s mainly in the United States of America (USA), however, the foundation of biomedical engineering was established during the late 1700s when Luigi Galvani initiated his research on electrophysiology [1, 3]. Galvani studied the 'animal electricity' by observing electricity in living organisms. Galvani observed that frog muscle fibers contracted with electrical discharge and he stated that the source of animal electricity was muscle tissues or

Sorumlu yazar/Corresponding Author: Mehlika KARAMANLIOGLU, **Tel:** +902124227000-286, **e-posta:** mkaramanlioglu@gelisim.edu.tr,
Gönderilme/Submitted: 14.06.2019, **Düzenleme/Revised:** 26.09.2019, **Kabul/Accepted:** 16.10.2019

nerve fibers [3, 4]. Engineering was initially associated with biology and medicine through only instrumentation [5]. At the end of 19th century, Wilhelm Roentgen invented X-Ray machine and in early 20th century, Willem Einthoven built the foundation of two medical instruments, the electrocardiograph and the electroencephalograph, via string galvanometer invention [5]. Therefore, initially biomedical engineering was mainly concerned with manufacturing of medical devices during 1950s and 1960s [1, 2] Engineers were introduced to hospitals in 1960s to protect patients from electrocution from medical devices during treatment by maintaining electrical safety of these instruments in hospitals [1]. The rapid growth of science and technology enhanced development of new techniques and methods in biomedical engineering as well [5]. Moreover, the research area of biomedical engineering has expanded from medical and laboratory instrumentation to artificial organs, biomaterials, biomechanics, medical imagining, computer analysis of medical research data, etc. mainly in the last 20 years [1–3]. As an academic field, biomedical engineering began to appear in the late 1950s [2]. At Drexel University in the USA, graduate biomedical engineering programs were taught and shortly after that PhD programs were taught at Johns Hopkins University and University of Pennsylvania [6–8]

1.2. A Brief History of Biomedical Engineering in Turkey

In Turkey, biomedical engineering first emerged in late 1970s as research on medical devices at Middle East Technical University (METU) [8]. Initially, biomedical engineering field was primarily concerned with the limited production of medical devices in Turkey [8, 9]. Biomedical engineering was introduced as a graduate program and then as PhD programs [9]. During the late 1970s and beginning of the 1980s, Boğaziçi University started teaching biomedical engineering as an elective course and opened graduate programs [8, 9]. METU opened graduate programs in 1985 and then Marmara University trained the first biomedical device technology technicians during the late 80s [8]. Junior technical colleges have been teaching biomedical device technology since 1980s [9]. The undergraduate studies of biomedical engineering began in the beginning of 2000s. As of 2018, approximately 51 universities have biomedical engineering undergraduate programmes in Turkey [10]. Since there are 175 universities in Turkey officially recognized by Turkish higher-education institutions [11], less than half of these universities have biomedical engineering undergraduate programs. In this paper, some of the challenges of biomedical engineering encountered in Turkey is presented and the prominent researches on biomedical engineering conducted in Turkey during the period 2008-2018 is summarized.

II. CHALLENGES REGARDING BIOMEDICAL ENGINEERING IN TURKEY

Biomedical engineering trainings began in 1980s, however, the number of graduates could not meet the number of biomedical engineers required especially in the hospitals [8, 9]. Due to this, the main problem in biomedical engineering during the 80's and 90's in Turkey was that many expensive biomedical devices were imported but none of them were used effectively due to the lack of trained biomedical technicians and researchers [8, 9]. Not only in biomedical engineering but in general, the number of researchers is reported to be 57% lower than EU average in 2014 according to European Research Area Progress Report [12]. Therefore, the lack of number of researchers in biomedical engineering still has not been completely resolved as biomedical engineering still is not being taught as undergraduate programs in many universities in Turkey [13]. Another problem is that the number of medical devices manufactured is very low and they do not have the advanced technology [13–15]. Therefore, most medical devices i.e. imaging and dialysis devices are imported from other countries which costs more than manufacturing of these devices [13]. According to a report 85% of the medical devices in the sector is imported from other countries [16]. Moreover, maintenance of these devices cost a lot more since they are imported from other countries [13]. Although the number of medical devices have been increasing over the years in Turkey, ultrasound machine being the most common, MR being the least common medical device, the total number of medical devices in Turkey compared to Organization for Economic Cooperation and Development (OECD) countries, is not sufficient [14, 16, 17]. Moreover, the distribution of medical devices is reported to be uneven throughout the country as big cities contain the most number of medical devices and small cities and generally south east of Turkey has the least number of medical devices [16]. Health expenditure has been increasing especially in the last 10 years in Turkey. As of 2016, total health expenditure was approximately 120 million Turkish Liras in general total which is almost 25 times more than the expenditure reported in 1999 [18]. Not only medical devices but also other medical supplies are also imported to great extent [19]. Therefore, there is an increasing need of biomedical supplies, efficient biomedical instruments, researchers and technicians to operate them. According to European Research Area Progress Report, 2016, Turkey still needs to improve national research systems as it falls behind EU [12].

Therefore, as in biomedical perspective, considering a 20-year gap between the USA and Turkey, today there is still need for development on this research area and proper use of medical devices.

In general, Turkey has been making progress in R&D projects as some university laboratories, research institutions and technology development zones have been associated to European Union (EU) Framework Programs (FP) since 2003 [20, 21]. Framework Programs are the European Community research and technological development activities and have been undertaken since 1984 [22]. Turkey has been participating in multi – annual FP series since FP6, which took place between 2002-2006. Turkey also participated in FP7, which was during 2007-2013; and currently to Horizon 2020 (2014-2020) which has a funding of about 80 billion Euros [23]. In FP7, more than 1000 participants with about 950 projects received approximately 200 million Euros in EU funding [23].Turkey's investment on R&D is reported to be below EU average, which is less than 1% of gross domestic product (GDP) [23]. Although there is an increase in R&D in biomedical engineering with participation to these EU FP, valorization and industrializing remain to be one of the main challenges in this research area [20]. Also Turkey only publishes 1,5% of scientific literature globally [24], therefore there is still need to do more scientific publishing including biomedical engineering.

There is still insufficient research on some research areas of biomedical engineering such as biotelemetry, bioimaging, bioinformatics in biomedical engineering in Turkey [13, 25]. Biotelemetry is the remote detection of a living organism's physiological functions and has been developing due to fast growing technology of smart phones specifically to trace elderly as it is estimated that by 2050, there will be a 70% increase in the number of people in the EU aged over 65 [26]. Biotelemetry is also important specifically for medical emergencies, however, there has not been any tangible research on this area in Turkey yet [13]. Bioinformatics is the analysis of biological data especially used in molecular biology and likewise, bioinformatics has not been taught or studied effectively in Turkey [13]. Biomedical tools used in sports medicine are also still insufficient [13].

III. MAIN BIOMEDICAL ENGINEERING RESEARCH AREAS IN TURKEY

According to data retrieved from Scopus, research and development in biomedical engineering has been increasing in Turkey since 1970 especially after 2000 (Figure 1) [20, 25]. In general, number of publications have increased in Turkey [24] and in accordance with this, there is a steady increase in the number of documents published in biomedical engineering area specifically after mid 90s (Figure 1) [25]. During the period 1970 – 2018, in total 4802 documents related to biomedical engineering were retrieved [25]. According to Scopus database, most of these studies were conducted at Hacettepe University (11%) and then at METU (9%), then at Ege University (8%), Gazi University (6%) and Istanbul University (5%) [25].

During 2008 – 2018, 3655 research documents were published [25]. When compared with the number of publications between 1970-2018 with the same search criteria except for the publication years, 76% of the publications were published during the period 2008-2018.

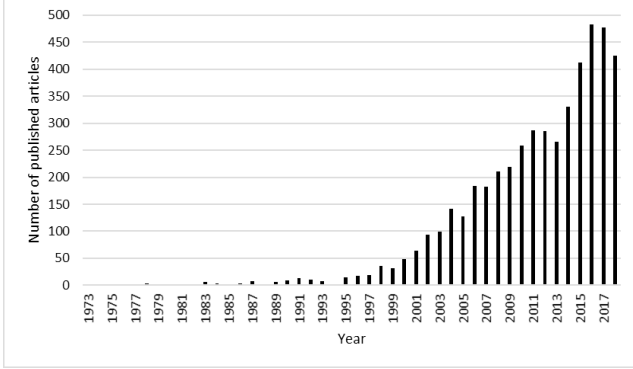

Figure 1. The number of published articles regarding biomedical engineering during 1970-2018 in Turkey. Data retrieved from *Scopus*; last accessed January 22, 2019 [25].

Scopus is an international citation database where peer-reviewed literature can be accessed [25] and since citation numbers show the scientific respectability of a specific research [24], first 100 most cited papers out of 3655 research documents published in between 2008-2018 regarding biomedical engineering on Scopus database were analyzed and the ones with significant results that would contribute to R&D in Turkey were summarized. Also the papers which were not in the first 100 most cited list but would and/or have a potential to contribute to R&D sector in Turkey were selected and summarized as well. Reviews and conference papers were excluded. The selected researches were mainly conducted in Turkey and some of them were collaborated with international institutions. As of 2018, The USA and Germany are the two countries collaborating with Turkey for biomedical engineering research according to Scopus database. The United Kingdom, The Netherlands and Italy were the other countries that were collaborated to publish articles related to biomedical engineering [25]. Most of the studies in biomedical engineering in Turkey have been

conducted as an interdisciplinary branch relating to the field of medicine, engineering, materials science, molecular biology, chemistry and dentistry [25]. Therefore, the studies published during the period 2008-2018 in biomedical engineering research area were divided into categories of tissue engineering, biomaterials and nanomaterials, biosensors and biomedical devices; and summarized for this review.

3.1. Tissue Engineering, Biomaterials and Nanoparticles

Tissue engineering is a new branch of engineering and has rapidly been growing since 1980s [2, 3]. It is an interdisciplinary field combining biological sciences (cell biology, histology) with engineering methods and materials sciences [2]. Tissue engineering mainly develops new therapeutic strategies, designs biocompatible artificial tissues and devices. Therefore it aims to regenerate impaired tissues, to provide function to organs that lost their ability and to treat wounds [2, 3, 27, 28]. Tissue engineering research areas include production of new biocompatible devices made of materials like polymers, ceramics and metals; and scaffold matrix materials to grow cells on; therefore academic and industrial communities have an increasing number of research and development projects on this subject [3, 28]. Tissue engineers treat the materials beforehand so that these materials are biocompatible and in case they are biodegradable, tissue engineers make sure biomaterials and their by-products do not have any side effects and toxicity [3].

Tissue engineering is increasingly becoming a popular research area in Turkey as well, especially the design and development of scaffold materials. Scaffolds are derived from native extracellular matrices (ECM) to offer three-dimensional support for regeneration of tissues and organs [29] and various studies have been conducted on scaffolds and improvement of their materials.

In materials sciences, biomaterials are widely used in tissue engineering applications and have many applications [30]. Biomaterials are mainly classified as metals, ceramics, polymers [29]. Biopolymers are polymers from natural sources which can either be synthetic or natural such as collagen, chitosan, etc.

Biomaterials can be used as scaffolds, implants, orthopedic devices and drug delivery systems [30]. Biodegradable biomaterials are mainly used as bioresorbable sutures, wound dressing materials, orthopedic devices since they slowly hydrolyze in the body and they do not need to be removed with an operation [31–34]. Function of biomaterials can be classified either as passive (e.g. a heart valve biomaterial) or bio active (e.g. hydroxyapatite-coated hip implants) [35].

Biomaterials research area in Turkey is mostly based on scaffold synthesis, tissue implants and drug delivery applications with the use of natural and synthetic polymers and also nano sized particles [21].

In scaffold synthesis studies involving biomaterials, polyhydroxybutyrates, PHB, as a polymeric scaffold, was synthesized from a bacterium strain and nanofibrilar scaffold of PHB was produced by electrospining technique [36]. Also when surface of PHB scaffold was modified, it improved cell attachment and proliferation which are necessary for optimal tissue engineering applications [36]. Developing scaffold materials with favourable mechanical qualities has also been studied. For instance, gelatin fibre-based scaffolds were mechanically improved with boron nitride nanotubes (BNNTs), which has a potential to improve mechanical properties of scaffolds for tissue engineering applications [37]. Auxetic PCL, polycaprolactone, nanofiber membranes were fabricated to be used as scaffolds with improved mechanical properties used in tissue engineering [38].

Scaffold synthesis for bone tissue applications, chitosan based scaffolds with sequential growth factor delivery system were constructed to increase bone cell proliferation for bone tissues [39]. A 3-D scaffold capable of releasing two bone morphogenetic proteins (BMP) was also designed [40]. New biomimetic scaffold materials were demonstrated to increase osteoblastic differentiation to form new bone tissue when electrospun polycaprolactone (PCL) nanofiber mats were synthesized in calcium phosphate solutions [41]. To repair bone deffects, scaffolds were obtained from strontium doped bioactive glass and these scaffolds were shown to release strontium for bone tissue regeneration [42].

In bone tissue engineering studies other than scaffold synthesis, biomaterials are used such as cerium oxide-bovine hydroxyapatite composites were prepared with improved mechanical properties [43]. Apatites are widely used in implants and Raman spectroscopy was used to analyze the effect of coating hydroxylapatite [44]. Bioactive glass fibers were prepared to be used in bone and soft tissue regeneration [45]. To treat bone, cartilage and adipose tissue defects in regenerative medicine, a synthetic polymeric agent, F68, was shown to enhance cell differentiation [46]. This particular study also employed human tooth germ stem cells (hTGSCs) isolated from wisdom teeth as stem cells to differentiate into bony tissues for skeletal repair [46]. In dental procedures zirconia, a ceramic material, is widely used and in a study Er:YAG laser irradiation was shown to improve mechanical properties i.e. shear bond strength of yttrium-stabilized tetragonal zirconia (Y-TZP) ceramics [47]. Additionally, roughening the surface of Y-TZP ceramic by

laser treatment was shown to decrease microleakage in the adhesive-ceramic interface [47]. Also PHB membranes were treated with NaOH for antimicrobial purposes to be used in orthopedic and dental tissue engineering applications [48].

Since chitin and chitosan have a wide range of applications in medicine as biomaterials, they were extracted for the first time from six different aquatic invertebrates [49]. Tannic Acid molecules were turned into poly(tannic acid) particles in a single step to be used as a biomaterial since poly(tannic acid) particles are determined to be more biocompatible than tannic acid molecules [50]. Sodium alginate was used in a drug delivery system to synthesize pH and temperature responsive beads to deliver an anti-inflammatory drug, indomethacine (IM) [51].

In other applications of biomaterials, a biodegradable nerve conduit was synthesized using polyesters which can be effective in nerve injury regeneration [52].

Environmentally friendly and biocompatible materials for organic field-effect transistors were developed to have wide range of applications including biomedical implants [53].

Mechanically improved hydrogels were produced from Poly(N,N-dimethylacrylamide; PDMA) for autonomous self-healing purpose of the tissue [54]. A promising wound dressing material with favourable properties was also fabricated using a silk protein, sericin, is also added to wound dressing material [55].

In order to heal tendon injuries, adipose-derived stem cells (ASC) were used instead of using mesenchymal stem cells which is commonly used in the literature [56]. ASCs were shown to increase primary tendon healing in this study collaborated with Japan [56]. Self healing hydrogel with strong adhesion and good self-healing properties to be applied in tissue engineering was produced with a poly(acrylic acid) having 30% catechol appendants on its backbone [57]. Adipose derived stem cells were used to synthesize hydrogels which were also UV crosslinked to increase vascularization in wounded tissues [58].

Peptide nanofibers were designed to interact with growth factors by mimicing heparin which is necessary for formation of new blood vessels in case of injuries [59]. This is an important study for tissue regeneration as there is no need to add growth factors exogenously to form new blood vessels [59]. In a follow up study, nanofiber gel which is again mimicking heparin was synthesized and shown to enhance scar free wound reperations [60].

Nanoparticles are also applied in clinical diagnostics and in therapeutic methods as they are suitable to be used in cancer therapy and bioimaging of specific cell targeting. In bioimaging applications of nanoparticles, gold–magnetite (Au–Fe_3O_4) hybrid nanoparticles (HNPs) were synthesized to be used in magnetic resonance imaging (MRI) as contrast agents (CAs) to enhance imaging quality for diagnosis [61]. These novel Au–Fe_3O_4 hybrid nanoparticles (HNPs) were found to be good candidates as MRI CAs [61].

Collagen is a natural biomaterial and recently its nanofibers are synthesized to be used in biomedical applications [62]. Collagen nanofibers were synthesized using electrospinning to be used in drug delivery systems since collagen is a highly biocompatible biomaterial [63]. Furthermore, structural properties of collagen nanofibers were observed [62] and different preparation parameters were tested when its nanofibers were synthesized by electrospinning [64].

Magnetic nanoparticles (MNPs) have been used in tissue engineering as new nanobiomaterials. The chitosan-coated magnetic nanoparticles (CS MNPs) were fabricated and characterized to be used in different biomedical applications such as drug delivery and magnetic resonance imaging (MRI) [65]. As another application of MNPs, they were encapsulated within cell-encapsulating hydrogels [66]. Since these hydrogels were degradable, the release of encapsulated MNPs were studied to be applied in tissue regenerative medicine and drug delivery systems [66].

Iron oxide particles were coated with PHB polymer and this magnetic carrier system was used as a drug delivery system for cancer treatment [67]. A new method to coat magnetic iron oxide nanoparticles (MIONPs) with polyethylene glycol (PEG) hydrogel was designed [68]. MIONPs are used in early tumor or cancer detection and in targeted therapies, this new method to coat MIONPs allowed specific tissues to be targeted and also enhanced viability and drug uptake of HeLA cell [68]. Gold-coated iron oxide magnetic nanoparticles were also synthesized to isolate bacteria in a biological sample facilitating bioassay studies [69].

Poly(acrylonitrile) (p(AN))-based materials such poly(acrylonitrile-co-(3-acrylamidopropyl)-trimethylammonium chloride (p(AN-co-APTMACl)), poly(acrylonitrile-co-4-viniyl pyridine)(p(AN-co-4-VP)) and poly(acrylonitrile-co-N-isopropylacrylamide) (p(AN-co-NIPAM)) were prepared, chemically modified and succesfully used in drug delivery systems [70]. Also some of the particles were shown to have antimicrobial activities [70].

Apart from drug delivery and bioimaging, nanoparticles can be used for antimicrobial purposes. For instance, to prevent bacterial infection of medical devices, instead of using antibiotics, adhesion of bacteria on medical devices were reduced through controlling surface properties of titanium nanotubes [71]. Four types of xeolites, the nanoporous alumina silicates, with different cation contents were synthesized and

their antimicrobial properties were tested [72]. Xeolite with silver Ag^{+} was shown to have more antimicrobial property than other xeolites containing copper (Cu^{+2}) and zinc (Zn^{+2}) [72]. This study suggests that zeolites with synthesized various materials can be used to manufacture antimicrobial surfaces, textiles, medical devices or household items [72].

3.2. Biosensors

Sensors are widely used in bioinstrumentation systems to monitor physiological variables and also non-physiological variables such as environment, agriculture and bioprocessing [1, 73]. Sensors mainly convert physical parameters to electrical signals [73]. Sensors with a biological sensing component i.e. enzyme, anti-body, etc. that can detect the presence of a specific agent such as a chemical group or a compound are classified as biosensors [2, 74]. Biomedical sensors are designed to detect and measure physiological variables and provide diagnostic information [1]. Research related to biosensors have been steadily increasing since 1980s [74].

Biosensors are studied substantially in Turkey as well. Biomedical engineering research in Turkey is mostly related to biosensor synthesis with a wide range of applications. The most prominent study in biosensor research in Turkey is a study collaborated with the USA and it involves graphene nanosheets as novel biosensor materials [75]. In that particular study, graphene nanosheets were chemically developed to detect some neurotransmitters such as dopamine and were shown to be more effective than single-walled carbon nanotubes [75].

Carbon nanotubes, a novel class of nanomaterial, can also be used in biosensor design to detect various molecules. In vivo detection of the marker and signalling molecule nitric oxide concentration was achieved by development of near-infrared-fluorescent single-walled carbon nanotubes sensors [76]. This optical sensor study would allow to detect tissue inflammation and cancer activity as well as to study cell signalling [76]. Multiwall carbon nanotubes (MWCNTs) and gelatin were employed in an amperometric biosensor detecting hydrogen peroxide in disinfector solutions biosensor [77]. Amperometric hydrogen peroxide biosensor was synthesized with myoglobin (Mb) on multi-walled carbon nanotube (MWCNT) –Nafion–nanobiocomposite film with gold electrode [78]. In order to detect phenol and its derivatives which are toxic to environment, an amperometric biosensor was developed by incorporating horseradish peroxidase (HRP) to carbon nanotube (CNT)/polypyrrole (PPy) nanobiocomposite film [79]. More recently, a new amperometric biosensor based on HRP immobilized on poly(glycidylmethacrylate)-grafted iron oxide nanoparticles was synthesized to detect phenol's and its derivatives' their presence in the environment [80].

A xanthine biosensor was fabricated with chitosan, Co_3O_4 nanoparticles and using multiwall carbon nanotubes (MWCNTs) [81]. A sensitive urea biosensor was also synthesized when urease enzyme was immobilized on polyamidoamine grafted multiwalled carbon nanotube (MWCNT-PAMAM) dendrimers [82].

A DNA biosensor was presented to determine anticancer drug, 6-mercaptopurine (6-MP) [83]. For this purpose, DNA was immobilized on a pencil graphite electrode which was modified with polypyrrole and functionalized multiwalled carbon nanotubes (MWCNT/COOH) [83].

A new DNA biosensor with cysteamine and gold nanoparticles was also fabricated to detect aflatoxin M1 in milk samples which provided good analytical results and in that particular study interaction of aflatoxin and DNA on gold nanoparticles were shown [84]. In a prominent study in 2014 by Yola et al, an electrochemical DNA bioensor with better stability and higher selectivity to certain DNA samples was prepared with iron-gold nanoparticles (Fe@AuNPs) using n-graphene oxide [85]. In relation to this study, an electrochemical biosensor with Fe@AuNPs was developed to detect cefexime in biological samples, i.e. human plasma [86]. This biosensor has potential to enable new β-lactam antibiotics recovery [86].

Since pathogen detection with biosensors have been becoming popular, a new quartz crystal microbalance (QCM) biosensor was developed to detect *Salmonella* pathogen that causes gastroenteritis in humans [87]. This QCM biosensor was based on DNA aptamers which are the bio-recognition molecules [87].

Glucose biosensors have wide range of applications such as in medical diagnosis, therefore, in the last decade many studies using different approaches and materials to be used as glucose biosensors were fabricated. A sensitive electrochemical glucose biosensor was synthesized using gold (Au) nanoparticles on a semiconductor, molybdenum disulfide (MoS_2) nanosheet in a single step reaction [88]. A new sensitive glucose sensor was fabricated using activated carbon (AC) and monodisperse nickel and palladium alloy nanocomposites by an in-situ reduction technique [89]. A highly sensitive amperometric glucose biosensor was designed with the immobilization of glucose oxidase (GOx) on poly(pyrrole propylic acid)/Au nanocomposite for diagnosis of diabetes [90].

microRNAs, miRNAs, are the small non-coding ribonucleic acids (RNAs) and have recently been gaining attention in

biomedical research due to its potential to be used as biomarkers in diagnosis and treatment of cancer [91, 92]. An enzyme biosensor for the early detection of breast cancer was developed by detection of mir21 which forms in cancer cells during the early stages of breast cancer [91]. A very sensitive and rapid electrochemical biosensor was also developed to detect mir21 using protein 19 [92].

Myocotoxins are found in meat and dairy products due to fungal infection of crops and cause serious health problems. Citrinin (CIT) is one of the most harmful mycotoxins and in order to detect mycotoxins in food, a sensitive molecular CIT imprinted surface plasmon resonance (SPR) biosensor was designed for the first time and was shown to successfully detect CIT in red yeast rice [93].

Biosensors using different materials to detect various molecules were also designed. For instance, a new approach to synthesize an ethanol biosensor, an amperometric biosensor was reported [94]. This amperometric biosensor containing polypeptide and ferrocene side was reported to detect ethanol content in alcoholic beverages [94]. Chitosan–ferrocene (CHIT–Fc) hybrid, a redox biopolymer, was synthesized to be used as an immobilization matrix for biomolecules in biosensor systems [95].

3.3. Biomedical Devices

Biomedical engineers have been contributing to modern health care by developing instruments for diagnosis, treatment and follow up of patients and also for prevention of diseases [2, 14]. Nowadays, these devices are engineered to use non – invasive methods and to provide rapid results with more information specific to each patient's requirements [2]. Biomedical devices can mainly be classified as diagnostic devices, which provide information about the condition of the patient (electrocardiography, X-ray, etc); and as therapeutic devices , which aim to cure a disease or a condition (defibrillators, heart pacemakers, etc.) [3].

A new effective biomedical instrument for kidney stone destruction was developed by using hydrodynamic cavitation where fluid pressure is used to trigger inception, growth, and implosion of cavities [96]. A new device named soft tissue stiffness meter (STSM) was also designed to assess soft tissue stiffness to diagnose dermatological pathologies [97]. This study has significance on on diagnosis of skin cancer since cancerous tissues are stiffer than healthy tissues [97, 98].

Data analysis techniques are very important for efficiency of biomedical devices. In a study, electroencephalogram (EEG) signal processing and analysis framework were developed to classify EEG data in order to determine the presence of epileptic seizure [99]. In EEG results, data can be incomplete due to electrode disconnections. For this purpose, an algorithm called CP-WOPT (CP Weighted OPTimization) was developed for incomplete data to factorize tensors which can be applied for EEG [100]. ECG signal classification system was initially developed [101]. Further on, a new fast electrocardiogram (ECG) data classification and monitoring specific to a patient has also been developed by using 1-D convolutional neural networks (CNNs) [102]. Therefore, long ECG data of a patient, such as a Holter device output which records ECG of a patient for more than 24 hours, can be processed rapidly and accurately. For this purpose, CNNs are used for ECG classification in this study for the first time [102]. Another signal classification for EEG was developed using a new deep learning approach [103]. A classification system for electromyography (EMG) was also developed for arm prosthesis control studies and for this purpose discriminant analysis and support vector machine (SVM) classifier were used to identify and classify EMG signals at a good accuracy [104].

Metamaterial absorbers (MA) are used in biomedical devices since MAs have high absorption at wide angles of incidence for both transverse electric (TE) and transverse magnetic (TM) waves and a new MA with polarization independency and with different configuration was presented to be used in metamaterial (MTM) applications was presented [105]. Then, an MA with electromagnetic properties was designed which can be used in medical technologies as well as in sensors [106].

Phonocardiogram (PCG) is a biomedical device which determines heart defects through auditory perception of heart sounds. Wavelet types of PCG were examined and for the accuracy of this method, different wavelets on PCG signals were tested and Morlet wavelet was determined to be the most suitable wavelet for the time– frequency analysis of PCG signals [107]. A dynamic receive beamformer integrated circuit (IC) for High-Frequency Medical Ultrasound Imaging was developed in a study on biomedical devices [108]. High-Frequency Ultrasound has more resolution of some organs and arteries and in this study beamformer IC is developed for efficient intravascular ultrasound (IVUS) imaging [108].

Apart from technology used in biomedical devices, there are various studies related to biomedical engineering using advanced technologies. Ablation cooling is a method used in aerospace engineering, however, it is recently applied in biomedical engineering to increase ablation rate of tissues without side effects [109]. In that particular study, specifically as a research area of biophotonics, which is concerned

with interaction of light and tissues, ultrafast laser pulses were used and ablation of brain tissue was achieved without a thermal damage [109]. Scaffold-free biomimetic aortic vascular structures were developed for 3D bioprinting and for this purpose, new algorithms and methods were designed [110]. A real human heart aorta was used to generate computer model of macro-vascular tissue so that the computer aided algorithms would be used to bioprint 3D scaffold free tissues [110].

IV. CONCLUSION

Turkey has a potential in biomedical engineering as there is a steady increase in published research in this area in the past 15 years (Figure 1). Turkey has been participating to EU funded framework programs and projects in recent years; therefore, its contribution to biomedical engineering is expanding [21–23]. Most of the studies in biomedical engineering area are conducted on biosensors, tissue engineering & biomaterials and biomedical devices with prominent results that would contribute to or has a potential to contribute to research and development sector in Turkey. More diverse study areas of biomedical engineering can be explored with the improvement of infrastructure in biomedical engineering and with the aid of fast developing technologies; therefore, Turkey can reach advanced countries in biomedical engineering research field.

REFERENCES

[1] Bronzino, J.D., (2012). Biomedical Engineering: A Historical Perspective. In Introduction to Biomedical Engineering, J.D. Bronzino, J.D. Enderle (ed.), 1-33, doi: 10.1016/B978-0-12-374979-6.00001-0.

[2] Saltzman, W.M., (2015). Biomedical engineering: bridging medicine and technology, Second Edi. Cambridge University Press.

[3] Nebeker, F., (2002). Golden accomplishments in biomedical engineering. *IEEE Eng. Med. Biol. Mag.,* 21:17–47.

[4] Humpolíčk, P., Radaszkiewicz, K.A., Capáková, Z., Pacherník, J., Bober, P., Kašpárková, V., Rejmontová, P., Lehocký, M., Ponížil, P., Stejskal, J., (2018). Polyaniline cryogels: Biocompatibility of novel conducting macroporous material. *Sci. Rep.,* 8:1–12.

[5] Requena-Carrion, J., & Leder, R. S. (2009, September). The natural history of the engineering in medicine and biology ociety from a modern perspective. In 2009 Annual International Conference of the IEEE Engineering in Medicine and Biology Society (pp. 1086-1088). IEEE.

[6] Schwan, H.P., (1991). Biomedical engineering: University of Pennsylvania-from research laboratory to a leader in educational institutions for bioengineering. *IEEE Eng Med. Biol. Mag.,* 10:47–49.

[7] Sun, H.H., (1991). Biomedical engineering: Drexel University-pioneer in a formal MS degree training program for doctors. *IEEE Eng. Med. Biol. Mag.,* 10:44–46.

[8] Çamurcu, A.Y., Alsan, S., (1998). Türkiye'de ve Dünyada Biyomedikal Mühendislik ve Biyomedikal Cihaz Teknolojisi Eğitimi. *Atatürk Eğitim Fakültesi Eğitim Bilimleri Dergisi*, 10: 51–58.

[9] Sezdi, M., Akan, A., Kalkandelen, C., (2009). Biyomedikal ve Klinik Mühendisliği Eğitimi ve Ülkemizin Bu Alandaki İhtiyaçlarının İncelenmesi. *EEBB09 Elektrik Elektronik Bilgisayar Biyomedikal Mühendislikleri Eğitimi 4. Ulus. Sempozyumu.* Eskişehir, Türkiye, 22-24.

[10] Yükseköğretim Kurulu Yükseköğretim Program Atlası. https://yokatlas.yok.gov.tr/#. Accessed 29 Apr 2018.

[11] World University Rankings & Reviews uniRank. https://www.4icu.org/tr/. Accessed 20 May 2019.

[12] European Research Area Progress Report 2016. https://ec.europa.eu/research/era/pdf/era_progress_report2016/era_progress_report_2016_com.pdf. Accessed 20 March 2018.

[13] Taşgetiren, S., Yuran, F., Özmen, N., Özkan, N., (2015). Biyomedikal Ar-Ge 2015: 2015 İtibariyle Türkiye'de Biyomedikal Teknolojileri Alanında Yapılan Araştırma Faaliyetlerinin Mevcut Durumu. doi: 10.13140/2.1.3053.9043.

[14] Bozer, A., Ağırbaş, İ., (2016). Tıbbi Görüntüleme Cihazlarının Sayısal Durumu ve Kullanımlarının Değerlendirilmesi – Quantitative Evaluation of the Status and Use of Medical Imaging Devices. *Ankara Üniversitesi Tıp Fakültesi Macmuası*, 69(3), 193-201, doi: DOI: 10.1501/Tıpfak_000000943.

[15] Kiper, M., (2013). Türkiye'de tıbbi cihaz sektörü ve strateji önerisi. *Türkiye Teknol. Geliştirme Vakfı*, 1–226.

[16] Mertler, A.A., Karadoğan, N., Tatarhan, G., (2015). Türkiye'de Tıbbi Cihazların Sayısal Durumu ve OECD Ülkeleri İle Karşılaştırmaları. *Int. J. Heal. Manag. Strateg. Res.* 1:52–70.

[17] T.C. Sağlık Bakanlığı, (2013). Sağlık İstatistikleri Yıllığı 2013. Sentez Matbaacılık ve Yayıncılık, Ankara.

[18] Türkiye Istatistik Kurumu Türkiye İstatistik Kurumu. http://www.tuik.gov.tr/PreTablo.do?alt_id=1084. Accessed 20 March 2018.

[19] Ministry of Health of the Republic of Turkey. Health Treansformation Programme.https://sbu.saglik.gov.tr/Ekutuphane/kitaplar/healthtransformation.pdf. Accessed 20 March 2018.

[20] Bakker, E., Nuijens, R., Kaplan, D., (2015). The Turkish life sciences and health sector: Identifying opportunities to exchange knowledge and products between the Netherlands and Turkey. https://healthholland.h5mag.com/healthholland/edit-update_may_2015/internationalisation/1944/Report_Turkish_Life_Sciences_and_Health_Sector_March_2015__1_.pdf?nocache=113.117.7427. Accessed 20 July 2018.

[21] Dundar, M., Akbarova, Y., (2011). Current State of Biotechnology in Turkey. *Curr. Opin. Biotechnol.,* 22S:S3-S6 doi: 10.1016/j.copbio.2011.05.509.

[22] Eurostat Research Projects under Framework Programmes – European Commission. https://ec.europa.eu/eurostat/cros/content/research-projects-under-framework-programmes-0_en. Accessed 1 May 2018.

[23] European Commission – PRESS RELEASES – Press release – Turkey joins Horizon 2020 research and innovation programme. http://europa.eu/rapid/press-release_IP-14-631_en.htm. Accessed 1 May 2018.

[24] Yaşar, T., (2017). TÜBİTAK Türkiye Adresli Uluslararası Bilimsel Yayınları Teşvik (UBYT) Programının Değerlendirilmes. TÜBİTAK Ulakbim.

[25] SciVerse SCOPUS. www.scopus.com. Accessed 22 January 2019.

[26] Health European Commission. https://ec.europa.eu/programmes/horizon2020/en/area/ health. Accessed 1 May 2018.

[27] Morouço, P., Biscaia, S., Viana, T., Franco, M., Malça, C., Mateus, A., Moura, C., Ferreira, F.C., Mitchell, G., Alves, N.M., (2016). Fabrication of poly(ϵ-caprolactone) scaffolds reinforced with cellulose nanofibers, with and without the addition of hydroxyapatite nanoparticles. *Biomed. Res. Int.*, 1-10, doi: 10.1155/2016/1596157.

[28] Andreu, V., Mendoza, G., Arruebo, M., Irusta, S., (2015). Smart dressings based on nanostructured fibers containing natural origin antimicrobial, anti-inflammatory, and regenerative compounds. *Materials (Basel),* 8:5154–5193.

[29] O'Brien, F.J., (2011). Biomaterials & scaffolds for tissue engineering. *Mater. Today,* 14:88–95.

[30] Langer, R., Tirrell, D.A., (2004). Designing materials for biology and medicine. *Nature*, 428:487–492.

[31] Kulkarni, R.K., Pani, K.C., Neuman, C., Leonard, F., (1966). Polylactic acid for surgical implants. *Arch. Surg.,* 93:839–843.

[32] Vert, M., Mauduit, J., Li, S., (1994). Biodegradation of PLA/GA polymers: increasing complexity. *Biomaterials*, 15:1209–13.

[33] Weir, N.A., Buchanan, F.J., Orr, J.F., Farrar, D.F., Boyd, A., (2004). Processing, annealing and sterilisation of poly-L-lactide. *Biomaterials,* 25:3939–3949.

[34] Zaman, H.U., Islam, J.M.M., Khan, M.A., Khan, R.A., (2011). Physico-mechanical properties of wound dressing material and its biomedical application. *J. Mech. Behav. Biomed. Mater.,* 4:1369–1375.

[35] Zorlutuna, P., Yilgör P., Başmanav, F.B., Hasirci, V., (2009). Biomaterials and tissue engineering research in Turkey: The METU biomat center experience. *Biotechnol. J.,* 4:965–980.

[36] Karahaliloğlu, Z., Demirbilek, M., Şam, M., Erol-Demirbilek, M., Sağlam, N., Denkbaş, E.B., (2013). Plasma polymerization-modified bacterial polyhydroxybutyrate nanofibrillar scaffolds. *J. Appl. Polym. Sci.,* 128:1904–1912.

[37] Şen, Ö., Culha, M., (2016). Boron nitride nanotubes included thermally cross-linked gelatin-glucose scaffolds show improved properties. *Colloids Surfaces B. Biointerfaces* 138:41–49.

[38] Bhullar, S.K., Rana, D., Lekesiz, H., Bedeloglu, A.C., Ko, J., Cho, Y., Aytac, Z., Uyar, T., Jun, M., Ramalingam, M., (2017). Design and fabrication of auxetic PCL nanofiber membranes for biomedical applications. *Mater. Sci. Eng. C,* 81:334–340.

[39] Yilgor, P., Tuzlakoglu, K., Reis, R.L., Hasirci, N., Hasirci, V., (2009). Incorporation of a sequential BMP-2/BMP-7 delivery system into chitosan-based scaffolds for bone tissue engineering. *Biomaterials,* 30:3551–3559.

[40] Basmanav, F.B., Kose, G.T., Hasirci, V., (2008). Sequential growth factor delivery from complexed microspheres for bone tissue engineering. *Biomaterials,* 29:4195–4204.

[41] Mavis, B., Demirtaş, T.T., Gümüşderelioğlu, M., Gündüz, G., Çolak, Ü. (2009). Synthesis, characterization and osteoblastic activity of polycaprolactone nanofibers coated with biomimetic calcium phosphate. *Acta Biomater.,* 5:3098–3111.

[42] Erol, M., Özyuğuran, A., Özarpat, Ö., Küçükbayrak, S., (2012). 3D Composite scaffolds using strontium containing bioactive glasses. *J. Eur. Ceram. Soc.,* 32:2747–2755.

[43] Gunduz, O., Gode, C., Ahmad, Z., Gökçe, H., Yetmez, M., Kalkandelen, C., Sahin, Y.M., Oktar, F.N., (2014). Preparation and evaluation of cerium oxide-bovine hydroxyapatite composites for biomedical engineering applications. *J. Mech. Behav. Biomed. Mater.,* 35:70–76.

[44] Saber-Samandari, S., Alamara, K., Saber-Samandari, S., Gross, K.A., (2013). Micro-Raman spectroscopy shows how the coating process affects the characteristics of hydroxylapatite. *Acta Biomater.,* 9:9538–9546.

[45] Deliormanli, A.M., (2014). Preparation and in vitro characterization of electrospun 45S5 bioactive glass nanofibers. *Ceram. Int*., 41:417–425.

[46] Doğan, A., Yalvaç, M.E., Şahin, F., Kabanov, A. V., Palotás, A., Rizvanov, A.A., (2012). Differentiation of human stem cells is promoted by amphiphilic pluronic block copolymers. *Int. J. Nanomedicine,* 7:4849–4860.

[47] Akin, H., Tugut F., Akin, G.E., Guney, U., Mutaf, B., (2012). Effect of Er:YAG laser application on the shear bond strength and microleakage between resin cements and Y-TZP ceramics. *Lasers Med. Sci.,* 27:333–338.

[48] Karahaliloglu, Z., Ercan, B., Taylor, E.N., Chung, S., Denkbaş, E.B., Webster, T.J., (2015). Antibacterial Nanostructured Polyhydroxybutyrate Membranes for Guided Bone Regeneration. *J. Biomed. Nanotechnol.,* 11:2253–2263.

[49] Kaya, M., Baran, T., Mentes, A., Asaroglu, M., Sezen, G., Tozak, K.O., (2014). Extraction and Characterization of α-Chitin and Chitosan from Six Different Aquatic Invertebrates. *Food Biophys.,* 9:145–157.

[50] Sahiner, N., Sagbas, S., Aktas, N., (2015). Single step natural poly(tannic acid) particle preparation as multitalented biomaterial. *Mater. Sci. Eng.* C, 49:824–834.

[51] Işiklan, N., Küçükbalci, G., (2012). Microwave-induced synthesis of alginate-graft-poly(N-isopropylacrylamide) and drug release properties of dual pH – and temperature-responsive beads. *Eur. J. Pharm. Biopharm.,* 82:316–331.

[52] Yucel, D., Kose, G.T., Hasirci, V., (2010). Polyester based nerve guidance conduit design. *Biomaterials,* 31:1596–1603.

[53] Irimia Vladu, M., Troshin, P.A., Reisinger, M., Shmygleva, L., Kanbur, Y., Schwabegger, G., Bodea, M., Schwödiauer, R., Mumyatov, A., Fergus, J.W., (2010). Biocompatible and biodegradable materials for organic field effect transistors. *Adv. Funct. Mater.,* 20:4069–4076.

[54] Algi, M.P., Okay, O., (2014). Highly stretchable self-healing poly(N,N-dimethylacrylamide) hydrogels. *Eur. Polym. J.,* 59:113–121.

[55] Akturk, O., Tezcaner, A., Bilgili, H., Deveci, M.S., Gecit, M.R., Keskin, D. (2011). Evaluation of sericin/collagen membranes as prospective wound dressing biomaterial. *J. Biosci. Bioeng.,* 112:279–288.

[56] Uysal, C.A., Tobita, M., Hyakusoku, H., Mizuno, H., (2012). Adipose-derived stem cells enhance primary tendon repair: biomechanical and immunohistochemical evaluation. *J. Plast. Reconstr. Aesthetic Surg.,* 65:1712–1719.

[57] Wang, W., Xu, Y., Li, A., Li, T., Liu, M., von Klitzing, R., Ober, C.K., Kayitmazer, A..B, Li, L., Guo, X., (2015). Zinc induced polyelectrolyte coacervate bioadhesive and its transition to a self-healing hydrogel. *Rsc. Adv.,* 5:66871–66878.

[58] Eke, G., Mangir, N., Hasirci, N., MacNeil, S., Hasirci, V., (2017). Development of a UV crosslinked biodegradable hydrogel containing adipose derived stem cells to promote vascularization for skin wounds and tissue engineering. *Biomaterials,* 129:188–198.

[59] Mammadov, R., Mammadov, B., Toksoz, S., Aydin,. B, Yagci, R., Tekinay, A.B., Guler, M.O., (2011). Heparin mimetic peptide nanofibers promote angiogenesis. *Biomacromolecules,* 12:3508–3519.

[60] Uzunalli, G., Mammadov, R., Yesildal, F., Alhan, D., Ozturk, S., Ozgurtas, T., Guler, M.O., Tekinay, A.B., (2016). Angiogenic heparin-mimetic peptide nanofiber gel improves regenerative healing of acute wounds. *ACS Biomater. Sci. Eng.,* 3:1296–1303.

[61] Umut, E., Pineider, F., Arosio, P., Sangregorio, C., Corti, M., Tabak, F., Lascialfari, A., Ghigna, P., (2012). Magnetic, optical and relaxometric properties of organically coated gold-magnetite (Au-Fe_3O_4) hybrid nanoparticles for potential use in biomedical applications. *J. Magn. Magn. Mater.,* 324:2373–2379.

[62] Bürck, J., Aras, O., Bertinetti, L., Ilhan, C.A., Ermeydan, M.A., Schneider, R., Ulrich, A.S., Kazanci, M., (2018). Observation of triple helix motif on electrospun collagen nanofibers and its effect on the physical and structural properties. *J. Mol. Struct.,* 1151:73–80.

[63] Aras, O., Kazanci, M., (2015). Production of collagen micro-and nanofibers for potential drug-carrier systems. *J. Enzyme Inhib. Med. Chem.,* 30:1013–1016.

[64] Kazanci, M., (2014). Solvent and temperature effects on folding of electrospun collagen nanofibers. *Mater. Lett.,* 130:223–226.

[65] Unsoy, G., Yalcin, S., Khodadust, R., Gunduz, G., Gunduz, U., (2012). Synthesis optimization and characterization of chitosan-coated iron oxide nanoparticles produced for biomedical applications. *J. Nanoparticle Res.,* 14:964.

[66] Xu, F., Inci, F., Mullick, O., Atakan, U., Sung, Y., Kavaz, D., (2012). Release of Magnetic Nanoparticles from Cell – Encapsulating Biodegradable Nanobiomaterials. *ACS nano*, 2012, 6.8: 6640-6649.

[67] Erdal, E., Kavaz, D., Şam, M., Demirbilek, M., Demirbilek, M.E., Sağlam, N., Denkbaş, E.B., (2012). Preparation and characterization of magnetically responsive bacterial polyester based nanospheres for cancer therapy. *J. Biomed. Nanotechnol.,* 8:800–808.

[68] Nazli, C., Ergenc, T.I., Yar, Y., Acar, H.Y., Kizilel, S., (2012). RGDS-functionalized polyethylene glycol hydrogel-coated magnetic iron oxide nanoparticles enhance specific intracellular uptake by HeLa cells. *Int. J. Nanomedicine,* 7:1903–1920.

[69] Tamer, U., Gündoğdu, Y., Boyaci, I.H., Pekmez, K., (2010). Synthesis of magnetic core-shell Fe3O4-Au nanoparticle for biomolecule immobilization and detection. *J Nanoparticle Res.,* 12:1187–1196.

[70] Silan, C., Akcali, A., Otkun, M.T., Ozbey, N., Butun, S., Ozay, O., Sahiner, N., (2012). Novel hydrogel particles and their IPN films as drug delivery systems with antibacterial properties. *Colloids Surfaces B. Biointerfaces,* 89:248–253.

[71] Ercan, B., Taylor, E., Alpaslan, E., Webster, T.J., (2011). Diameter of titanium nanotubes influences anti-bacterial efficacy. *Nanotechnology,* 22:295102.

[72] Demirci, S., Ustaoğlu, Z., Yilmazer, G.A., Sahin, F., Baç, N., (2014). Antimicrobial properties of zeolite-X and zeolite-A ion-exchanged with silver, copper, and zinc against a broad range of microorganisms. *Appl. Biochem. Biotechnol.,* 172:1652–1662.

[73] Khandpur, R.S., (2003). Handbook of biomedical instrumentation, Second Edi. Tata McGraw-Hill Education.

[74] Turner, A.P.F., (2013). Biosensors: sense and sensibility. *Chem. Soc. Rev.,* 42:3184–3196.

[75] Alwarappan, S., Erdem, A., Liu, C., Li, C-Z., (2009). Probing the electrochemical properties of graphene nanosheets for biosensing applications. *J. Phys. Chem. C.,* 113:8853–8857.

[76] Iverson, N.M., Barone, P.W., Shandell, M., Trudel, L.J., Sen, S., Sen, F., Ivanov, V., Atolia, E., Farias, E., McNicholas, T.P., (2013). In vivo biosensing via tissue-localizable near-infrared-fluorescent single-walled carbon nanotubes. *Nat. Nanotechnol.,* 8:873.

[77] Kaçar, C., Dalkiran, B., Erden, P.E., Kiliç, E., (2014). An amperometric hydrogen peroxide biosensor based on Co_3O_4 nanoparticles and multiwalled carbon nanotube modified glassy carbon electrode. *Appl. Surf. Sci.,* 311:139–146.

[78] Canbay, E., Şahin, B., Kiran, M., Akyilmaz, E., (2015). MWCNT-cysteamine-Nafion modified gold electrode based on myoglobin for determination of hydrogen peroxide and nitrite. *Bioelectrochemistry,* 101:126–131.

[79] Korkut, S., Keskinler, B., Erhan, E., (2008). An amperometric biosensor based on multiwalled carbon nanotube-poly (pyrrole)-horseradish peroxidase nanobiocomposite film for determination of phenol derivatives. *Talanta,* 76:1147–1152.

[80] Çevik, E., Şenel, M., Baykal, A., Abasiyanik, M.F., (2012). A novel amperometric phenol biosensor based on immobilized HRP on poly(glycidylmethacrylate)-grafted iron oxide nanoparticles for the determination of phenol derivatives. *Sensors Actuators*, B. Chem., 173:396–405.

[81] Dalkiran, B., Kaçar, C., Erden, P.E., Kiliç, E., (2014). Amperometric xanthine biosensors based on chitosan-Co_3O_4-multiwall carbon nanotube modified glassy carbon electrode. *Sensors Actuators*, B. Chem., 200:83–91.

[82] Dervisevic, M., Dervisevic, E., Şenel, M., (2018). Design of amperometric urea biosensor based on self-assembled monolayer of cystamine/PAMAM-grafted MWCNT/Urease. *Sensors Actuators B. Chem.,* 254:93–101.

[83] Karimi-Maleh, H., Tahernejad-Javazmi, F., Atar, N., Yola, M.L., Gupta, V.K., Ensafi, A.A., (2015). A Novel DNA Biosensor Based on a Pencil Graphite Electrode Modified with Polypyrrole/Functionalized Multiwalled Carbon Nanotubes for Determination of 6-Mercaptopurine Anticancer Drug. *Ind. Eng. Chem. Res.,* 54:3634–3639.

[84] Dinçkaya E, Kinik Ö, Sezgintürk MK, Altuğ Ç, Akkoca A (2011). Development of an impedimetric aflatoxin M1 biosensor based on a DNA probe and gold nanoparticles. *Biosens. Bioelectron,* 26:3806–3811.

[85] Yola, M.L., Eren, T., Atar, N., (2014). A novel and sensitive electrochemical DNA biosensor based on Fe@Au nanoparticles decorated graphene oxide. *Electrochim. Acta,* 125:38–47.

[86] Yola, M.L., Eren, T., Atar, N., (2014). Molecularly imprinted electrochemical biosensor based on Fe@Au nanoparticles involved in 2-aminoethanethiol functionalized multi-walled carbon nanotubes for sensitive determination of cefexime in human plasma. *Biosens. Bioelectron,* 60:277–285.

[87] Ozalp, V.C., Bayramoglu, G., Erdem, Z., Arica, M.Y., (2015). Pathogen detection in complex samples by quartz crystal microbalance sensor coupled to aptamer functionalized core-shell type magnetic separation. *Anal Chim. Acta,* 853:533–540.

[88] Parlak, O., İncel, A., Uzun, L., Turner, A.P.F., Tiwari, A., (2017). Structuring Au nanoparticles on two-dimensional MoS_2 nanosheets for electrochemical glucose biosensors. *Biosens. Bioelectron.,* 89:545–550.

[89] Koskun, Y., Şavk, A., Şen, B., Şen, F., (2018). Highly sensitive glucose sensor based on monodisperse palladium nickel/activated carbon nanocomposites. *Anal. Chim. Acta,* 1010:37–43.

[90] Şenel, M., Nergiz, C., (2012). Novel amperometric glucose biosensor based on covalent immobilization of glucose oxidase on poly(pyrrole propylic acid)/Au nanocomposite. *Curr. Appl. Phys.,* 12:1118–1124.

[91] Kilic, T., Topkaya, S.N., Ariksoysal, D.O., Ozsoz, M., Ballar, P., Erac, Y., Gozen, O., (2012). Electrochemical based detection of microRNA, mir21 in breast cancer cells. *Biosens. Bioelectron,* 38:195–201.

[92] Kilic, T., Topkaya, S.N., Ozsoz, M., (2013). A new insight into electrochemical microRNA detection: A molecular caliper, p19 protein. *Biosens. Bioelectron.* 48:165–171.

[93] Atar, N., Eren, T., Yola, M.L., (2015). A molecular imprinted SPR biosensor for sensitive determination of citrinin in red yeast rice. *Food. Chem.,* 184:7–11.

[94] Kesik, M., Akbulut, H., Söylemez, S., Cevher, Ş.C., Hızalan, G., Udum, Y.A., Endo, T., Yamada, S., Çırpan, A., Yağcı, Y., (2014). Synthesis and characterization of conducting polymers containing polypeptide and ferrocene side chains as ethanol biosensors. *Polym. Chem.,* 5:6295–6306.

[95] Yilmaz Ö, Demirkol DO, Gülcemal S, Kilinç A, Timur S, Çetinkaya B (2012). Chitosan-ferrocene film as a platform for flow injection analysis applications of glucose oxidase and Gluconobacter oxydans biosensors. *Colloids Surfaces B.* Biointerfaces, 100:62–68.

[96] Perk, O.Y., Şeşen, M., Gozuacik., D., Koşar, A., (2012). Kidney stone erosion by micro scale hydrodynamic cavitation and consequent kidney stone treatment. *Ann. Biomed. Eng.,* 40:1895–1902.

[97] Oflaz, H., Baran, O., (2014). A new medical device to measure a stiffness of soft materials. *Acta Bioeng. Biomech.,* 16:125–131.

[98] Yen, P-L., Chen, D-R., Yeh, K-T., Chu, P-Y. (2008). Lateral exploration strategy for differentiating the stiffness ratio of an inclusion in soft tissue. *Med. Eng. Phys.,* 30:1013–1019.

[99] Subasi, A., Gursoy, M.I., (2010). EEG signal classification using PCA, ICA, LDA and support vector machines. *Expert Syst. Appl.,* 37:8659–8666.

[100] Acar, E., Dunlavy, DM., Kolda, T.G., Mørup, M., (2011). Scalable tensor factorizations for incomplete data. *Chemom. Intell. Lab. Syst.,* 106:41–56.

[101] Ince, T., Kiranyaz, S., Gabbouj, M., (2009). A generic and robust system for automated patient-specific classification of ECG signals. *IEEE Trans. Biomed. Eng.,* 56:1415–1426.

[102] Kiranyaz, S., Ince, T., Gabbouj, M., (2016). Real-Time Patient-Specific ECG Classification by 1-D Convolutional Neural Networks. *IEEE Trans. Biomed. Eng.,* 63:664–675.

[103] Tabar, Y.R., Halici, U., (2016). A novel deep learning approach for classification of EEG motor imagery signals. *J. Neural Eng.,* 14:16003.

[104] Alkan, A., Günay, M., (2012). Identification of EMG signals using discriminant analysis and SVM classifier. *Expert. Syst. Appl.,* 39:44–47.

[105] Dincer, F., Karaaslan, M., Unal, E., Sabah, C., (2013). Dual-band polarization independent meta-material absorber based on omega resonator and octastarstrip configuration. *Prog. Electromagn. Res.,* 141:219–231.

[106] Sabah, C., Dincer, F., Karaaslan, M., Unal, E., Akgol, O., Demirel, E., (2014). Perfect metamaterial absorber with polarization and incident angle independencies based on ring and cross-wire resonators for shielding and a sensor application. *Opt. Commun.,* 322:137–142.

[107] Ergen, B., Tatar, Y., Gulcur, H.O., (2012). Time-frequency analysis of phonocardiogram signals using wavelet transform: A comparative study. *Comput. Methods, Biomech. Biomed. Engin.,* 15:371–381.

[108] Gurun, G., Zahorian, J.S., Sisman, A., Karaman, M., Hasler, P..E, Degertekin, L.F., (2012). An analog integrated circuit beamformer for high-frequency medical ultrasound imaging. *IEEE Trans. Biomed. Circuits Syst.* 6:454–467.

[109] Kerse, C., Kalaycıoğlu, H., Elahi, P., Çetin, B., Kesim, D.K., Akçaalan, Ö., Yavaş, S., Aşık, M.D., Öktem, B., Hoogland, H., (2016). Ablation-cooled material removal with ultrafast bursts of pulses. *Nature,* 537:84.

[110] Kucukgul, C., Ozler, S.B., Inci, I., Karakas, E., Irmak, S., Gozuacik, D., Taralp, A., Koc, B., (2015). 3D bioprinting of biomimetic aortic vascular constructs with self-supporting cells. Biotechnol Bioeng 112:811–821.

Int. J. Adv. Eng. Pure Sci. 2019, 4: 328-335
DOI: 10.7240/jeps.579624

RESEARCH ARTICLE / ARAŞTIRMA MAKALESİ

Yeni Bir Yaklaşımla Genç Bireylerde Kalp Sağlığı Takibi için Web ve Mobil Uygulama Geliştirilmesi

Developing Web and Mobile Applications for Heart Health Monitoring in Young People with a New Approach

Zehra Aysun ALTIKARDEŞ [1], Mensur BAJGORA [1], Ufuk SARIKAYA [1], Buket DOĞAN [1], Ali Serdar FAK [2]

[1] Marmara Üniversitesi, Teknoloji Fakültesi, Bilgisayar Mühendisliği Bölümü, 34722, Kadıköy / İstanbul

[2] Marmara Üniversitesi, Hipertansiyon ve Ateroskleroz Araştırma Merkezi, 34854, Maltepe / İstanbul

Öz

Kardiyovasküler hastalık riskini tetikleyen hipertansiyon, obezite, diyabet gibi önlenebilir hastalıkların ve risk faktörülerinin sıklığı ülkemizdeki genç bireylerde hızla artmaktadır. Bu hastalıkların kontrollü bir şekilde takip edilebilmesi ve önlenebilmesi için Marmara Üniversitesi öğrencilerinin demografik ve sağlık verilerinin kayıt altına alınmasını ve izlenmesini sağlayan web ve mobil uygulamanın geliştirilmesi sağlanmıştır. Böylece, Framingham risk skoruna göre öğrencilerin 10 yıllık kardiyovasküler risklerinin hesaplanarak görüntülendiği ve kişiye özel hale getirilmiş tıbbi önerilerin e-posta yoluyla bildirildiği bir web platformu PHP ve MySQL kullanılarak oluşturulmuştur. Öğrencilerin ilerleyen zamandaki kardiyovasküler hastalık risklerinin takip edilebildiği bu platform, yüksek risk grubunda olan bireylerin risk seviyelerinin normale indirilebilmesi için farkındalıklarını arttıran bir işlevselliğe sahiptir. Hazırlanan web platformunun desteklenmesi için, Marmara Üniversitesi öğrencilerinin kendi sağlık durumlarını takip edebilecekleri, kalp sağlığı konusunda bilinçlendirici bildirimlerle destekleneceği ve yaşam kalitelerini arttırabilmeleri için bir standart oluşturulmasına yardımcı olacak "Sağlıklı Kalpler" adında Android ve iOS platformlarında kullanılmak üzere bir mobil uygulama geliştirilmiştir. Bu uygulama içerisinde adım sayar, egzersiz ekleme, listeleme, sağlıklı beslenme ve güncel sağlık durumunu izleme gibi fonksiyonlar bulunmaktadır.

Anahtar Kelimeler: Kalp Sağlığı, Sağlıklı Kampüs, Mobil Uygulama, Web Platformu

Abstract

The incidence of preventable diseases such as hypertension, obesity and diabetes which triggers the risk of cardiovascular disease increases rapidly in young individuals in our country. In order to monitor and prevent these cardiovascular risk factors and diseases in a controlled way, a web and mobile application was developed to record and monitor demographic and health data of Marmara University students. Thus, a web platform was created using PHP and MySQL, in which 10-year cardiovascular risks of students were calculated according to Framingham Risk Score and displayed and personalized medical recommendations were notified to them via e-mail. This platform, in which students can monitor the risks of cardiovascular disease in the future, has a functionality that increases the awareness of individuals in high-risk groups in order to normalize their risk levels. In order to support the web platform, a mobile application has been developed for use on Android and iOS platforms called "Healthy Hearts" which will allow Marmara University students to follow their own health status, be supported with awareness-raising notifications about heart health and help to establish a standard for improving their quality of life. This app includes functions such as step counts, exercise addition, listing, healthy eating and monitoring of current health status.

Keywords: Heart Health, Healthy Campus, Mobile Application, Web Platform

I. GİRİŞ

Günümüzde, bireylerin eğitim ve gelir düzeyinin yükselmesi, beslenme alışkanlıklarının değişmesi, bulaşıcı hastalıkların kontrolü gibi etkenler yaşam süresinin artmasına olanak sağlamıştır. Artan yaşam süresinin yanında bulaşıcı olmayan

Sorumlu yazar/Corresponding Author: Zehra Aysun ALTIKARDEŞ, **Tel:** +905057398000, **e-posta:** aaltikardes@marmara.edu.tr,
Gönderilme/Submitted: 19.06.2019, **Düzenleme/Revised:** 26.09.2019, **Kabul/Accepted:** 16.10.2019

hastalıkların (BOH) sayısı ve sıklığı da artmaktadır. 2012 yılında dünyada gerçekleşen 56 milyon ölümün 38 milyonu kalp ve damar hastalıkları, kanser, kronik solunum yolu gibi BOH'lardan kaynaklanmıştır. Sağlık Bakanlığı raporuna göre bu hastalıklara sebep olan faktörlerden birisi yapılan fiziksel aktivitelerin yetersiz olmasıdır [1]. Bu raporda, sağlıklı kalma ile ilgili (wellness) teknolojilerin ve uygulamaların kullanımlarının özendirilmesi gerektiği başlığına da yer verilmiştir [2].

Üniversite öğrencileri arasında cep telefonu kullanımının çok yaygın olması, mobil uygulamaların kullanılmasına yönelik olumlu görüşleri ve mobil sağlık sistemlerine katılma konusunda istekli olmaları yönünde araştırmalar da bulunmaktadır [3]. Bu nedenle, üniversiteye devam eden öğrenciler arasında mobil sağlık uygulamaları konusunda farkındalık oluşturmak, ilerleyen zamanda bireylerin sağlıklarına olumlu katkı yapacak niteliktedir. Artık disiplinlerarası bir çalışma konusu haline gelen mobil sağlık sistemlerine öğrencilerin katılım göstermesi, hem özel hayatlarında hem de iş dünyasındaki faaliyetlerinde olumlu etki etme potansiyeli taşımaktadır.

Bu çalışma kapsamında, kalp sağlığını takip etmek isteyen Marmara Üniversitesi öğrencileri arasında gönüllülük ilkesi temelinde bu çalışma gerçekleştirilmiştir. Çalışmada, demografik, boy, kilo, bel çevresi, kolesterol, kan şekeri, kan basıncı, sigara kullanımı gibi verilerinin toplanması, kalp sağlığı risk skorlarının belirlenmesi, elde edilen ölçüm sonuçlarına göre risk durumlarının takip edilmesi, gerçekleştirilen fiziksel aktivitelerin izlenmesi, aktivite durumlarının raporlanması ve kişiye özel tıbbi önerilerle öğrencilerin yaşam kalitelerini yükseltmelerine olanak sağlanması için web ve mobil uygulamaları geliştirilmiştir.

1.1 İlgili Çalışmalar

Günümüzde kullanılan akıllı telefonların bilgi işleme yeteneği yükselmiş ve bununla birlikte kullanım kolaylığı artmıştır. Mikrofon ve kameranın yanı sıra ivmeölçer, GPS, nabız ölçer gibi sensörler ile donanımları güçlendirilmiştir. Bu özellikler dikkate alındığında akıllı telefonlarda sağlık uygulamalarının geliştirilmesi yaygınlaşmıştır. Geliştirilen mobil sağlık uygulamaları, bireylerin çeşitli tıbbi ve fiziksel aktivite verilerinin saklanmasına, takip edilmesine, raporlanmasına ve böylece bireylere daha sağlıklı bir yaşam sunulmasına olanak sağlamaktadır [4].

Ülkemizde, diğer gelişmiş ülkelerde olduğu gibi genç nüfusta hipertansiyon, obezite ve şeker hastalığı sıklığı fazladır ve hızla artmaktadır. Önümüzdeki yıllarda erişkinlerde daha fazla kalp damar hastalığı ve bunlara bağlı ölümlerle karşılaşmamak için genç bireylerde kalp damar hastalığı riskleriyle daha etkin mücadele edilmesi gereklidir. Bu bağlamda yapılan bu özgün çalışma ile benzer konuları işleyen literatür tarama sonuçları aşağıda paylaşılmıştır.

Richardson ve arkadaşları tarafından gerçekleştirilen çalışma sonuçlarına göre üniversite yaşamının ilk yıllarında, öğrencilerin kilolarında yaklaşık %15'lik bir artış olduğu ortaya konmuştur. Bu çalışma, üniversitenin ilk yılında, birçok öğrencide kilo artışı görüldüğü özellikle de erkeklerde üniversite öğrenciliğinin ikinci yılında kilo artışlarının devam ettiğini göstermektedir [5].

Farinelli ve arkadaşları tarafından gerçekleştirilen çalışma 18-35 yaş arası bireyler üzerinde gerçekleştirilmiştir. Bu çalışma kilo alımını önlemeye yönelik bir mobil sağlık uygulaması olup, dokuz aylık süreçte uygulamayı kullananların kullanmayanlara göre daha fazla kilo verdiği tespit edilmiştir [6].

Walsh ve arkadaşlarının çalışması, yaşları 17-26 arasında değişen 58 kişilik bir grup üzerinde gerçekleştirilmiştir. Bu mobil uygulamanın sonuçları incelendiğinde, belirlenen hedefler doğrultusunda, kendi kendini izleyen ve geri bildirimlere göre aktivitelerini düzenleyen genç erişkin bireylerin fiziksel aktivitelerini gerçekleştirme oranlarının önemli ölçüde arttığı tespit edilmiştir [7].

Bir mHealth uygulaması olan iCardia [8] çalışmasında, akıllı telefon kullanan kullanıcılardan fiziksel aktiviteleri ve kalp atışı gibi verileri gerçek zamanlı olarak merkezi bir sunucuda toplanmış ve kardiyovasküler hastalıkların uzmanlar tarafından takibi sağlanmıştır. mHealth uygulamaları, geleneksel kardiyovasküler programların kapsamını genişletmenin yanı sıra, daha fazla kullanıcı katılımını sağlayarak daha fazla veri toplama olanağı sağlamaktadır. Böylelikle hastaların problemlerinin daha hızlı ve net bir biçimde çözümüne ulaşma imkânı sunulmaktadır.

WE-CARE ise EKG işaretlerini okuyan bir donanım vasıtasıyla akıllı cep telefonuna ulaşan kalp atış sinyallerini, gerçek zamanlı olarak bir merkezde toplayan ve böylece kalp sağlığı takibini sağlayan bir mHealth uygulamasıdır. Geliştirdikleri algoritmalar vasıtasıyla, sunucuya gelen EKG işaretlerini inceleyerek, hastaların kalp sağlığı riskini takip etmektedirler. Anpeng ve arkadaşları çalışmalarının sonucunda mHealth kavramının umut verici olduğunu ve gelecekte gerçek uygulamalara dönüştürülebileceğini belirtmişlerdir [9].

Gerçekleştirilen bu pilot çalışma, tamamen özgün olarak tasarlanmış olup, öğrencilerin üniversiteye kayıtlarından mezuniyetlerine kadar kardiyovasküler risk durumlarının değerlendirildiği, web ve mobil platformlarda bireyselleştirilmiş önerilerin sunulduğu, öğrenci merkezli etkinlikleriyle ve "kalp dostu üniversite kampüsü" hedefiyle henüz

ülkemizde benzeri olmayan Marmara Üniversitesi Öğrenci Kalp Sağlığı Projesi'nin teknik altyapısı için ilk adımlardır.

II. MATERYAL VE YÖNTEM

Temel olarak web ve mobil platformu olmak üzere iki kısımdan oluşan uygulama, Facebook, Twitter, Instagram gibi sosyal medya platformları ile desteklenmiştir.

2.1 Materyal

Çalışmada gönüllülük ilkesi temelinde 770 öğrenciye ait yaş, cinsiyet, kilo, boy, bel çevresi, kan şekeri, sistolik ve diyastolik kan basıncı, kolesterol, sigara kullanımı, ilaç kullanımı ve diyabet geçmişi verileri toplanarak bir veritabanı oluşturulmuştur. Öğrencilerden verilerin toplanabilmesi için M.Ü. Tıp Fakültesi Klinik Araştırma Etik Kurulu Onayı alınmıştır (Protokol No: 09.2017.327 Onay Tarihi: 07.04.2017). Bu verilere ek olarak öğrencilere, kalp sağlığı konusundaki bilgilerini ve farkındalıklarını tespit etmek amacıyla bazı anketler uygulanmış ve her bir öğrencinin anketlere verdikleri cevaplar da veritabanına kaydedilmiştir.

10 yıllık kardiyovasküler risk hesaplaması için Framingham Risk Score kullanılmıştır [10].

2.2 Veritabanı

Geliştirilen web ve mobil uygulamalarında MySQL veritabanı kullanılmıştır. Veritabanında oluşturulan tablolar ve açıklamaları Tablo 1'de görülmektedir.

Tablo 1. Kullanılan veritabanı tabloları ve açıklamaları

Tablo Adı	***Açıklaması***
Ogrenciler	*Öğrencilerin kişisel ve demografik tüm bilgilerinin tutulduğu tablodur.*
Ogrenci_ bilgileri	*Sağlık ölçümleri yapılan öğrencilerin tüm sağlık verilerinin tutulduğu tablodur. Ogrenciler tablosu ile ilişkilidir.*
Kullanicilar	*Sistemde öğrenci, veri girişi yapan ve analizleri inceleyen sağlık personeli ile yönetici tiplerinde 3 farklı kullanıcı bulunmaktadır. Bu kullanıcıların tümünün sisteme girişleri için kullanıcı adı&şifre gibi bilgilerinin tutulduğu tablodur.*
Kullanici_ tipleri	*Giriş yapan kullanıcının öğrenci, sağlık personeli veya yönetici olduğunu belirten tablodur. Kullanıcılar tablosu ile ilişkilidir.*
Anket_ tipleri	*Öğrencilere uygulanan 4 farklı anket bulunmaktadır. Bu anketlerin listesinin tutulduğu tablodur.*
Anket_ sorulari	*Her bir ankette yer alan soruların tutulduğu tablodur. Anket_tipleri tablosu ile ilişkilidir.*
Anket_ ogrenci	*Anket dolduran öğrencilerin fakülte, bölüm, sınıf ve hangi anketi doldurduğu bilgilerinin tutulduğu tablodur. Anket_sorulari tablosu ile ilişkilidir.*
Anket_ cevaplari	*Öğrencilerin her bir anket için verdikleri cevapların tutulduğu tablodur. Anket_tipleri, anket_sorulari ve anket_ ogrenci tablolarıyla ilişkilidir.*
Fakulteler	*Marmara Üniversitesi'nde yer alan tüm fakülte, yüksekokul ve enstitülerin adlarının yer aldığı tablodur.*
Fakulte_ bolumleri	*Marmara Üniversitesi'nde yer alan her bir fakültedeki bölümlerin adlarının yer aldığı tablodur. Fakulteler tablosu ile ilişkilidir.*
Ogrenci_ yorumlari	*Sisteme kayıtlı öğrencilerden, hazırlanan web platformu ve yapılan tüm çalışmalar hakkında değerlendirmelerinin ve görüşlerinin yer aldığı tablodur. Ogrenciler tablosu ile ilişkilidir.*
İslem_log	*Veri girişi veya güncellemeleri sırasında yapılan tüm işlemlerin kimin tarafından ve ne zaman yapıldığı bilgilerinin tutulduğu tablodur. Bu işlemlerden bazıları bir öğrencinin sağlık bilgilerinin sisteme eklenmesi, anket cevaplarının girilmesi, kişisel bilgilerinden bazılarının güncellenmesi, silinmesi vb. işlemlerdir.*
Egzersizler	*Kullanıcıların yapmış oldukları egzersizler, bu egzersizlerin tarihi, zamanı, süresi gibi detayları ile birlikte bu tabloda tutulmaktadır.*
Doktorlar	*Sisteme dahil olan doktorların bilgilerinin tutulduğu tablodur.*
Beslenme	*Kullanıcıların beslenme alışkanlıkları ile ilgili yapmış oldukları veri girişleri bu tabloda tutulmaktadır.*
PlanlıBildirimler	*Kullanıcılara gönderilecek olan standart bildirimler bu tabloda tutulmaktadır.*
AppLog	*Kullanıcıların mobil uygulamayı kullanım istatistikleri bu tabloda tutulmaktadır.*

2.3 Web Uygulaması

PHP programlama dili kullanılarak oluşturulan web platformu, 3 ana modülden oluşmaktadır. Bu modüller sırasıyla aşağıdaki gibidir.

Sağlık personeli: Öğrencilere ait demografik, sağlık ve anket verilerinin sisteme girilmesi, öğrencilere ait tüm bilgilerin ve çeşitli raporların görüntülenmesi, bilgilerin güncellenmesi ve silinmesi işlemlerinin gerçekleştirildiği bölümdür.

Öğrenci paneli: Sisteme kaydı yapılan öğrencilerin giriş yaparak, kendi bilgilerinin görüntülenmesi, yapılan ölçümlere göre kişisel gelişim grafiği, yapılan anketlere ait sorulara verilen cevap yüzdelerinin görüntülenmesi işlemlerinin gerçekleştirildiği bölümdür.

Yönetim paneli: Veri girişleri için yeni kullanıcıların tanımlama işlemlerinin gerçekleştirildiği bölümdür.

Oluşturulan web platformunun site haritası Şekil 1'de görülmektedir.

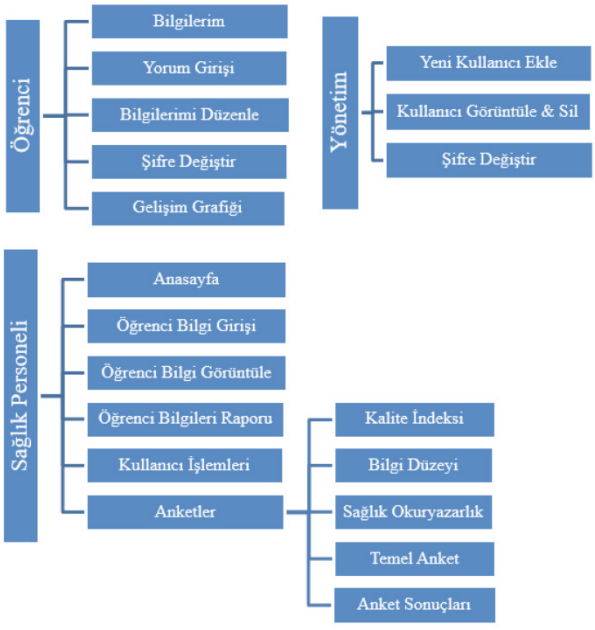

Şekil 1. Sağlıklı kalpler site haritası

2.4 Mobil Uygulama

Hazırlanan mobil uygulamanın içerdiği fonksiyonlar aşağıdaki gibidir:

Mobil cihazın sensörleri kullanılarak kullanıcının attığı adım sayısının takip edilmesi,

Kullanıcının yaptığı yürüme, koşma, bisiklet sürme gibi aktivitelerin takip edilmesi ve bu aktivitelerin mesafe ve süre gibi değerlerinin tutulması,

Yapılan bu aktivitelerin listelenmesi,

Önceden kayıt edilmiş sağlık verilerinin gösterilmesi,

Kullanıcılara verilmiş önerilerin bildirim olarak gönderilmesi

Bu çalışmada gerçekleştirilen uygulamanın sistem mimarisi Şekil 2'de görülmektedir. Uygulamanın kullanıcıları, akıllı telefonları sayesinde internete bağlanıp, uygulamalarından sunucuya yaptıkları fiziksel aktivitelerin verilerini göndermektedirler. Gönderilen veriler veritabanına kaydedilmekte ve gerekli hesaplamalar gerçekleştirilmektedir. Kullanıcılar, aktivitelerinin raporunu günlük, haftalık, aylık veya yıllık gibi farklı zaman aralığında görüntüleme imkânına sahiptirler.

Bu kapsamda toplanan veriler aşağıdaki gibi listelenebilir.

Hareketlilik: Kullanıcının yapmış olduğu yürüme, koşma, bisiklet sürme ve benzeri fiziksel aktivitelerin verilerini kullanıcı profili ile ilişkilendirerek veritabanına kaydedilmesi,

Beslenme: Kullanıcıların gün içerisinde tükettiği yiyecek ve içeceklerin sağlıklı/sağlıksız gibi bilgilerinin kaydedilmesi,

Kullanım: Kullanıcıların uygulamayı kullanım süresinin ölçülmesi, bunun sonucunda fiziksel aktivitelerindeki değişiklerinin belirlenmesi ve bu konuya ilişkin istatistiksel bilgilerin çıkarabilmesi

API ve web uygulaması Linux sunucu içerisinde yer almaktadır. Bu sunucuda "CentOS 7" işletim sistemi çalışmaktadır. Veritabanı ise farklı bir Linux sunucusunda yer almaktadır. Mobil uygulamasına gönderilen bildirimler için "One Signal" adlı bir eklenti kullanılmaktadır. API ve mobil uygulaması, ortak çalışma özelliğine sahiptir [11]. Yani API tarafında tetiklenen bildirimler, bu eklenti sayesinde mobil uygulamasına ulaştırılabilmektedir. Gerçekleştirilen mobil uygulama "Android" ve "iOS" işletim sistemlerinin her ikisinde de kullanılabilmektedir.

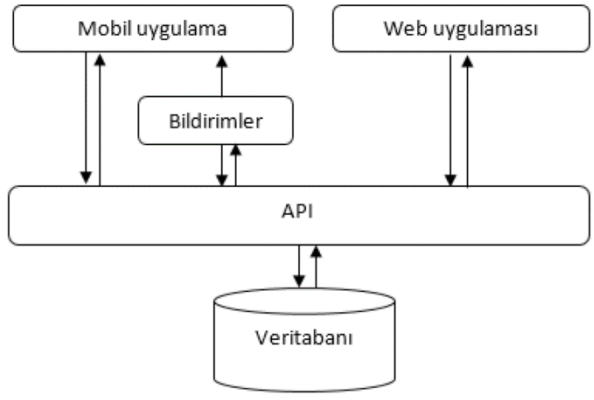

Şekil 2. Sistemin genel mimarisi

API, uygulamada veritabanı, web uygulaması, mobil uygulaması ve bildirim mekanizması gibi diğer mimari bileşenler arasında köprü görevi üstlenmektedir. Bu nedenden dolayı mimarinin tam ortasında yer almaktadır ve çok kritik bir öneme sahiptir. API ile ilgili dikkat edilmesi gereken en önemli unsurlar güvenlik ve sürekliliktir. Hem veritabanı ile hem de mobil uygulaması ile direkt iletişim kurabilen tek bileşen API'dir.

API'nin bulunduğu sunucular yedekli olarak iki farklı konumda tutulup, birbiriyle sürekli iletişimde bulunarak birinci sunucuda yapılan herhangi bir değişiklik ikinci sunucuya yansımaktadır. Böylece birinci sunucuda herhangi bir problem veya arıza meydana geldiği durumda ikinci sunucu üzerinde en güncel yazılım hali ile sistemin işlemesi devam

etmektedir. API'nin diğer bir rolü ise oturum yönetimidir. Oturum yönetimi kullanıcıların erişim izin kontrolü ve veri güvenliğinin sağlanması için gereken bir mekanizmadır. Mobil uygulamalarda kurulması gereken oturum yönetimi, web uygulamalarından işlem süresi ve işlem sürekliliği gibi noktalarda farklılıklar göstermektedir. Mobil uygulamalarda oturum yönetimi için jeton (token) kullanılır. Mobil uygulamada kullanıcı giriş yaparken bir jeton üretilmekte, bu jeton kullanıcıya gönderilerek kullanıcının mobil cihazında kaydedilir ve daha sonra yapılan her bir istekte bu jetonun parametre olarak kullanılması sağlanır. API tarafından yeniden üretilen jeton ile kullanıcıdaki jeton aynı ise işlem yapılması sağlanarak bir kontrol mekanizması çalıştırılır. Bu jeton, kullanıcının bilgileri ve anahtar kelimeleri şifrelenerek, her kullanıcı için eşsiz olacak şekilde üretilmektedir. Böylece kullanıcıdan gelen ve üretilen jeton kontrol edilerek veri akışının ilk aşamasındaki güvenlik ve kullanıcının oturum yönetimi sağlanmaktadır.

Android ve iOS için gerekli olan NodeJs, Ionic 3, Android SDK ve Xcode bileşenleri ile yazılım altyapısı hazırlanmıştır. Uygulamanın geliştirmesi için IONIC platformu kullanılmıştır. Bu platformun seçilmesinin nedeni, yazılım geliştirme sürecinin hızlandırılması, web tabanlı teknolojilerin kullanılması ve birçok ortam için aynı kaynak kodu kullanılarak uygulama geliştirilmesi gibi avantajlara sahip olmasıdır.

Mobil uygulaması, iki servis sağlayıcı (provider) ve birkaç yardımcı ekran olmak üzere toplamda altı ekrandan oluşmaktadır. Bu ekranlarda, oturum açılması, veri toplanması, geçmiş verilerin gösterilmesi, özet sağlık durumunun gösterilmesi ve sağlıklı yaşam ile ilgili genel bilgilerin gösterilmesi gibi özellikler bulunmaktadır. Servis sağlayıcıları ise API ile iletişim kurmak ve yerel depolama alanı yönetmek gibi işlemleri gerçekleştirmektedir.

2.4.1 Bildirimler

Geliştirilen sistemde bildirimlerin kullanım amacı, kullanıcılara belli zamanlarda kalp sağlığı ile ilgili öneriler sunmak ve daha fazla aktivite yapmalarını teşvik etmektir. Bu bildirimler gönderilirken her zaman makul ölçüde olmasına dikkat edilmektedir.

Bildirimlerin gönderilebilmesi için OneSignal platformu kullanılmaktadır. Bu platform ile basit web ve mobil bildirimleri ücretsiz olarak gönderilebilmektedir. Bu platformun kullanıcı dostu arayüze sahip olması sayesinde giden bildirimler, kayıtlı olan kullanıcıların listelenmesi ve izlenmesine olanak sağlamaktadır. Platformun API hizmeti de iyi tasarlanmış olup farklı platformlardan kullanılma imkânı sunmaktadır. Bu API'nin çeşitli metotları sayesinde kullanıcılara toplu veya özel bildirimler gönderme imkânı bulunmaktadır. OneSignal platformunun grafiksel arayüzü sayesinde bildirim gönderilen kullanıcı sayısı takip edilebilmektedir.

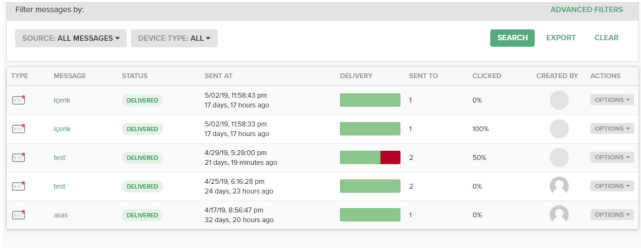

Şekil 3. Onesignal bildirim listesi

Şekil 3'te OneSignal'ın göndermiş olduğu bildirimlerin listesinin yer aldığı panel gösterilmektedir. Bu ekranda bildirimin başlığı ve içeriğinin yanı sıra bildirimin gönderilme zamanı, kaç kullanıcıya başarılı olarak gönderildiği, kaç kullanıcıda başarısız olduğu ve kaç kullanıcı tarafından tıklandığı gibi bilgiler de takip edilebilmektedir. Bu takip sayesinde kullanıcılar tarafından hangi bildirimlerin daha çok dikkate alındığı, hangi saatlerin bildirim göndermek için daha verimli olduğu ve kullanıcıların uygulamaya olan ilgisi gibi bilgiler edinilebilmektedir. Bu bilgiler kullanılarak gönderilen bildirimlerin optimizasyonu mümkün kılınmaktadır.

Gönderilen bildirimler iki gruba ayrılır. Birinci gruptaki bildirimler, önceden planlanmış genel kalp sağlığı ile ilgili bildirimlerdir ve bu bildirimlerden bir liste oluşturulmuştur. Hangi bildirimin hangi günde gideceğine karar verilmiştir. Daha sonra kullanıcının uygulamayı kullanmayı başladıktan sonra zamanlanmış bir görev tanımlayarak günlük olarak bu bildirimler gönderilecektir. İkinci gruptaki bildirimler ise, kullanıcının yaptığı egzersizlere bağlı oluşan bildirimlerdir. Kullanıcının egzersiz verilerinin analizinden sonra öğrencinin kalp sağlığı risk skoru dikkate alınarak, belirlenen günlük aktivite hedefine ulaşıldıysa olumlu içerikli, hedefin altında kalındıysa olumsuz içerikli bir bildirim gönderilebilmektedir.

2.4.2 Sağlıklı kalpler mobil uygulamasının kullanıcı arayüzleri

Bu başlık altında, geliştirilen "Sağlıklı Kalpler" mobil uygulamasının aktivite ile ilgili olan kullanıcı arayüz ekranları ve açıklamalarına yer verilmiştir.

2.4.2.1 Uygulama hakkında ekranı

Şekil 4'te görülen ekranda kullanıcılara mobil uygulama hakkında bilgi verilmektedir.

Şekil 4. Uygulama hakkında sayfası ekran görüntüsü

2.4.2.2. Anasayfa ekranı

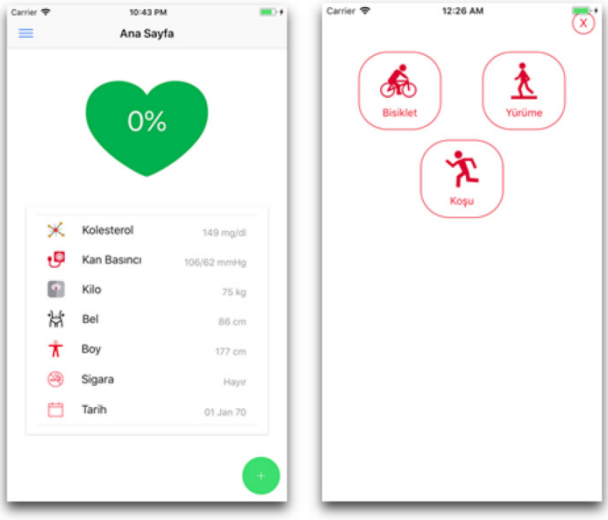

Şekil 5. (a) Uygulamanın ana sayfası ve **(b)** fiziksel aktivite başlatma ekranı

Şekil 5 (a)'da gösterilen ekran kullanıcı, uygulamaya giriş yaptıktan sonra açılan ilk ekrandır. Bu ekranda kullanıcının yapılan son sağlık kontrolündeki ölçülen bilgileri gösterilmektedir. Böylece kullanıcı her zaman güncel sağlık durumunu görebilmektedir. Ekranın üst kısmında gösterilen kalp şekli, kullanıcının kardiyovasküler risk değerini gösterecek şekilde hesaplanan FRAMINGHAM skor puanı [12] renklendirilerek görüntülenmektedir. Bu değerler elektronik veri tabanında kayıt edilerek, katılan her öğrenci için hesaplanmaktır. Risk skoru yüksek olan öğrencilerin profesyonel destek alabilmeleri için imkân sağlamak hedeflenmiştir. Eğer FRAMINGHAM skor değeri bir veya birden küçük ise yeşil, birden büyük ve ikiden küçük ise sarı, iki veya daha büyük bir değer ise kırmızı rengini almaktadır [12]. Ana sayfanın sağ alt köşesinde bulunan yeşil renkli butona basılarak, kullanıcı yeni bir fiziksel aktivite başlatabilmektedir.

Şekil 5 (b)'de görülen fiziksel aktivite başlatma ekranında, bisiklet, yürüme ve koşu olmak üzere üç farklı aktivite başlatılabilmektedir. Öğrencinin fiziksel aktive performansının gözlemlenmesi ve bu gözlem sonucunda gerekli önerilerin verilmesi için bu ekran en önemli rolü oynamaktadır.

2.4.2.3 Fiziksel aktivite ekranı

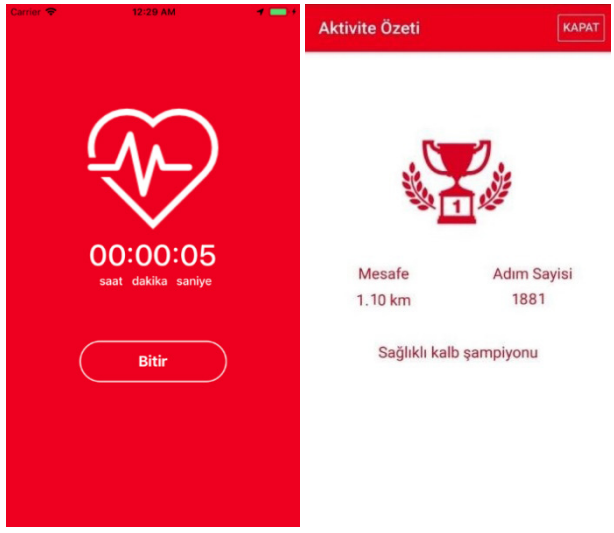

Şekil 6. (a) Fiziksel aktivite ekranı ve **(b)** bitmiş fiziksel aktivitenin özeti

Şekil 6 (a)'da görülen ekran, fiziksel aktivite gerçekleştirme sırasında kullanıcıya gösterilmektedir. Bu ekran, kullanıcının ilgili fiziksel aktivitesinin süresini göstermektedir. Böylece kullanıcı hedeflediği süreye ulaşıp ulaşmadığını kontrol edebilmektedir. Şekil 6 (b)'de ise yapılan fiziksel aktivitenin kat edilen mesafe ve adım sayısını içeren özet ekranı görülmektedir.

2.4.2.4 Egzersiz geçmişi ekranı

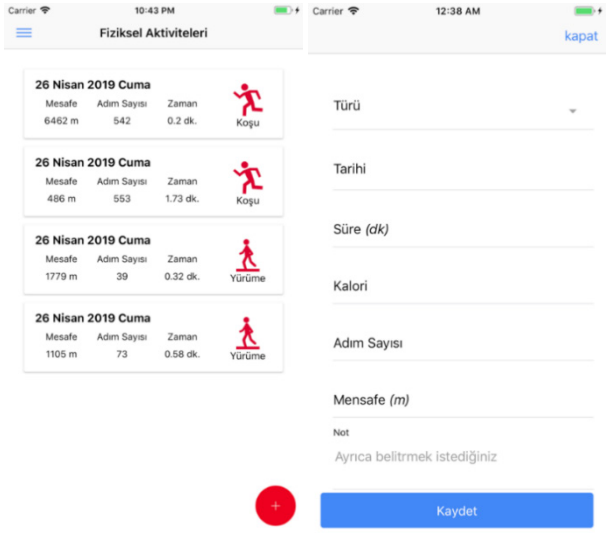

Şekil 7. (a) Egzersiz geçmişi ekranı ve **(b)** egzersiz ekleme ekranı

Şekil 7 (a)'da görülen ekranda, kullanıcının yapmış olduğu fiziksel aktivitelerin listesi gösterilmektedir. Kullanıcı, ekranı aşağıya doğru kaydırarak geçmişe doğru zaman, mesafe, süre, egzersiz çeşidi ve adım sayısı gibi tüm fiziksel aktivite bilgilerini görebilmektedir.

Ekranın sağ alt köşesinde gösterilen düğme (+) ise kullanıcının yaptığı fiziksel aktivitelerini ekleyebildiği ekranı açmaktadır. Şekil 7 (b)'de gösterilen bu ekran, fiziksel aktivite ekleyebilmek için gerekli bilgilerin giriş yapılabileceği ekrandır. Bu ekrandan eklenen fiziksel aktivitelerin doğruluğu tespit edilemediği için kullanıcının performans hesabı yapılırken dikkate alınamayabilir.

2.4.2.5 Geçmiş kontroller ekranı

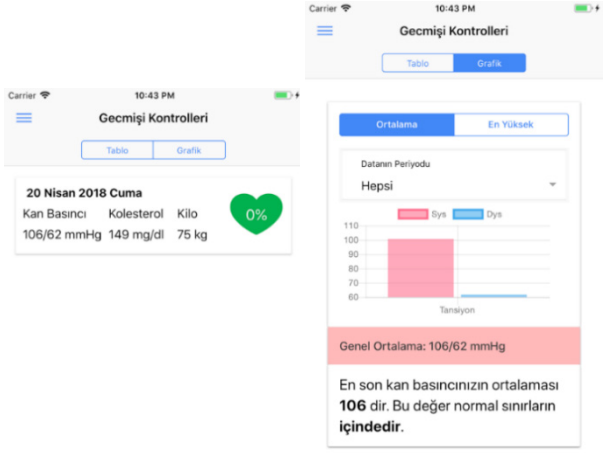

Şekil 8. Geçmiş kontroller liste ve grafik ekranı

Şekil 8'de görülen ekranda, yapılan sağlık kontrolleri tarihe göre listelenmiştir ve kan basıncı, kolesterol, kilo, kalp sağlığı risk skoru gibi bilgiler gösterilmektedir. Bu listede kullanıcı, sağlık durumunun değişimi hakkında bilgi alabilmektedir. Ayrıca grafik sekmesinde, yapılan ölçümlerde alınan kan basıncı değerleri grafiksel olarak gösterilmektedir.

2.4.2.6 Sağlıklı beslenme ekranı

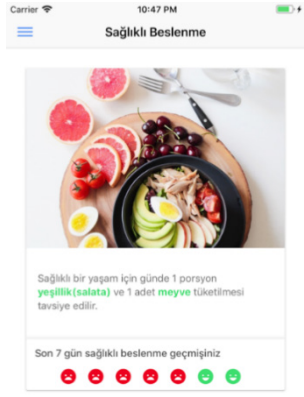

Şekil 9. Sağlıklı beslenme ekranı

Şekil 9'da görülen sağlık beslenme ekranında, kullanıcı o gün ile ilgili yapılan beslenme durumunu değerlendirebilmektedir. Ayrıca bu ekranda, kullanıcıdan alınan son 7 güne ait değerlendirmeler gösterilmektedir. Böylelikle kullanıcı, beslenmesine ne kadar dikkat ettiğini takip edebilmektedir.

III. BULGULAR VE TARTIŞMA

Bu çalışma ile Marmara Üniversitesi öğrencilerinin kalp sağlığı konusunda farkındalıklarını arttırmaya yönelik, önümüzdeki 10 yıllık süreç için kardiyovasküler hastalıklara yakalanma risklerini öğrenebilmelerine, risk düzeylerini düşük tutabilmek için fiziksel aktivite, doğru beslenme ve temel sağlık verilerini düzenli olarak kontrol etmelerine olanak sağlayan, böylece yaşam kalitelerini yükseltmelerine yardımcı olacak bir web platformu ve bunu destekleyen bir mobil uygulaması geliştirilmiştir. 770 öğrenciye ulaşan başlangıç seviyesindeki bu küçük projenin başarılı ve öncü bir çalışma olduğu ortaya konmuş olup Marmara Üniversitesi başta olmak üzere ülkemizdeki tüm üniversitelerde sağlıklı kampüs adı altında çeşitli projelere öncülük etmesi hedeflenmektedir.

Marmara Üniversitesi Öğrenci Kalp Sağlığı Projesi kapsamında gerçekleştirilen bu çalışma üniversite öğrencilerinin demografiki klinik ve bazı biyolojik verilerinin kendi katkı ve katılımlarıyla mobil cihaz ve yöntemlerle takibinin

mümkün olabileceğini pilot olarak göstermiş ve farkındalık yaratmıştır. Bu durum biraz büyük bir destekle üniversite öğrencilerinin kalp damar sağlığının korunmasında önemli ve etkin katkı sağlayabilir.

TEŞEKKÜR

Bu çalışma, FEN-C-YLP-150.218.0054 ve FEN-C-YLP-170.118.0018 numaralı Marmara Üniversitesi BAPKO Lisansüstü Tez projeleri kapsamında desteklenmiştir.

Bu projenin gerçekleştirilebilmesi için M.Ü. Tıp Fakültesi Klinik Araştırma Etik Kurulu Onayı alınmıştır (Protokol No: 09.2017.327 Onay Tarihi:07.04.2017).

Bu projeyi destekleyen, Marmara Üniversitesi HİPAM Müdürü Sayın Prof. Dr. Ali Serdar FAK ile Yönetim Kurulu Üyelerine ve emeği geçen tüm ekibe katkılarından dolayı teşekkür ederiz.

KAYNAKLAR

[1] Tosun, N., Erkoç, Y., Buzgan, T., Keskinkılıç, B., Aras, D., Yardım, N., Soylu, M. (2014). Türkiye Kalp Ve Damar Hastalıklarının Önleme ve Kontrol Programı (2010-2014). Ankara: Anıl Matbaası. Anthropology And Medicine, 3-12.

[2] Tezcan, C. (2016). Sağlığa Yenilikçi Bir Bakış Açısı: Mobil Sağlık.

[3] Kazemi, D. M., Cochran, A. R., Kelly, J. F., Cornelius, J. B., & Belk, C. (2014). Integrating Mhealth Mobile Applications To Reduce High Risk Drinking Among Underage Students. Health Education Journal, 73(3), 262-273.

[4] Samiei-Zonouz, R., Memarzadeh-Tehran, H., & Rahmani, R. (2014, June). Smartphone-Centric Human Posture Monitoring System. In 2014 IEEE Canada International Humanitarian Technology Conference-(IHTC) (Pp. 1-4).

[5] Lloyd-Richardson, E. E., Bailey, S., Fava, J. L., Wing, R., & Tobacco Etiology Research Network. (2009). A Prospective Study Of Weight Gain During The College Freshman And Sophomore Years. Preventive Medicine, 48(3), 256-261.

[6] Allman-Farinelli, M., Partridge, S. R., Mcgeechan, K., Balestracci, K., Hebden, L., Wong, A., Bauman, A. (2016). A Mobile Health Lifestyle Program For Prevention Of Weight Gain In Young Adults (TXT2BFiT): Nine-Month Outcomes Of A Randomized Controlled Trial. JMIR Mhealth And Uhealth, 4(2), E78.

[7] Walsh, J. C., Corbett, T., Hogan, M., Duggan, J., & Mcnamara, A. (2016). An Mhealth Intervention Using A Smartphone App To Increase Walking Behavior In Young Adults: A Pilot Study. JMIR Mhealth And Uhealth, 4(3), E109.

[8] Kitsiou, S., Thomas, M., Marai, G. E., Maglaveras, N., Kondos, G., Arena, R., & Gerber, B. (2017, February). Development Of An Innovative Mhealth Platform For Remote Physical Activity Monitoring And Health Coaching Of Cardiac Rehabilitation Patients. In 2017 IEEE EMBS International Conference On Biomedical & Health Informatics (BHI) (Pp. 133-136).

[9] Huang, A., Xu, W., Li, Z., Xie, L., Sarrafzadeh, M., Li, X., & Cong, J. (2013). System Light-Loading Technology For Mhealth: Manifold-Learning-Based Medical Data Cleansing And Clinical Trials In WE-CARE Project. IEEE Journal Of Biomedical And Health Informatics, 18(5), 1581-1589.

[10] Sarıkaya U. (2019).Web Platformunda Kardiyovasküler Risk Takibi Ve Bireyselleştirilmiş Öneri Sistemi, Yüksek Lisans Tezi, Istanbul.

[11] Bajgora M. (2019). Genç Bireylerde Kalp Sağlığı Takibi İçin Mobil Uygulama, Yüksek Lisans Tezi, Istanbul.

[12] Güleç, S. (2009). Kalp Damar Hastalıklarında Global Risk ve Hedefler. Türk Kardiyol Dern. Arş, 37, 3-5.

Int. J. Adv. Eng. Pure Sci. 2019, 4: 336-354
DOI: 10.7240/jeps.590618

RESEARCH ARTICLE / ARAŞTIRMA MAKALESİ

Auxiliary Air Conditioner for Vehicles Storing Liquid Hydrogen

Sıvı Hidrojenli Taşıtlar İçin Yardımcı Bir Klima Sistemi

Adem Uğurlu[1]

[1] *Kırklareli Üniversitesi, Mekatronik Mühendisliği Bölümü, 39000, Kırklareli, Türkiye.*

Abstract

Current Vehicle Air Conditioning (VAC) systems, which are operated by compressors driven by Internal Combustion Engines (ICEs) or batteries, increase the fuel consumption and emissions depending on the thermal load of the vehicle passenger cabin. Since decreasing the thermal load of the vehicle will decrease the fuel consumption and emissions, studies in this area is very important from the economic and environmental aspects. In this study, an Auxiliary Air Conditioning (AAC) system for Internal Combustion Engine Vehicles (ICEVs) or Fuel Cell Vehicles (FCVs) that store Liquid Hydrogen (LH_2) as a powering source has been proposed to make contribution to the works in this significant area. ICEVs were evaluated as Gasoline Equivalent Hydrogen Internal Combustion Engine Vehicles (GEHICEVs) and Diesel Equivalent Hydrogen Internal Combustion Engine Vehicles (DEHICEVs) considering their average fuel consumption rates according to the New European Driving Cycle (NEDC). According to the analyses, approximate hydrogen consumption values have been found that reach 0.7 g/s for GEHICEVs, 1.6 g/s for DEHICEVs, and 0.6 g/s for FCVs with maximum cooling rates of 326 W, 704 W, and 250 W, respectively.

Keywords: Liquid hydrogen, air conditioning, internal combustion engines, fuel cell vehicles.

Öz

İçten yanmalı motor veya batarya ile hareket ettirilen bir kompresör ile çalışan günümüz taşıt klimaları, taşıt yolcu kabininin ısıl yüküne bağlı olarak yakıt tüketimini ve emisyonları artırmaktadır. Kabin ısıl yükünün düşürülmesi yakıt tüketimi ve emisyonları azaltacağı için, bu alandaki çalışmalar ekonomik ve çevresel yönden çok önemlidir. Bu çalışmada, içten yanmalı motor veya yakıt hücresinde yakıt olarak sıvı hidrojen kullanan taşıtlar için yardımcı bir klima sistemi önerilmektedir. İçten yanmalı motoru olan taşıtlar, benzin (GEHICEV) ve dizele (DEHICEV) eşdeğer hidrojen yakıtlı taşıtlar olmak üzere ikiye ayrılmakta ve bu taşıtların yakıt tüketimleri Avrupa Yeni Sürüş Çevrimi'ne (NEDC) göre hesaplanmaktadır. Analizlere göre; GEHICEV, DEHICEV ve yakıt hücreli taşıtlarda (FCV) yaklaşık hidrojen tüketim değerlerinin sırasıyla 0.7-1.6-0.6 g/s olduğu ve değerlere göre yapılabilecek en yüksek soğutma değerlerinin yine sırasıyla 326-704-250 W olarak ortaya çıktığı bulunmuştur.

Anahtar Kelimeler: Sıvı hidrojen, klima, içten yanmalı motorlar, yakıt hücreli taşıtlar.

1. INTRODUCTION

Since fossil fuel sources are depleting rapidly and the enormous environmental effects of their utilization can no longer be ignored, there have been many advances in alternative fuel technology in recent years [1-3]. Being one of the alternative fuels to create clean and environment friendly future with energy-efficient and low-polluting nature, hydrogen is increasingly studied as a potential candidate to replace these fossil fuels. One of the areas that fossil fuels are being used is vehicles, which mainly benefit from internal combustion engines to convert the chemical energy of these fuels into wheel movement. Hydrogen vehicles, on the other hand, have become increasingly popular since the first hydrogen-powered fuel cell vehicle launched, and being right beside FCVs, some ICEVs with hydrogen can also be seen on the market. When hydrogen is used in a fuel cell to generate electricity or is combusted with air, the only products are water and a small amount of Nitrogen Oxides (NO_x) [4-6]. The high energy density and absence of carbon is the main advantages of the hydrogen. But, problems

Sorumlu yazar/Corresponding Author: Adem UĞURLU **Tel:** +902882142083/3315, **e-posta:** adem.ugurlu@klu.edu.tr,
Gönderilme/Submitted: 11.07.2019, **Düzenleme/Revised:** 26.09.2019, **Kabul/Accepted:** 16.10.2019

such as cost of production, storage issues, hydrogen embrittlement, and percolation through the tank and the fuel line are the main drawbacks of the hydrogen usage in vehicles [7]. Though most hydrogen vehicles store hydrogen in gaseous form in their tanks like Ford Zetec 2.0 L [8, 9] and Toyota Mirai FCV, some examples like first GM FCV Electro Van (1966), GM HydroGen3, BMW Mini Hydrogen and BMW 750hl [10-12] use liquid hydrogen as a fuel, which is stored in vacuumed cryogenic tanks [13, 14]. Liquefaction of hydrogen is one of the best ways to store hydrogen [15], thus LH_2 constitutes a promising part of hydrogen applications [16]. LH_2 is presently used for some other areas such as space applications and the semiconductor industry. Gasification of LH_2 in those applications results in waste energy that can be used for refrigeration purposes with auxiliary equipments at small costs. This study deals with one of the areas where this applies: VAC systems.

Considering the safety and comfort functions, an AC system is one of the essential subsystems of vehicles. But, fuel consumption of vehicles increases due to the mechanical compressor of the AC system that uses a significant power. This increase can reach to the values of 12-17% according to indeterminate conditions such as road factors, environmental factors and driver factors for subcompact to midsize cars [17-18]. In a study, it is maintained that air conditioning usage can increase the vehicle fuel consumption by 20% on average [19]. Farrington et al. [20] reported that the driving range of an electric vehicle decreases by nearly 40% due to the use of AC system. Welstand et al. [21] investigated the effects of AC system on vehicle exhaust emissions and fuel consumption variations, and they found out a high correlation among them. For these reasons, reducing the energy consumption of the VAC systems will help to improve overall energy efficiency and environment friendly state of vehicles [22-24]. Many systems and methods have been proposed to improve energy efficiency of VAC systems so far. A few of these systems and methods include: alternative systems to the conventional vapor compression cycles [25-31], new designs of compressors [32-34], and evaporators [35], alternative driving sources to the engine of the vehicle [36], additional functionalities like calculating skin temperatures of the vehicle passengers by an infrared sensor [37] and some control methods such as PID [38, 39], rule based [40], and fuzzy [41-45]. Linder and Kulenovic [46] proposed a prototype of a hydrogen open sorption system to decrease the cooling load of air-conditioning systems. They experimentally investigated the system on a laboratory circumstances using metal hydrides. They derived the energy source of the system from a compressed hydrogen storage tank, which is used in hydrogen powered vehicles. Not wasting the compression of hydrogen and using it for additional cooling purpose, the proposed system could increase the overall energy efficiency of hydrogen powered vehicles. In their system, supply pressure of the hydrogen was 53 bar and they reach a cooling power of about 900 W. Pino et al. [47] analyzed the behavior of an FCV on AC usage in terms of hydrogen consumption under standard urban and highway driving cycles at extreme and smooth ambient conditions and different passenger loads. They found the increase of hydrogen consumption as varying value of between 3-12.1% when the air conditioning system of the FCV is on. The nominal capacity and COP of their system were 3 kW and 3, respectively. They also found out that the most effective parameters of the hydrogen consumption increment are: number of passengers and weather conditions. Thus, it can be concluded that the VAC systems are crucial systems [48] in vehicles to develop both efficient and environmental friendly vehicles, having internal combustion engines, fuel cells, or batteries. On the other hand, there are limited studies on cryogenic fluids (including hydrogen, helium, nitrogen, oxygen, and air) and their usage to generate cooling by researchers. For instance, Liquid Natural Gas (LNG) was used to provide cooling during its gasification process in an open Rankine power cycle in some studies [49-54]. Deng et al. [50] reports that providing only cooling or only power is not an efficient way to wholly extract the stored energy of the LNG. Therefore, it requires a combined system to provide both cooling and powering ability of LNG at a maximum degree. In some other studies [55, 56], Liquid Nitrogen (LN_2) was investigated as a cryogenic fluid to provide cooling in refrigerators. Dakhil [57] used LN_2 by spraying it in a cooling space to generate cooling in a refrigerator system. LN_2 was also evaporated using the ambient temperature and low heat source and then expanded to generate power in an open Rankine cycle in some studies [58-62]. The reported literature indicates that there is a need to investigate combined cooling and power systems to extract more energy from cryogenic fluids, and to see the feasibility of using these systems to meet economical and environmental concerns.

In the present paper, the use of LH_2 to provide both cooling for air conditioning and power for wheel movement in vehicles has been theoretically investigated, where several thermodynamic equations and calculations apply in terms of the consumption, cooling, COP, and AC saving. The analyses were conducted for vehicles in two groups: GEHICEV and DEHICEV as ICEVs and FCVs, mainly depending on their fuel consumption and latent heat of evaporating hydrogen. Parking analysis was also performed for vehicles. Proposing an auxiliary air conditioner, it is aimed at the study that LH_2 can be feasibly used in ICEVs and FCVs as the main power source

together with the supplementary refrigerant at the same time. Therefore, fuel economy and environmental friendly operation will be improved in LH_2 powered vehicles.

2. LIQUID HYDROGEN AS A FUEL FOR VEHICLES

2.1. Liquid Hydrogen

Having an element number of one, hydrogen is located at the top left of the periodic table. It is abundant in nature as in many natural compounds. It is lighter than air when present in gaseous form. It rises and dissipates without toxic effects if released to the air. Hydrogen is currently used for commercial purposes in petroleum refining, glass purification, semiconductor manufacturing, aerospace applications, fertilizer production, welding, annealing and heat-treating metals, pharmaceuticals, hydrogenation of unsaturated fatty acids in vegetable oil, food production, electric generation, and in the petrochemical industry to reformulate fuels. Electrolysis of water (H_2O) and steam reformation of natural gas (CH_4) are the main typically separation methods of hydrogen from other elements to form pure hydrogen. With hydrogen, we can produce power without harmful air emissions in burners or fuel cells. Hydrogen can be stored physically in gaseous form like conventional fuels, such as propane and natural gas or liquid form in cryogenic tanks [63]. Since the energy density by weight of hydrogen is too large to be compared with the energy density by volume, which are 120 MJ/kg and 10.05 MJ/m^3, respectively, liquefaction of hydrogen is one of the best ways to store hydrogen [64-67]. Table 1 shows this and some other prominent properties of hydrogen. Some remarking properties of hydrogen are its low heating value by volume but high heating value by mass, high heat of vaporization, ultralow boiling point, extra-large flammability limits in air, zero carbon rate, and high octane number. It is important that these properties must be taken into account in the design of hydrogen fuel systems in ICEVs or FCVs.

Table 1. Properties of hydrogen/liquid hydrogen [68-70]

Property	H_2/LH_2
Molecular weight (kg/kmol)	2.016
Lower heating value (MJ/m^3)	10.05
Lower heating value (MJ/kg)	120
Higher heating value (MJ/kg)	142
Heat of vaporization (kJ/kg at 1atm)	446
Liquid density (kg/m^3 at 283 K)	71
Boiling point (K at 1 atm)	20.27
Freezing point (K)	14.40
Specific heat (kJ/kg K)	9.69
Diffusion velocity in air (m/s)	≤2.00
Flammability limits in air (% by volume)	4.0-75.0
Buoyant velocity in air (m/s)	1.2-9
Minimum ignition energy in air (mJ)	0.02
Burning velocity in air (cm/s)	265-325
Flame temperature in air (K)	2318
Thermal energy radiated to surroundings (%)	17-25
C/H ratio	0
Octane number	130

In the past years, the demand of liquid hydrogen has constantly increased in some prominent areas. For instance, as an alternative to kerosene, liquid hydrogen is used for rocket propulsion systems in space applications [71] and for unmanned aeronautic vehicles [72]. Another area is the semiconductor industry [73]. There is no need for liquid hydrogen in this area, but a minimum 99.999 mol.% extremely high purities are required, and this is achieved by a temperature close to liquid hydrogen temperature in pre-purification at ambient conditions and fine purifications at cryogenic conditions. There are also some studies on LH_2 as an alternative fuel for air transportation [68, 74-76]. Another area that liquid hydrogen is used is clean energy vehicles such as hydrogen cars, hydrogen buses, and hydrogen forklifts [77]. Although some brands like GM/Opel have introduced the feasibility of LH_2 as a fuel in vehicles since 1960s [10], a rather excessive increase in demand are not encountered in this area, however, due to the reduction policies in carbon free vehicle emissions, a probable increasing demand can be expected in the near future. Liquid hydrogen will play a major role in this development with the help of cost reducing large scale liquefaction plants and efficient transport of this energy through great distances, or on site production solutions [78].

2.2. Internal Combustion Engine Vehicles

There are mainly two types of internal combustion engines: Spark Ignition (SI) and Compression Ignition (CI). Spark ignition engines operate according to Otto cycle consuming gasoline fuel, while compression ignition engines operate according to Diesel cycle consuming diesel fuel. There are some basic differences between Otto and Diesel cycles. These differences are specified in Table 2 [62, 70, 77, 79]. SI engines take air and fuel mixture in intake stroke, compress it in the ratios of about 1/7-1/14, and ignite this compressed mixture by spark plugs. They are mostly used for speed purposes as nearly every racing cars have engines that operates according to Otto cycle. On the other hand, CI engines take only air in intake stroke, compress it in the ratios of about 1/14-1/24 that is higher than SI engines have, and start combustion with this highly compressed air by injecting fuel. They are mostly used for torque purposes as nearly every heavy duty vehicles have engines that operates

according to Diesel cycle. In other respects, initial and maintenance costs of gasoline engines are lower than equivalent diesel engines, but it is vice versa for fuel consumption rates.

Table 2. Main differences of Otto and Diesel cycles [62, 70, 77, 79]

	Otto cycle	Diesel cycle
Fuel	Gasoline	Diesel
Intake stroke	Air + fuel mixture	Only air
Compression rate	1/7 – 1/14	1/14 – 1/24
Energy efficiency	Lower	Higher
Ignition	By spark plugs	By fuel injection
General purpose	Speed	Torque
Equivalent energy efficiency	Lower	Higher
Equivalent weight	Lower	Higher
Equivalent cost & maintenance	Lower	Higher
Equivalent fuel consumption	Higher	Lower
Equivalent noise level	Lower	Higher

In internal combustion engines, not only gasoline or diesel is burned; but fuels such as Liquid Petroleum Gas (LPG), Compressed Natural Gas (CNG), ethanol, methanol, biodiesel or hydrogen may also be used. In the case of flexible fuel engines, it is possible to use two or more fuel mixtures. Engines that utilize fuel blends such as gasoline-ethanol, gasoline-methanol, or diesel-biodiesel are examples of flexible fuel engine. Many vehicles in the market today are able to work with similar fuel mixtures without the need for any modifications. Table 3 shows which fuels are burned by which fuel systems in what types of engines [69, 77, 79]. As seen from the table, hydrogen can be used in both SI and CI engines and in Fuel Cell (FC) systems in mono or bi-fuel form fuel systems [79].

Table 3. Appropriate fuels for engine types and fuel systems [69, 77, 79]

Fuel	Engine type	Fuel system
Gasoline	SI	mono
Diesel	CI	mono
LPG	SI	mono, bi-fuel
CNG	CI, SI	mono, bi-fuel
Hydrogen	SI, CI, FC	mono, bi-fuel
Ethanol	SI, CI, FC	mono, ff
Methanol	SI, CI, FC	mono, ff
Biodiesel	CI	mono, ff
mono : only one fuel is used		
bi-fuel : more than one fuel is used without mixing		
ff : more than one fuel is used with mixing		

Table 4 shows a comparison of gasoline, diesel and hydrogen in some items [1, 69, 77, 79]. Since hydrogen does not include any carbon content as gasoline and diesel fuels do, hydrogen powered engines do not give main ICE emissions such as Carbon Monoxide (CO) or Hydrocarbon (HC) [80-81]. Referring to Table 4, hydrogen has a high auto-ignition temperature when compared to gasoline and diesel fuels. Auto-ignition temperature is an important parameter for ICEs that it specifies the compression ratio of the engine, since if the auto-ignition temperature of the fuel is low, it may cause pre-ignition problems during compression process that rises the temperature of the combustion chamber before the spark plugs ignite the compressed air/fuel mixture. With its high auto-ignition temperature, compression ratios of hydrogen powered ICEs can be set to high values without any pre-ignition problems such as engine knocking, overheating, and mechanical damages in this context. Ignition range in percent by volume in air is the flammability proportion of a combustible fuel in air. Between these limits, the fuel/air mixture is flammable. It is seen from Table 4 that the ignition range of hydrogen in air is between about 4–74% which means that hydrogen has a wide range of flammability compared to gasoline and diesel fuels. This is a good property of hydrogen in terms of a high range of lean-rich mixtures can be maintained, however, it also causes undesirable results such as misfiring and backfiring. Proper designs of spark plugs, optimized designs of engine cooling passages to avoid hot spots, special hydrogen injection systems, optimizations of air-fuel charging strategies, and variable valve timings for effective exhaust discharging are some of precaution methods to avoid misfiring and backfiring problems in hydrogen powered ICEs [79]. On the other hand, hydrogen has an approximately 3 times more energy content per weight than gasoline and diesel fuel. This property is important to extent the driving period of vehicle without refueling. Therefore, when hydrogen is utilized in liquid form, the cruising time of vehicles can be considerably improved. If we briefly summarize the main properties of hydrogen when it is used as a fuel in ICEs, advantageously, it has a zero carbon rate, a higher auto-ignition temperature, and a higher heating value by mass. Disadvantageously, on the other hand, it has a large ignition range in air according to the table.

Table 4. Properties of gasoline, diesel and hydrogen [1, 69, 77, 79]

Property	Gasoline	Diesel	Hydrogen
Chemical formula	C_8H_{18}	$C_{12}H_{23}$	H_2
Molecular weight (kg/kmol)	114	167	2
Carbon rate (% by mass)	84	86	0
Hydrogen rate (% by mass)	16	14	100
Oxygen rate (% by mass)	0	0	0
Heat of vaporization (kJ/kg)	350	270	446
Specific heat (kJ/kg K)	2.4	2.2	9.69
Auto-ignition temperature (°C)	280	210	565

Higher heating value (kJ/kg)	47.3	46.1	141.8
Lower heating value (kJ/kg)	44.0	42.8	120.0
Burning velocity in air (cm/s)	37.43	30	265-325
Octane number	92-98	30	130
Flammability limits in air (% by volume)	1.4-7.6	0.7-5.0	4.0-75.0
Liquid density (kg/m^3 at 283 K)	737	856	71

2.3. Fuel Cell Vehicles

Hydrogen flows from the tank to the combustion chambers to be burned with air generating power in hydrogen powered internal combustion engines. A similar flow is encountered in state of the art fuel cell vehicles. Differently in fuel cell vehicles hydrogen is used to generate electricity [82]. The fuel cell vehicles are electric vehicles that utilize hydrogen in fuel cell units to generate electricity onboard of the vehicle, eliminating the need for heavy batteries and long periods of recharging times. As soon as Zero Emission Vehicle (ZEV) mandates begin in the near future, FCVs are expected to be commercially released in bulks by automotive companies for public and fleet use. The main obstacles encountered in FCVs are their higher costs, shorter life span, hydrogen cost and availability. Fuel cell technology has a potential of the highest efficiency and the lowest emissions among vehicle energy sources, if the hydrogen is produced from the right energy source with the right method [83].

Fuel cell unit converts hydrogen energy into electrical energy by electrochemical principle. This operation is not a process of combustion. Hydrogen is combined in a fuel cell by a chemical reaction with oxygen from the air. As a result of this reaction, the electric energy to be used for the mechanical movement of the vehicle is obtained. Only water vapor is emitted through the fuel cell unit as the end product of the reaction. With different types of batteries and electrolytes, there are several types of fuel cells available in the market, where the Proton Exchange Membrane (PEM) fuel cell units are the most commonly used [84].

2.4. Vehicle Air Conditioners

VAC systems regulate temperature, humidity, air quality, and air flow of vehicle cabins for occupants. The vapor compression cycle is still dominant in VAC systems. The power source of this system is a compressor, which is driven mechanically by the engine of the vehicle in ICEVs or electrically by the battery of the vehicle in FCVs. When the system is turned on, the compressor causes an increase in the load of the engine. The engine has to increase the fuel consumption to meet this load. The compressor is the heart of the system. It pumps the refrigerant through the system, also heating up the refrigerant at the same time. This warming period of the refrigerant is a required process so as to establish a big temperature difference with outside and discharge more heat to the environment by the condenser of the VAC system. The refrigerant gets into the condenser in gas phase and leaves it in liquid phase. Then the liquid refrigerant is directed to the expansion valve through a group of valves, switches, and fluid reservoirs for controlling the flow. The main purpose of using an expansion valve in VAC systems is to decrease the pressure of the refrigerant to prepare it for evaporation. The refrigerant is sent to the evaporator device in spray form from the expansion valve unit. This vaporization process, which is a heat drawing process, causes the air to cool down. Pressure decrease of the refrigerant leads to the decrease of the evaporation temperature of the refrigerant. Therefore, the refrigerant will be easily vaporized by the air, which can be totally fresh air taken from the outside or return air taken from the vehicle cabin, or mixture of both, and thereby cooling of the vehicle interior cabin can be maintained. After the refrigerant is vaporized by the air, the cycle is completed, and then the refrigerant goes to the compressor again starting a new course. Actually, it is difficult to use hydrogen as a refrigerant in these AC systems with its ultralow critical temperature, but, since hydrogen has good refrigerant properties such as low boiling temperature and high latent heat, it can be used as refrigerant in addition to their main purpose in the systems that store liquid hydrogen and use it in gaseous form. An evaporator and air blower unit may be added to these systems to get the cooling ability of hydrogen.

As briefly discussed above, refrigerants circulate through the pipes between the equipments of AC systems in a closed loop. For doing their job in the best possible way, ideal refrigerants should have some properties such as low boiling point, high latent heat of vaporization, and high critical temperature. In addition to these required properties, ideal refrigerants also should not have some undesirable characteristics like being corrosive, toxic, explosive, and flammable. In the past, R11 (Trichlorofluoromethane), R12 (Dichlorodifluoromethane), and R22 (Chlorodifluoromethane) were generally used as refrigerants in VAC systems. They are no longer in use due to their high Ozone Depletion Potential (ODP) and Global Warming Potential (GWP) values. R134a (1,1,1,2-Tetrafluoroethane) has been replacing the previous ones for a while, and is the dominant refrigerant in VAC systems today [48]. But, R1234yf (2,3,3,3-tetrafluoro-1-propene) and R744 (Carbon dioxide) are currently started to be used as new VAC refrigerants in most countries [18, 85, 86] due to their lower GWP potentials. In Table 5, together with new refrigerants, mostly used VAC system refrigerants are compared to hydrogen which is the very topic of this study. Although the extremely low critical temperature

Table 5. Comparison of hydrogen with some refrigerants [88-95]

Refrigerant	R11	R12	R22	R134a	R744	R1234yf	R702
Common name	Trichlorofluoro-methane	Dichlorodifluo-romethane	Chlorodifluoro-methane	1,1,1,2-Tetraflu-oroethane	Carbon di-oxide	2,3,3,3-tetrafluo-ropropene	Hydrogen
Chemical formula	CCl_3F	CCl_2F_2	$CHClF_2$	$CH_2FC\ F_3$	CO_2	$C_3H_2F_4$	H_2
Refrigerant class	CFC	CFC	HCFC	HFC	Natural	HFO	Natural
Molecular mass (g/mol)	137.37	120.91	86.47	102.03	44.01	114	2.016
Density (kg/L)	1.47	1.34	1.21	1.22	0.298	1.094	0.0707
Vapor density (kg/m^3)	4.8	4.2	3	3.5	1.977	5.98	0.0898
Boiling point (°C)	-23.8	-29.8	-40.8	-26.1	-78.4	-29.45	-252.8
Critical point (°C)	198	111.8	96.2	101.08	31.06	94.7	-239.95
Critical pressure (bar)	44.1	41.1	49.9	40.6	73.84	33.8	1300
ODP	1	1	0.07	0	0	0	0
GWP (100 years)	3400	8500	1700	1300	1	4	5.8
Latent heat of vaporization at 1 atm (kj/kg)	227.3	165.24	233.75	216.87	230.5	180.1	445.7
Life in the atmosphere (years)	45	130	15	16	29.3k-36.1k	0.030116	-
Flammability	A1 (No)	A1 (No)	A1 (No)	A1 (No)	A1 (No)	A2L (Low)	A3 (High)

(−239.95 °C) of hydrogen makes it not appropriate for normal refrigeration cycle [87], it can be used in some other system designs for refrigerating purposes, thus it is compared to the conventional and new refrigerants.

Regarding the information given in Table 5, main advantages and disadvantages of hydrogen as a refrigerant can be specified briefly as in the following:

+ Hydrogen has a lower boiling point, which provides easily evaporation of a liquid refrigerant in the evaporator that is exposed to the temperature of the blown air at the outside surface. If the boiling temperature of the refrigerant is higher than the air temperature, no boiling of the refrigerant takes place, no heat is absorbed from the air, and air cannot be cooled down.

+ Hydrogen has a higher latent heat of vaporization, which ensures higher heat absorption from the air with a lower hydrogen amount during the evaporation process. If the latent heat of vaporization is low, too much refrigerant should be circulated through the system to perform adequate cooling.

+ Hydrogen has a lower ODP and GWP, which effect environment badly. These numbers of a refrigerant should be very low or preferably zero, so that utilization of that refrigerant could not harm the environment.

- Hydrogen has a lower critical temperature, which means it easily exceeds its critical temperature. This results that it cannot be liquefied in the condenser and cannot throw away the heat that it absorbs from the air. This negative property of hydrogen prevents it to be used in conventional cooling devices.

- Hydrogen has a lower vapor density, which causes the vapor to occupy a maximum volume at the outlet of the evaporator coil, and thus pipeline diameter and compressor size cannot be kept small and compact.

- Hydrogen has a higher flammability, which causes fire hazards in some dangerous circumstances.

- Hydrogen is readily available in nature, but it is expensive to produce it in today's technology.

Researchers work on more efficient and environmental friendly AC systems, and thus they propose not only alternative refrigerants or refrigerant blends but also new systems, new equipments, controlling algorithms, insulation materials, insulation strategies, auxiliary systems, and so on. With its good refrigerating properties, hydrogen may be evaluated as a refrigerant in some special systems that store liquid hydrogen. Therefore, refrigerating capability of hydrogen may not be wasted in vain, which is an important phenomenon today as the costs and emissions of energy have been gaining importance each passing day.

3. METHODOLOGY

3.1. Description of the VAAC system

The proposed VAAC system aims to use the latent heat energy of LH_2 to provide for cooling while gasified hydrogen produces power or electricity in ICEVs or FCVs, respectively. As the layout of the system is shown in Fig. 1, the system consists of two main circuits: hydrogen and air. While the hydrogen circuit maintains hydrogen for internal combustion engine or fuel cell unit of the vehicle, the air circuit supplies additional cooling capacity for the vehicle cabin. Cooling down of the air is provided by the gasification of the hydrogen passing through the evaporator of the system and decreases the cooling load of the vehicle, which is the most significant additional load in today's vehicles; its energy consumption even outweighs the energy loss to rolling and aerodynamic resistances, or power train losses for typical vehicles [96]. Therefore, the more hydrogen is supplied to the powering of the vehicle, the more cooled-down air is supplied to the cooling of the vehicle cabin. Hydrogen is stored in the cryogenic tank in liquid form under pressure. Vehicle power generator needs hydrogen in gaseous form at atmospheric pressure. A pressure regulation valve decreases the pressure of the hydrogen. An evaporation process follows this pressure decrease. Hydrogen is evaporated by the air blown along the outer surface of the evaporator. This cooled-down air is sent to the vehicle compartment to decrease the AC cooling load, which depends on the environmental factors such as: the sun, outside temperature and humidity, number of passengers, etc. There is a similar scheme in parking vehicles that has no need to hydrogen for power production but needs an amount of hydrogen leakage according to the environmental circumstances for safety reasons. This required amount of hydrogen to be delivered from the tank is sent to the atmosphere through the evaporator unit cooling down the air. This air will decrease the AC load of the vehicle when parking; even it is at a slight amount. FCVs can also generate power using this small amount of hydrogen at the time of parking, establishing cooling of the cabin at the same time.

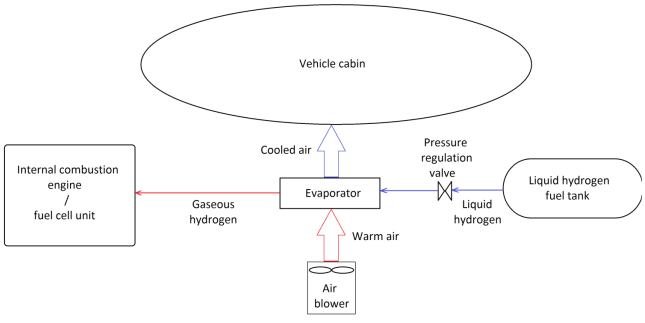

Figure 1. Layout of the auxiliary air conditioning system for vehicles storing liquid hydrogen

3.2. GEHICEV Analysis

Analyses of GEHICEVs have been conducted according to Eqs. (1-6). Eq. (1) shows the calculation of the average gasoline consumption (l/s) of a Gasoline Internal Combustion Engine Vehicle (GICEV). $\mathbf{FC_g}$ (l/100 km), which is declared by the manufacturer of the GICEV, is determined according to the NEDC. This cycle lasts 1180 s and the vehicle covers a road of 11,007 km during the cycle [97-98]. In this study, analyses of GEHICEVs have been conducted using $\mathbf{FC_g}$ values between 0 and 30 l/100 km as to be consisted to vehicles on the market. Therefore, the calculation of $\dot{v}_g$ at different conditions can be performed, and an easy comparison of GICEVs and GEHICEVs can be established through the analysis.

$$\dot{v}_g = \frac{\frac{FC_g \times 11{,}007}{100}}{1180} \quad (1)$$

The average gasoline consumption in mass flow rate ($\dot{m}_g$) is calculated as seen from Eq. (2) using ρ_g, which is the average density of gasoline taken from the literature [93] which specifies between 0.72-0.78 kg/l.

$$\dot{m}_g = \dot{v}_g \times \rho_g \quad (2)$$

Approximate hydrogen consumption of the vehicle in mass flow rate ($\dot{m}_{h,GEHICEV}$) is calculated using the equivalent heating value rate of gasoline and hydrogen ($r_{HV,h/g}$) as seen in Eq. (3). Arithmetic means of lower and higher heating values for gasoline and hydrogen were used in this equivalent rate. Lower and higher heating values for gasoline and hydrogen are 44,000 kJ/kg, 47,300 kJ/kg, 120,000 kJ/kg, and 141,800 kJ/kg, respectively [93]. Since heating values of hydrogen is higher than that of gasoline, the required amount of hydrogen mass flow rate is found to be approximately 0.3488 times lower than mass flow rate of gasoline, which is also comparable to the works encountered in the literature [11, 69, 99].

$$\dot{m}_{h,GEHICEV} = \dot{m}_g \times r_{HV,h/g} \quad (3)$$

Calculation of the cooling capacity to be maintained from the gasification of liquid hydrogen is given in Eq. (4). In this formula, $\dot{Q}_c$ shows the cooling amount (W) that the system takes from the air to be sent to the vehicle cabin, $\dot{m}_{h,GEHICEV}$ is the approximate hydrogen mass flow rate (kg/s), and $h_{fg,h}$ is the enthalpy of vaporization (kJ/kg) of hydrogen. $h_{fg,h}$ is taken as 446 J/kg from the literature [93].

$$\dot{Q}_{c,GEHICEV} = \dot{m}_{h,GEHICEV} \times h_{fg,h} \quad (4)$$

AC savings (%) of the VAAC system on vehicles at various cooling loads are calculated through Eq. (5). S_{AC} is the percent saving, $\dot{Q}_{c,GEHICEV}$ is cooling capacity of the system (W), and $\dot{L}_c$ is the cooling load of the vehicle (W). $\dot{L}_c$ values are chosen according to the literature [100], which reports that average cooling load values for subcompact, compact, and standard automobiles are 3,62 kW, 4,15 kW, and 5,12 kW, respectively. As $\dot{L}_c$ of vehicles constantly takes different values according to the weather conditions, size of the vehicles, and number of the occupants, 1000 W, 2000 W, 3000 W, 4000 W, 5000 W, and 6000 W values were chosen for the determination of the AC savings at different conditions. These values are compatible with the works of Meier et al. [82] and Fayazbakhsh and Bahrami [96] also.

$$S_{AC,GEHICEV} = \frac{\dot{Q}_{c,GEHICEV}}{\dot{L}_c} \quad (5)$$

Last part of the GEHICEV analysis constitutes COP calculation of the VAAC system as shown in Eq. (6). $COP_{R,GEHICEV}$ is the performance measurement of the VAAC system that is an air conditioning system. The COP calculation of the VAAC system has been performed regarding Peltier effect thermoelectric coolers. Unlike conventional air conditioners and refrigerators, there is no compressor in thermoelectric coolers. Similarly the VAAC system proposed in this work does not have any compressor, because the liquid hydrogen in the tank is pressurized. And if the pressure becomes insufficient for the flow, the tank is refilled with hydrogen in fuel stations. The operating costs of the engine that consumes hydrogen are not included in energy consumption of the VAAC. The only energy consumed by the VAAC system creating cooling effect is fan power (P_f) required to circulate the air through the hydrogen evaporator. The fan used in the calculations of the VAAC system is selected as a standard one working at three positions. The energy amounts of the fan which draws from the battery are 24 W, 48 W, and 72 W, respectively for the three positions. These constant electric fan powers were chosen accordingly that they are widely used in literature and suitable for the proposed VAAC system [101]

$$COP_{R,GEHICEV} = \frac{\dot{Q}_c}{P_f} \quad (6)$$

3.3. DEHICEV Analysis

Analyses of DEHICEVs have been conducted similar to GEHICEV analysis as seen Eqs. (7-12). Differently in Eq. (7), FC_d values between 0 and 60 l/100 km were chosen for the calculations regarding both automobiles and heavy vehicles appear on the market. ρ_d in Eq. (8), which is the average density of diesel fuel, was taken from the literature [93] as between 0.78-0.88 kg/L. The equivalent heating value rate of diesel and hydrogen ($r_{HV,h/d}$) in Eq. (9) was calculated using the arithmetic means of lower and higher heating values for diesel and hydrogen with the values of 42,800 kJ/kg, 46,100 kJ/kg, 120,000 kJ/kg, and 141,800 kJ/kg, respectively [93]. The required amount of hydrogen mass flow rate is found to be approximately 0.3394 times lower than mass flow rate of diesel. Calculations of the cooling capacity, AC savings, and COP have similar formulas with GEHICEV analysis.

$$\dot{v}_d = \frac{\frac{FC_d \times 11,007}{100}}{1180} \quad (7)$$

$$\dot{m}_d = \dot{v}_d \times \rho_d \quad (8)$$

$$\dot{m}_{h,DEHICEV} = \dot{m}_d \times r_{HV,h/d} \quad (9)$$

$$\dot{Q}_{c,DEHICEV} = \dot{m}_{h,DEHICEV} \times h_{fg,h} \quad (10)$$

$$S_{AC,DEHICEV} = \frac{\dot{Q}_{c,DEHICEV}}{\dot{L}_c} \quad (11)$$

$$COP_{R,DEHICEV} = \frac{\dot{Q}_{c,DEHICEV}}{P_f} \quad (12)$$

3.4. FCV Analysis

In FCV analysis, although the calculation of the cooling capacity, AC savings, and COP have the same formulas with the previous GEHICEV and DEHICEV analyses, some differences are encountered in the calculation of the $\dot{m}_{h,FCV}$. Fuel consumption of commercial FCVs is generally given as kg H_2/100 km. Eq. (13) shows the calculation of the average hydrogen consumption (kg/s) of an FCV. $\dot{m}_{h,FCV,NEDC}$ (kg/100 km), which is declared by the manufacturer of the FCV, is determined according to the NEDC. The analyses of FCVs have been conducted using $\dot{m}_{h,FCV,NEDC}$ values between 0 and 6 kg/100 km as to be easily comparable to vehicles on the market. Today's commercially available FCVs like Toyota Mirai, Honda Clarity Fuel Cell, Hyundai Nexo etc. have an average hydrogen consumption, which is calculated using the hydrogen tank capacity and total range in NEDC with full capacity of the tank, of 1 kg/100 km is also compatible with the literature [82]. Therefore, $\dot{m}_{h,FCV,NEDC}$ values between 0 and 6 kg/100 km are suitable for a great variety of vehicles in a wide range of driving conditions.

$$\dot{m}_{h,FCV} = \frac{\frac{m_{h,FCV,NEDC} \times 11,007}{100}}{1180} \quad (13)$$

$$\dot{Q}_{c,FCV} = \dot{m}_{h,FCV} \times h_{fg,h} \quad (14)$$

$$S_{AC,FCV} = \frac{\dot{Q}_{c,FCV}}{L_c} \quad (15)$$

$$COP_{R,FCV} = \frac{\dot{Q}_{c,FCV}}{P_f} \quad 16)$$

3.5. Parking Analysis of All Types of Vehicles Storing Liquid Hydrogen

Since it has a very low evaporating temperature, liquid hydrogen can only be stored in special tanks in special circumstances. When hydrogen consumption of a vehicle stops, hydrogen pressure in the tank increases in time depending on to the environmental conditions. The hydrogen in the tank should be discharged in a required amount so as not to damage the tank due to the increasing pressure of evaporating hydrogen [10]. So, in this part of the study, cooling effect of this amount of hydrogen has been analyzed for parking vehicles. Eq. (17) shows the calculation of cooling capacity of hydrogen venting out from the tank through the evaporator. Here, c_v is the venting coefficient of the tank according to outside conditions (temperature, capacity, fullness etc.). For c_v, values between 0 and 3 have been taken for the analysis. $\dot{m}_{h,PV}$ is the average venting flow rate of the hydrogen when the vehicle is parking. A constant value of 16 g/h has been taken for $\dot{m}_{h,PV}$ in the parking analysis, which is compatible with the literature [10, 64]. Therefore, venting fluctuations of the hydrogen have been established by just the c_v coefficient. As to the COP of the VAAC system when the ICE/FC is not working, it depends on the cooling capacity ($\dot{Q}_{c,PV}$) and the fan power (P_f) as given in Eq. (18).

$$\dot{Q}_{c,P} = c_v \times \dot{m}_{h,P} \times h_{fg,h} \quad (17)$$

$$COP_{R,P} = \frac{\dot{Q}_{c,P}}{P_f} \quad (18)$$

3.6. Validity of the Methodology

The most important term in the calculations of the methodology of this work is the latent heat of hydrogen. Latent heat is important for air conditioning systems, since the cooling capacity is mainly depends on the heat amount derived by the refrigerant when changing state from liquid to vapor. This heat absorption, which occurs at the time of the refrigerant changes state, makes the air cooler. Then the cooled air is sent to the vehicle indoor cabin blown by an air fan through the air channels. Therefore, analyses of cooling capacities, COP and AC saving variations were conducted using latent heat of hydrogen for LH_2 powered vehicles. It is assumed in the analyses that continuously evaporated hydrogen takes all of its latent heat of vaporization from the air, blown to the hydrogen evaporator, at 100% efficiency. Losses in the evaporator or other system equipments are neglected in this context. Sensible heat gain of hydrogen is also neglected for the analyses. This simple but logical approach provides a great convenience to determine whether the proposed system is feasible or not. Since the VAAC system does not include a compressor, the analysis performed in this study does not include compressor based expressions which AC systems with compressor have.

4. RESULTS AND DISCUSSION

4.1. Results of the GEHICEV Analysis

Table 6 shows hydrogen flow rate, cooling capacity, COP, and AC saving variations of GEHICEVs according to the GEHICEV analysis, conducted for fuel consumption values between 0-30 l/100 km. Although SI engines consume less fuel when they are operated at a constant speed, their fuel consumptions increase if their speeds are changed. And also they spend too much fuel in some circumstances such as cold start, excessive loads, sudden acceleration, steep ways climbing etc. Increasing fuel consumption in gasoline vehicles increases hydrogen consumption as well, which GEHICEV demonstrates gasoline vehicles converted to be powered by hydrogen fuel. According to Table 6, hydrogen consumption rises to the value of about 0.0007 kg/s for 30 l/100 km gasoline consumption. For this consumption, cooling capacity of the VAAC system is 326 W, which means the system can absorb and throw out 326 J heat from the vehicle cabin per second. This cooling power may be sufficient for the vehicle when the system is operated even alone in some cases. In other occasions with a high cooling load, the VAAC system will assist the main AC system of the vehicle. As to the COP variations of the proposed VAAC system, since the only energy wasting equipment is the fan in the system, and the calculation method includes accordingly, COP variations are higher than normal AC systems. The highest COP values of the system are 13.6, 6.8, and 4.5 respectively for 24 W, 48 W, and 72 W fan powers. The highest assisting percentages of the VAAC system to the main AC system are as follows: 33% for 1 kW AC load, 16%, for 2 kW AC load, 11% for 3 kW AC load, 8% for 4 kW AC load, 7% for 5 kW AC load, and 5% for 6 kW AC load. Decreasing fuel consumption and increasing AC load in the cabin decrease the assisting percentages of the VAAC system as seen from the table. It can be concluded that these AC saving values are high enough for the proposed VAAC system, since it cuts the AC system operation by one third, also cutting the fuel consumption increase of the vehicle due to the AC system with a low

power consuming fan. If we do not use this cooling capacity of the evaporating hydrogen in liquid hydrogen powered vehicles, it will be wasted in vain. This waste of energy is aimed to be prevented with the proposed VAAC system.

4.2. Results of the DEHICEV analysis

Hydrogen flow rate, cooling capacity, COP and AC saving results of the DEHICEV analysis are given in Table 7. As diesel engines are generally utilized in heavy vehicles and they consume much fuel when compared to gasoline vehicles, between 0-60 l/100 km fuel consumption values were determined for DEHICEVs. However, the first few lines of the table also demonstrate today's light-duty diesel vehicles, which have low fuel consumptions. When a diesel vehicle is converted to operate by hydrogen fuel, the amount of the hydrogen that the vehicle consumes is shown in the second column of the table. The highest hydrogen flow rate occurs 0.0016 kg/s for 60 l/100 km diesel consumption according to the DEHICEV analysis. For this flow rate, the VAAC system gives a 704 W cooling power. And the highest achievable COPs of the system at this cooling capacity are 29.3, 14.7, 9.8 for 24 W, 48 W, 72 W fan powers, respectively. The proposed VAAC system can substitute as highly as 70% of the main AC system of the vehicle when the AC load is 1 kW. If the AC loads of the vehicle passenger compartment are taken as 2, 3, 4, 5 and 6 kW, the assistance of the VAAC system decreases to the percentages of 35%, 23%, 18%, 14%, and 12%, respectively. Even for the highest AC load in the analysis, the proposed VAAC system can supply a high cooling power which substitutes 12% of the AC unit of the vehicle. It is clear from the DEHICEV analysis that the proposed VAAC system is more suitable for heavy vehicles, considering their small cabin volumes – that means small AC loads – and high fuel consumption values. With the use of this system in LH_2 powered heavy duty vehicles, little or no usage of main AC system provides little or no compressor operation, and thus lower fuel consumption and exhaust emissions. Main AC systems can be designed very compact in those vehicles, and even in some vehicle examples, there can be included no AC system at all, since the VAAC system can maintain required cooling power for all operation scenarios.

4.3. Results of the FCV Analysis

Hydrogen consumption (in kg/s), cooling power, COP, and AC saving variations according to the FCV analysis are given in Table 8. FCVs with hydrogen consumptions of between 0-6 kg/100 km were considered in the analysis. This consumption range is suitable for FCVs encountered in the market. It is also compatible for the vehicles examined in literature, which are mainly automobiles. Although some academic and commercial circles started to build fuel cell heavy vehicle prototypes, which have probably large hydrogen consumption values, they are not included in the FCV analysis. In the near future, it is estimated that fuel cell systems will be used for vehicles of any size; however, they are only used in some automobiles in small numbers. According to the table, cooling capacity of the VAAC system in FCVs rises to the highest value of 250 W, which is the lowest cooling power among all the vehicle types in the analyses. The reason for this is mainly FCVs are consuming less fuel when compared to equivalent gasoline and diesel vehicles. Therefore the cooling ability of the VAAC system decreases in FCVs. As to the COP of the system, it negatively varies by the increase of the fan power, which have the highest values of 10.4, 5.2, and 3.5, respectively for 24 W, 48 W, and 72 W fan powers. On the other hand, AC saving variations of the VAAC system, which are lower than that of GEHICEV and DEHICEV analyses as the hydrogen consumption in FCVs is lower when compared to GEHICEVs and DEHICEVs. The highest reachable AC savings are 25%, 12%, 8%, 6%, 5%, 4%, respectively for 1-6 kW AC loads. The VAAC system can supply a cooling power that decreases the main AC usage as high as 25% when the vehicle consumes 6 kg hydrogen per 100 km and the AC load of the cabin is 1 kW according to the analysis. If the hydrogen consumption increases –e.g. heavy FCVs – or the AC load decreases, the VAAC system would provide all the cooling need of the vehicle when the fuel cell unit is in operation consuming hydrogen.

4.4. Results of the Parking Analysis

Table 9 shows the hydrogen ventilation flow rate, cooling capacity, and COP variations according to the changing of hydrogen ventilation coefficient in parking vehicles. When the ventilation coefficient is at its peak value, which is taken as 3 in this analysis, the cooling capacity of the VAAC system is 5.9 W, which supplies very low cooling effect for the vehicle cabin. However, there are some systems that just ventilate the vehicle cabin with a fan without the cooling of the air when the vehicle is parking. Therefore, the proposed VAAC system will assist those systems blowing some cooled air instead of the ventilated warm air in the cabin even at a small amount. The VAAC system operates with COP values of 0.25, 0.12, and 0.08, respectively for 24 W, 48 W, and 72 W fan powers.

Table 6. Approximate hydrogen consumption, cooling, COP, and AC Saving variations according to the GEHICEV analysis

FC_g (l/100 km)	$\dot{m}_{h,GEHICEV}$ (kg/s)	$\dot{Q}_{c,GEHICEV}$ (W)	$COP_{R,GEHICEV}$ @P_f=24 W	$COP_{R,GEHICEV}$ @P_f=48 W	$COP_{R,GEHICEV}$ @P_f=72 W	$S_{AC,GEHICEV}$ @1 kW load (%)	$S_{AC,GEHICEV}$ @2 kW load (%)	$S_{AC,GEHICEV}$ @3 kW load (%)	$S_{AC,GEHICEV}$ @4 kW load (%)	$S_{AC,GEHICEV}$ @5 kW load (%)	$S_{AC,GEHICEV}$ @6 kW load (%)
0	0.0000	0	0.0	0.0	0.0	0	0	0	0	0	0
1	0.0000	11	0.5	0.2	0.2	1	1	0	0	0	0
2	0.0000	22	0.9	0.5	0.3	2	1	1	1	0	0
3	0.0001	33	1.4	0.7	0.5	3	2	1	1	1	1
4	0.0001	44	1.8	0.9	0.6	4	2	1	1	1	1
5	0.0001	54	2.3	1.1	0.8	5	3	2	1	1	1
6	0.0001	65	2.7	1.4	0.9	7	3	2	2	1	1
7	0.0002	76	3.2	1.6	1.1	8	4	3	2	2	1
8	0.0002	87	3.6	1.8	1.2	9	4	3	2	2	1
9	0.0002	98	4.1	2.0	1.4	10	5	3	2	2	2
10	0.0002	109	4.5	2.3	1.5	11	5	4	3	2	2
11	0.0003	120	5.0	2.5	1.7	12	6	4	3	2	2
12	0.0003	131	5.4	2.7	1.8	13	7	4	3	3	2
13	0.0003	141	5.9	2.9	2.0	14	7	5	4	3	2
14	0.0003	152	6.3	3.2	2.1	15	8	5	4	3	3
15	0.0004	163	6.8	3.4	2.3	16	8	5	4	3	3
16	0.0004	174	7.3	3.6	2.4	17	9	6	4	3	3
17	0.0004	185	7.7	3.9	2.6	19	9	6	5	4	3
18	0.0004	196	8.2	4.1	2.7	20	10	7	5	4	3
19	0.0005	207	8.6	4.3	2.9	21	10	7	5	4	3
20	0.0005	218	9.1	4.5	3.0	22	11	7	5	4	4
21	0.0005	229	9.5	4.8	3.2	23	11	8	6	5	4
22	0.0005	239	10.0	5.0	3.3	24	12	8	6	5	4
23	0.0006	250	10.4	5.2	3.5	25	13	8	6	5	4
24	0.0006	261	10.9	5.4	3.6	26	13	9	7	5	4
25	0.0006	272	11.3	5.7	3.8	27	14	9	7	5	5
26	0.0006	283	11.8	5.9	3.9	28	14	9	7	6	5
27	0.0007	294	12.2	6.1	4.1	29	15	10	7	6	5
28	0.0007	305	12.7	6.3	4.2	30	15	10	8	6	5
29	0.0007	316	13.2	6.6	4.4	32	16	11	8	6	5
30	0.0007	326	13.6	6.8	4.5	33	16	11	8	7	5

Table 7. Approximate hydrogen consumption, cooling, COP, and AC Saving variations according to the DEHICEV analysis

FC_d (l/100 km)	$\dot{m}_{h,DEHICEV}$ (kg/s)	$\dot{Q}_{c,DEHICEV}$ (W)	$COP_{R,DEHICEV}$ @P_f=24 W	$COP_{R,DEHICEV}$ @P_f=48 W	$COP_{R,DEHICEV}$ @P_f=72 W	$S_{AC,DEHICEV}$ @1 kW load (%)	$S_{AC,DEHICEV}$ @2 kW load (%)	$S_{AC,DEHICEV}$ @3 kW load (%)	$S_{AC,DEHICEV}$ @4 kW load (%)	$S_{AC,DEHICEV}$ @5 kW load (%)	$S_{AC,DEHICEV}$ @6 kW load (%)
0	0.0000	0	0.0	0.0	0.0	0	0	0	0	0	0
2	0.0001	23	1.0	0.5	0.3	2	1	1	1	0	0
4	0.0001	47	2.0	1.0	0.7	5	2	2	1	1	1
6	0.0002	70	2.9	1.5	1.0	7	4	2	2	1	1
8	0.0002	94	3.9	2.0	1.3	9	5	3	2	2	2
10	0.0003	117	4.9	2.4	1.6	12	6	4	3	2	2
12	0.0003	141	5.9	2.9	2.0	14	7	5	4	3	2
14	0.0004	164	6.8	3.4	2.3	16	8	5	4	3	3
16	0.0004	188	7.8	3.9	2.6	19	9	6	5	4	3
18	0.0005	211	8.8	4.4	2.9	21	11	7	5	4	4
20	0.0005	235	9.8	4.9	3.3	23	12	8	6	5	4
22	0.0006	258	10.7	5.4	3.6	26	13	9	6	5	4
24	0.0006	281	11.7	5.9	3.9	28	14	9	7	6	5
26	0.0007	305	12.7	6.4	4.2	30	15	10	8	6	5
28	0.0007	328	13.7	6.8	4.6	33	16	11	8	7	5
30	0.0008	352	14.7	7.3	4.9	35	18	12	9	7	6
32	0.0008	375	15.6	7.8	5.2	38	19	13	9	8	6
34	0.0009	399	16.6	8.3	5.5	40	20	13	10	8	7
36	0.0009	422	17.6	8.8	5.9	42	21	14	11	8	7
38	0.0010	446	18.6	9.3	6.2	45	22	15	11	9	7
40	0.0011	469	19.5	9.8	6.5	47	23	16	12	9	8
42	0.0011	492	20.5	10.3	6.8	49	25	16	12	10	8
44	0.0012	516	21.5	10.7	7.2	52	26	17	13	10	9
46	0.0012	539	22.5	11.2	7.5	54	27	18	13	11	9
48	0.0013	563	23.5	11.7	7.8	56	28	19	14	11	9
50	0.0013	586	24.4	12.2	8.1	59	29	20	15	12	10
52	0.0014	610	25.4	12.7	8.5	61	30	20	15	12	10
54	0.0014	633	26.4	13.2	8.8	63	32	21	16	13	11
56	0.0015	657	27.4	13.7	9.1	66	33	22	16	13	11
58	0.0015	680	28.3	14.2	9.4	68	34	23	17	14	11
60	0.0016	704	29.3	14.7	9.8	70	35	23	18	14	12

Table 8. Approximate hydrogen consumption, cooling, COP, and AC Saving variations according to the FCV analysis

$\dot{m}_{h,FCV,NEDC}$ (kg/100 km)	$\dot{m}_{h,FCV}$ (kg/s)	$\dot{Q}_{c,FCV}$ (W)	$COP_{R,FCV}$ @P_f=24 W	$COP_{R,FCV}$ @P_f=48 W	$COP_{R,FCV}$ @P_f=72 W	$S_{AC,FCV}$ @1 kW load (%)	$S_{AC,FCV}$ @2 kW load (%)	$S_{AC,FCV}$ @3 kW load (%)	$S_{AC,FCV}$ @4 kW load (%)	$S_{AC,FCV}$ @5 kW load (%)	$S_{AC,FCV}$ @6 kW load (%)
0	0.0000	0	0.0	0.0	0.0	0	0	0	0	0	0
0.2	0.0000	8	0.3	0.2	0.1	1	0	0	0	0	0
0.4	0.0000	17	0.7	0.3	0.2	2	1	1	0	0	0
0.6	0.0001	25	1.0	0.5	0.3	2	1	1	1	0	0
0.8	0.0001	33	1.4	0.7	0.5	3	2	1	1	1	1
1	0.0001	42	1.7	0.9	0.6	4	2	1	1	1	1
1.2	0.0001	50	2.1	1.0	0.7	5	2	2	1	1	1
1.4	0.0001	58	2.4	1.2	0.8	6	3	2	1	1	1
1.6	0.0001	67	2.8	1.4	0.9	7	3	2	2	1	1
1.8	0.0002	75	3.1	1.6	1.0	7	4	2	2	1	1
2	0.0002	83	3.5	1.7	1.2	8	4	3	2	2	1
2.2	0.0002	92	3.8	1.9	1.3	9	5	3	2	2	2
2.4	0.0002	100	4.2	2.1	1.4	10	5	3	2	2	2
2.6	0.0002	108	4.5	2.3	1.5	11	5	4	3	2	2
2.8	0.0003	116	4.9	2.4	1.6	12	6	4	3	2	2
3	0.0003	125	5.2	2.6	1.7	12	6	4	3	2	2
3.2	0.0003	133	5.5	2.8	1.8	13	7	4	3	3	2
3.4	0.0003	141	5.9	2.9	2.0	14	7	5	4	3	2
3.6	0.0003	150	6.2	3.1	2.1	15	7	5	4	3	2
3.8	0.0004	158	6.6	3.3	2.2	16	8	5	4	3	3
4	0.0004	166	6.9	3.5	2.3	17	8	6	4	3	3
4.2	0.0004	175	7.3	3.6	2.4	17	9	6	4	3	3
4.4	0.0004	183	7.6	3.8	2.5	18	9	6	5	4	3
4.6	0.0004	191	8.0	4.0	2.7	19	10	6	5	4	3
4.8	0.0004	200	8.3	4.2	2.8	20	10	7	5	4	3
5	0.0005	208	8.7	4.3	2.9	21	10	7	5	4	3
5.2	0.0005	216	9.0	4.5	3.0	22	11	7	5	4	4
5.4	0.0005	225	9.4	4.7	3.1	22	11	7	6	4	4
5.6	0.0005	233	9.7	4.9	3.2	23	12	8	6	5	4
5.8	0.0005	241	10.1	5.0	3.4	24	12	8	6	5	4
6	0.0006	250	10.4	5.2	3.5	25	12	8	6	5	4

Table 9. Average hydrogen ventilation, cooling and COP variations according to the parking analysis

c_v	$\dot{m}_{h,P}$ (kg/s)	$\dot{Q}_{c,P}$ (W)	$COP_{R,P@P_f=24\ W}$	$COP_{R,P@P_f=48\ W}$	$COP_{R,P@P_f=72\ W}$
0	0.000000	0.0	0.00	0.00	0.00
0.1	0.000000	0.2	0.01	0.00	0.00
0.2	0.000001	0.4	0.02	0.01	0.01
0.3	0.000001	0.6	0.02	0.01	0.01
0.4	0.000002	0.8	0.03	0.02	0.01
0.5	0.000002	1.0	0.04	0.02	0.01
0.6	0.000003	1.2	0.05	0.02	0.02
0.7	0.000003	1.4	0.06	0.03	0.02
0.8	0.000004	1.6	0.07	0.03	0.02
0.9	0.000004	1.8	0.07	0.04	0.02
1	0.000004	2.0	0.08	0.04	0.03
1.1	0.000005	2.2	0.09	0.05	0.03
1.2	0.000005	2.4	0.10	0.05	0.03
1.3	0.000006	2.6	0.11	0.05	0.04
1.4	0.000006	2.8	0.12	0.06	0.04
1.5	0.000007	3.0	0.12	0.06	0.04
1.6	0.000007	3.2	0.13	0.07	0.04
1.7	0.000008	3.4	0.14	0.07	0.05
1.8	0.000008	3.6	0.15	0.07	0.05
1.9	0.000008	3.8	0.16	0.08	0.05
2	0.000009	4.0	0.17	0.08	0.06
2.1	0.000009	4.2	0.17	0.09	0.06
2.2	0.000010	4.4	0.18	0.09	0.06
2.3	0.000010	4.6	0.19	0.09	0.06
2.4	0.000011	4.8	0.20	0.10	0.07
2.5	0.000011	5.0	0.21	0.10	0.07
2.6	0.000012	5.2	0.21	0.11	0.07
2.7	0.000012	5.4	0.22	0.11	0.07
2.8	0.000012	5.6	0.23	0.12	0.08
2.9	0.000013	5.7	0.24	0.12	0.08
3	0.000013	5.9	0.25	0.12	0.08

5. CONCLUSIONS

Conventional air conditioning systems significantly contribute to energy consumption in vehicles. Liquid hydrogen powered vehicles, on the other hand, have a potential of latent heat of hydrogen to be vaporized for the need of feeding the internal combustion engine or fuel cell unit of the vehicle depending on its type. Therefore there is a need to produce a new technology that utilizes this energy and reduces costs. An auxiliary air conditioning system for liquid hydrogen vehicles has been proposed and theoretically analyzed in this study. The internal combustion engine vehicles and fuel cell vehicles were included in the analyses. Hydrogen consumption, cooling capacity, COP, and AC saving variations were presented according to the vehicles that have specified fuel consumptions. Parking analyses of vehicles were also performed. The results of the analyses show that the system can supply adequate cooling with a COP that is comparable to the conventional vapor compression cycle. This system can assist VAC systems in ICEVs or FCVs storing liquid hydrogen with small initial and operating costs.

Since the achievable cooling capacity of the VAAC system proposed in this study for vehicles consuming high hydrogen is more sufficient for assisting the VAC system, vehicles like lorries or trucks with a higher fuel consumption and lower indoor volume seem to be more suitable than the vehicles that have lower fuel consumption and higher cooling demand. However, the system reduces the main air conditioning operation, thus reducing fuel consumption and emissions in any case.

On the other hand, the analyses reveal that the auxiliary system proposed in this study could supply adequate cooling capacity to the vehicle compartment only in mild weather conditions when the main AC system of the vehicle is off. If

the same situation is in question, performance of the system would decrease dramatically with decreasing fuel consumption and outside ambient temperature. At this condition, the main VAC system should be automatically activated, which in any case puts a lower load on the engine of the ICEVs or battery of the FCVs.

It is also important to discuss the effect of varying hydrogen flow rates on the cooling behavior of the VAAC system. Depending on the varying vehicle loads such as different traffic situations, number of occupants, baggage loads, and slope of the road, hydrogen flow changes thus changing the cooling capacity of the VAAC system. Therefore, there should be a higher requirement of a control strategy for the VAC system when the VAAC system is implemented. New system regulating algorithms have to be developed for optimized working conditions between the proposed VAAC and the VAC system to avoid not regulating the desired air conditions in the cabin of the vehicle and unnecessary usage of the VAC system, which influences the driving performance of the vehicle and increases fuel consumption.

In addition, apart from the application of the VAAC system for the vehicle interior cabin, especially for FCVs, a further possible integration concept of the system is the cooling of the vehicle components such as the power electronics, the battery or the electric motor, which, for an overall propulsion efficiency of 80%, between 0.75-2.5 kW of waste heat of an FCV is produced from these components [82].

As a result, the proposed VAAC system is a suitable and environmental friendly system for vehicles that use liquid hydrogen as fuel. It can support the conventional air-conditioning system of the vehicles that have low fuel consumption with a high air conditioning load, or replace it for vehicles that have high fuel consumption with low air conditioning load like lorries or trucks. A further promising integration concept is the direct cooling of vehicle interior or propulsion components. In future studies, the system has to be directly coupled with a fuel cell and solutions for a homogeneous cooling power have to be examined.

Nomenclature

AAC	Auxiliary Air Conditioning
AC	Air Conditioning
c_v	Venting Coefficient of the Tank
CH_4	Natural Gas
CI	Compression Ignition
CNG	Compressed Natural Gas
CO	Carbon Monoxide
COP	Coefficient Of Performance
COP_R	Refrigeration Coefficient Of Performance
DEHICEV	Diesel Equivalent Hydrogen Internal Combustion Engine Vehicle
FC	Fuel Cell
FC_d	Diesel Fuel Consumption, l/100 km
FC_g	Gasoline Fuel Consumption, l/100 km
FCV	Fuel Cell Vehicle
GEHICEV	Gasoline Equivalent Hydrogen Internal Combustion Engine Vehicle
GICEV	Gasoline Internal Combustion Engine Vehicle
GWP	Global Warming Potential
H_2O	Water
$h_{fg,h}$	Enthalpy of Vaporization of Hydrogen, kJ/kg
HC	Hydrocarbon
ICE	Internal Combustion Engine
ICEV	Internal Combustion Engine Vehicle
$\dot{L}_c$	Cooling Load of the Vehicle
LH_2	Liquid Hydrogen
LN_2	Liquid Nitrogen
LNG	Liquid Natural Gas
LPG	Liquid Petroleum Gas
$\dot{m}_d$	Diesel Fuel Consumption, kg/s
$\dot{m}_g$	Gasoline Fuel Consumption, kg/s
$\dot{m}_h$	Hydrogen Consumption, kg/s
NEDC	New European Driving Cycle
NO_x	Nitrogen Oxides
ODP	Ozone Depletion Potential
P_f	Fan Power, W
PEM	Proton Exchange Membrane
$\dot{Q}_c$	Cooling Capacity, W
ρ_d	Diesel Density, kg/L
ρ_g	Gasoline Density, kg/L
$r_{HV,h/d}$	Equivalent Heating Value Rate of Diesel and Hydrogen
$r_{HV,h/g}$	Equivalent Heating Value Rate of Gasoline and Hydrogen
S_{AC}	AC Saving, %
SI	Spark Ignition
VAAC	Vehicle Auxiliary Air Conditioning

VAC	Vehicle Air Conditioning
$\dot{v}_d$	Diesel Fuel Consumption, L/s
$\dot{v}_g$	Gasoline Fuel Consumption, L/s
ZEV	Zero Emission Vehicle

REFERENCES

[1] Ciniviz, M. and Köse, H., (2011) "The use of hydrogen in internal combustion engine: a review". International Journal of Automotive Engineering and Technologies, 1.

[2] Tüccar, G., Tosun, E., Özcanlı, M. and Aydın, K., (2013) "Possibility of Turkey to transit Electric Vehicle-based transportation", International Journal of Automotive Engineering and Technologies 2: 64-69.

[3] Akar, M.A., Kekilli, E., Bas, O., Yildizhan, S., Serin, H. and Ozcanli, M., (2018) "Hydrogen enriched waste oil biodiesel usage in compression ignition engine", International Journal of Hydrogen Energy, 43, 38, 18046-18052.

[4] Baltacioglu, M.K., Arat, H.T., Özcanli, M. and Aydin, K., (2016) "Experimental comparison of pure hydrogen and HHO (hydroxy) enriched biodiesel (B10) fuel in a commercial diesel engine", International Journal of Hydrogen Energy, 41, 19, 8347-8353.

[5] Ozcanli, M., Akar, M.A., Calik, A. and Serin, H., (2017) "Using HHO (Hydroxy) and hydrogen enriched castor oil biodiesel in compression ignition engine", International Journal of Hydrogen Energy, 42, 36, 23366-23372.

[6] Ozcanli, M., Bas, O., Akar, M.A., Yildizhan, S. and Serin, H., (2018) "Recent studies on hydrogen usage in Wankel SI engine", International Journal of Hydrogen Energy, 43, 38, 18037-18045.

[7] Serin, H. and Yıldızhan, Ş., (2018) "Hydrogen addition to tea seed oil biodiesel: Performance and emission characteristics", International Journal of Hydrogen Energy, 43, 38, 18020-18027.

[8] Stockhausen, W.F., Natkin, R.J., Kabat, D.M., Reams, L., Tang, X., Hashemi, S., " Ford P2000 hydrogen engine design and vehicle development program", SAE Paper No. 2002-01-0240.

[9] Tang, X. Kabat, D.M., Natkin, R.J., Stockhausen, W.F., Heffel, J., "Ford P2000 hydrogen engine dynamometer development", SAE Paper No. 2002-01-0242.

[10] Arnold, G., and Wolf, J.,, (2005) "Liquid Hydrogen for Automotive Application Next Generation Fuel for FC and ICE Vehicles", Teion Kogaku (J. Cryo. Soc. Jpn.), 40, 6.

[11] Wallner, T., Lohse-Busch, H., Gurski, S., Duoba, M., Thiel, W., Martin, D., Korn, T., (2008) "Fuel economy and emissions evaluation of BMW Hydrogen 7 Mono-Fuel demonstration vehicles", International Journal of Hydrogen Energy, 33, 24, 7607-7618.

[12] Kiesgen, G., Kluting, M., Bock, C., Fischer, H., "The new 12-cylinder hydrogen engine in the 7 series: the H2 ICE age has begun", SAE Paper No. 2006-01-0431.

[13] Pehr, K., (1996) "Aspects of safety and acceptance of LH2 tank systems in passenger cars", International Journal of Hydrogen Energy, 21, 5, 387–395.

[14] Michel, F., Fieseler, H., Meyer, G., Theissen, F., (1998) "On-board equipment for liquid hydrogen vehicles", International Journal of Hydrogen Energy, 23, 3, 191–199.

[15] Ansarinasab, H., Mehrpooya, M. and Mohammadi, A., (2017) "Advanced exergy and exergoeconomic analyses of a hydrogen liquefaction plant equipped with mixed refrigerant system", Journal of Cleaner Production, 144, 248-259.

[16] Theiler, G., Gradt, T., (2018) "Friction and wear behaviour of polymers in liquid hydrogen", Cryogenics, 93, 1-6.

[17] Lambert, M.A., Jones, B.J., (2006) "Automotive adsorption air conditioner powered by exhaust heat. Part1: conceptual and embodiment design", Journal of Automobile Engineering, 220, 959-972.

[18] Khayyam, H., (2013) "Adaptive intelligent control of vehicle air conditioning system", Applied Thermal Engineering, 51, 1154-1161.

[19] Javani, N., Dincer, I., Naterer, G.F., (2012) "Thermodynamic analysis of waste heat recovery for cooling systems in hybrid and electric vehicles", Energy, 46, 1, 109-116

[20] Farrington, R., Cuddy, M., Keyser, M., and Rugh, J., "Opportunities to Reduce Air-Conditioning Loads Through Lower Cabin Soak Temperatures," Presented at the 16th Electric Vehicle Symposium, China, October 13-16, 1999.

[21] Welstand, J., Haskew, H., Gunst, R., and Bevilacqua, O., "Evaluation of the Effects of Air Conditioning Operation and Associated Environmental Conditions on Vehicle Emissions and Fuel Economy," SAE Technical Paper 2003-01-2247.

[22] Dincer, I., (2007) "Environmental and sustainability aspects of hydrogen and fuel cell systems", International Journal of Energy Research, 31, 1, 29-55.

[23] Randaxhe, F., Lemort, V., Lebrun, J., (2015) "Global Optimization of the Production and the Distribution System for Typical European HVAC Systems", Energy Procedia, 78, 2452-2457.

[24] Linder, M., Mertz, R., Laurien, E., (2010) "Experimental results of a compact thermally driven cooling system based on metal hydrides", International Journal of Hydrogen Energy, 35, 14, 7623-7632.

[25] Weckerle, C., Bürger, I., Linder, M., (2017) "Novel reactor design for metal hydride cooling systems", International Journal of Hydrogen Energy, 42, 12, 8063-8074.

[26] Qin, F., Chen, J., Lu, M., Zhijiu, C., Zhou, Y., Yang, K., (2007) "Development of a metal hydride refrigeration system as an exhaust gasdriven automobile air conditioner", Renew Energy, 32, 2034-2052.

[27] Ni, J., Liu, H., (2007) "Experimental research on refrigeration characteristics of a metal hydride heat pump in auto air-conditioning", Int J Hydrogen Energy, 32, 2567-2572.

[28] Ron, M., (1984) "A hydrogen heat pump as a bus air conditioner", J Less Common Met, 104, 259-278.

[29] Linder, M., (2010) "Automotive cooling systems based on metal hydrides", University of Stuttgart.

[30] Jiang, L., Wang, R.Z., Li, J.B., Wang, L.W., Roskilly, A.P., (2018) "Performance analysis on a novel sorption air conditioner for electric vehicles", Energy Conversion and Management, 156, 515-524.

[31] Gillet, T., Andres, E., El-Bakkali, A., Lemort, V., Rulliere, ., Haberschill, P., 2018 "Sleeping evaporator and refrigerant maldistribution: An experimental investigation in an automotive multi-evaporator air-conditioning and battery cooling system", International Journal of Refrigeration, 90, 119-131.

[32] Yang, X., Dong, C., Qu, Z., (2017) "Design and dynamic analysis of a novel double-swing vane compressor for electric vehicle air conditioning systems", International Journal of Refrigeration, 76, 52-62.

[33] Dahlan, A.A., Zulkifli, A.H., Nasution, H., Aziz, A.A., Perang, M.R.M., Jamil, H.M., Zulkifli, A.A., (2014) "Efficient and 'Green' Vehicle Air Conditioning System Using Electric Compressor", Energy Procedia, 61, 270-273.

[34] Cuevas, C., Fonseca, N., Lemort, V., (2012) "Automotive electric scroll compressor: Testing and modeling", International Journal of Refrigeration, 35, 4, 841-849.

[35] Zhang, Q., Canova, M., (2015) "Modeling air conditioning system with storage evaporator for vehicle energy management", Applied Thermal Engineering, 87, 779-787.

[36] Pang, W., Yu, H., Zhang, Y., Yan, H., (2019) "Solar photovoltaic based air cooling system for vehicles", Renewable Energy, 130, 25-31.

[37] Wei, K.C., Dage, G.A., (1995) "An intelligent automotive climate control system", IEEE Systems, Man and Cybernetics, Intelligent Systems for the 21st Century, Vancouver, BC, Canada, 1995, 2977-2982.

[38] Zhang, J., Qin, G., Xu, B., Hu, H., Chen, Z., (2010) "Study on automotive air conditioner control system based on incremental-PID", Advanced Material Research 129-131, 17-22.

[39] Khayyam, H., Kouzani, A.Z., Hu, E.J., Nahavandi, S., (2011) "Coordinated energy management of vehicle air conditioning system", Applied Thermal Engineering" 31, 750-764.

[40] Khayyam, H., Kouzani, A.Z., Hu, E.J., "Reducing energy consumption of vehicle air conditioning system by an energy management system", in: IEEE The 4th International Green Energy Conference, Beijing, China, 2009.

[41] Thompson, R., Dexter, A., (2005) "A fuzzy decision-making approach to temperature control in air-conditioning systems", Control Engineering Practice, 13, 689-698.

[42] Calvino, F., Gennusa, M., Roizzo, G., Scaccianoce, G., (2004) "The control of indoor thermal comfort conditions: introducing a fuzzy adaptive controller", Energy and Buildings, 36, 97-102.

[43] Sousa, J.M., Babuska, R., Verbruggen, H.B., (1997) "Fuzzy predictive control applied to air-conditioning system", Control Engineering Practice, 5, 1395-1406.

[44] Farzaneh, Y., Tootoonchi, A.A., (2008) "Controlling automobile thermal comfort using optimized fuzzy controller", Applied Thermal Engineering, 28, 1906-1917.

[45] Khayyam, H., Nahavandi, S., Eric, H., Kouzani, A., Chonka, A., Abawajy, J., Marano, V., Sam, D., (2011) "Intelligent energy management control of vehicle air conditioning via look-ahead system", Applied Thermal Engineering, 31, 3147-3160.

[46] Linder, M., Kulenovic, R., (2011) "An energy-efficient air-conditioning system for hydrogen driven cars", International Journal of Hydrogen Energy, 36, 4, 3215-3221.

[47] Pino, F.J., Marcos, D., Bordons, C., Rosa, F., (2015) "Car air-conditioning considerations on hydrogen consumption in fuel cell and driving limitations", International journal of hydrogen energy, 40, 11696-11703.

[48] Zhang, Z., Wang, J., Feng, X., Chang, L., Chen, Y., Wang, X., (2018)"The solutions to electric vehicle air conditioning systems: A review", Renewable and Sustainable Energy Reviews, 91, 443-463.

[49] Popov, D., Fikiin, K., Stankov, B., Alvarez, G., Youbi-Idrissi, M., Damas, A., Evans, J., Brown, T., (2019) "Cryogenic Heat Exchangers for Process Cooling and Renewable Energy Storage: A Review", Applied Thermal Engineering.

[50] Deng, S., Jin, H., Cai, R., Lin, R., (2004) "Novel cogeneration power system with liquefied natural gas (LNG) cryogenic exergy utilization", Energy, 29, 4, 497–512.

[51] Dispenza, C., Dispenza, G., La Rocca, V., Panno, G., (2009) "Exergy recovery during LNG regasification: electric energy production–Part one", Appl Therm Eng, 29, 2, 380–387.

[52] Liu, Y., Guo, K., (2011) "A novel cryogenic power cycle for LNG cold energy recovery", Energy, 36, 5, 2828–2833.

[53] Dispenza, C., Dispenza, G., La Rocca, V., Panno, G., (2009) "Exergy recovery during LNG regasification: electric energy production – part two", Appl Therm Eng, 29, 2, 388–399.

[54] Jan, S., Ireneusz, S., (2009) "Utilization of the cryogenic exergy of liquid natural gas (LNG) for the production of electricity", Energy, 34, 7, 827–837.

[55] Garlov, R., Saveliev, V., Gavrylov, K., Golovin, L., Pedolsky, H., (2002) "Refrigeration of a food transport vehicle utilizing liquid nitrogen", Google Patents.

[56] Skobel, R.M., Davey, D., (2012) "Liquid nitrogen cooled beverage dispenser", Google Patents.

[57] Dakhil, F., (1999) "Air conditioning apparatus using liquid nitrogen", Google Patents.

[58] Manning, L., Schneider, R., (1974) "Nitrogen vapor engine", Google Patents.

[59] Ordonez, C.A., Plummer, M.C., (1997) "Cold thermal storage and cryogenic heat engines for energy storage applications", Energy Sources, 19, 4, 389–396.

[60] Ordonez, C.A., Plummer M.C., Reidy R.F., "Cryogenic heat engines for powering zero emission vehicles", In: Proceedings of 2001 ASME international mechanical engineering congress and exposition, US: IMECE; 2001. p. 11.

[61] Knowlen, C., Williams, J., Mattick, A., Deparis, H., Hertzberg, A., "Quasi-isothermal expansion engines for liquid nitrogen automotive propulsion", SAE Technical Paper; 1997 0148-7191.

[62] Chen, H., Ding, Y., Li, Y., Zhang, X., Tan, C., (2011) "Air fuelled zero emission road transportation: a comparative study", Appl Energy, 88, 1, 337–342.

[63] Jorgensen, S.W., (2011) "Hydrogen storage tanks for vehicles: Recent progress and current status", Current Opinion in Solid State and Materials Science, 15, 2, 39-43.

[64] Babac, G., Sisman, A., Cimen, T., (2009) "Two-dimensional thermal analysis of liquid hydrogen tank insulation", International Journal of Hydrogen Energy, 34, 15, 6357-6363.

[65] Durbin, D.J., Malardier-Jugroot, C., (2013) "Review of hydrogen storage techniques for on board vehicle applications", International Journal of Hydrogen Energy, 38, 34, 14595-14617.

[66] Chen, W., Gao, R., Sun, J., Lei, Y., Fan, X., (2018) "Modeling of an isolated liquid hydrogen droplet evaporation and combustion", Cryogenics, 96, 151-158.

[67] Ansarinasab, H., Mehrpooya, M., Mohammadi, A., (2017) "Advanced exergy and exergoeconomic analyses of a hydrogen liquefaction plant equipped with mixed refrigerant system", Journal of Cleaner Production, 144, 248-259.

[68] Janic, M., (2014) "Greening commercial air transportation by using liquid hydrogen (LH2) as a fuel", International journal of hydrogen energy, 39, 16426-16441.

[69] Verhelst, S., Wallner, T., (2009) "Hydrogen-fueled internal combustion engines", Progress in Energy and Combustion Science 35, 490–527.

[70] Das, L.M., Gulati, R., Gupta, P.K., (2000) "A Comparative Evaluation of The Performance Characteristics of A Spark Ignition Engine Using Hydrogen and Compressed Natural Gas as Alternative Fuels", International Journal of Hydrogen Energy, 25, 783-793.

[71] Linde, A.G., (2015) "Gases and Applications".

[72] Xu, W., Li, Q., Huang, M., () "Design and analysis of liquid hydrogen storage tank for high-altitude long-endurance remotely-operated aircraft", International Journal of Hydrogen Energy, 40, 46, 16578-16586.

[73] Kloeppel, S., Dittmar, N., Haberstroh, C., Quack, H., (2017) "Mixed refrigerant cycle with neon, hydrogen, and helium for cooling sc power transmission lines", IOP Conf. Series: Materials Science and Engineering, 171.

[74] Janić, M., (2018) "An assessment of the potential of alternative fuels for "greening" commercial air transportation", Journal of Air Transport Management, 69, 235-247.

[75] Janic, M., (2010) "Is liquid hydrogen a solution for mitigating air pollution by airports?", International Journal of Hydrogen Energy, 35, 5, 2190-2202.

[76] Janic, M., (2008) "The potential of liquid hydrogen for the future 'carbon-neutral' air transport system", Transportation Research Part D: Transport and Environment, 13, 7, 428-435.

[77] Hipp, E., Kerschl, S., Pflanz, T., Gruber, C., (2003) "Hydrogen Supplied ICEs and Fuel Cells for Commercial Vehicles", FUEL CELLS, 3, 3.

[78] Ohlig, K., and Decker, L., (2013). "The Latest Developments and Outlook for Hydrogen Liquefaction Technology", AIP conference proceedings. 1573. 10.1063/1.4860858.

[79] Fayaz, H., Saidur, R., Razali, N., Anuar, F.S., Saleman, A.R., Islam, M.R., (2012) "An overview of hydrogen as a vehicle fuel", Renewable and Sustainable Energy Reviews, 16, 8, 5511-5528.

[80] Yilmaz, I.T., Gumus, M., (2018) "Effects of hydrogen addition to the intake air on performance and emissions of common rail diesel engine", Energy, 142, 1104-1113.

[81] Yilmaz, I.T., Demir, A., Gumus, M., (2017) "Effects of hydrogen enrichment on combustion characteristics of a CI engine", International Journal of Hydrogen Energy, 42, 15, 10536-10546.

[82] Meier, K., Kurtz, C., Weckerle, C., Hubner, M., Bürger, I., (2018) "Air-conditioning system for vehicles with on-board hydrogen", Applied Thermal Engineering, 129, 1150–1159.

[83] Veziroglu, A. and Macario, R., (2011) "Fuel cell vehicles: State of the art with economic and environmental concerns", International Journal of Hydrogen Energy, 36, 1, 25-43.

[84] Gurz, M., Baltacioglu, E., Hames, Y., Kaya, K., (2017) "The meeting of hydrogen and automotive: A review", International Journal of Hydrogen Energy, 42, 36, 23334-23346.

[85] Regulation (EC) no 842/2006 of the European Parliament and of the Council of 17 May 2006 on certain fluorinated greenhouse gases. Official Journal of the European Union. 2006.6.14. L161/1-11.

[86] Baakeem, S.S., Orfi, J., Alabdulkarem, A., (2018) "Optimization of a multistage vapor-compression refrigeration system for various refrigerants", Applied Thermal Engineering, 136, 84-96.

[87] Abas, N., Kalair, A.R., Khan, N., Haider, A., Saleem, Z., Saleem, M.S., (2018) "Natural and synthetic refrigerants, global warming: A review", Renewable and Sustainable Energy Reviews, 90, 557-569.

[88] Mohanraj, M., Jayaraj, S., Muraleedharan, C., (2009), "Environment friendly alternatives to halogenated refrigerants – A review", International Journal of Greenhouse Gas Control, 3, 108-119.

[89] World Meteorological Organization, (1991), "Scientific assessment of ozone depletion: 1991", global ozone research and monitoring project – Report No. 25, Geneva.

[90] Wongwises, S., Kamboon, A., Orachon, B., (2006) "Experimental investigation of hydrocarbon mixtures to replace HFC-134a in an automotive air conditioning system", Energy Conversion and Management, 47, 1644–1659.

[91] Hesselgreaves, J.E., (2001) "Compact heat exchangers", Elsevier Science & Technology Books.

[92] Cavallini, A., "Properties of CO_2 as a refrigerant", in: European Seminar, Carbon Dioxide as a Refrigerant: Theoretical and Design Aspects, 2004 November 27, Milan, Italy.

[93] Cengel, Y.A. and Boles, M.A., (2005) "Thermodynamics: An Engineering Approach", 5th ed., McGraw-Hill, New York.

[94] Lorentzen, G. and Pettersen, J. (1993) "A new, efficient and environmentally benign system for car air-conditioning", Int. J. Refrig, 16, 1, 4–12.

[95] Lorentzen, G., (1994) "Revival of carbon dioxide as a refrigerant", Int J Refrig, 17, 5, 292–301.

[96] Fayazbakhsh M.A. and Bahrami, M., "Comprehensive Modeling of Vehicle Air Conditioning Loads Using Heat Balance Method", SAE International, 2013-01-1507.

[97] Pacheco, F.A., Martins, M.E.S., Zhao, H., (2013) "New European Drive Cycle (NEDC) simulation of a passenger car with a HCCI engine: Emissions and fuel consumption results", Fuel, 111, 733-739.

[98] Marachlian, J., Benelmir, R., El Bakkali, A., Olivier, G., (2011) "Exergy based simulation model for vehicle HVAC operation", Applied Thermal Engineering, 31, 5, 696-700.

[99] Sáinz, D., Diéguez, P.M., Sopena, C., Urroz, J.C., Gandía, L.M., (2012) "Conversion of a commercial gasoline vehicle to run bi-fuel (hydrogen-gasoline)", International Journal of Hydrogen Energy, 37, 2, 1781-1789.

[100] Ruth, D.W., (1975) "Simulation of modelling of automobile comfort cooling requirements", ASHRAE Journals, 53-55.

[101] Gendebien, S., Parthoens, A., Lemort, V., (2019) "Investigation of a single room ventilation heat recovery exchanger under frosting conditions: Modeling, experimental validation and operating strategies evaluation", Energy and Buildings, 186, 1-16.

Int. J. Adv. Eng. Pure Sci. 2019, 4: 355-361
DOI:10.7240/jeps.607857

RESEARCH ARTICLE / ARAŞTIRMA MAKALESİ

Farklı Uzunluklarda Dinamik Kalça Vidası Yan Plakaları ile İntertrakkanterik Kalça Kırığı Tedavisinin Biyomekanik Analizi

Biomechanical Analysis of Intertracranteric Hip Fracture Treatmentwith Dynamic Hip Screw Side Plates of Different Lengths

Oğuz Kayabaşı[1]

[1]*Düzce Üniversitesi, Mühendislik Fakültesi, Biyomedikal Mühendisliği Bölümü, 81620 Konuralp Düzce*

Öz

Dinamik kalça vidası (DKV), stabil tip intertrokanterik kalça kırıklarını tedavi etmek için kullanılan yaygın bir implanttır. Cerrahinin başarısını etkileyebilecek birçok faktör vardır. Yan plakaların uzunluğu faktörlerden biridir. Bu nedenle, DKV yan plakaların uzunluklarının biyomekaniğini araştırmak önemlidir. İmplant başarısızlıklarını azaltmak ve farklı uzunluklarda yan plaka etkilerini anlamak için, bu çalışmanın amacı DKV'daki farklı uzunluklarda yan plakaları araştırmak için sonlu elemanlar analizini kullanmaya çalışmaktır. Bu sonlu elemanlar analizi çalışmasında intertrokanterik kalça kırıkları için, farklı uzunluklardaki DKV implantasyonunu simüle etmek için kortikal kemik, süngerimsi kemik, yan plaka, gecikme vidası için 3D model inşa edilmiştir. Yükleme koşulu, bir süje dik dururken femur başı üzerindeki kuvveti (400N) simüle etmek için kullanılmıştır. Bu çalışmada gecikme vidası, yan plaka, kortikal vidalar ve femurdaki gerilme dağılımını araştırılmıştır. En büyük gerilme, vidaların kortikal kemiklerle temas ettiği noktaların çevresinde meydana gelmiştir. Femurdaki en distal kortikal vidadaki gerilme en fazla olmuştur. Yan plakanın uzunluğu kısaldıkça kortikal vidalar üzerindeki gerilme artar ve bu da kortikal vidaları çevreleyen femur üzerindeki gerilmeyi arttırır. Yan plakanın uzunluğu (2 delikli yan plaka) ve femur üzerindeki en uzak vida ile DHS kullanımı, yan plakanın dışarı çekilme riskini artırabilir. Bu çalışmanın sonuçları, ortopedik cerrahlar tarafından DKV implant uzunluklarının seçilmesi için biyomekanik bir analiz sağlayabilir.

Anahtar Kelimeler: Biyomekanik, Sonlu elemanlar analizi, Dinamik kalça vidası, İntertrokanterik kalça kırığı

Abstract

Dynamic hip screw (DKV) is a common implant used to treat stable type intertrochanteric hip fractures. There are many factors that may affect the success of surgery. The length of the side plates is one of the factors. Therefore, it is important to investigate the biomechanics of the lengths of the DKV side plates. To reduce implant failures and to understand the side-plate effects of different lengths, the aim of this study is to try to use finite element analysis to investigate side-lengths of different lengths in the DKV. In this finite element analysis study, a 3D model was constructed for intertrochanteric hip fractures, cortical bone, spongy bone, side plate, delay screw to simulate DKV implantation of different lengths, was used. In this study, the stress distribution in the delay screw, side plate, cortical screws and femur was investigated. The greatest stress occurred around the points where the screws contacted the cortical bones. The most distal cortical screw in the femur was most stressed. As the length of the side plate is shortened, the tension on the cortical screws increases, which increases the tension on the femur surrounding the cortical screws. The use of DHS with the length of the side plate (2-hole side plate) and the furthest screw on the femur can increase the risk of pulling out the side plate. The results of this study may provide a biomechanical analysis for the selection of DKV implant lengths by orthopedic surgeons.

Keywords: Biomechanics, Finite element analysis, Dynamic hip screw, Intertrochanteric hip fracture

Sorumlu yazar/Corresponding Author: Oğuz KAYABAŞI, **Tel:** +903805421036, **e-posta:** oguzkayabasi@duzce.edu.tr,
Gönderilme/Submitted: 20.08.2019, **Düzenleme/Revised:** 26.09.2019, **Kabul/Accepted:** 16.10.2019

1. GİRİŞ

Dinamik kalça vidası (DKV), stabil tip intertrokanterik kalça kırıkları için tercih edilen implanttır [1-3]. DKV kırılma bölgesinde kompresyon sağlar ve kullanımı nispeten kolaydır [4-8]. Lag vidası kesilmesi DKV ile karşılaşılan en yaygın komplikasyonlardan biridir. Uygun uç apeks mesafesi ve kırığın azaltılmasının gecikme vidası kesme riskini azalttığı düşünülmektedir [9-12]. Femur şaftından yan plaka çekilmesi DKV'nin bir komplikasyonudur [13], ancak bu konudaki tartışmalar yetersizdir. Daha uzun bir yan plaka kemikleri kavramak için daha fazla vida sağlayabilir, ancak bu daha uzun bir yara ve daha yumuşak doku tahribatına neden olur. Birçok çalışma farklı yan plaka uzunluklarının klinik gözlemlerle etkilerini araştırmış olmasına rağmen, [13-17], araştırmalar için biyomekaniği az sayıda çalışma kullanılmıştır [18-19]. Bu nedenle, ortopedi cerrahlarının, hastaları için uygun uzunluktaki yan plakaları seçmek için biyomekanik bir analize ihtiyacı vardır, bu da ameliyat sonrası komplikasyonları azaltabilir.

Önceki çalışmalarda, 4 delikli yan plakaların tedavi için ortak seçimler olduğu belirtilmiştir, ancak bazı araştırmacılar 2 delikli yan plakaların biyomekanik analiz ve klinik uygulamada yeterli stabilite sağladığını düşünmüşlerdir [13-19]. McLoughlin vd. implantasyon sonrası 2 ve 4 delikli yan plakanın biyomekanik durumunu araştırmak için kadavra deneysel bir çalışma yürütmüş, ve sonuçlar 2 delikli ve 4 delikli yan plaka arasındaki kararlılıkta önemli bir fark olmadığını göstermiştir [18]. 2 delikli DKV, döngüsel ve arıza yüklerinde 4 delikli DKV kadar biyomekanik olarak kararlıdır.

Bazı çalışmalar, 2 delikli yan plakaları kullanmanın yan plakanın dışarı çekilmesine neden olabileceğini bulmuştur. Laohapoonrungsee vd. 2 delikli yan plaka ile DKV implantasyonu alan 83 hastayı gözden geçirmiş ve 2 hastanın yan plakadan çekildiğini görmüştür [13]. Ríha vd. bir 2 delikli yan plaka ile DKV implantasyonu alan 32 hastanın, bir tanesi yan plaka çekilmesi yaşadığını bildirmiştir [14]. Bu çalışmalar, DKV'nin iki delikli bir yan plaka ile kullanılmasının tatmin edici sonuçlar verdiğini bulmuştur. Ancak vidaların çıkarıldığı veya kırılmanın düştüğü birkaç durum vardır. Yian vd. sabit yan plaka sabitlemesi için gereken optimal kortikal vida sayısını araştırmış ve üç kortikal vidanın optimal gerilim dağılımı sağladığını tespit etmiştir [20]. Her ne kadar birçok çalışma yan plakanın uzunluğunu ve kortikal vida numaralarını incelemiş olsa da [13-21], az sayıda çalışma farklı yan plaka uzunlukları için komple bir biyomekanik analiz gerçekleştirmiştir [19].

Sonlu elemanlar analizinin (SEA) tıbbi araştırmalardaki uygulamaları çoğunlukla ortopedik veya dental biyomekanik analizlerdedir [22-25]. SEA'nın avantajları, deneysel gözlemlerden elde edilemeyen genel yapının mekanik statüsünü sağlayan, gerilme dağılımı, yer değiştirme, zorlanma gözlemi için kullanılabileceğidir. Bazı araştırmacılar, farklı uzunluktaki uç vidalarının ve farklı uzunluklardaki namluların etkilerini araştırmak için SEA'yı kullanmışlardır [22]. Rooppakhun vd. SEA'in farklı uzunluklarda yan plaka uzunluklarına sahip DKV'nin mekanik performansını araştırmak için kullanılmış ve sonuçlar, implant gerilmesinde ve kırılma stabilitesinde artan plaka uzunluğunda anlamlı bir fark olmadığını göstermiştir [19]. Bununla birlikte, çalışmalarında gerilme dağılımının femur ve kortikal vidalar üzerindeki etkilerinin araştırılması yer almamıştır.

Yukarıda belirtilen çalışmalardaki açıklamalara ve farklı yan plaka uzunluklarının hasta üzerindeki etkilerini anlamaya dayalı olarak, bu çalışmanın amacı, farklı uzunluklarda üç farklı yan plakaların biyomekanik bir analizini yapmak için SEA kullanmaya çalışılmıştır. Çalışmada (2 delikli, 4 delikli ve 6 delikli) DKV'de kullanılmıştır. Çalışmada esas olarak gecikme vidası, yan plaka, kortikal vidalar ve femur üzerindeki stres dağılımı incelenmiştir. Bu çalışmanın sonuçları ortopedi cerrahlarına ideal cerrahi sonuçlar elde etmeleri için biyomekanik bir analiz sağlayabilir ve gelecekteki tasarım ve implantların geliştirilmesi için biyomekanik bir temel sağlayabilir.

2. MATERYAL VE YÖNTEM

Bu çalışma genel olarak DKV'daki farklı uzunluklarda yan plakaların üç boyutlu (3-D) SEA bilgisayar simülasyonunu; bu nedenle, klinik uygulamada sıkça karşılaşılan, farklı uzunluklarda (2 delik, 4 delik ve 6 delik) 3 grup DKV'nın SEA modeli kurulmuştur (Şekil 1 (a)). Bu çalışmada kullanılan modeller esas olarak kortikal kemik, süngerimsi kemik, yan plaka, gecikme vidası ve kortikal vidalar olmak üzere 5 bileşene ayrılmıştır. ABD'de Ulusal Sağlık Enstitüleri tarafından sağlanan bilgisayarlı tomografi görüntüleri (Görünür İnsan Projesi) kullanılarak bir femur modeli oluşturulmuştur (bu çalışmada kullanılan kemik modeli erkeğin sağ femurudur). Bu model esas olarak kortikal ve sünnetli kemikler olmak üzere 2 bileşene bölünmüştür ve büyük trokanterde 1 mm'lik bir kırılma alanı oluşturulmuştur. DKV ve kortikal vidalarla ilgili olarak, bu çalışmada çizim için 3B bilgisayar destekli tasarım (CAD) yazılımı (Pro/Engineer Wildfire 5.0) kullanılmıştır. Ayrıca, CAD yazılımı femur, DKV, vidalı vida ve kortikal vidaları montaj etmek için kullanılmıştır. (4,5 mm çapında, kullanılan vidalar dişlere sahiptir).

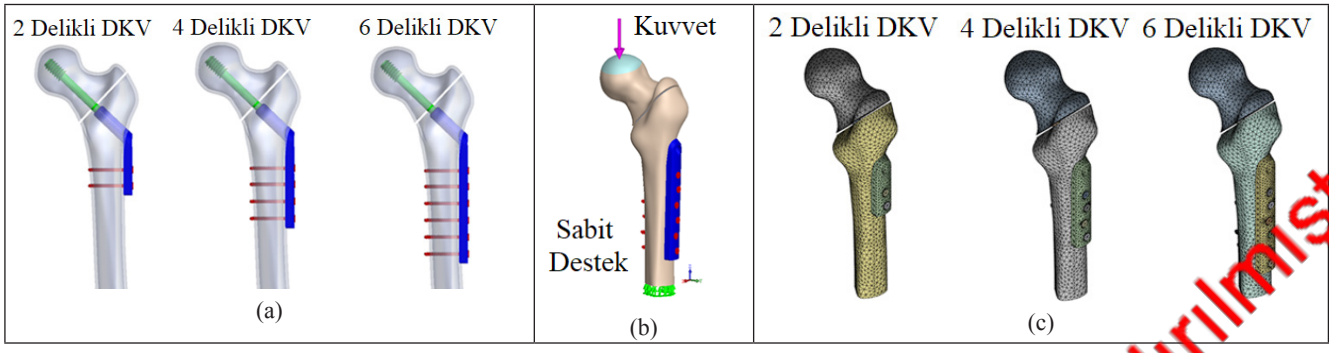

Şekil 1. (a) Bu çalışmada kullanılan 3 boyutlu bilgisayar modeli. (b) Yükleme koşulları ve sınır koşulları. (c) 3B bilgisayar modellerinin ağ yapısı

Gecikme vidası femur başının ortasına yerleştirilmiştir. İmplant için temel olarak gecikme vidasının ucundan femur kafasının tepesine 10 mm'lik bir mesafe kullanılmıştır. Ek olarak, uç-tepe mesafesi (TAD) değeri 22,5 mm (TADAP = 10 mm, TADLAT = 12,5 mm) (TAD = lateral radyografide ölçülen ön-arka radyograf (TADAP) + uç-tepe mesafesi üzerinde ölçülen uç-tepe mesafesi) TADLAT)). Bu çalışma DKV'ları boylarına göre 3 gruba ayırmıştır: 2 delikli DKV (birinci grup), 4 delikli DKV (ikinci grup) ve 6 delikli DKV grupları (üçüncü grup). Üç boyutlu bilgisayar modeli tamamlandıktan sonra, oluşturulan model analiz için FEA yazılımına (ANSYS Workbench 15.0, ANSYS, Inc., Canonsburg, PA) aktarılmıştır.

Bu çalışma temel olarak femur başı üzerindeki kuvveti, bir erkeğin dik durduğu bir senaryoda simüle etmiştir. Bu çalışma bir yük koşulu ve bir sınır koşulu sağlamıştır (Şekil 1 (b)). Yükleme koşulu, bir özne dik dururken femur başı üzerindeki kuvveti simüle etmek için kullanılır. Bu nedenle her iki bacaktaki kuvveti taklit etmek için femur başı için 400 N (Z ekseni yönü) aşağı doğru bir kuvvet uygulanmıştır [25]. Ek olarak, bu çalışmada kullanılan sınır koşulları için femurun distal ucunda sabit bir destek sağlanmış, böylece X ekseni, Y ekseni ve Z eksenindeki yer değiştirme 0 olarak ayarlanmıştır. gecikme vidası ve yan plakanın namlusu ayırma tipi olarak ayarlanmamış ve diğer parçalar arasındaki temas, bağlı bir tip olarak ayarlanmıştır. SEA yazılımı ANSYS Workbench'de "ayırma yok" seçeneği, temas halindeyken bir miktar kaymaya izin verir. Öte yandan, "bağlı" seçeneği, iki yüzü (veya kenarı) birbirine bağlayarak boşluk bırakmaz [27].

Bu çalışmada kullanılan model femoral kortikal kemik, femoral süngerimsi kemik, gecikme vidası, yan plaka ve kortikal vidalar olmak üzere beş bölümden oluşmuştur. Bu çalışmada oluşturulan malzeme özellikleri önceki çalışmalardan elde edilmiştir [22-25]. Tüm malzemelerin homojen, izotropik ve doğrusal elastik olduğu varsayılmıştır. Bu nedenle, malzeme özelliklerini ifade etmek için iki bağımsız parametre (Young'ın modülü ve Poisson'ın oranı) kullanılmıştır. Tablo 1, bu simülasyonda kullanılan malzeme özelliklerini göstermektedir.

Tablo 1. Malzeme özellikleri [22-25]

Malzeme	Young modülü (MPa)	Poisson oranı
Cortical kemik	17.000	0.3
Cancellous kemik	1.000	0.3
Yan levha	200.000	0.3
Gecikme vidası	200.000	0.3
Kortikal vida	118.000	0.3

SEA analizinden sonra, bu çalışma çoğunlukla von Mises gerilmesinin dağılımını gözlem göstergesi olarak kullanılmıştır. Gözlenen von Mises gerilme bölgeleri, gecikmeli vida, yan plaka ve kortikal vidalardaki bölgelerdir. Femurun lateral ve medial tarafındaki stres dağılım durumu, farklı uzunluklarda yan plakalar kullanıldığında DKV'deaki farklılıkları incelemek için belirlenmiştir.

SEA gerçekleştirmeden önce, inşa edilen modelde bir yakınsama testi yapılmalıdır. Bu, bir simülasyon analizi yaparken SEA modeliyle daha doğru sonuçlar elde etmek içindir. Yakınsama testi modeli ile ilgili olarak, bu çalışmada temel olarak test yakınsama testinin sonucunu elde etmek için ağ büyüklüğü kontrolü kullanılmıştır. Ağın boyutları 5, 4, 3 ve 2 mm olarak seçilmiş ve karesel tetrahedral elemanlar çoğunlukla ağ için ANSYS Workbench yazılımında kullanılmıştır. Bu çalışma ağın ebatını vermiş olmasına rağmen, yazılım ağda otomatik olarak ağın işlevinde büyük bir eğriliği olan bir yerde, vida üzerindeki dişler gibi arındırır. Femur başı üzerine yük koşulu olarak 400 N (Z ekseni) aşağı doğru kuvvet uygulanmıştır. Femurun distal ucunda sınır durumu olarak sabit bir destek kullanılmıştır (Şekil 1 (b)). Yakınsama testi için farklı mesh boyutları kullanılmıştır. Bu çalışma, Tablo 2'de listelenen yakınsama değerleri için bir işaretleyici olarak kortikal kemiğin daha küçük trokanteri üzerinde

bulunan von Mises gerilmesinin maksimum değerini, Tablo 2'de sıralanan yakınsama değerleri için bir belirteç olarak gözlemlemiştir. Üç farklı modelde, % 2.450, % 0.974 ve % 0.368 yakınsaklıklarında farklılıklar saptanmıştır (yakınsama düzeyi,% 97.549, % 99.025 ve % 99.631). Daha önceki çalışmalardan bu yakınsama sonucunun bu çalışma için kabul edilebilir olduğunu ve yakınsama testi için % 5 yakınsamanın durma kriteri olduğu bulunmuştur [25,28]. Bu sonuçlar, bu çalışmada kullanılan modelin birbirine yaklaştığını göstermektedir. Bu nedenle, bu sonlu elemanlar ağ modellerinin farklı uzunluklardaki DKV'ları incelemek için kullanılması makul olacaktır. Yakınsama testinden sonra, çalışmada kullanılan üç FEA modelinin tümü, kuadratik tetrahedral elemanlar için ağ bölümlendirmesi için bir standart (Şekil 1 (c)) ve ANSYS Workbench FEA yazılımındaki mekanikler için bir analiz simülasyonu olarak 3 mm'lik bir ağ kullanılmıştır. Çalışmada 2 delikli modelde 93.965 düğüm noktası ve 53.089 elaman, 4 delikli modelde 117.724 düğüm noktası ve 67.054 eleman, 6 delikli modelde 141.475 düğüm noktası ve 80.971 eleman kullanılmıştır.

Tablo 2. Yakınsama test sonuçları.

Ağ ölçüsü	2 Delikli model (MPa)	Yakınsama Seviyesi (%)	4 Delikli model (MPa)	Yakınsama Seviyesi (%)	6 Delikli model (MPa)	Yakınsama Seviyesi (%)
5mm	5.0928	95.467	4.5765	98.256	4.5089	99.252
4mm	5.0944	95.973	4.6009	98.780	4.6232	99.560
3mm	5.2039	97.549	4.6123	99.025	4.6265	99.631
2mm	5.3346	-	4.6577	-	4.6436	-

3. SONUÇLAR

Bu sonlu elemanlar analiz çalışmasında, analiz edilen sonuçlar renk grafiği ile gösterilebilir. Şekil 2 (a) gecikme vidaları üzerindeki gerilme dağılımını göstermektedir. Üç grup arasında, her gecikme vidasındaki en büyük von Mises gerilme değerleri aşağıdaki gibidir. (2 delikli DKV, 281.18MPa; 4 delikli DKV, 280.15MPa; ve 6 delikli DKV, 280.4Mpa). En büyük gerilme değerlerinin tümü kırık bölgesinde bulunmuştur. Üç gruptaki gecikme vidaları arasındaki en büyük gerilme değerleri arasındaki farklar dikkate değer değildir. Şekil 2 (b), kortikal vidalar üzerindeki gerilme dağılımını göstermektedir. Her gruptaki kortikal vidalar üzerindeki en büyük von Mises gerilme değerleri aşağıdaki gibidir: (2 delikli DKV, 71.934MPa; 4 delikli DKV, 34.684MPa; ve 6 delikli DKV, 29.606Mpa). En büyük gerilme değerleri, vidaların kortikal kemikle temas ettiği noktaların etrafında meydana gelmiştir. 2 delikli DKV grubunda kortikal vidalar üzerindeki stres en büyüktür. Şekil 3 (a) implant yerleştirilmesinden sonra yanal olarak gözlendiğinde femurdaki stres dağılımını göstermektedir. Yan plakanın uzunluğu daha uzun olduğunda, düşük stresli geniş bir alanın olacağını tespit edilmiştir. Şekil 3 (b), femur medial olarak gözlendiğinde gerilme dağılımını gösterir. Kortikal vidalar ile femurun medial korteksi arasındaki temas noktası çevresinde daha fazla gerilmenin üretildiğini göstermektedir. Sonuçlar en distal vidanın etrafındaki kemiğin daha fazla stres yaşayacağını göstermektedir. 2 delikli DHS grubunda bu stres değeri en büyüktür. Şekil 3 (a), femurdaki enine kesit gerilme dağılımını gösterir.

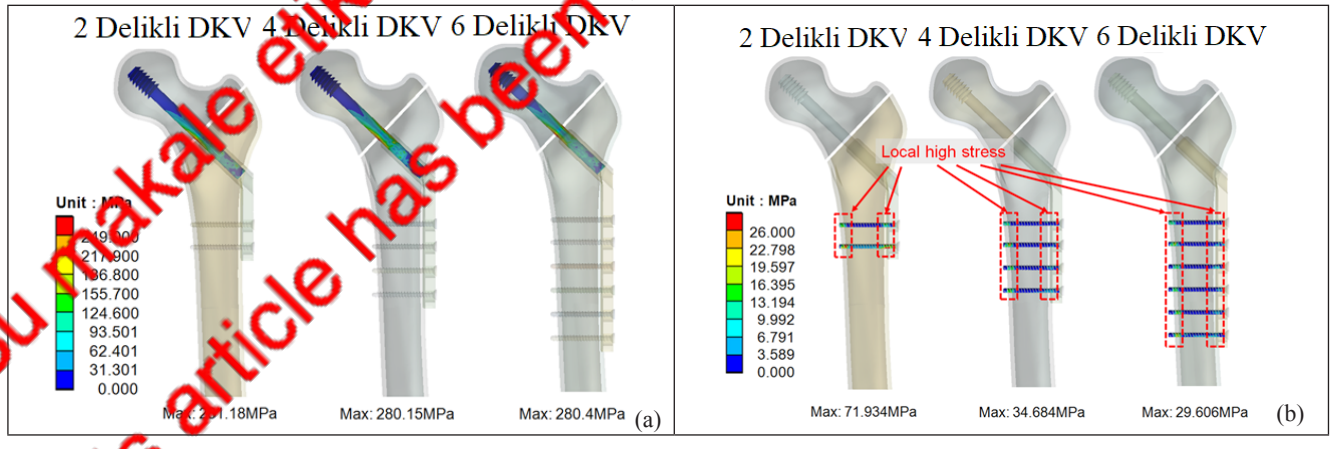

Şekil 2. (a) Gecikme vidalarındaki gerilme dağılımı. (b) Kortikal vidalarda gerilme dağılımı.

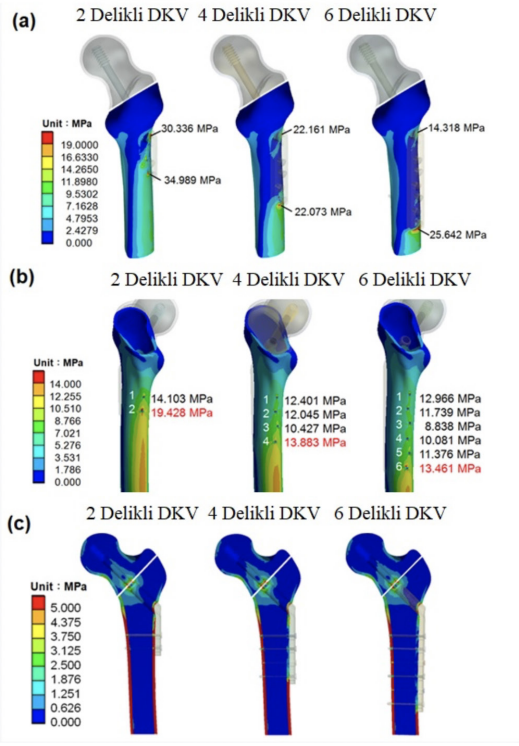

Şekil 3. (a) Femurun lateral tarafındaki gerilme dağılımı. (b) Femurun medial tarafında gerilme dağılımı. (c) Femurda kesitsel gerilme dağılımı.

4. TARTIŞMA

DKV, stabil tip intertrokanterik kalça kırıklarını tedavi etmek için kullanılan yaygın bir implanttır. DKV'sının intertrokanterik kırıkların fiksasyonundaki başarısını belirleyen faktörler arasında kırık paterni, kırık azalmasının kalitesi ve gecikme vidasının konumu yer alır [4,5,9,10,11,29]. Geçmeli vida kesimi ve yan plaka sökülmesi DKV yetmezliğinin ortak komplikasyonlarıdır. Genellikle daha uzun bir yan plakanın daha fazla stabilite sağlayabileceğine ve yan plakanın dışarı çekilme riskini en aza indireceğine inanılmaktadır. Bununla birlikte, daha uzun bir yan plaka daha uzun bir yara ve daha yumuşak doku hasarına neden olur. Bazı çalışmalar daha küçük bir insizyona sahip 2 delikli bir yan plakanın implantasyonunun yeterli fiksasyon sağlayabileceğini belirtmiştir, ancak bu yan plaka çekmesi yine de gerçekleşebilir [13,14,15,16]. Bazı çalışmalar da kortikal vida kırılmasından dolayı başarısız olduğunu bildirmiştir [13]. Bu çalışma, implantasyon sonrası farklı uzunluklarda DHS yan plakalarının biyomekanik etkilerini araştırmak için FEA'yı başarıyla kullanılmıştır. Bu çalışma aynı zamanda, yan plakanın uzunluğunun, femur kemiğinin kortikal kemiği üzerindeki stresin daha fazla artmasına neden olabileceğini göstermiştir. Bu çalışmanın sonuçları ortopedi cerrahları tarafından yan plaka uzunluklarının seçimi için mekanik bir temel sağlayabilir.

Bu çalışmanın sonuçları, her gruptaki gecikme vidası üzerindeki stres değerlerinde önemli bir farklılık göstermemiştir (Şekil 2 (a)). Bunun ana nedeni, bu çalışmada kullanılan gecikme vidasının ve namlunun uzunluklarının sabit olması olabilir. Daha önceki çalışmalar, daha uzun bir gecikme vidası kullanıldığında, gecikme vidası üzerindeki gerilmenin daha kısa bir gecikme vidası kullanıldığında olduğundan daha büyük olduğunu belirtmiştir [25]. Daha kısa namlulu bir yan levhanın kullanılması, gecikme vidası ve namlu üzerinde daha fazla strese neden olacaktır. Bu çalışmada aynı uzunlukta gecikme vidaları ve varilleri kullanılmıştır; bu nedenle, her gruptaki gecikme vidası ve namlu üzerindeki gerilme farklılıkları dikkate değer değildir. Ek olarak, bu çalışma kortikal vidalardaki gerilme dağılımını da incelemiştir. En büyük gerilme vidaların kortikal kemiklerle temas ettiği noktaların çevresinde meydana gelmiştir (Şekil 2 (b)). Bunun sebebi, kortikal vidaların kortikal kemik ve süngerimsi kemik içinden geçtiği zaman, Young'ın kortikal kemiğin modülü daha büyük olduğu için (kortikal kemik üzerindeki stres, süngerimsi kemikte olduğundan daha büyüktü), kortikal vida kortikal kemik ile bağlandı; bu nedenle, kortikal vida her iki tarafta da kortikal kemikle temas ettiği yerde daha fazla stres sağlamıştır. Her ne kadar bu çalışmanın kortikal vidaları üzerindeki tepe gerilimi, nihai dayanımdan (paslanmaz çeliğin nihai mukavemeti yaklaşık 850MPa) [30] daha düşük olmasına rağmen, kortikal vida kırılması yorulma arızası ile indüklenebilir [31]. Bazı DKV yetersizliği vakalarında, kortikal vidaların kırılma yeri bu çalışmanın sonuçlarıyla uyumlu olmuştur [13]. Ek olarak, yan levhanın uzunluğu ne kadar uzun olursa kortikal vidalar o kadar çok kullanılır ve kortikal vidalar üzerindeki baskı o kadar düşük olur.

Asıl sebep, kortikal vidalar ne kadar çok kullanılırsa, kortikal vidalar ile femur arasındaki temas yüzey alanı o kadar büyük olur ki bu da kortikal vidalar üzerindeki baskıyı azaltabilir. Femur üzerindeki gerilme değerlerine bakıldığında bu çalışma, yan plakla temas tarafında implantın desteğinden dolayı femur stresinin göreceli olarak daha düşük olduğunu göstermiştir. Bu, gerilme koruma etkisiyle açıklanabilir. Gerilme koruyucu etki, implante edilen malzeme ile kemik arasındaki elastik modülde fark büyük olduğunda ortaya çıkar. Başlangıçta kemik tarafından sağlanan geilme, implant tarafından korunur ve böylece kemikteki gerilmeyi azaltır. Ek olarak, femurun medial tarafının gözlemleri, kortikal vidaları çevreleyen kemiğin, özellikle kemik üzerindeki stresin en büyük olduğu en distal kortikal vida olan daha fazla gerilmeye maruz kaldığını ortaya koymuştur ve

2 delikli DKV grubundaki gerilme diğer 2 gruptakilerden daha büyüktü (4 delikli ve 6 delikli DKV grubu; Tablo 3). Önceki literatürler, normal kemikte, nihai mukavemet değerinin yaklaşık 105 ila 120Mpa [30, 32] olduğunu göstermiştir. Bununla birlikte, yaş ve hastalık aynı zamanda kortikal kemiğin nihai kuvvet değerini de etkiler. Bu nedenle, vida çekme işlemi daha büyük gerilme değerleriyle ortaya çıkabilir. Bu nedenle, 2 delikli DHS'nin hastalarda kullanılması, yan plakanın dışarı çekilme riskini artırabilir ve vidanın çıkarılmasını önlemek için daha uzun bir yan plaka seçilebilir. Ek olarak, klinik olarak, kortikal vidadaki iplik, stres konsantrasyonundan dolayı kortikal kemikte daha yüksek gerilmeye neden olabilir.

Bu çalışmada bu SEA'de bazı sınırlamalar vardır. Materyal özelliklerinin, bu çalışmada simülasyonu basitleştirmek için homojen, izotropik ve doğrusal elastik olduğu varsayılmıştır ve başkalarının çalışmalarına atıfta bulunarak ayarlanmıştır [22,25,28]. Bu varsayımın sonuçları gerçek durumlardan farklı olsa da, çalışma eğilimleri değişmeyecektir. Ek olarak, femur modelinde, bu çalışma sadece femurun proksimal kısmını kullanılmıştır. Bunun ana nedeni femurun proksimal kısmının bu çalışmada gözlemlenen konum olmasıydı ve bu sadeleştirme bilgisayar simülasyon süresini kısaltabilir. Ek olarak, kortikal vidalar vida dişlerine sahip olduğundan, kemik implantı (vida dişleri) arayüzünde üretilen yüksek gerilme, gerilme konsantrasyonunun geometrik görünümünün neden olduğu yüksek gerilme nedeniyle olabilir. Bu nedenle çalışma kemik-implant arayüzünü gözlemlerse; sonlu elemanlar analizi kullanılarak hatalı araştırma sonuçlarına yol açabilir (stresin yoğunlaştığı yeri bulmak için sonlu elemanlar analizinin kullanılması genellikle doğru değildir). Daha önceki biyomekanik çalışmalar proksimal femur 23'e kas kuvveti eklemiş olmasına rağmen, proksimal femur ve kalça ekleminde abduktörler, addüktörler, fleksörler, ekstensörler, dış rotatorler ve iç rotatorlar da dahil olmak üzere birçok kas grubu vardır. Her bir kas grubu farklı kasları içerdiğinden, her kasın kuvvet ve kuvvet yönü hareket sırasında farklı olacaktır. Bu nedenle, kas faktörlerinin mekanik analizi daha karmaşık hale getirmesine izin vermemek için, bu çalışma yalnızca femur başından femura iletilen aşağı doğru dış kuvveti bir yükleme koşulu olarak kullanılmıştır. Böyle bir dış kuvvet yaklaşımı, farklı dış kuvvetlerin çalışmanın sonuçları üzerindeki etkisinden kaçınabilir. Her ne kadar bu çalışmada bazı basitleştirmeler yapılmış ve gerçek durumlarla farklı olan koşullar kullanılmış olsa da, araştırılan konu için net bir eğilim göstermiştir.

Bu çalışmada FEA gözlemlerine dayanarak, farklı uzunluklarda DHS yan plakalarının biyomekanik durumu araştırılmıştır. Bu analizden elde edilen sonuçların gerçek durumlarla bazı farklılıkları olsa da, veriler farklı uzunluklarda yan plakaları seçerken ortopedi cerrahları için referans sağlamıştır. Bu aynı zamanda implant başarısızlıklarını azaltarak hastaların daha iyi prognoz kazanmalarını sağlayabilir.

5. SONUÇ

Bu çalışmada genel olarak DKV'daki farklı uzunluklardaki yan plakaların etkilerini araştırılmıştır. Bu çalışmanın sonuçları, farklı yan plakalar implante edildiğinde gerilme vidası ve namlu üzerindeki baskıda önemli bir fark olmadığını göstermiştir. Bu çalışma aynı zamanda yan plakanın (2 delikli) uzunluğu ne kadar kısa olursa kortikal vidalar üzerindeki gerilmenin o kadar yüksek olduğunu göstermiştir. Bu, kortikal vidaları çevreleyen femur üzerindeki stresi artıracaktır. 2 delikli yan plaka ile DKV kullanımı, yan plaka çekme riskini artırabilir. Bu çalışmanın sonuçları, ortopedik cerrahlar tarafından DKV implant uzunluklarının seçilmesi için biyomekanik bir analiz sağlayabilir.

KAYNAKLAR

[1] Kaplan K, Miyamoto R, Levine BR, Egol KA, Zuckerman JD, (2008). Surgical Management of Hip Fractures: An Evidence-based Review of the Literature. II: Intertrochanteric Fractures, *J Am Acad Orthop Surg* 16(11):665-673.

[2] Ahn, J, Bernstein J, (2010). Fractures in brief: intertrochanteric hip fractures, *Clin Orthop Relat Res* 468(5):1450-1452.

[3] Lorich DG, Geller DS, Nielson, JH, (2004). Osteoporotic pertrochanteric hip fractures: management and current controversies, *J Bone Joint Surg Am* 86(2):398-410.

[4] Mainds CC, Newman RJ, (1989). Implant failures in patients with proximal fractures of the femur treated with a sliding screw device, *Injur*,20(2):98-100.

[5] Davis TR, Sher JL, Horsman A, Simpson M, Porter BB, Checketts RG, (1990). Intertrochanteric femoral fractures. Mechanical failure after internal fixation, *J Bone Joint Surg Br* 72(1):26-31.

[6] Spivak JM, Zuckerman JD, Kummer FJ, Frankel VH, (1991). Fatigue failure of the sliding screw in hip fracture fixation: a report of three cases, *J Orthop Trauma* 5(3):325-331.

[7] Arastu MH, Phillips L, Duffy P, (2013). An unusual failure of a sliding hip screw in the immediate post-operative period, *Inj Extra* 44(2):23-297.

[8] Amis AA, Bromage JD, Larvin M, Fatigue fracture of a femoral sliding compression screw-plate device after bone union, *Biomaterials* 8(2):153–157, 1987.

[9] Haidukewych GJ, (2009). Intertrochanteric fractures: ten tips to improve results, *J Bone Joint Surg Am* 91(3):712-719.

[10] Rubio-Avila J, Madden K, Simunovic N, Bhandari M, Tip to apex distance in femoral intertrochanteric fractures: A systematic review, J Orthop Sci 18(4):592–598, 2013.

[11] Andruszkow H, Frink M, Frömke C, Matityahu A, Zeckey C, Mommsen P, Suntardjo S, Krettek C, Hildebrand F, (2012). Tip apex distance, hip screw placement, and neck shaft angle as potential risk factors for cut-out failure of hip screws after surgical treatment of intertrochanteric fractures, *Int Orthops* 36(11):2347–2354.

[12] Sommers MB, Roth C, Hall H, Kam BC, Ehmke LW, Krieg JC, Madey SM, Bottlang M, (2004). A laboratory model to evaluate cutout resistance of implants for pertrochanteric fracture fixation, *J Orthop Trauma* 18(6):361-368.

[13] Laohapoonrungsee A, Arpornchayanon O, Phornputkul C, (2005). Two-hole side-plate DHS in the treatment of intertrochanteric fracture: Results and complications, *Injury* 36(11):1355–1360.

[14] Ríha D, Bartonícek J, (2010). Internal fixation of pertrochanteric fractures using DHS with a two-hole side-plate, *Int Orthop* 34(6):877–882.

[15] Bolhofner BR, Russo PR, Carmen B, (1999). Results of intertrochanteric femur fractures treated with a 135-degree sliding screw with a two-hole side plate, *J Orthop Trauma* 13(1):5-8.

[16] DiPaola M, Rozbruch SR, Helfet DL, (2004). Minimal incision technique using a two-hole plate for fixation of stable intertrochanteric hip fractures, *Orthopedics* 27(3):270–274.

[17] Baird RP, O'brien P, Cruickshank D, (2014). Comparison of stable and unstable pertrochanteric femur fractures managed with 2-and 4-hole side plates, Can *J Surg* 57(5):327-330.

[18] McLoughlin SW, Wheeler DL, Rider J, Bolhofner B, (2000). Biomechanical evaluation of the dynamic hip screw with two – and four-hole side plates, *J Orthop Trauma* 14(5):318-323.

[19] 19. Rooppakhun S, Siamuna K, (2012). Finite element analysis of dynamic hip screw for intertrochanteric fracture, *Int J Model Opt* 2(2):158-161.

[20] Yian EH, Banerji I, Matthews LS, (1997). Optimal side plate fixation for unstable intertrochanteric hip fractures, *J Orthop Trauma* 11(4):254-259.

[21] Rog D, Grigsby P, Hill Z, Finette W, Inceoglu S, Zuckerman L, (2017). A biomechanical comparison of the two- and four-hole side-plate dynamic hip screw in an osteoporotic composite femur model, *J Orthop Surg* 25(2):1-6.

[22] Chen DW, Lin CL, Hu CC, Wu JW, Lee MS, (2012). Finite element analysis of different repair methods of Vancouver B1 periprosthetic fractures after total hip arthroplasty, *Injury* 43(7):1061–1065.

[23] Seral B, García JM, Cegoñino J, Doblaré M, Seral F, (2004). Finite element study of intramedullary osteosynthesis in the treatment of trochanteric fractures of the hip: Gamma and PFN, Injury 35(2):130-135.

[24] Taheri NS, Blicblau AS, Singh M, (2011). Comparative study of two materials for dynamic hip screw during fall and gait loading: titanium alloy and stainless steel, *J Orthop Sci* 16(6):805–813.

[25] Tzeng CY, Huang KC, Wu YC, Chang CL, Lee KR, Su KC, Biomechanical effect of different lag screw lengths with different barrel lengths in dynamic hip screw system: a finite element study, J Mech Med Biol 17(1):1750008, 2017.

[26] Hofmann-Fliri L, Nicolini TI, Barlaet J , Gueorguiev B, Richards RG, Blauth M,

[27] Windolf M, Cement augmentation of implants—no general cure in osteoporotic

[28] fracture treatment. (2016). A biomechanical study on non-displaced femoral neck fractures, *J Orthop Res*, 34(2):314-319.

[29] ANSYS User's Manual (2014).

[30] Ke MJ, Huang KC, Lee CH, Chu HY, Wu YT, Chang ST, Chiang SL, Su KC, (2017). Influence of three different curvatures flex-foot prosthesis while single-leg standing or running: a finite element analysis study, *J Mech Med Biol* 17(3):1750055

[31] Goffin JM, Pankaj P, Simpson AH, (2013). The importance of lag screw position for the stabilization of trochanteric fractures with a sliding hip screw: a subject-specific finite element study, *J Orthop Res* 2013;31:596-600

[32] Enderle JD, Bronzino JD, (2012). Introduction to Biomedical Engineering. *Burlington, MA: Academic Press;*

[33] Zand MS, Goldstein SA, Matthews LS, (1983). Fatigue failure of cortical bone screws, *J Biomech* 16(5):305-311,

[34] Bartel DL, Davy DT, Keaveny TM, (2006). Orthopaedic biomechanics: mechanics and design in musculoskeletal systems, *Pearson Prentice Hall, Upper Saddle River*,